



VNIVERSITAT
DE VALÈNCIA

**FACULTY OF CHEMICAL
SCIENCES**

P[®]TS

polypeptide
therapeutic
solutions

**POLYPEPTIDE THERAPEUTIC
SOLUTIONS S.L.**

Department: **Organic Chemistry**

Doctoral Program: **Chemistry**

**POLYAMINO ACID CARRIERS IN DRUG DELIVERY
AND THEIR PRODUCTION UNDER GOOD
MANUFACTURING PRACTICE COMPLIANCE**

Daniel Morelló Bolumar

**Doctoral Thesis - University of Valencia
April 2021**

Thesis Directors: **Dr. Vicent J. Nebot Carda** and **Dr. María J. Vicent Docón**

Dr. Vicent J. Nebot Carda, Ph.D. in Chemistry, and Chief Technical Officer at Polypeptide Therapeutic Solutions S.L.

AND

Dr. María J. Vicent Docón, Ph.D. in Chemistry, Head of the Polymer Therapeutics Laboratory at the Centro de Investigación Príncipe Felipe (Valencia Spain), and Chief Scientific Officer at Polypeptide Therapeutic Solutions S.L.

CERTIFY, that the work:

“POLYAMINO ACID CARRIERS IN DRUG DELIVERY AND THEIR PRODUCTION UNDER GOOD MANUFACTURING PRACTICE COMPLIANCE”

has been developed by Daniel Morelló Bolumar under their supervision at Polypeptide Therapeutic Solutions S.L. in Paterna, as a thesis project to obtain a Ph.D degree in Chemistry from the University of Valencia, Faculty of Chemical Sciences.



María J. Vicent, PhD



Vicent J. Nebot, PhD



Daniel Morelló (PhD candidate)

INDEX

ACKNOWLEDGEMENTS	7
ABBREVIATIONS	8
ABSTRACT	11
AIMS	13
<u>CHAPTER I: GENERAL INTRODUCTION</u>	<u>15</u>
1. WHAT IS A POLYAMINO ACID?	16
2. SYNTHESIS OF PAA VIA RING OPENING POLYMERIZATION OF ALPHA AMINO ACID N-CARBOXYANHYDRIDE MONOMERS	18
3. POLYAMINO ACID-BASED MATERIALS IN DRUG DELIVERY TECHNOLOGY: CURRENT STATE OF THE ART	26
3.1. DRUG DELIVERY: CROSSING BIOLOGICAL BARRIERS	26
3.2. THERAPEUTIC APPLICATIONS.....	28
3.3. RATIONAL DESIGN OF PAA-BASED MATERIALS.....	29
4. INDUSTRIALIZATION OF POLYAMINO ACIDS: FROM R&D BENCH TO GMP AND COMMERCIAL PHASES	45
4.1. BRIEF INTRODUCTION TO DRUG PRODUCT PROCESS DEVELOPMENT.....	45
4.2. LESSONS LEARNED FROM PAA-BASED MARKETED DRUGS	49
4.3. REGULATORY: INTERNATIONAL COUNCIL FOR HARMONIZATION QUALITY GUIDELINES (ICH-Q).....	50
4.4. CRITICAL ANALYTICAL METHODS TO ADDRESS QUALITY CONTROL OF PAA-BASED DRUGS	54
5. ADDRESSING CMC APPROACH FOR PAA-BASED MATERIALS.....	58
6. REFERENCES.....	58
<u>CHAPTER II: AMPHIPHILIC POLYAMINO ACID BASED MICELLES FOR DRUG DELIVERY</u>	<u>69</u>
1. INTRODUCTION.....	70
1.1. BRIEF INTRODUCTION TO POLYMERIC MICELLES BASED ON APAA MATERIALS IN DRUG DELIVERY.....	70

1.2. DRUG DELIVERY APPLICATIONS OF APAA-BASED MICELLES AND THE IMPORTANCE OF PEG AND ITS ALTERNATIVES	71
1.3. MICELLE FORMULATION	75
1.4. DESIGN OF APAA MICELLES IN THE PRESENT WORK.....	76
1.5. EXPLORING OTHER KINDS OF POLYMERIC MICELLES: TOCOPHERSOLAN AND ITS BIODEGRADABLE ALTERNATIVE	77
2. RESULTS AND DISCUSSION	79
2.1. DEVELOPMENT OF AMPHIPHILIC POLYAMINOACIDS (APAA) BY ROP OF NCAS THROUGH NAM.....	80
2.2. MICELLAR PROPERTIES CHARACTERIZATION FOR SELECTED CANDIDATES.....	112
2.3. POLYMERIC MICELLES CONTAINING AN ACTIVE HYDROPHOBIC MOLECULE.....	118
3. CONCLUSIONS	118
4. MATERIALS AND METHODS	119
4.1. MATERIALS.....	119
4.2. METHODS.....	119
5. REFERENCES.....	122

**CHAPTER III: DEVELOPMENT OF A
HYALURONATE-POLYGLUTAMATE CROSS-
POLYMER AS PERMEATION ENHANCER IN
SKIN DELIVERY APPROACHES 128**

1. INTRODUCTION.....	129
2. RESULTS AND DISCUSSION	131
2.1. SYNTHESIS AND CHARACTERIZATION OF A NEW HYBRID BIOMATERIAL.....	131
2.2. HA-CP CROSS-POLYMER-BASED MATERIALS AS SAFE PENETRATION ENHANCERS FOR TOPICAL ADMINISTRATION.....	137
3. CONCLUSION.....	143
4. MATERIALS AND METHODS	144
4.1. MATERIALS.....	144
4.2. METHODS.....	145

5.	SUPPORTING INFORMATION.....	154
6.	REFERENCES.....	160
<u>CHAPTER IV: MANUFACTURING PROCESS</u>		
<u>DEVELOPMENT FOR ALPHA POLY-L-LYSINES</u>		
<u>UNDER DRUG SUBSTANCE QUALITY GRADE IN</u>		
<u>GOOD MANUFACTURING PRACTICE</u>		
<u>COMPLIANCE.....</u>		
		164
1.	INTRODUCTION.....	165
1.1.	POLY-L-LYSINE.....	166
1.2.	GOOD MANUFACTURING PRACTICES AND MANUFACTURING PROCESS DEVELOPMENT	167
1.3.	AIMS AND APPROACH	170
2.	RESULTS & DISCUSSION.....	174
2.1.	MANUFACTURING PROCESS DEVELOPMENT.....	174
2.2.	DESIGN SPACE & CONTROL STRATEGY	202
2.3.	ANALYTICAL METHODS DEVELOPMENT	205
2.4.	PROCESS PERFORMANCE: GMP COMPLIANCE AND DATA SUMMARY 205	
2.5.	ICH FORMAL STABILITY	213
2.6.	SUBMISSION OF CMC PACKAGE.....	216
3.	CONCLUSIONS	216
4.	MATERIALS & METHODS.....	217
4.1.	MATERIALS.....	217
4.2.	METHODS.....	217
5.	SUPPORTING INFORMATION.....	217
6.	REFERENCES.....	218
	GENERAL DISCUSSION AND FINAL CONCLUSIONS..	220
	APPENDIX I. THESIS PROJECT, OBJECTIVES, MAIN METHODOLOGY, RESULTS AND CONCLUSIONS IN SPANISH.....	231
1.	INTRODUCCIÓN Y MARCO TEMÁTICO DE LA TESIS	231

2. OBJETIVOS.....	233
3. METODOLOGÍA PRINCIPAL	234
3.1. MATERIALES E INSTRUMENTACIÓN	234
4. RESULTADOS.....	234
4.1. MICELAS BASADAS EN POLIAMINO ÁCIDOS AMFIFÍLICOS PARA LA ADMINISTRACIÓN DE FÁRMACOS (CAPÍTULO 2).....	235
4.2. SISTEMA HÍBRIDO POLÍMÉRICO ENTRECruzADO COMO VEHÍCULO CAPAZ DE AUMENTAR LA PERMEACIÓN CUTÁNEA (CAPÍTULO 3)	236
4.3. DESARROLLO DEL PROCESO DE FABRICACIÓN DE ALPHA POLI-L-LISINAS BAJO EL GRADO DE CALIDAD DE SUSTANCIA FÁRMACÉUTICA CONFORME A LAS BUENAS PRÁCTICAS DE FABRICACIÓN (CAPÍTULO 4) 238	
5. CONCLUSIONES.....	239
6. REFERENCIAS	241

ACKNOWLEDGEMENTS

Me gustaría brindar mi agradecimiento a toda la gente que me ha acompañado en este gran viaje, sobre todo a mis padres, mi hermano, a Alba y a Pau. Así como a mis directores y todo el personal de PTS y del CIPF que tanto me ha enseñado. Y también al Ministerio de Economía y Competitividad por la subvención recibida para realizar esta tesis dentro del marco de Doctorados Industriales con código DI-14-06926.

ABBREVIATIONS

3-D	Three-Dimensional		
aa	Amino Acid(s)	Dil	1,1'-dioctadecyl-3,3,3',3'-tetramethylindocarbocyanine perchlorate
ABC	Accelerated Blood Clearance		
AcOEt	Ethyl acetate		1,1'-dioctadecyl-3,3,3',3'-tetramethylindocarbocyanine perchlorate
AFM	Atomic Force Microscopy	DilC18(3)	
Ala	Alanine		
AMM	Activated Monomer Mechanism	DLS	Dynamic Light Scattering
ANOVA	Analysis of variance	D-Lys	D-lysine
APAA	Amphiphilic Poly(Amino Acid)	DMEM	Dulbecco's Modified Eagle Medium
API	Active Pharmaceutical Ingredient	DMF	Dimethylformamide
ATP	Adenosine tri phosphate	DMF-d ₇	Deuterated Dimethylformamide
ATPR	Atom Transfer Radical Polymerization	DMSO	Dimethyl Sulfoxide
Ba(OH) ₂	Barium Hydroxide	DMSO-d ₆	Deuterated Dimethyl Sulfoxide
BBB	Blood-Brain Barrier		4-(4,6-Dimethoxy-1,3,5-triazin-2-yl)-4-methylmorpholinium tetrafluoroborate
BF ₄ ⁻	Tetrafluoroborate	DMTMMBF ₄	
Boc	Tert-butyloxycarbonyl		4-(4,6-Dimethoxy-1,3,5-triazin-2-yl)-4-methylmorpholinium chloride
Br	Bromide	DMTMMC1	
BSA	Bovine Serum Albumin	DNA	Deoxyribonucleic Acid
Ca(OH) ₂	Calcium Hydroxide	DP	Degree of Polymerization
CAC	Critical Aggregation concentration	DQ	Design Qualification
Cbz	Carboxybenzyl	ECM	Extracellular Matrix
CC	Chiral Chromatography		1-ethyl-3-(3-dimethylaminopropyl)-1-carbodiimide hydrochloride
CD	Circular Dichroism	EDC	
CDCl ₃	Deuterated Chloroform	EG	Ethylene Glycol
CDDP	Cisplatin	EMA	European Medicines Agency
CDI	Carbonyldiimidazole	EU	Endotoxin Unit
CDMT	2-Chloro-4,6-dimethoxy-1,3,5-triazine	FBS	Fetal Bovine Serum
CFU	Colony-Forming Unit	FDA	Food and Drugs Administration
CHCl ₃	Chloroform	FMECA	Failure Mode, Effects and Criticality Analysis
CMC	Chemistry, Manufacturing and Control	Fmoc	9-Fluorenylmethoxycarbonyl
CMO	Contract Manufacturing Organization	FTIR	Fourier Transform Infrared Spectroscopy
CO ₂	Carbon Dioxide	GC-FID	Gas Chromatography - Flame Ionization Detector
CoA	Certificate Of Analysis	GLP	Good Laboratory Practice
cP	Centipoise	GLP TOX	Good Laboratory Practice Toxicological
CP	Cross-Polymer	GMP	Good Manufacturing Practice
CPP	Critical Process Parameters	GPC	Gel Permeation Chromatography
CQA	Critical Quality Attribute	HA	Hyaluronic Acid
cryo-EM	Cryogenic electron microscopy	HAase	Hyaluronidase
CTD	Common Technical Documents	HaCaT	Human immortalized non-tumorigenic keratinocyte cell line
Cys	Cystine	HA-CP	Hyaluronic Acid Cross-Polymer
D	Dextrogyre	HBF ₄	Tetrafluoroboric Acid
Đ	Dispersity	HBr	Hydrobromic acid
DAPI	6-diamidino-2-phenylindole	HCl	Hydrochloric Acid
DCM	Dichloromethane	HClO ₄	Perchloric Acid
	trans-2-[3-(4-tert-Butylphenyl)-2-methyl-2-propenylidene] malononitrile	H-E	Hematoxylin-Eosin
DCTB		HFIP	1,1,1,3,3,3-Hexafluoro-2-propanol
Dh	Hydrodynamic Diameter		

His	Histidine	NaNO ₃	Sodium Nitrate
H-L	Hydrophilic - Lipophilic	NaOH	Sodium Hydroxide
HMDS	Hexamethyldisilane	NCA	N-CarboxyAnhydride
HNK-1	Human Natural Killer-1	NCE	New Chemical Entity
hOSEC	Human Organotypic Skin Explant Culture	nHeNH ₂	n-Hexylamine
		nBuNH ₂	n-Butylamine
HPLC	High Performance Liquid Chromatography	NHS	N-hydroxysuccinimide
HP-BM	Hydrophilic Polymer Bio Molecule	NMM	4-Methylmorpholine
HVT	high vacuum techniques	NMR	Nuclear Magnetic Resonance
IC	Ionic Chromatography	O/W	Oil Water
ICH	International Council for Harmonization	OBzl	O-Benzyl
Ile	Isoleucine	OMe	O-Methyl
IND	Investigational New Drug	OOS	Out Of Specification
IP	Intellectual Property	OQ	Operational Qualification
IPC	In-Process Control	OtBu	O-tertbutyl
IQ	Installation Qualification	P(Glu-co-Orn)	Poly(L-glutamate co-statistical L-ornithine) random polymer
IUPAC	International Union of Pure and Applied Chemistry	PAA	Poly(Amino Acid) / PolyPeptide
K ⁺	Potassium Ion	PAR	Proven Acceptable Range
KBr	Potassium Bromide	PArg	Poly(L-arginine)
KF	Karl Fischer	PB	Phosphate Buffer
KOH	Potassium Hydroxide	PBS	Phosphate-Buffered Saline
KTFA	Potassium Trifluoroacetate	PDI	PolyDispersity Index
L	Levogyre	PEG	Poly(ethylene glycol)
Leu	Leucine	PEI	Poly(ethylene imine)
LiBr	Lithium Bromide	PFA	Paraformaldehyde
L-Lys	L-lysine	PGlu	Poly(L-glutamate)
LS	Light Scattering	Phe	Phenylalanine
M	Molar	PIC	Polyion Complex
M&M	Materials and Methods	PLys	Poly(L-lysine)
MAG	Myelin-associated glycoprotein	PLysHBr	Poly(L-lysine hydrobromide)
MALDI-TOF	Matrix-Assisted Laser	PLysTFA	Poly(L-lysine trifluoroacetamide)
MS	Desorption/Ionization Mass Spectrometry	PMASS	Polymethacrylic Acid Sodium Salt
MALLS	Multi Angle Laser Light Scattering	PMDA	Pharmaceuticals and Medical Devices Agency
MALS	Multi Angle Light Scattering	PMet(O)	Poly(L-methionine sulfoxide)
MeOD-d ₄	Deuterated Methanol	PMMA	Polymethylmethacrylate
MeOH	Methanol	PMS	Phenazine Methosulfate Minimum
Mn	Molecular Weight average in Number	POrn	Poly(L-ornithine)
MP	Melting Point	PPhe	Poly(L-phenylalanine)
Mp	Molecular Weight at the Maximum Peak	PQ	Performance Qualification
		PQAS	Pharmaceutical Quality Assessment System
MTS	3-(4,5-dimethylthiazol-2-yl)-5-(3-carboxymethylphenyl)-2-(4-sulfophenyl)-2H tetrazolium	PSar	Poly(sarcosine)
		PTMC	Poly(trimethylene carbonate)
Mw	Molecular Weight average in Weight	PTFE	Polytetrafluoroethylene
MWCO	Molecular Weight Cut-Off	PTX	Paclitaxel
Na ⁺	Sodium Ion	PVal	Poly(L-valine)
NaBF ₄	Sodium tetrafluoroborate	QA	Quality Assurance
NaBr	Sodium Bromide	QC	Quality Control
NaCl	Sodium Chloride	R&D	Research And Development
NAM	Normal Amine Mechanism	RES	Reticuloendothelial System
		Rh	Hydrodynamic radius
		RI	Refraction Index
		RID	Refractive Index Detector
		ROP	Ring-Opening Polymerization

rpm	Revolutions Per Minute
RT	Room Temperature
SAS	Safety Access System
SC	Stratum Corneum
SEC	Size Exclusion Chromatography
SEM	Scanning Electron Microscopy
SI	Supporting Information
siRNA	Small Interfering Ribonucleic Acid
SOP	Standard Operating Procedures
SPPS	Solid Phase peptide Synthesis
TEA	Triethylamine
TEM	Transmission Electron Microscopy
TFA	Trifluoroacetic acid
TFA-	Trifluoroacetate
TFA-d1	Deuterated Trifluoroacetic Acid
TFF	Tangential Flow Filtration
THF	Tetrahydrofuran
TNBSA	2,4,6-trinitrobenzene sulfonic acid
TPGS	D-alpha-tocopherol-poly(ethylene glycol)-succinate
U	Activity units
USA	United States of America
USP	United States Pharmacopeia
UV	Ultra Violet
UV-Vis	Ultra Violet-Visible
Val	Valine
w/w	Weight / Weight
Z	Carboxybenzyl
ξ	Zeta potential
3-D	Three-Dimensional
aa	Amino Acid(s)
ABC	Accelerated Blood Clearance
AcOEt	Ethyl acetate
AFM	Atomic Force Microscopy
Ala	Alanine

ABSTRACT

Poly(Amino Acids) (PAA)s are biocompatible, biodegradable and multifunctional polymers, which have been effectively used as building blocks in polymer-based delivery carriers for various medical applications. In addition, PAAs are envisaged to achieve a major impact on biomedical areas due to their structural versatility, biocompatibility, water-solubility and the important advances made on the synthetic strategies. Control on polymer chain length and stereochemistry have been one of the major challenges in PAA synthesis over the past years. Their physico-chemical properties can be modulated in terms of the manufacturing process, size, electrostatic charge, conformation, geometry, topology, monomer composition. Also, the structural elements such as the Active Pharmaceutical Ingredient (API) nature, the API-carrier interaction and the supramolecular architecture of the drug delivery system (micelle, vesicle, polymer-drug conjugate, polyplex, hydrogel, or nanoparticle) can be designed and controlled.

Within the current state of the art of PAA-based materials, the vast majority of compounds are in the early stages of R&D or Proof of Concept (POC) with few examples of PAA-based therapeutics in clinical trials or marketed. The process to move a candidate from R&D to the market is a long travel that must be performed under the Good Manufacturing Practice (GMP) regulation. And inside of this GMP regulation, the Chemistry Manufacturing and Control (CMC) activities must be applied to support, control, and secure the travel. The CMC activities encompass the development, optimization, and performance of the manufacturing process and the analytical methodologies, as well as quality management systems, quality grade definition, facilities, equipment, laboratory controls, materials, packaging, labeling, and even shipment. Moreover, the quality management systems of CMC activities also contain the deviation identification, investigation, and risk management of the manufacturing process, and also the analytical methodologies qualification and validation.

Within the current framework of this thesis dissertation, the two first chapters have been focused on a work based on R&D activities for PAA-based materials that can be considered inside of the POC stage (or feasibility study or bench stage) before engaging the manufacturing process development. Through the synthetic technic of Ring-Opening Polymerization of N-carboxyanhydrides monomers of amino acids (ROP of NCAs) we obtained a pipeline of polymeric micelles based on Amphiphilic PAA (APAA). We modulated their physico-chemical properties in terms of electrostatic charge, secondary structure, and hydrophilic and hydrophobic compositions, to use them as carriers to transport hydrophobic APIs for drug delivery applications.

Furthermore, another family of polymeric micelles were studied focusing the work on the D-alpha-tocopherol-poly(ethylene glycol)-succinate (**TPGS**) molecule. This material is being highly employed for drug delivery applications and it is approved by the Regulatory Agencies. A new biodegradable analog employing a polysarcosine as water-soluble segment instead of poly(ethylene glycol) (PEG) and maintaining the D-alpha-

tocopherol as hydrophobic part was designed, developed and characterized properly comparing it face-to-face with the commercial PEGylated version finding similar results.

Besides, a novel platform for skin drug delivery and topical applications based on a cross-polymer composed of Hyaluronic acid (HA) cross-linked with poly(L-glutamate) through L-lysine named **HA-CP** was designed and developed. The new material was fully characterized and its biological properties as penetration enhancer in topical skin delivery were studied employing *in vitro*, *ex vivo*, and *in vivo* assays, comparing it with the parent linear HA with similar Mw. Substantial improvements in terms of resistance to hyaluronidase degradation, intrinsic human skin permeation capability, and excellent human skin compatibility were observed. The safety and pharmacological properties not only as skin permeation enhancer but also due to its hydration capabilities pave the way to the use of the **HA-CP** as an ingredient in cosmetic products currently marketed under the name of **Biomimetic PBT®**.

To closely reflect one of the main expertise at PTS as a company, the final chapter shows two real examples of alpha-poly(L-lysine) (PLys) currently being used as part of therapies in clinical trials. For these PLys we performed the CMC activities under GMP compliance following the quality guidelines of *The International Council for Harmonization of Technical Requirements for Pharmaceuticals for Human Use* (ICH) to achieve the drug substance quality. The optimization and development of: (i) manufacturing process at 2 Kg scale, (ii) analytical methodologies, (iii) control strategy, and (iv) submission of results to obtain PAA (concretely alpha-poly(L-lysine)) is our main contribution to the current state of the art of the PAA-based materials in the nanomedicine field for drug delivery. This work allows our customers to defend properly their products with the health regulatory authorities without problems to test them in preclinical and clinical studies to improve the life of the patients. To date, both *European Medicines Agency* (EMA) and *Food and Drugs Administration* (FDA) have evaluated our CMC package for PAA related materials with very good feedback allowing our partners to clear their path to clinical trials. These GMP grade PLys already reached human use as key components of nanomedicines under clinical evaluation for the treatment of different pathologies ranging from neurodegenerative disorders to oncology.

AIMS

The present thesis dissertation is focused on the design and development of Poly(Amino Acid) (PAA) based materials to generate versatile and tunable carriers manufactured under Good Manufacturing Practice (GMP) compliance to be used in drug delivery applications.

This general goal, involves several specific tasks that can be summarized as follows:

- 1) To adapt the synthetic methodology described in literature-based on Ring-Opening Polymerization (ROP) of alpha-amino acids N-carboxyanhydride (NCA) monomers via Normal Amine Mechanism (NAM) to obtain PAA and amphiphilic polyamino acids (APAA) block copolymers with well-defined and narrowly distributed Mw.
- 2) To explore the synthetic strategy to modulate the physico-chemical properties of APAA such as electrostatic charge (neutral, positive, negative, and zwitterionic), secondary conformation (alpha-helix, beta-sheet, and random coil), and hydrophilic – hydrophobic balance. Study of selected compositions in terms of self-assembly in aqueous solutions into micellar structures to encapsulate and transport hydrophobic bioactives (APIs).
- 3) To explore other kinds of amphiphilic block copolymers containing a biomolecule as their hydrophobic part (HP-BM). Specifically, towards the design and development of a biodegradable alternative to D-alpha-tocopherol-poly(ethylene glycol)-succinate (TPGS) based on polysarcosine to replace the polyethylene glycol as the hydrophilic segment.
- 4) To design and develop a novel platform as drug penetration enhancer for topical administration. PAA cross-polymer materials in combination with APAAs-based micelles will be develop for skin drug delivery applications.
- 5) To develop exhaustive physico-chemical characterization techniques to study the Critical Quality Attributes (CQA) in all PAA-based materials synthesized.
- 6) To evaluate the PAA-derived drug delivery systems in relevant preclinical models (*in vitro* and *ex vivo*) for skin delivery including safety as well as skin permeation profiles.
- 7) To design and develop a robust, reproducible, and scalable manufacturing process to generate PAA-based materials under GMP compliance applying the quality standards grade for drug substances following the International Council for Harmonization of Technical Requirements for Pharmaceuticals for Human Use (ICH) guidelines.

- 8) To generate a Chemical, Manufacturing and Control (CMC) package documentation over the manufacturing process of PAA-based materials. This means: (i) develop the scale-up process (POC and Pilot Batches), (ii) identify the CQA and define the Critical Process Parameters (CPP) to secure the target product quality, (iii) develop the analytical techniques and the In-Process Controls (IPC), (iv) define the work-flow, (v) select the starting materials and source materials, (vi) define the control strategy, (vii) design the facilities and set-ups with the adequate capability to perform a reproducible scale-up and (viii) manage the submission of results defining the CQA (physical, chemical and biological), the impurities profile, the related degradation substances and their limits to generate the Certificate of Analysis (CoA).

CHAPTER I: GENERAL INTRODUCTION

1. WHAT IS A POLYAMINO ACID?

Amino acids (aa) are the building blocks of life. They are biomolecules that are naturally combined in precise sequences forming peptides and proteins with specific activities. There are more than 250 types of aa described, but only 20 of them are proteinogenic. All aa have at least two chemical functional groups: (i) a carboxylic acid, and (ii) an amine. They can join through these groups forming an amide bond, also called a peptide bond [1].

Amino acids can be used as monomers to synthesize polymers with biodegradable and biocompatible properties. These bio-polymers are commonly termed polypeptides, or polyamino acids (PAA) [1]. In this thesis dissertation, the term PAA is used to describe these polymers, whose architecture consists of single repeating aa units, thereby avoiding confusion with peptides that are composed of multiple aa arranged in a specific sequence.

Due to the wide variety of available amino acids, the architectures that can be imagined and designed are unlimited. Depending on the aa used in the architectural composition of the PAA, we can tune their properties and characteristics. The functional groups present in the starting amino acid are transferred to the corresponding polymer, offering a multivalent biomaterial that may be further modified with bioactive cargos of different nature (ranging from small drugs to biologics) cell-targeting groups, cross-linkers, and fluorescent tags, among other biomedically-relevant features [2]. Through the amines, carboxylic acids, alcohols, or thiol groups present in the polymer mainchain as terminal group as well as in the side chains. Additionally, non-polar groups also can be employed to provide the PAA with hydrophobic attributes widely used for self-assembly into ordered and stable conformations [3] (see Figure 1.1).

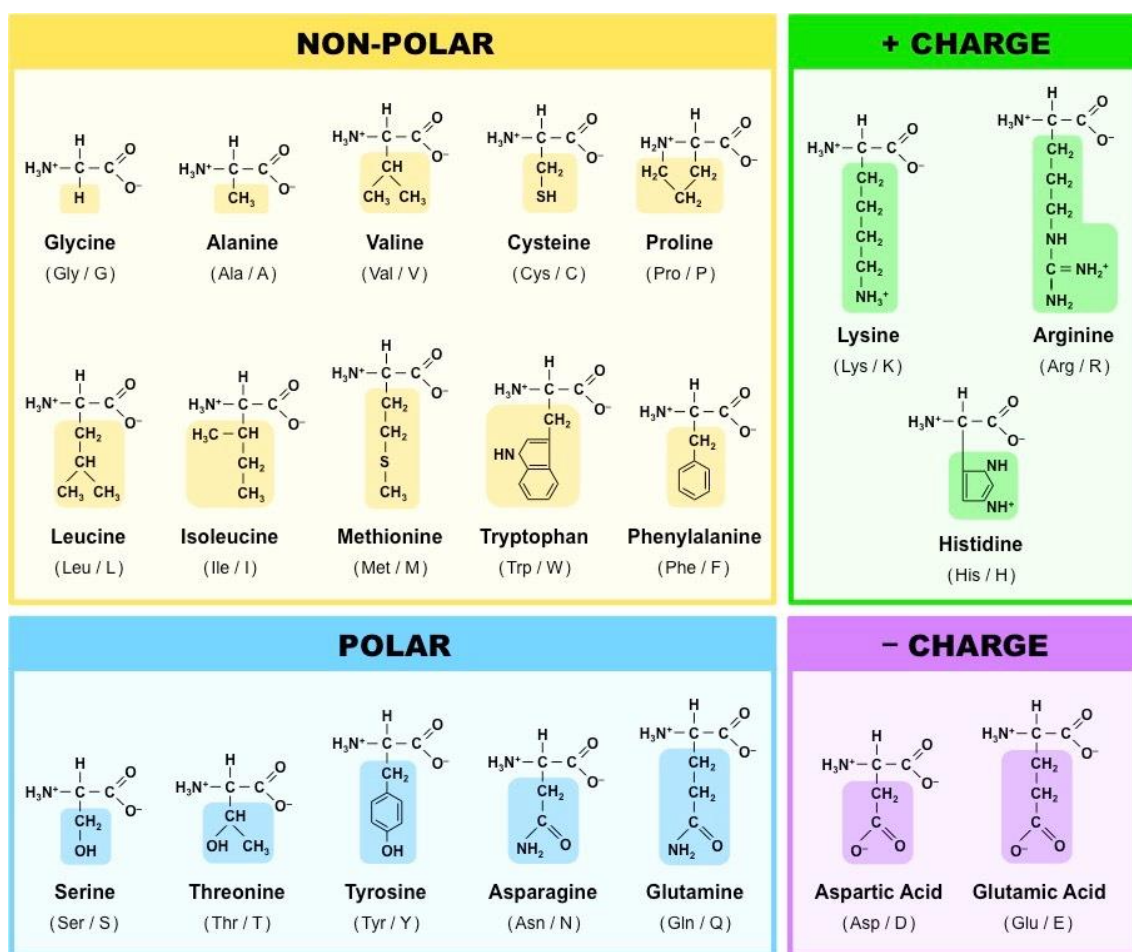


Figure 1.1. The proteinogenic amino acids classified into non-polar, polar, positive charge and negative charge. Figure obtained from the Online Science Notes website [4].

In addition to the 20 amino acids that are present in the genetic code, numerous non-natural amino acids may also be polymerized to form polymers that present different functional groups, including alkenes and alkynes pendant to the polymer chains [5, 6]. Such polymers may be further modified by contemporary, highly-efficient reactions, thus offering an effective route to modified polymers [7, 8]. The possibility of combining natural PAA with either natural non-poly(amino acid) macromolecules [e.g. hyaluronic acid (HA) [9, 10] or synthetic non-poly(amino acid) macromolecules [e.g. polyethylene glycol (PEG) [11] or polysarcosine (PSar) which is a N-methyl polyamino acid] [12] allows the creation of hybrid materials, which boast functional versatility and other desirable physico-chemical attributes [13]. Combinations between aa as monomers and other polymers can be done in the form of random, block, graft, branched and cross-linked polymers generating a great portfolio of PAA-based materials [14, 15].

These combinations and architectures offer us a wide spectrum of toolboxes of PAA-based materials in the form of gels or hydrogels, nanofilms, nanofibers, nanorods, nanotubes, cross-polymers, micelles, and vesicles [2, 15, 16]. Furthermore, the biomimeticism, biocompatibility, and biodegradability of PAA make them excellent biomaterials for applications in biomedicine, pharmaceuticals, personal care product

formulation, tissue engineering, food technology, and controlled drug delivery [15, 17, 18].

In recent years, the number of publications dealing with polypeptides or PAA has increased in agreement with the publications in drug delivery and medicine (see Figure 1.2.), demonstrating the high interest in the use of PAA in drug delivery for medical applications.

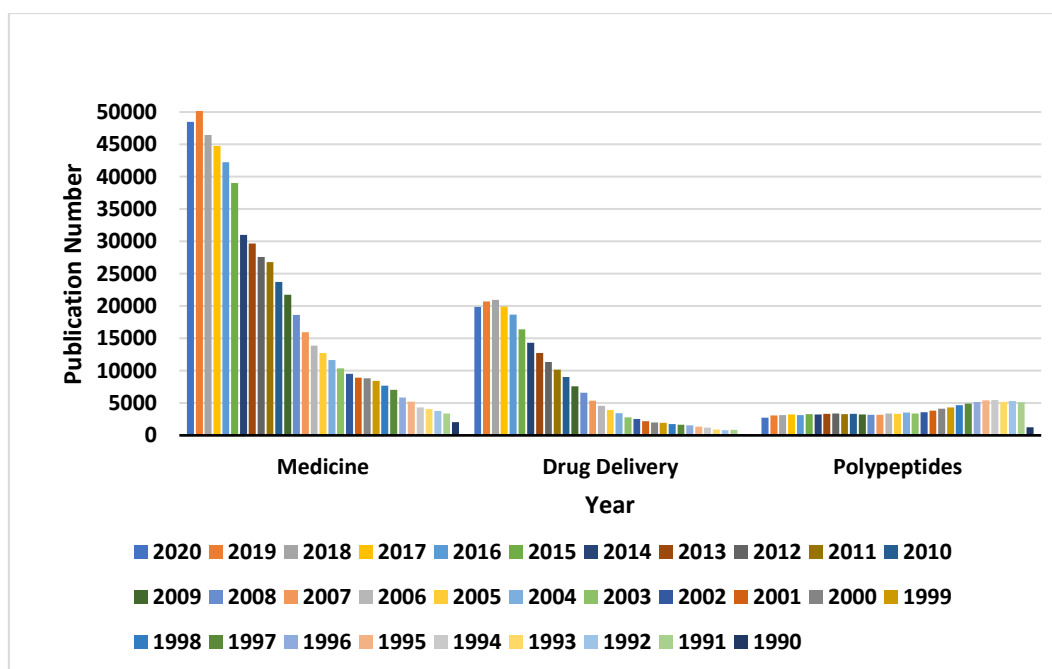
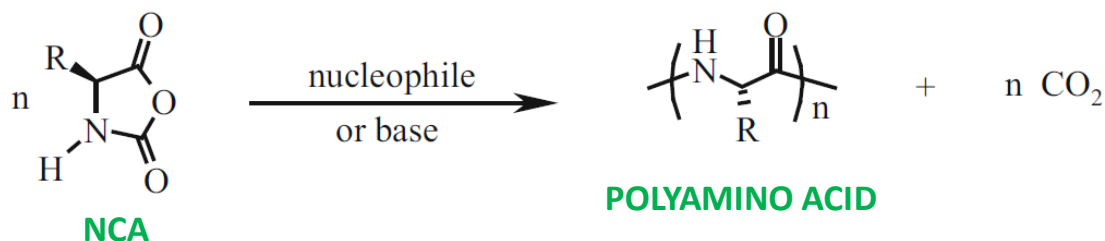


Figure 1.2. Publication numbers obtained from the Web Of Science database since 1990. The graphic is based on the data until December of 2020 in the Web Of Science database. Search based on the displayed keywords.

2. SYNTHESIS OF PAA VIA RING OPENING POLYMERIZATION OF ALPHA AMINO ACID *N*-CARBOXYANHYDRIDE MONOMERS

PAA or polypeptides can be synthesized by several techniques, such as recombinant DNA expression of proteins, Native Chemical Ligation, solid-phase peptide synthesis (SPPS), and Ring-Opening Polymerization (ROP) of α -Amino Acid *N*-Carboxyanhydrides (NCAs) [19]. Herein, we will focus on the latter, since it is the main technique to obtain homo-PAA, PAA-based block and random copolymers, as well as linear, star, graft and branched systems on a wide range of molecular weight even including large PAAs and even allowing PAA designs that would be difficult to reach through biotechnological approaches [15]. Although the polymers obtained are less defined than natural peptides or proteins, ROP synthesis allows us to achieve complex architectures based on PAA materials, such as polymeric micelles, polymersomes, polymer-drug conjugates, polyplexes and hydrogels, as well as nanoparticles for several applications [15].

The first NCA was synthesized by Leuchs in 1906 [20]. Since then, they have been used to synthesize multiple PAAs with different architectures and structures, due to the wide variety of natural and non-natural amino acids compatible with this versatile polymerization method [21-23].



Scheme 1.1. General scheme for ring-opening polymerization (ROP) of α -amino acid *N*-carboxyanhydrides (NCAs). Scheme adapted from Deming [24].

A desirable goal in the development of polymer-based materials is the construction of well-defined, reproducible and homogenous architectures, as well as a scalable and robust manufacturing process. The synthesis of narrowly distributed PAA for their potential use in biomedicine or other applications is a desirable aim. It is widely known that through the ROP of NCAs cannot currently provide perfect control in PAA synthesis, but the living character of this polymerization method allows us to get ever closer. The living character can be described as the successful synthesis of PAA through the elimination of side reactions in favour of the chain-growth process allowing multiple monomer additions to each chain yielding the free amine in the N-terminus [25].

To achieve these goals, it is necessary to use NCA monomers of high purity, thereby minimizing the secondary undesired reactions explained below. The purity of NCAs is a limiting factor in the ROP of NCAs since certain electrophilic impurities are potential catalysts for side reactions during PAA synthesis. For example, some electrophilic impurities are potential chain transfer agents that may negatively affect the chain length distribution and the polydispersity of the polymers produced. The chloride amount in the NCA is also a key parameter to control because chloride can affect the polymerization [22]. Chloride is present in the NCA since they are generally obtained from phosgene derivatives yielding HCl as a byproduct [26]. A robust and effective purification step in the manufacturing process of NCAs is essential to ensure that monomer purity is high. The mode of purification should be cost-effective and straightforward to conduct at an industrial scale if the ROP of NCAs is to become a viable method of creating polymers that can compete commercially with other polymers such as PEG. Repeated crystallization of NCA monomers under anhydrous conditions is the most commonly applied purification method at laboratory scale. The purity obtained with this method is satisfactory but recrystallization itself is always a time-consuming process [27].

When the purity and manufacturing process to obtain NCAs are controlled, they provide an excellent opportunity to build polymers of natural aa or aa derivatives due to the high chemical versatility possible in the orthogonal functional groups (see Figure 1.3).

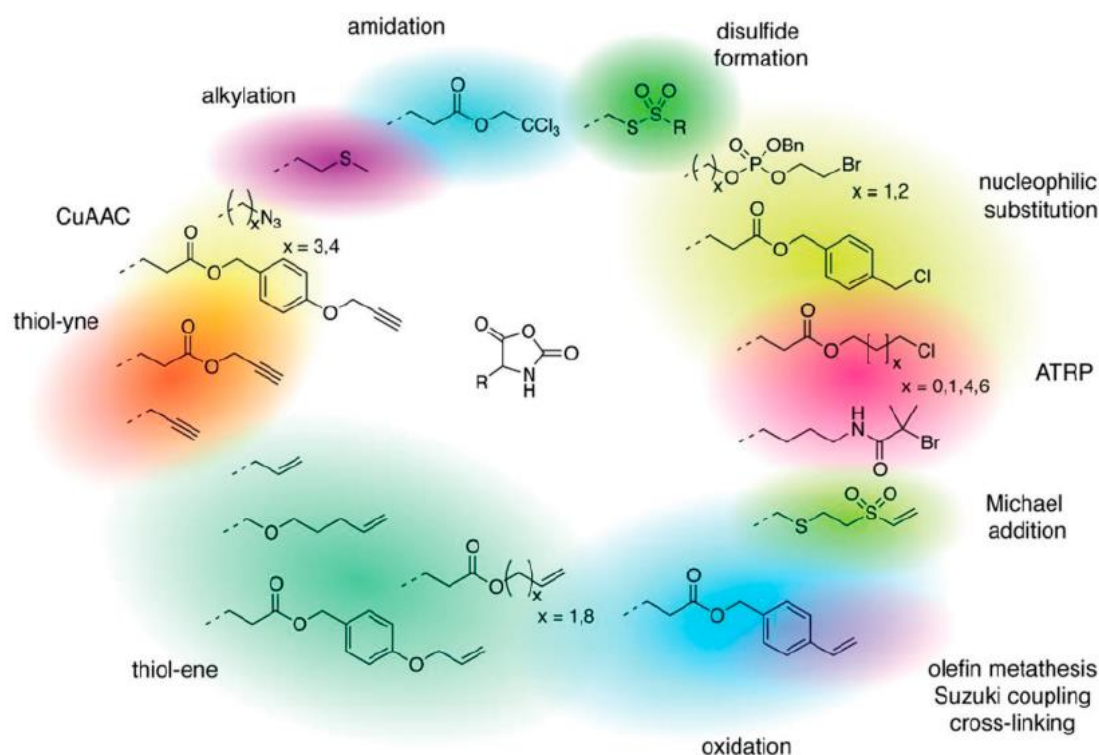
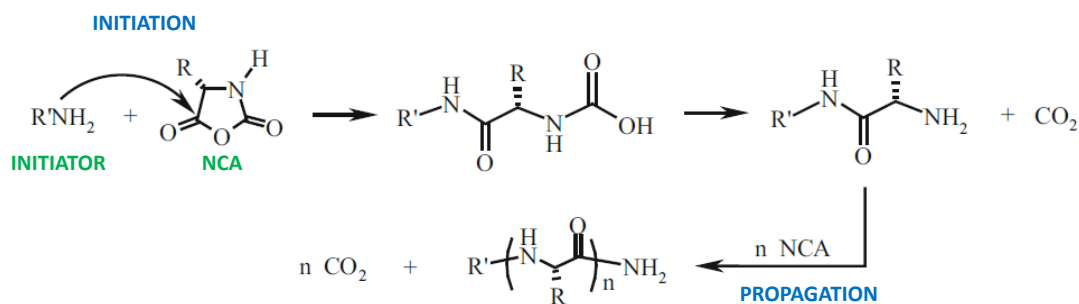


Figure 1.3. Orthogonally reactive NCAs for polypeptide synthesis from Huesmann et al [5].

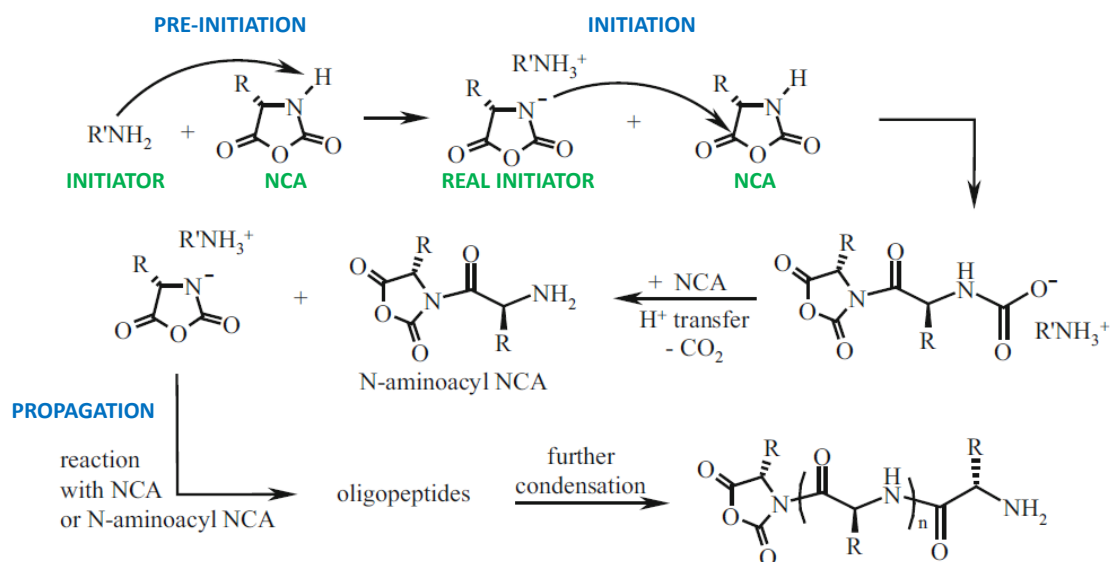
Scientific knowledge indicates that every NCA molecule can be polymerized by a nucleophile or a base reagent. Both initiation steps lead to a different propagation mechanism. However, it should be noted that, in aprotic solvents, every nucleophile can also act as a base leading to the coexistence of both mechanisms. This can be one of the main reasons why undefined polypeptides are sometimes obtained. Therefore, the ROP of NCAs can proceed via two mechanisms: the normal amine mechanism (NAM, induced by nucleophilic substitution), and the activated monomer mechanism (AMM, induced by deprotonation).

A proof of NAM was demonstrated independently by Peggion et al [28] and Goodman et al [29] by confirming the incorporation of the initiator fragment in the final polymer. As cited above, this mechanism is based on the nucleophilic attack of the initiator. The intermediate formed is an unstable carbamic acid that decarboxylates yielding a new free amine group, propagating the polymerization and releasing CO_2 . Therefore, primary amines are mainly used to polymerize NCAs. Scheme 1.2 shows the initiation and propagation steps. Importantly, this strategy is ideal to achieve block copolymers using a polymer itself as the initiator [30].



Scheme 1.2. Initiation and propagation steps according to NAM. Scheme adapted from Deming [24].

In contrast, AMM (first proposed by Ballard et al) [31] is based on the basic character of the initiator and its ability to deprotonate the N-H of the NCA ring in a preinitiation step generating the “real initiator”. This real initiator attacks the electrophilic carbonyl to give a tadpole dimer, followed by reaction with another NCA, creating a new anion with the simultaneous release of CO₂. This tadpole dimer is attacked by a new anion to give a tadpole trimer, and so on, followed by the creation of an NCA anion in each new addition (see Scheme 1.3). For that reason, this latter mechanism is attributed to reagents with a strong basic character such as tertiary amines or metal alkoxides. In the case of secondary amine and alkali halide-initiated polymerizations, it is believed that AMM and NAM coexist [32]. Whereas NAM is valid for both *N*-unsubstituted and *N*-substituted NCAs, the AMM mechanism can only be used with *N*-unsubstituted NCAs (due to the deprotonation in the preinitiation step). Furthermore, it should be noted that the NCA anion itself can rearrange into an α -isocyanatocarboxylate (See Scheme 1.4).



Scheme 1.3. Preinitiation, initiation and propagation steps in AMM. Scheme adapted from Deming [24].

A fast initiation is one of the key requirements for a controlled polymerization, leading to polymers with controlled Mw and low dispersities, since every molecule of initiator is supposed to start a polymer chain in this scenario. On the contrary, as AMM

proceeds via anionic attack, it is expected that the propagation rate is faster than in NAM leading to higher Mw. However, polypeptides with higher polydispersity indices (PDI) are obtained with this method [32]. Therefore, AMM should generally be avoided to achieve controlled polymerizations, but it can be controlled, and also well-defined PAA can be obtained. Since amines are both nucleophilic and basic, polymerization will always switch back and forth between the “amine” and “activated monomer” mechanisms. The use of secondary amines is especially unfavorable, because such compounds are sterically more hindered and have a more basic character. In summary, primary amines with reduced basic character seem to be the key to polymerization exclusively via NAM.

Besides the aforementioned polymerization mechanisms, several unwanted side reactions exist destroying the living nature of ROP of NCAs. It is important to take into account all factors hindering their controlled polymerization, such as the purity of the NCA and the rest of the reaction system (purity of solvents, etc.) [33], presence of water or moisture [34], CO₂ pressure [35], pH, temperature, presence of salts [36, 37], cleavage of protecting groups [38], and undesired termination processes (carbamate mechanisms or reaction with α -isocyanatocarboxylates) [39, 40]. The carbamate mechanism is based on the nucleophilic attack of the intermediate carbamate to another NCA, leading to the formation of urea groups within the polymer and termination of the chain growth reaction (see Scheme 1.4). ROP of NCAs via AMM should be avoided to yield block copolymers, given that control over polymer end groups is essential for the synthesis of multiblock architectures or end group functionalization. Classic NCA polymerization tends to be very problematic, even when initiated by primary amines, leading in most cases to reduced control of the polymerization process itself. Especially whenever a higher degree of polymerization or more complex architectures are desired, the occurring side reactions interfere.

Aside from the ROP of NCA chemistry drawbacks or limitations, there are others that might hinder the synthesis of target PAA architectures such as the conformational constraints affecting the living polymerization character (e.g. secondary structures, the bulkiness of the growing polymer chain with steric hindrance over the terminal amine, and impact on chain propagation, etc.) [41]. Recently it has been published a solubility-aggregation in the reaction solvent composition. In the first instance, this can be considered a drawback but also an opportunity to develop a one-pot synthesis of nanoparticles via Polymerization-Induced Self-assembly [41].

For these reasons, efforts have been devoted to developing new approaches in order to overcome these drawbacks, such as the use of heavy metal catalysts [25], high vacuum techniques (HVT) [42], primary amine hydrochloride salts [43] and tetrafluoroborate salts [44], the combination of low temperature with primary amines [45], the use of silazane derivatives as initiators [46] or the optimization of reaction conditions (pressure, temperature, etc.) [42, 45]. Unfortunately, all methods present limitations and they are described below.

In 1997 Deming [25] developed a new class of NCA-initiators based on organonickel and cobalt (0) compounds, capable of overcoming the termination reaction and useful for a wide range of NCAs, resulting in homo and block copolypeptides with narrow PDI (<1.2), controlled Mw from 500 to 500.000 Da, and preservation of chirality [47, 48].

In 2003, Schlaad et al reported the use of primary amine hydrochloride salts as macroinitiators to avoid the AMM mechanism [43]. The nucleophilic amino terminus is transferred into a dormant (i.e. protonated) state. The reactivity of primary amine hydrochlorides toward NCAs was first investigated by Knobler et al in the 1960s [49]. The main drawbacks are that polymerization time increases due to reduced reactivity of the active sites leading to incomplete monomer conversion, and the presence of nucleophilic chloride anions which can also act as initiators of NCA polymerization. Therefore, the remaining monomer must be removed before a second block can be synthesized. In their work, Schlaad and co-workers reported PDI < 1.1 and Mn no higher than 22 kDa [43].

The use of primary amines and High Vacuum Techniques (HVT) for living polymerization was proposed by Hadjichristidis and his team in 2004 [50]. According to the authors, HVT enables the synthesis of well-defined homo and copolypeptides with complex macromolecular architectures that are also valid for polypeptide hybrids. However, HVTs require a complex and expensive experimental setup, complicating synthesis. In addition, the closed system generates a pressure gradient during polymerization, which may influence polymerization kinetics. The use of low temperatures with primary amines was reported by Vayaboury et al in 2004 [45], decreasing termination reactions. At 0 °C, the activation energy barrier for chain propagation becomes lower than that of side reactions. The main disadvantage of this methodology is that reaction times increase 2-4 fold while yields decrease. Finally, the use of silazane derivatives as initiators was carried out by Lu and co-workers in 2007 [46], leading to polymers with low PDI, the expected Mw and almost quantitative yields. The weak point of this approach is the poor reaction scope; it cannot be used for the polymerization of *N*-unsubstituted NCAs, and hexamethyldisilazane (HMDS) amines are sensitive to hydrolytic reactions. Scheme 1.4 represents the complexity involved in the chemistry of NCA polymerizations.

In 2013, the research group led by María Jesús Vicent in collaboration with Matthias Barz developed a novel method to prepare well-defined PAA based on the use of initiators containing a primary amine as a tetrafluoroborate ammonium salt [44]. The non-nucleophilic character of the BF₄⁻ counteranion maximizes the nucleophilic behavior of the amine and decreases its basic character. This was a novel advantage over the commonly used counterions (Cl⁻ or Br⁻) in the ammonium salts of amines. Given that chloride and bromide anions are nucleophilic they are able to activate the polymerization, competing with the desired amine initiator and altering the stoichiometry between initiator and monomer, and as such yielding PAA with undesired Mw distributions [43,

49]. These initiators can be prepared easily through treatment of the primary amine with the HBF_4 ether complex [51]. This strategy allows us to obtain homo and block PAA copolymers through the living polymerization mechanism [44].

3. POLYAMINO ACID-BASED MATERIALS IN DRUG DELIVERY TECHNOLOGY: CURRENT STATE OF THE ART

The high versatility of the NCA polymerization strategy provides scientists and researchers with a powerful tool to generate well-defined homo or hetero materials based on PAAs. Employing this technology, the structures and architectures that can be designed are unlimited. Depending on the application and intended purpose, the polymer can be built with specific properties. Based on the composition and architectures of the PAA, the size, the electrostatic charge, the conformation, the geometry, and the topology of materials can all be modified.

The use of PAA-based materials can be corroborated by the number of publications over the last few years according to Web Of Science. This number is shown in the next figure, including the number of publications relating to PAA of the 20 essential aa, as well as polyethylene glycol, hyaluronic acid, poly-L-ornithine and polysarcosine, which are all polymers employed in this thesis dissertation. The figure displays that the PEG and HA are the highest materials employed. This is related with the synthesis and characterization techniques to obtain cost-eficiency process for PAA are being developed recently, and the PEG and HA are polymers more developed in these terms.

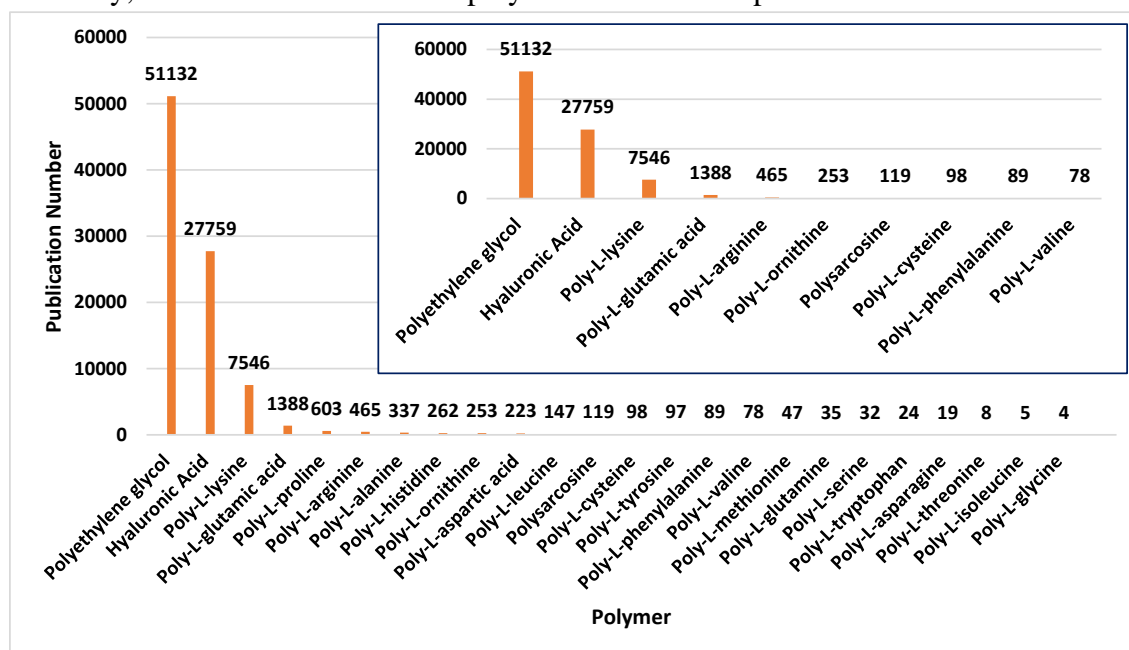


Figure 1.4. The number of publications obtained for PAA of the 20 essential aa, as well as polyethylene glycol, hyaluronic acid, poly-L-ornithine and polysarcosine. The specific polymers employed in this thesis dissertation are highlighted. The graphic is based on the data until December of 2020 in the Web Of Science database. The searches were carried out for the exact names shown here.

3.1. DRUG DELIVERY: CROSSING BIOLOGICAL BARRIERS

As mentioned, PAA-based materials present biomimetism, biocompatibility, and biodegradability. These attributes make them excellent biomaterials for applications in biomedicine, pharmaceuticals, personal care product formulation, tissue engineering, food technology and controlled drug delivery [1, 53]. These materials have gained much

attention in the field of biomedicine over recent decades and the number of compounds present in preclinical studies and clinical trials has increased [54]. The advances and increasing knowledge in the chemistry for the manufacturing process as well as in the physico-chemical characterization techniques have allowed scientists to develop a high variety of PAA-based materials as drug delivery system to treat life-threatening diseases such as cancer, Parkinson or Alzheimer [19, 54-56].

Drug delivery can be defined as the technology field that studies and develops materials for the transport of a pharmaceutical compound or active pharmaceutical ingredient (API) in the body to perform a therapeutic effect. Drug delivery systems have provided great benefits to current therapies by (i) increasing stability and bioavailability of therapeutic molecules, (ii) decreasing their side effects, and/or (iii) enabling alternative and better administration routes. Multi-encapsulation of drugs, bioadhesion, enhanced uptake properties, biocompatibility, drug sustained-release, or surface modification with target moieties to achieve a localized delivery of the drug transported are some of the appealing properties that drug delivery systems can offer [53].

Depending on the desired therapeutic effect, the composition and architecture of the PAA-based material has a crucial role. In order to rationally design PAA-based carriers, it is crucial to understand where the cargo should be released and which biological barriers it will encounter (Figure 1.5) [54].

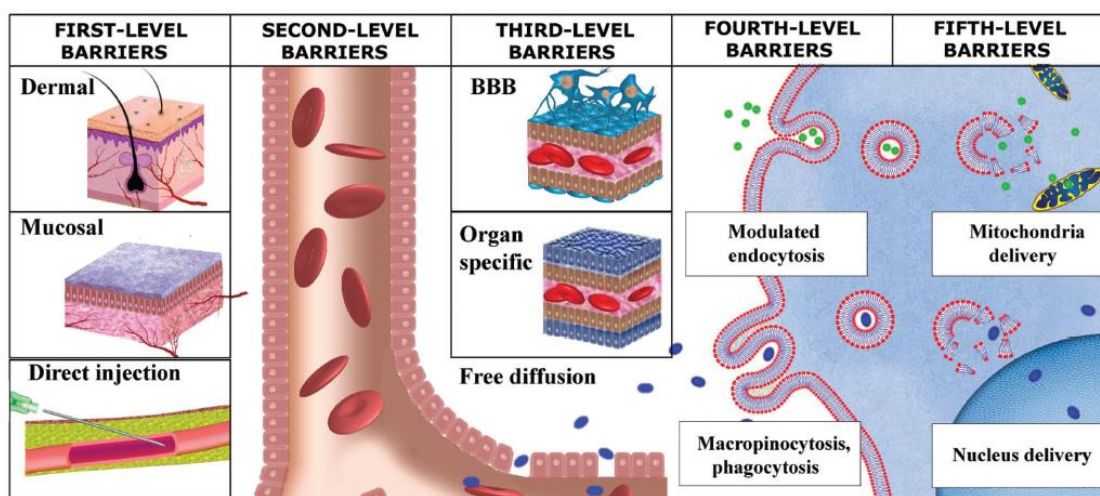


Figure 1.5. General representation of biological barriers present in the body published by Zagorodko et al in 2017 [54].

The known biological barriers can be classified into five hierarchical levels as shown in Figure 1.5.

Level 1 (absorption: reaching the bloodstream). Depending on the administration route the percentage of PAA reaching the bloodstream could be significantly different. Intravenous (i.v.) administration allows for increased drug bioavailability in comparison with other routes including oral, intranasal or topical, administration, with each route requiring the optimization of the final therapeutic

formulation to take into account the range of parameters that affect interactions with biological interfaces such as the mucosa or the skin. Alternative routes of administration for PAAs include topical, oral, and pulmonary, delivery through different mucus barriers (buccal, nasal, vaginal, ocular, etc.), and through direct injection to the site of disease (intraocular, intraperitoneal etc.) [54].

Level 2 (circulatory barriers). In the bloodstream, the immune, reticuloendothelial, and hepatic systems are the main obstacles for adequate delivery. Physico-chemical parameters such as size, charge, geometry, or solution conformation govern the *in vivo* distribution and fate. The design of effective PAA-based materials must ensure their chemical stability and integrity during blood circulation at physiological conditions (ionic strength, redox potential, pH, presence of proteases, etc.) until arrival at the desired site of action.

Level 3 (tissue-specific barriers and tumor stroma). Some organs are provided with highly specific blood-tissue barriers (blood-brain, blood-ocular, blood-retinal, blood-testis, blood-thymus and blood-air). Crossing the blood-brain barrier (BBB) using PAA-based materials has only recently gained attention following the publication of the so-called “Trojan Horse” strategy [57, 58].

Level 4 (cellular barriers). The passive diffusion of molecules with a molecular mass above 1 kDa is efficiently blocked by the cell membrane. Most PAA-based materials enter the cell through energy-dependent endocytosis mechanisms. Upon derivatization with targeting residues on the carrier surface (e.g., folic acid, cholesterol, or Arginylglycylaspartic acid-based peptides) receptor-mediated transport could be also explored) [59, 60].

Level 5 (subcellular barriers). Targeting of specific organelles (e.g., the nucleus or mitochondrion) represents the most challenging area within drug delivery. PAA-based materials can be designed to pass these barriers by different endocytic mechanism, which will determine the trafficking to different subcellular vesicles or organelles. Most PAAs are designed to enter the cell by clathrin-mediated endocytosis to be actively transported to lysosomes for further degradation, a process which is advantageous for bioresponsive-drug release. To note, after endocytosis, endosomal escape is needed to ensure cytosolic release of the PAA if organelles different from lysosome are the target [61, 62].

As stated, it is necessary to design the PAA-based materials, not only to cross the biological barriers, but also to reach the target-specific location into the body to release the API in a controlled manner towards an effective therapy.

3.2. THERAPEUTIC APPLICATIONS

PAA-based materials in drug delivery can be applied in several areas such as oncology, regenerative medicine, gene delivery, or immunotherapy to treat cancer [15, 19, 63, 64]. These materials can also be used for infectious [65], inflammatory diseases

[66], and for diagnostics with a variety of imaging agents, in fact several materials have been tested as nanoprobes for disease monitoring [19, 67]. Surprisingly few literature examples for topical and skin applications are available employing PAA-based materials [65, 68]. Table 1.1 shows examples of PAA-based therapeutics in early preclinical stage, clinical trials and also in the market.

3.3. RATIONAL DESIGN OF PAA-BASED MATERIALS

For an adequate targeted delivery of an API to the site of action, it is necessary to control the **physico-chemical parameters** of the PAA-based material carriers such as the size, electrostatic charge, conformation, geometry and topology as well as **structural elements** such as API nature, API-carrier interaction, and the supramolecular architecture of the resulting drug delivery system. See Figure 1.6.

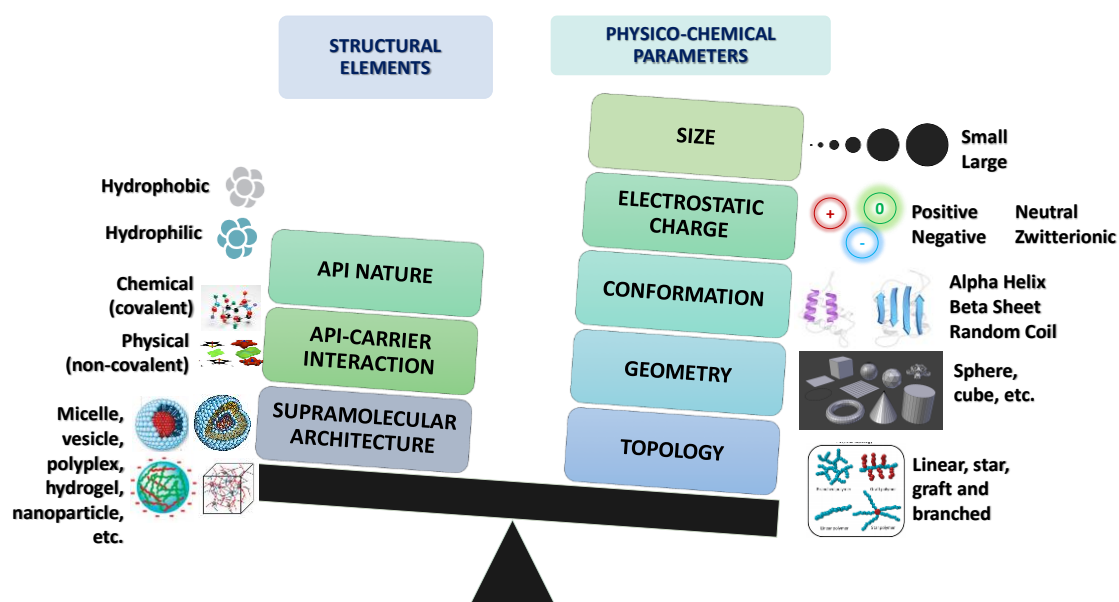


Figure 1.6. Schematic representation of attributes to design the PAA-based material vehicle in terms of structural elements and physico-chemical parameters.

3.3.1. PHYSICO-CHEMICAL PARAMETERS

To properly design the PAA-vehicle, it is important to take into account the effect of the following physico-chemical properties.

Size effect. The diameter of the transport system suitable for *in vivo* application should be in the range from 5 to 200 nm. This is due to the rapid penetration of capillary fenestrae by nano-systems smaller than 5 nm, allowing them to equilibrate with the extracellular matrix and be rapidly cleared by renal glomerular capillaries. On the other hand, systems with larger than 200 nm exhibit prolonged circulation (except in cases where clearance is guided by factors other than size), although the reticuloendothelial system (RES) does eventually eliminate them [54]. Size effects are directly related to the Mw of the polymers employed in the PAA-based material carrier. Furthermore, an increase in size is generally observed when an API is added to a polymer system. For

example, the modification of dendrimeric PLys nanosystems with folic acid [69] and PEG-b-PAsp nanosystems with biotin [70] both resulted in a size increase.

Electrostatic charge effect. The electrostatic charge or Z potential (ξ) on the surface of the transport system should be negative or neutral to inhibit opsonization and RES elimination. It is described that positively charged species such as (P(L-Glu-hydrazide)-b-poly(N,N-dimethylaminopropyl methacrylamide)) 3-g-PEG-Dox ($\xi = +46.3$ mV) are not directly applicable *in vivo* due to charge associated toxicity, but they can be transformed into negatively charged nanoconstructs by conjugation or complexation with anionic molecules (e.g. siRNA) [71].

Conformation effect. There is no preferred or recommended secondary structure conformation for the carrier design. The conformation of the PAA-based material can be modified according to the aa monomers employed in the polymer composition. If an alpha helix conformation is required, Ala, Phe or Leu aa can be used, whereas the use of Ile or Val results in a beta-sheet secondary structure [54, 72-74]. Not only the nature of hydrophobic aa can determine the conformation, but the stereochemical conformation of the alpha carbon is also a key parameter to control the secondary structure. For example, in 2014 Kataoka's team reported that PEG-b-P(L-Glu)-CDDP and PEG-b-P(D-Glu)-CDDP, which both adopt helical conformations, displayed no differences in biodistribution or anti-cancer activity. However, micelles with a random P(D,L-Glu) copolymer matrix, which are unable to form helical conformation, were less active and cleared faster, even though the size of the resulting nano-system was similar [75].

Geometry effect. Particle shape, which could have a strong impact on carrier performance, has not been investigated in detail [76]. However, according to some scientists, the shape of the vehicle may be the main driving attribute in some biological scenarios [77]. Several studies have demonstrated that shape, and in particular local particle shape rather than size, has a dominant influence on phagocytosis when exposing alveolar macrophages to non-spherical particles of different sizes and shapes [78]. PAA-based materials with spherical shape changes may lead to increased cell attachment, resistance to detachment, as well as increased cell internalization [76]. However, nanodisks, as compared to nanospheres, tend to localize within phospholipid bilayers and do not penetrate the membrane [79].

Topology effect. Similarly, there is no specific topology for polymer architecture to use in drug delivery, although it is described that topology is a very important parameter to design and build a transport system. In a recent study, star-shaped polyglutamates St-P(L-Glu) were directly compared with their linear analogs P(L-Glu) with regards to cell trafficking, as well as *in vivo* biodistribution and pharmacokinetics [80]. Both topologies of polyglutamates (lineal versus stars of 3 arms) showed similar biodistribution profiles, with renal excretion and no specific accumulation in any organ. However, the star-shaped polymer displayed longer retention times, greater distribution

volume, and a 3-fold cell uptake enhancement when compared to a linear counterpart [54].

3.3.2. STRUCTURAL ELEMENTS

As mentioned, structural elements such as **API nature**, **API-carrier interaction** and **supramolecular architecture** must be taken into account to design the drug delivery system. API nature and API-carrier interaction will be discussed together in the following section.

API NATURE AND API-CARRIER INTERACTION IN PAA-BASED MATERIALS

API or drugs can display different water-solubility properties. According to these, APIs can be classified as hydrophilic (water-soluble), hydrophobic (water-insoluble), or even partially water-soluble. Depending on the nature of the API, the route of administration, and the application, the carrier is designed with different properties to successfully reach the target site of action.

API transport in drug delivery can be done through two strategies. The first is establishing a covalent bond (chemical interaction) between the carrier system and the API, thereby generating a new compound or new chemical entity (NCE) including the API in the molecular structure [81]. When this is performed with a polymer, it is considered a Polymer Therapeutic. The second strategy is based on non-covalent (physical) interactions between the vehicle and API [81]. This approach consists of the transport of the API within a supramolecular architecture based on the specific vehicle attribute without chemical bond formation. It is necessary to keep in mind that the physical interaction is solely between the API and transport system. In the case of designing a drug delivery system by means of physical interactions, usually amphiphilic polyamino acid (APAA)-based materials promoting self-assembly and capable to encapsulate the API are used. Summarizing, in the chemical interaction the API must include adequate functional groups in its structure to allow chemical conjugation with the PAA carrier yielding a NCE. And for physical interaction, the vehicle can be (or not) a NCE but the API is not included in the molecular structure of the carrier system. See Figure 1.7.

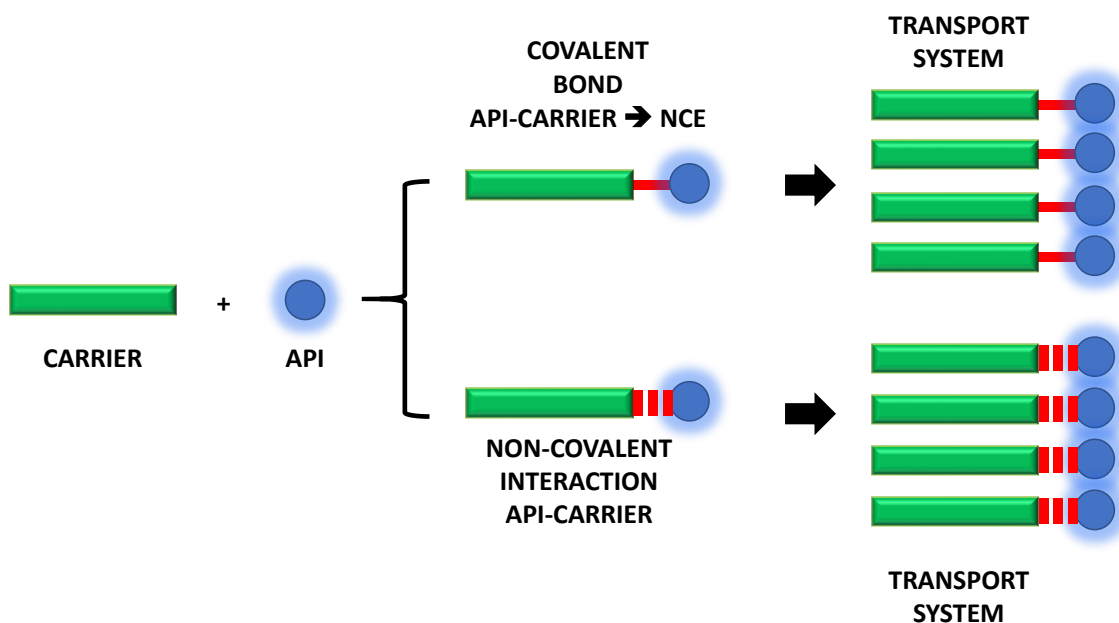


Figure 1.7. Brief schematic representation of interactions between carrier and API in the transport system.

DESIGN OF PAA-BASED THERAPEUTICS BY COVALENT BOND CONJUGATION

In 2003, Professor Ruth Duncan defined Polymer Therapeutics as a family of NCEs considered the first polymeric nanomedicines [82]. This term covers a variety of complex macromolecular systems, their common feature being the presence of a rationally-designed covalent bond between a water-soluble polymeric carrier (with or without inherent activity) and the bioactive molecule(s). Within the 40 nano-products in routine use for healthcare, Polymer Therapeutics is considered one of the most revolutionary systems with two of them within the Top 10 selling drugs [19, 63, 83].

The classical definition of Polymer Therapeutics includes five different families classified depending on the bioactive molecule: (i) **polymeric drugs**, polymers with inherent activity, (ii) **polymer-protein conjugates** bearing a covalent bond between polymer and protein, (iii) **polymer-drug conjugates** bearing a covalent bond between polymer and a small Mw drug, (iv) **polyplexes** which are multi-component systems developed as non-viral vectors, and (v) **polymeric micelles** where the bioactive agent is covalently bound to an amphiphilic polymeric carrier [19] (see Figure 1.8). Examples are shown in Table 1.X.

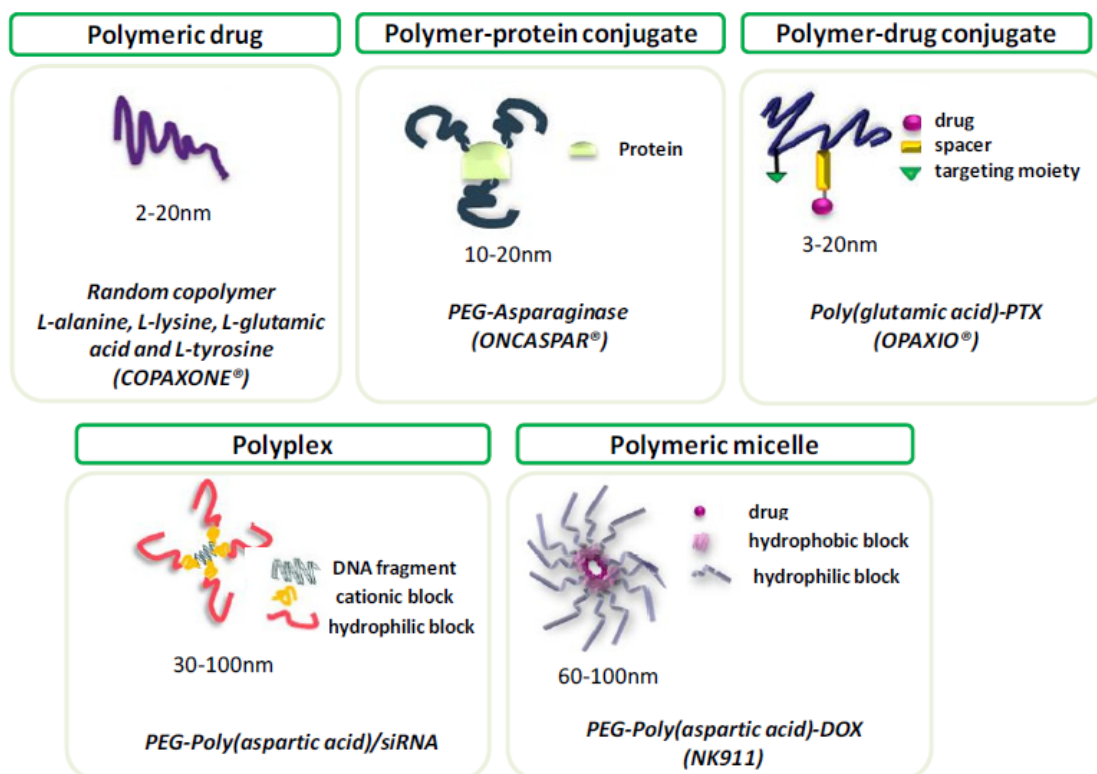


Figure 1.8. Schematic representation of polymer therapeutic families containing examples published by Duro and Conejos in 2014 [19].

Polymer-drug conjugate. In the mid-1970s, Ringsdorf proposed that polymer-drug conjugates could improve the delivery of anticancer drugs to tumors. He envisioned that when an anticancer drug is conjugated to a polymeric carrier, its pharmacological properties could be manipulated by changing the physicochemical properties of the polymer [53]. To achieve this kind of PAA platform in drug delivery, the selected aa are Asp, Glu, and Lys, because they have reactive chemical groups (carboxylic acids and amines) which can be exploited to easily form a covalent bond to the API [53]. Importantly, within this type of architecture, the non-covalent interaction PAA-API is not considered, it is performed only by chemical interaction and as such always generates a NCE.

As mentioned above, polymer-drug conjugates based on PAA materials can display self-assembling structures if the polymer and API form an amphiphile. Normally, the polymer is hydrophilic and the API hydrophobic, and the conjugate is generated to improve the API water solubility. This can be illustrated perfectly with Opaxio® (formerly known as Xyotax®), Opaxio® is a polymer-drug conjugate which uses Glu as the aa monomer to build the PAA and Paclitaxel as the hydrophobic drug or API [53]. Currently, this PAA-drug conjugate is in Phase III for the treatment of various cancers including ovarian, breast, or non-small cell lung [63]. On the other hand, it is also possible to conjugate hydrophilic molecules, such as small saccharides. In 2014, Perdih and colleagues reported the conjugation of D-(+)-Glucosamine to linear PGlu to form nanoparticles, prepared by polyelectrolyte complexation methods [84]. Examples with

PLys conjugated to small saccharides can also be found. In 2017, Herrendorff and coworkers published the use of high Mw PLys to conjugate a sulfated trisaccharide yielding an antigen-specific treatment option for anti-myelin associated glycoprotein neuropathy, a rare but disabling autoimmune disorder that affects the peripheral nervous system [85].

Polymeric Micelles. Employing amphiphilic polymers in aqueous solutions, polymeric micelles can be formed. The hydrophilic and hydrophobic blocks to form the corona and the core of the micelles, respectively [81]. Normally they have spherical geometry that can be corroborated by electronic microscopy techniques like TEM and SEM [86]. If it takes a look at the state of the art of polymeric micelles containing APAA materials, quickly it can see that the main polymer used for the hydrophilic water-soluble block is the PEG [11, 52, 87]. A very key player with these materials is Kataoka and coworkers. They have published a lot of reviews in the last decade about polymeric-based micelles as Polymer Therapeutic for several drug delivery applications [88-91]. They have reported the use of some PAA to yield block copolymers-drug conjugated like PEG-b-PLys-cyclophosphamide or PEG-b-PAsp-doxorubicin or cisplatin conjugates [11]. In this case, the interaction between API and the vehicle is through a covalent bond and the API is forming part of the carrier. Another very interesting example from Kataoka's team is the use of PEG-b-PGlu-cisplatin micelle. In 2011 this polymeric micelle started its clinical trials Phase I under the name of NC-6004 and produced by the company NanoCarrier Co. (Japan). This product is being employed to treat solid tumors [92]. Currently, this polymeric micelle is in Phase III for pancreatic cancer treatment [63].

Polyplexes. The main application for polyplexes based on PAA materials is gene therapy to treat cancer [93]. These materials are based on ionic complexation between polycations and polyanions. The main aa monomer employed to build the polycation is the Lys, due to its positive electrostatic charge in water solution at $\text{pH} < 10$, thanks to its protonated amine. Positive charges in polycations can be complexed with polyanionic materials such as proteins, DNA, and RNA among others. Residues of Arg and Orn can also be employed [93]. Not only homo-PAA are reported for this, but completely hydrophilic block copolymers containing Lys and HPMA are also described for the transport of DNA [94], as well as PEG and PLys, of course [95]. For these materials, APAA-based polyplexes also are employed. In 2017, Kataoka and colleagues published the use of micelles for gene delivery applications. The micelles were based on poly(ethylene glycol)-block-poly(L-lysine) with residual lysine chain modification with 2-iminothiolane, and were subsequently generated with crosslinking disulfides in oxidative media [96]. However, cationic aa are not the monomers of choice for the construction of polyplexes. The use of Glu modified with amine-containing moieties has been explored due to the potential toxicity of polycations. Also, Kataoka and coworkers developed a PGlu-amine polymers to form polyplexes with siRNA to induce gene silencing for cancer treatment [97]. This was illustrated by Niño-Pariente et al in 2017 when they modified the carboxylic acids of PGlu with covalent amide bonds to pentameric succinyl tetraethylene pentamines, and used this to complex DNA [98].

PAA-BASED DELIVERY SYSTEMS BY NON-COVALENT INTERACTIONS

As mentioned above, the other approach for drug delivery systems based on PAA materials is the encapsulation of APIs normally obtained with APAA-based materials [99].

This approach is based on the self-assembly capability of PAA or APAA-based materials to transport of the APIs. This fascinating area in materials science and nanochemistry is concerned with the creation of supramolecular architectures with well-defined shapes and functions. The obtention of self-assembled nanostructures can be achieved through non-covalent forces, such as van der Waals forces, electrostatic interactions, hydrogen bonding, and metal complexation. Various self-assembled morphologies with spherical, rod-like and lamellar structures have been described and offer numerous possibilities to tailor their physical, chemical and biological properties by variation of their chemical structure or by conjugation to biomolecules [100]. This is possible thanks to the amphiphilic properties of the polymers. Figure 1.9 depicts possible self-assembly structures for APAA-based materials. This fantastic illustration of amphiphiles self-assembly was published by Song and co-workers in 2014 [101].

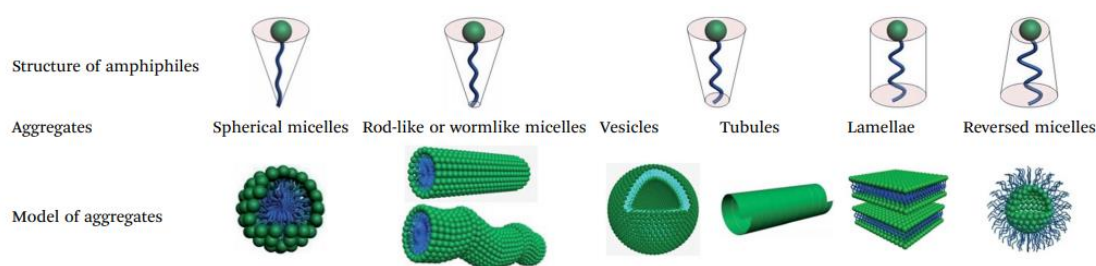


Figure 1.9. Schematic representation of the supramolecular self-assembly structures of amphiphiles published by Song and co-workers in 2014 [101].

By means of these supramolecular structures, APIs can be encapsulated and transported through biological barriers to reach the desired site of action. Of course, the design of the vehicle to encapsulate the API is specific for each API and depends intimately on the nature of the API. If the API has a hydrophobic or lipophilic nature, the PAA-based material designed to act as a carrier must also have a hydrophobic part to interact with and properly encapsulate the API for transport [81]. Examples include:

Polymeric Micelles. Regarding the API encapsulation, micelles are employed mainly for hydrophobic drugs performing their transport in the core such as doxorubicin [102]. As well as in the Polymeric Micelles described for the carrier-API covalent bond, the main polymer used for the hydrophilic water-soluble block is the PEG [11, 52, 87]. And for hydrophobic block, non-polar aa can be used, such as Phe and Leu and also polar aa like Tyr [103]. Also protected aa monomers like Asp(OBzl) and Glu(OBzl) are used to form the hydrophilic length in polymeric micelles [11]. These are the conventional diblock copolymers and the API-carrier interaction is physical. Of course, other

alternatives at PEG have been explored in the last years employing hydrophilic aa as monomers like Glu [104], Orn [105], Lys combined with poly-L-lactide and hyaluronic acid [9], and also a very interestingly peptoid called sarcosine [12, 106]. These topics will be described with more detail in the introduction of the next chapter dedicated to APAA micelles, as well as the use of non-polar aa as monomers to control the secondary structure in polymeric micelles based in APAA. Also, PEG and their alternatives are discussed.

Polymersomes. Similar to the aforementioned polymeric micelles, the most widely used hydrophilic block used in polymersomes is PEG [13]. There are two main topologies used to construct APAA-based polymersomes, graft and block copolymers [81]. In contrast to micelles, polymersomes can be loaded with hydrophobic APIs as well as hydrophilic molecules such as oligonucleotides, proteins, etc. [107, 108]. For this, the aqueous core allows the encapsulation of hydrophilic components while the hydrophobic part of the shell provides a compartment for hydrophobic drugs [109]. In 2003, a very interesting article was published in the Journal of Controlled Release where authors indicated that longer hydrophilic PEG lengths (higher PEG molar ratios) promote the formation of curved micelles rather than stable lipid membranes [110]. Such results explain why PEG-5000 liposomes show similar or even reduced circulation times compared to PEG-2000 vesicles at similar doses; although the PEG is smaller, vesicle formation is favored, and vesicles are generally larger than micelles [111-113]. Although these results are from PEG-lipid, not for PEG-PAA materials, researchers can apply this principle to design polymersomes based on APAA materials, taking into account the specific architecture and hydrophobic parts, of course..

An example developed by Brown and coworkers in 2000 was the use of PEG in graft form. They built cationic graft copolymers with lysine or ornithine backbones to form polymersomes with a covalent bonds to PEG-5000 and the hydrophobic small molecule palmitoyl, PLys-g-PEG-g-palmitoyl and POrn-g-PEG-g-palmitoyl respectively. Researchers found that these APAA-based materials showed self-assembly into polymeric vesicles in the presence of cholesterol. They used these cationic polymersomes as non-viral gene delivery systems to complex DNA, and also tested their amphiphilic properties to encapsulate doxorubicin [114].

The use of polysarcosine for the hydrophilic block to reach a liposomal architecture has also been reported. Weber et al described in 2017 the use of an amphiphilic PSar-based copolymer with 111 units and Glu(OBzl) as the hydrophobic aa monomer with 46 units, PSar111-b-PGlu(OBzl)46, obtaining polypept(o)ide-based polymersomes around 40 nm in diameter for vaccine applications. They called this technology *peptosomes* [109].

Pure APAA have also been described to build polymeric vesicle architectures. This was illustrated by Deming and coworkers in 2005 and 2007. The authors obtained vesicles through an amphiphilic block copolymer approach using Lys, Glu and Arg as aa monomers for the hydrophilic block, and Leu for the hydrophobic segment [115, 116].

Furthermore, they illustrated that the ratio between aa determines the architecture of the self-assembly in aqueous media. Through differential interference contrast microscopy images they determined the structure of the self-assemblies resulting from different DP ratios of Lys and Leu. APAA PLys20-b-PLeu20 forms a membrane sheet, PLys40-b-PLeu20 generates fibers, PLys60-b-PLeu20 yields vesicles and when the hydrophobic PLeu segment was decreased to 10 units, PLys60-b-PLeu10 forms micelles [115]. This great work indicates that the hydrophilic-hydrophobic ratio and the DP for each aa monomer are very important parameters to build the self-assembling supramolecular architectures.

Another example to describe the importance of these parameters can be found with PGlu-b-PPhe. High DPs promote vesicle formation and small DPs form nanoparticles. In 2016 Vlakh and co-workers described the use of poly(L-glutamic acid)-block-poly(L-phenylalanine) with polypeptide blocks containing up to 117 L-glutamic acid and 165 L-phenylalanine residues to obtain polymersomes [117]. This work can be compared with a small length of the same block copolymer reported by Kim et al in 2009 describing the synthesis of poly(L-glutamic acid)-b-poly(L-phenylalanine) copolymers with small DPs of just 7 for PGlu and 2 for PPhe, which resulted in nanoparticles [118].

Another interesting example using pure PAA without a hydrophobic part to form pH-responsive polymeric vesicles was reported by Lecommandoux's group in 2004. They reported the use of PLys15-b-PGlu15 (same DPs), which self-assembles under both acidic (pH < 4) and basic (pH > 10) conditions [119].

Hydrogels. According to Peppas et al “*hydrogels are three-dimensional, hydrophilic, polymeric networks capable of imbibing large amounts of water or biological fluids*” [120]. Hydrogels are a class of gelating materials and are normally highly branched, porous, and possess a similar water enveloped network to that of the extracellular matrix (ECM), which is an advantageous characteristic when considering criteria for biomaterial design [121]. Concerning PAA-based hydrogels, the water crosslinked network can be achieved through several strategies, including non-covalent interactions, covalent interactions, and stimuli-responsive interactions [122, 123].

For those based on non-covalent interactions, APAA materials are generally used. Gelation can be achieved by polyion complexation (PIC). Sun and Deming reported complex architectures of diblock co-PAA hydrogels generated via PIC between the poly[(L-methionine sulfoxide)-co-(L-alanine)]-block-poly(L-glutamate) as the anionic part, and the cationic poly[(L-methionine sulfoxide)-co-(L-alanine)]-block-poly(L-lysine). The same authors also reported the use of triblocks and pentablocks to form hydrogels via PIC [124, 125]. PLys-b-PLeu is also described as forming antimicrobial hydrogels for topical applications. Depending on the ratio between Lys and Leu and their DPs, hydrogels with alpha-helices or beta-sheets at low concentration (0.1 g/L) are prepared. This was reported by Bevilacqua and his colleagues in 2017 [65]. In this sense, PEG-b-PVal also is used to form hydrogels through physical interactions based on

secondary conformation [125]. Other systems are based on pi-pi stacking [126] or cooperative hydrogen-bonding in well known supramolecular scaffolds [127].

For chemical cross-linking, as the name indicates, the hydrogel formation is performed through a chemical reaction. An interesting example was published in 2016 by Shirbin et al. using random copolymers of PLys and PGlu. In this work, the researchers generated macroporous ($\geq 100 \mu\text{m}$) hydrogels upon cooling these zwitterionic PLys-co-PGlu copolymers to $0 \text{ }^\circ\text{C}$ and adding EDC/sulfo-NHS. These hydrogels were found to be suitable for applications in tissue engineering [128].

In terms of stimuli-response hydrogel formation, Popescu et al in 2015 demonstrated that an APAA triblock composed of PAla5-b-PGlu11-b-PAla5 can transition between an alpha-helix or beta-sheet conformation by changing the pH [129]. Furthermore, in 2016 Deming and his team once again developed a PAA block copolymer-based on poly(L-lysine)-block-poly(oNB-L-lysine) that formed hydrogels that could be degraded by Ultra Violet (UV) irradiation. This is based on the o-nitrobenzyloxycarbonyl (oNB) moiety in the Lys residues. To achieve this, they prepared the L-Lys(NCA) with an oNB protecting group [130].

Polymeric nanoparticles. The term nanoparticles envelops all nano-structures that materials can form including micelles, vesicles, polymer-drug conjugates and polyplexes. Herein, we have considered polymeric nanoparticles the structures that cannot be classified easily within those architectures. As with the others, polymeric nanoparticle architectures can be very elaborate. For example, in 2014, Shixian Lv and coworkers published pH-responsive polymeric nanoparticles achieved via complexation through electrostatic interactions between the positively charged Lys monomers and the negatively charged Glu segments, as well as hydrophobic interactions between aromatic rings of Phe, and using PEG as the hydrophilic block. The mixed nanoparticles were prepared by a mixture of anionic PEG-b-poly(L-glutamic acid-co-L-phenylalanine) and cationic PEG-b-poly(L-lysine-co-L-phenylalanine). They then used these nanoparticles to encapsulate doxorubicin via physical interaction for lung cancer therapy [131]. Apart from PEG, other non-PAA polymers have also been reported to form nanoparticles within PAA-based systems. In 2012, Lecomandoux and Heise published novel amphiphilic glycopolyptide nanoparticles containing PAA, describing them as “tree-like”. For this, they employed Glu(OBzl) as the hydrophobic monomer and hyaluronic acid and dextran for the hydrophilic block. TEM and AFM were used to study the size and morphology of the resulting nanoparticles [132].

But not only alpha-PAA can be used for nanoparticles preparation. Zhu et al. developed nanoparticles for protein delivery using a poly(γ -glutamic acid)-block-poly(lactide) graft copolymer. They controlled the self-assembly using both enantiomers (D and L) of lactide monomer [133]. Another example of the use of APAA is poly(γ -glutamic acid)-graft-poly(L-phenylalanine ethyl ester), which also gives solid 150 – 200

nm nanoparticles by self-assembly in aqueous media. They are used to encapsulate ovalbumin at a level of around 10% w/w [134].

Homo-PAA materials also are involved in other nanoparticle architectures such as nanocapsules. In 2017, Alonso's research group reported the use of PArg to prepare nanocapsules as nanocarriers with potential applications in transmucosal drug delivery. In this example, the role of the cationic PAA is to coat the nanocapsules, which contain an oil core [135]. Furthermore, atypical nanoparticles have been described. In 2017, Duro and coworkers published a novel platform based on star-shaped polyglutamates. This star-shaped topology with negative charges from Glu monomers generates the self-assembly of polymers by means of electrostatic charges, with the resulting nanoparticles reaching diameters not observed in linear polyglutamates of 30 – 100 nm not observed in linear polyglutamates [8].

SUPRAMOLECULAR ARCHITECTURES FOR PAA-BASED DRUG DELIVERY SYSTEMS

The final size, shape and deformability are features driving the biodistribution and fate of a given PAA-based drug delivery system [1].

As seen in the previous paragraph APAA-based materials show self-assembly in aqueous media into a variety of structures. The nature of these carriers depends directly on the covalent and non-covalent interactions of the self-assembling molecules [3]. Self-assembly is driven by the entropy gain associated with the dehydration of the hydrophobic moieties, and the resulting hydrophobic associations [136]. Water molecules adjacent to the hydrophobic part of the molecule are unable to hydrogen bond freely, and this generates a lower entropy state [3]. The migration of water molecules from the hydrophobic environment is favored because in the hydrophilic environment hydrogen bonding is not disrupted. When this migration occurs, the entropy increases and therefore the water molecules drive the self-assembly [137].

The organization of supramolecular architectures resulting from self-assembly of APAA-based materials can be encountered as (i) polymeric micelles [81], (ii) polymersomes forming vesicles [138], (iii) hydrogels [122, 123] and (iv) nanoparticles [139], described above. Although the polymer-API conjugates [19] and polyplexes [93] present covalent bond, they have been also included.

Figure 1.10 shows a schematic representation of PAA synthesis by ROP of NCAs, the possible composition and topology of the resulting PAA, as well as the types of PAA-based biomaterials for drug delivery.

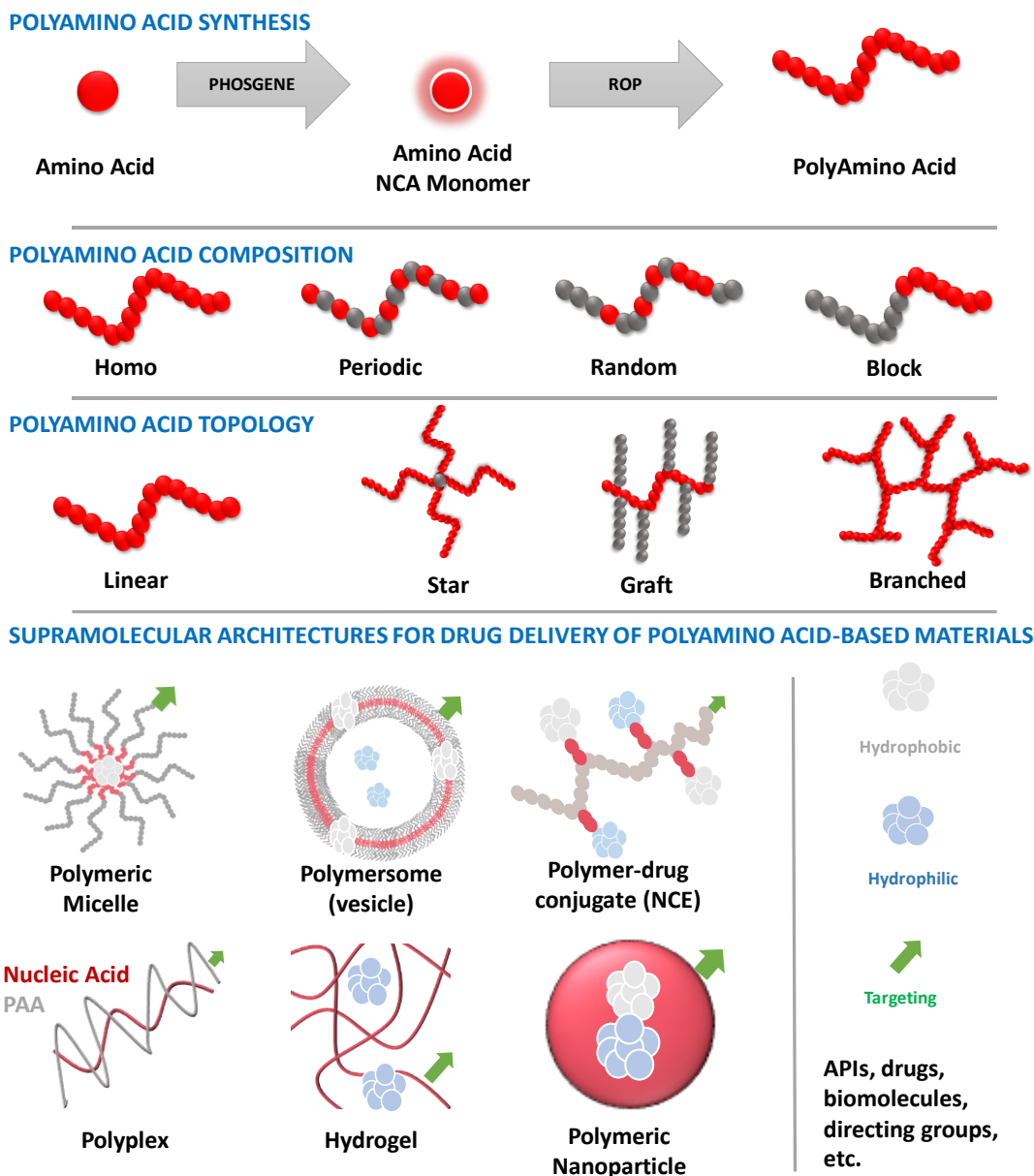


Figure 1.10. Schematic of PAA synthesis by ROP of NCAs, the PAA composition, the PAA topology and the types of supramolecular architectures for drug delivery of PAA-based materials.

For all of these reasons, the following physico-chemical parameters and structural elements must be controlled to guarantee the proper design and effective action of PAA-based materials for drug delivery in specific therapeutic application: polymer Mw; monomer nature (cationic, anionic, neutral, zwitterionic, polar, non-polar, hydrophilic, hydrophobic to promote alpha helix or beta sheet promotor); polymer composition (homo, random or block); polymer topology (linear, star, brush or graft); API nature (hydrophobic and hydrophilic); API-carrier interaction (covalent or non-covalent); and supramolecular architecture (micelle, vesicle, polymer-drug conjugate, polyplex, hydrogel or nanoparticle).

In Table 1.1. several examples for PAA-based materials used in drug delivery are shown indicating their related attributes explained in this section built as a summary of the current state of the art of PAA-based materials in drug delivery.

The vast majority are in the early stages of development, but there are some examples in preclinical and clinical trials, as well as on the market (highlighted in green). As shown below, these compounds are most commonly employed for applications in cancer therapy, and Lys is the most extensively used aa monomer, followed by Glu. As can be observed, the use of PAA in skin drug delivery is poorly described, and in this thesis dissertation, Chapter 3 will focus on such application.

Table 1.1. Summary of PAA-based materials (definitions can be found in the abbreviations section).

Compound	API-Carrier Interaction	Proteinogenic Amino Acid	Other Polymer	API	Polymer Composition	Drug Delivery Based Material	Therapeutic Application	Current State	Ref.
Copaxone®	-	Glu, Lys, Ala and Tyr	-	Polymer itself	Random	Polymer	Multiple sclerosis	Marketed, Teva	[140, 141]
PLys-block-PLeu	-	Lys and Leu	-	Polymer itself	Block	Hydrogel	Antimicrobial	Preclinical	[65, 142]
PLys and PGlu	-	Glu and Lys	-	Polymer itself	Homo	PIC Hydrogel	Skin wound healing	Early Stage	[68]
VivaGel®	Covalent	Lys	-	Naphthalene disulfonic acid	Dendrimer	Polymer Drug Conjugate	Sexually transmitted infections	Marketed, Starpharma	[143, 144]
Opaxio®	Covalent	Glu	-	Paclitaxel	Homo	Polymer Drug Conjugate	Ovarian cancer, non-small cell lung cancer, breast cancer	Phase III	[63, 145]
NC-6300, K-912	Covalent	Asp	PEG	Epirubicin	Block	Micellar Polymer Drug Conjugate	Advanced or recurrent solid tumor	Phase I/II	[146]
DEP® DOCETAXEL	Covalent	Lys	PEG	Docetaxel	Dendrimer	Polymer Drug Conjugate	Breast, lung, and prostate cancer	Phase II	[147]
DEP® CABAZITAXEL	Covalent	Lys	PEG	Cabazitaxel	Dendrimer	Polymer Drug Conjugate	Colon and pancreatic cancer	Phase II	[147]
DEP® IRINOTECAN	Covalent	Lys	PEG	Irinotecan	Dendrimer	Polymer Drug Conjugate	Colon and pancreatic cancer	Phase I/II	[147]
DEP® AZD0466	Covalent	Lys	PEG	AZD0466	Dendrimer	Polymer Drug Conjugate	Solid and hematological tumors	Phase I	[147]
PLys-DOTA-Gd	Covalent	Lys	-	DOTA-Gd	Dendrimer	Polymer Drug Conjugate	MRI contrast agent	Preclinical	[148]
PLys-RGD-DTPA-Gd	Covalent	Lys	-	RGD-DTPA-Gd	Dendrimer	Polymer Drug Conjugate	MRI contrast agent	Preclinical	[149]
PGlu-DTPA-Gd	Covalent	Glu	-	DTPA-Gd	Homo	Polymer Drug Conjugate	MRI contrast agent	Preclinical	[150]
NK-911	Covalent	Asp	PEG	Doxorubicin	Block	Micellar Polymer Drug Conjugate	Metastatic pancreatic cancer	Phase II	[151]
NK-012	Covalent	Glu	PEG	SN-38 (active metabolite of irinotecan)	Block	Micellar Polymer Drug Conjugate	Refractory solid tumors and metastatic or recurrent colorectal cancer	Phase I/II	[152]

Compound	API-Carrier Interaction	Proteinogenic Amino Acid	Other Polymer	API	Polymer Composition	Drug Delivery Based Material	Therapeutic Application	Current State	Ref.
CT-2106	Covalent	Glu	-	CPT	Homo	Polymer Drug Conjugate	Refractory solid tumor malignancies	Phase I/II	[153]
PEG-PGlu-Cisplatin	Covalent	Glu	PEG	Cisplatin	Block	Micelle	Cancer	Phase II	[53, 154]
PEG-PAsp-Paclitaxel	Covalent	Asp	PEG	Paclitaxel	Block	Micelle	Cancer	Phase II	[53, 155]
PLys-mimHNK1	Covalent	Lys	PEG	HNK-1 trisaccharide epitope	Homo	Polymer Drug Conjugate	Anti-MAG neuropathy	Early Stage	[85]
PGlu-FLUO	Covalent	Glu	-	Fluocinolone acetonide	Homo	Micellar Polymer Drug Conjugate	Psoriasis	Early Stage	[66]
PLys-block-PTyr	Non-Covalent	Lys and Tyr	-	Fluorouracil and doxorubicin	Block	Polymersome	Cancer	Early Stage	[156]
PLys-block-PGlu(OBzl)-block-PLys	Non-Covalent	Glu and Lys	-	Plasmid DNA	Block	Polymersome	Gen delivery	Early Stage	[157]
PTMC-block-PGlu	Non-Covalent	Glu	PTMC	Doxorubicin	Block	Polymersome	Cancer	Early Stage	[158]
PArg-block-PLeu	Non-Covalent	Arg and Leu	-	Texas-Red-labeled dextran	Block	Polymersome	Cell-penetrating	Early Stage	[116]
PLys-block-PGly	Non-Covalent	Lys and Gly	-	Nile red	Block	Polymersome	Imaging	Early Stage	[159]
PAsp-block-PPhe	Non-Covalent	Asp and Phe	-	4-amino-2-trifluoromethyl-phenyl retinate	Block	Micelle	Gastric cancer	Early Stage	[160]
PEG-block-PGlu-block-PPhe	Non-Covalent	Glu and Phe	PEG	Paclitaxel and Cisplatin	Block	Micelle	Ovarian cancer	Early Stage	[161]
PEG-blockP-Lys-block-PLeu	Non-Covalent	Lys and Leu	PEG	OVA antigens	Block	Micelle	Vaccine-induced immune	Early Stage	[162]
RadProtect®	Non-Covalent	Glu	PEG	Amifostine (with FeCl ₂)	Block	Micellar Polyplex	Acute radiation syndrome	Phase I	[163]
PEG-block-PPhe-block-PGlu and PEG-block-PPhe-block-PLys	Non-Covalent	Glu, Lys and Phe	PEG	Doxorubicin	Block	Nanoparticle	Cancer	Early Stage	[131]

Compound	API-Carrier Interaction	Proteinogenic Amino Acid	Other Polymer	API	Polymer Composition	Drug Delivery Based Material	Therapeutic Application	Current State	Ref.
Cys-PLys30-PEG10*CFTR	Non-Covalent	Lys and Cys	PEG	CFTR expression plasmid pKCPIRCFTRBGH	Block	Polyplex	Cystic fibrosis	Phase I	[164]
POrn-block-Pphe	Non-Covalent	Phe	POrn	siRNA	Block	Polyplex	Gen delivery	Early Stage	[105]
PLys - Cell Penetrating Peptides	Non-Covalent	Lys	-	DNA/siRNA	Dendrimer	Polyplex	Gen delivery	Early Stage	[165]
PLys dendrimers	Non-Covalent	Lys	-	DNA/siRNA	Dendrimer	Polyplex	Gen delivery	Early Stage	[166]
P(Lys-co-His) dendrimers-DNA	Non-Covalent	Lys and His	-	DNA	Dendrimer	Polyplex	Gen delivery	Preclinical	[166]
PSar-block-PGlu(OBzl)	Non-Covalent	Glu	PSar	Antigen and adjuvant	Block	Polymersome	Vaccine	Early Stage	[109]
P(Lys-co-Phe)	Non-Covalent	Lys and Phe	-	DNA/siRNA	Random	Polyplex	Gen delivery	Early Stage	[167]
PGlu(OBzl)-block-HA (Dox)	Non-Covalent	Glu	HA	Doxorubicin	Block	Polymersome	Cancer	Early Stage	[167]
PLys with HIV tat protein sequences	Non-Covalent	Lys	-	DNA/siRNA	Block	Nanoparticle	Gen delivery	Early Stage	[168]

4. INDUSTRIALIZATION OF POLYAMINO ACIDS: FROM R&D BENCH TO GMP AND COMMERCIAL PHASES

4.1. BRIEF INTRODUCTION TO DRUG PRODUCT PROCESS DEVELOPMENT

Globally, the process of taking a newly discovered API, developing it in the lab within an R&D environment, and incorporating it into a medicine or final drug product that is commercially available on the market takes many years and requires an intensive investment. Importantly, the API or drug substance is the active molecule in the drug product. This process, encompassing all the activities that researchers, companies, and agencies carry out to finally achieve the commercialization of a drug product is described as the *drug development process* [169]. In this pathway of drug development process, the desired goals are: (i) having a robust manufacturing process that is reproducible and scalable, (ii) having the appropriate tools to perform the appropriate physico-chemical characterization and (iii) executing all the documentation packages for regulatory agencies. These documents are called Common Technical Documents (CTD). Depending on the country, there are different agencies, such as the Food and Drugs Administration (FDA), European Medicines Agency (EMA) or Pharmaceuticals and Medical Devices Agency (PMDA) from the USA, the European Union and Japan respectively. As can be imagined, the execution of the drug development process is very complex. Fortunately, several harmonized guidelines exist with excellent and precise information to guarantee that the scientists and manufacturers successfully achieve a robust, reproducible and scalable manufacturing process inside the Good Manufacturing Practices (GMP) environment. These guidelines are set by the ICH (International Council for Harmonization), and also secure the lifecycle of the product and the traceability of the manufacturing batches.

A general summary of this road for the drug development process can be found in Figure 1.11. There is no standardized life cycle for the process, although the FDA website [169] describes the drug development process in five steps: (i) discovery and development, (ii) preclinical research, (iii) clinical research, (iv) FDA review, and (v) FDA post-marketing safety monitoring.

These steps are outlined in Figure 1.11. In this figure, the process starts with an **idea and rational design** defining the critical quality attributes (CQA) for the API applied in a specific therapeutic area. Then, an **R&D feasibility study**, also called Proof of Concept (POC) or bench stage is carried out to develop several candidates. In terms of PAA-based materials, this stage is when researchers design the attributes for the drug delivery system. This is reached applying all the scientific knowledge previously described, including *polymerization techniques*, rational design of the PAA taking into account the *physico-chemical parameters* such as **size** (small or large), **electrostatic charge** (positive, negative, neutral or zwitterionic), **conformation** (alpha-helix, beta-sheet, random coil, etc.), **geometry** (sphere, nanotube, etc.), **topology** (linear, star, graft

or branched) and **monomer composition** (homo, random, or block). The aforementioned **structural elements** should also be taken into account: the **API nature** (hydrophilic or hydrophobic), the **API-carrier interaction** [covalent or non-covalent] and the **supramolecular architecture of drug delivery system** (micelle, vesicle, polymer-drug conjugate, polyplex, hydrogel or nanoparticle). Then, *in vitro* studies are carried out and synthetic processes at the scale of a few grams, as well as developing and challenging the appropriate physico-chemical characterization techniques to control the basic CQA.

Next are the **pre-clinical studies**, which include animal studies and evaluations of drug production and purity. Animal studies explore: (i) the API safety in doses equivalent to approximate future human trials, (ii) pharmacodynamics (mechanisms of action, and the relation between drug levels and clinical response), and (iii) pharmacokinetics (drug absorption, distribution, metabolism, excretion, and potential drug-drug interactions) [170]. These studies are commonly called Good Laboratory Practice Toxicological (GLP TOX) studies. This data must be submitted for Investigational New Drug (IND) approval if the API is to be further studied in human subjects. Herein, pre-IND and IND documents are submitted to the FDA (in other countries there are similar documents) [171]. Those documents include the Chemistry, Manufacturing and Control (CMC) activities. At this stage, the manufacturing process should be developed to a relevant scale optimizing the critical process parameters (CPP) to control the CQA of the APIs.

Moreover, the analytical techniques to characterize the API need to be developed accordingly to guarantee an appropriate control strategy, including controls of raw materials, in-process controls to monitor the process performance, and release methods that allow a refined control on analytical parameters that determine the CQAs and the Pharmaceutical Quality Assessment System (PQAS). The methods do not need to be validated at this stage [172, 173], but given the importance and expenses involved in carrying out GLP TOX studies and submitting the IND, it is usually recommended that analytical methods are developed to minimum compliance (SOPs within qualified labs, challenged for accuracy, precision, reproducibility, etc.) to ensure that they are appropriate and can be validated under ICH in future stages. Overall, this makes it possible to secure the CQAs of the products to be administered in humans. Usually, for IND filing, GMP batches are required to prove that the process has been appropriately developed and allows the sponsors of the therapy to secure the supply chain for the imminent human trials.

CMC activities mainly involve the development, optimization and performance of the manufacturing process with high yields, analytical methodologies, and quality management systems. The CMC quality management systems include GMP, quality grade definition, production, facilities, equipment, laboratory controls, materials, packaging and labeling [174]. Moreover, the quality system of CMC activities also contains the deviation identification, investigation, and risk management of the manufacturing process. The analytical methodologies qualification and validation and

also the CMC documentation and data integrity management are also part of the CMC tasks [174-176]. Usually, these CMC activities are performed by Contract Manufacturing Organization (CMO) companies, which are entities specialized in these activities providing to other companies services from new drug development through drug manufacturing following the ICH guidelines.

Clinical trials are then carried out in 4 phases; although the vast majority of databases define the clinical trials in 3 phases (I, II and III), Phase 0 is also important [177]. At this stage, the API, as well as the drug product, must be manufactured under GMP compliance at Kg scale. Before the commercial stage, the GMP manufacturing process for drug substances and drug products must be validated with at least 3 batches including the concomitant stability study [169].

Phase 0. The FDA, in combination with industry experts and academia, identifies many factors responsible for the failure of new APIs. A preliminary phase is performed utilizing much lower drug doses, provide an opportunity to explore the clinical behavior of new APIs very early in the drug development process. This helps to identify the promising candidates and eliminate the less promising ones, thus improving the efficiency of the overall drug development process with significant savings of resources [177].

Phase I. Researchers test a new API or treatment in a small group of people for the first time to evaluate its safety, determine a safe dosage range, and identify side effects [178].

Phase II. The API or treatment is given to a larger group of people to see if it is effective and to further evaluate its safety [178].

Phase III: The API or treatment is given to large groups of people to confirm its effectiveness, monitor side effects, compare it to commonly used treatments, and collect information that will allow the drug or treatment to be used safely [178].

After that, the regulatory agencies approve the drug product system and it can be **commercialized**. During the commercialization, **Phase IV** is performed. In this phase, the studies are carried out after the drug or treatment has been marketed to gather information on the drug's effect in various populations and any side effects associated with long-term use [178].

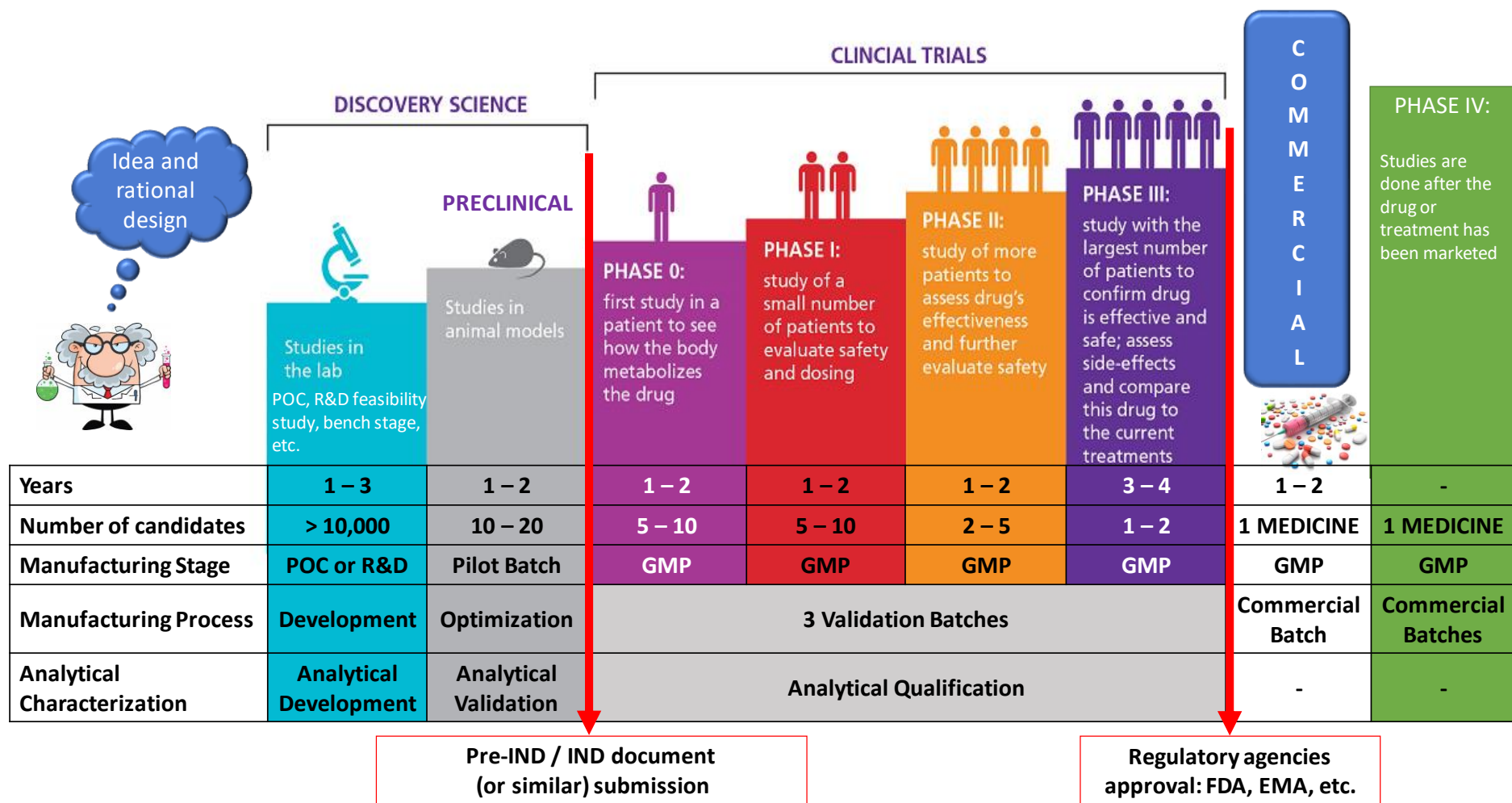


Figure 1.11. Scheme of the drug development process including the timeline, development stages, number of API candidates, manufacturing stage and process and analytics, as well as the regulatory agencies actions. Figure adapted from several websites [179-181].

4.2. LESSONS LEARNED FROM PAA-BASED MARKETED DRUGS

The Copaxone® is a commercial drug product in which the API is a Polymer Therapeutic [19], namely glatiramer acetate. This active ingredient is a random co-PAA composed of 4 aa monomers: (i) L-glutamic acid, (ii) L-alanine, (iii) L-tyrosine, and (iv) L-lysine. These monomers are present in an average molar fraction of 0.14, 0.43, 0.09, and 0.34, respectively, containing the acetate salt. The average molecular weight of glatiramer acetate is 4,7 –11 kDa [1]. This random co-PAA material was declared a NCE and it was classified as a polymeric drug in Polymer Therapeutics since the random co-PAA itself is the drug substance or API [19]. It was developed by Teva Pharmaceutical Industries Ltd. to treat multiple sclerosis [182]. In 1996, the FDA approved it in USA [140]. Since then, several generics have been also approved [140, 183].

PGlu-paclitaxel (PGlu-PTX, also known as CT-2103, PPX, or Opaxio™ produced by Cell Therapeutics Inc.) represents one of the few PAA-drug conjugates that has achieved the phase III clinical trials [63]. The drug conjugation bond is driving through an ester bond exhibiting a high drug loading capacity and high stability in blood. Unfortunately, the clinical development of PGlu-PTX was halted in 2016 due to a lack of significant improvement compared to the current standard of care [184]. Many of the lessons learned from the preclinical and clinical studies of Opaxio® can and must be applied to the development of more efficient PAA-drug conjugates. These include a more profound understanding of the mechanisms of action, the requirement for patient stratification in clinical trials, the optimized design from the bench to the clinics, and the need for effective academic-industry partnerships during the API and drug product development [63]

With these examples, both Teva Pharmaceutical Industries Ltd. and Cell Therapeutics Inc. had to implement a manufacturing process for both Polymer Therapeutics and, as mentioned previously, the PAA in question are manufactured using alpha-aa NCA monomers. Thus, from a point of view of the manufacturing process, the first question could be, who can produce the necessary monomers at large scale? As stated earlier, the NCA is a key raw material in the manufacturing process of PAA via ROP. Additionally, a critical point in PAA production is to have a good CMO which can guarantee the purity and reproducibility of NCA monomers. The next question then, could be which CMO can accurately perform the ROP at a large scale followed by the deprotection step? In the case of Opaxio®, who can carry out the conjugation of paclitaxel? And of course, who is the supplier of paclitaxel?

Finding the CMOs and having access to the “*know-how*” of CMC activities is very difficult to track in public data since the Pharmaceutical industry is very hermetic and a huge effort is invested to protect intellectual property. This is their “*know-how*” and they maintain their CMC, analytics, formulation procedures, equipment, set-ups, etc. extremely secret. Nevertheless, to have products in the market or advance in clinical trial phases it is necessary to obtain approval from regulatory authorities such as the FDA or

the EMA, and these agencies follow the aforementioned ICH guidelines to ensure the manufacturers work properly.

4.3. REGULATORY: INTERNATIONAL COUNCIL FOR HARMONIZATION QUALITY GUIDELINES (ICH-Q)

The ICH, according to its website, can be described as “*The International Council for Harmonization of Technical Requirements for Pharmaceuticals for Human Use (ICH) is unique in bringing together the regulatory authorities and pharmaceutical industry to discuss scientific and technical aspects of drug registration. Since its inception in 1990, ICH has gradually evolved, to respond to the increasingly global face of drug development. ICH's mission is to achieve greater harmonization worldwide to ensure that safe, effective, and high-quality medicines are developed and registered in the most resource-efficient manner.*” These ICH guidelines are organized into 4 families: (i) Quality, (ii) Safety, (iii) Efficacy, and (iv) Multidisciplinary [185].

From the point of view of PAA industrialization and manufacturing process development, the most important guideline type is the Quality Guidelines, called ICH-Q. They are based on the harmonization achievements in the Quality area, and include pivotal milestones such as the conduct of stability studies, defining relevant thresholds for impurities testing, and a more flexible approach to pharmaceutical quality based on GMP risk management [185]. There are 14 topics in ICH-Q containing 55 guidelines which are shown in the next Table.

It's clear to see that all the important topics are covered in these guidelines, such as stability and analytical validation, impurities, pharmacopeia regulation, quality risk, GMP, pharmaceutical development, development and manufacture drug substance, etc. Full compliance for the companies of these guidelines secures approbation from regulatory authorities.

Focusing on PAA-based materials, depending on the application, the applicable guidelines differ. For example, if the PAA of interest is to perform the encapsulation of the API (non-covalent interaction between PAA and the API), the PAA can be considered an excipient, and their manufacturing process is not considered “critical” and it would be arguable the need to manufacture under GMP compliance. However, if we are talking about a covalent bond between the PAA and the API resulting in a NCE, or the PAA itself is the API, they are the drug substances and the regulatory pathway needs to follow strictly the quality guidelines. . Another case is if the PAA is to be used as a starting material or key intermediate to obtain the drug substance. In this case, depending on the remaining manufacturing stages, the regulation is stricter when the starting material is closer to the drug substance and as the consequence, to the drug product.

Table 1.2. List of ICH Quality guidelines.

ICH-Q Number	Main Topic	Guideline Numbers	ICH-Q Active Models and Specific Topic
1	Stability	6	Q1A(R2) Stability Testing of New Drug Substances and Products
			Q1B Stability Testing: Photostability Testing of New Drug Substances and Products
			Q1C Stability Testing for New Dosage Forms
			Q1D Bracketing and Matrixing Designs for Stability Testing of New Drug Substances and Products
			Q1E Evaluation of Stability Data
			Q1F Stability Data Package for Registration Applications in Climatic Zones III and IV
2	Analytical Validation	2	Q2(R1) Validation of Analytical Procedures: Text and Methodology
			Q2(R2)/Q14 EWG Analytical Procedure Development and Revision of Q2 (R1) Analytical Validation
3	Impurities	7	Q3A(R2) Impurities in New Drug Substances
			Q3B(R2) Impurities in New Drug Products
			Q3C(R6) Maintenance of the Guideline for Residual Solvents
			Q3C(R8) Maintenance EWG Maintenance of the Guideline for Residual Solvents
			Q3D(R1) Guideline for Elemental Impurities
			Q3D(R2) Maintenance EWG Revision of Q3D(R1) for cutaneous and transdermal products
			Q3D Implementation of Guideline for Elemental Impurities
4	Pharmacopoeias	19	Q4A Pharmacopoeia Harmonization
			Q4B Evaluation and Recommendation of Pharmacopoeia Texts for Use in the ICH Regions
			Q4B Annex 1(R1) Residue on Ignition/Sulphated Ash General Chapter
			Q4B Annex 2(R1) Test for Extractable Volume of Parenteral Preparations General Chapter
			Q4B Annex 3(R1) Test for Particulate Contamination: Sub-Visible Particles General Chapter

ICH-Q Number	Main Topic	Guideline Numbers	ICH-Q Active Models and Specific Topic
			Q4B Annex 4A(R1) Microbiological Examination of Non-Sterile Products: Microbial Enumeration Tests General Chapter Q4B Annex 4B(R1) Microbiological Examination of Non-Sterile Products: Tests for Specified Microorganism General Chapter Q4B Annex 4C(R1) Microbiological Examination of Non-Sterile Products: Acceptance Criteria for Pharmaceutical Preparations and Substances for Pharmaceutical Use General Chapter Q4B Annex 5(R1) Disintegration Test General Chapter Q4B Annex 6 Uniformity of Dosage Units General Chapter Q4B Annex 7(R2) Dissolution Test General Chapter Q4B Annex 8(R1) Sterility Test General Chapter Q4B Annex 9(R1) Tablet Friability General Chapter Q4B Annex 10(R1) Polyacrylamide Gel Electrophoresis General Chapter Q4B Annex 11 Capillary Electrophoresis General Chapter Q4B Annex 12 Analytical Sieving General Chapter Q4B Annex 13 Bulk Density and Tapped Density of Powders General Chapter Q4B Annex 14 Bacterial Endotoxins Test General Chapter Q4B FAQs Frequently Asked Question
5	Quality of Biotechnological Products	6	Q5A(R1) Viral Safety Evaluation of Biotechnology Products Derived from Cell Lines of Human or Animal Origin Q5A(R2) informal WG Viral Safety Evaluation of Biotechnology Products Derived from Cell Lines of Human or Animal Origin Q5B Analysis of the Expression Construct in Cells Used for Production of r-DNA Derived Protein Products Q5C Quality of Biotechnological Products: Stability Testing of Biotechnological/Biological Products Q5D Derivation and Characterization of Cell Substrates Used for Production of Biotechnological/Biological Products Q5E Comparability of Biotechnological/Biological Products Subject to Changes in their Manufacturing Process
6	Specifications	2	Q6A Specifications: Test Procedures and Acceptance Criteria for New Drug Substances and New Drug Products: Chemical Substances

ICH-Q Number	Main Topic	Guideline Numbers	ICH-Q Active Models and Specific Topic
			Q6B Specifications: Test Procedures and Acceptance Criteria for Biotechnological/Biological Products
7	Good Manufacturing Practice	2	Q7 Good Manufacturing Practice Guide for Active Pharmaceutical Ingredients
			Q7 Q&As Questions and Answers: Good Manufacturing Practice Guide for Active Pharmaceutical Ingredients
8	Pharmaceutical Development	2	Q8(R2) Pharmaceutical Development
			Q8/9/10 Q&As (R4) Q8/Q9/Q10 - Implementation
9	Quality Risk Management	2	Q9 Quality Risk Management
			Q8/9/10 Q&As (R4) Q8/Q9/Q10 - Implementation
10	Pharmaceutical Quality System	2	Q10 Pharmaceutical Quality System
			Q8/9/10 Q&As (R4) Q8/Q9/Q10 - Implementation
11	Development and Manufacture of Drug Substances	2	Q11 Development and Manufacture of Drug Substances (Chemical Entities and Biotechnological/Biological Entities)
			Q11 Q&As Questions & Answers: Selection and Justification of Starting Materials for the Manufacture of Drug Substance
12	Lifecycle Management	1	Q12 EWG Technical and Regulatory Considerations for Pharmaceutical Product Lifecycle Management
13	Continuous Manufacturing of Drug Substances and Drug Products	1	Q13 EWG Continuous Manufacturing of Drug Substances and Drug Products
14	Analytical Procedure Development	1	Q2(R2)/Q14 EWG Analytical Procedure Development and Revision of Q2 (R1) Analytical Validation

An example case to illustrate the interpretability and risk assessment is Copaxone®, where the glatiramer acetate random copolymer of Ala, Tyr, Glu and Lys is the API or drug substance. The NCAs of these aa are the starting materials, but they can also be considered intermediates. The aa to obtain the NCA aa monomers are also starting materials. However, thinking of the manufacturing process shown in Figure 1.12., the authorities may consider that the starting aa can be manufactured outside the GMP environment, but the subsequent synthesis of NCA aa monomers is recommended in GMP environment, since after the NCA, the glatiramer acetate is obtained which is the drug substance. Harmonized guidelines for GMP compliance of excipients are under discussion and regulatory bodies will release specific guidelines briefly. However, novel excipients that are incorporated into the drug product at the very latest stages remain highly critical components and therefore sponsors tends to request CMOs to provide full GMP compliance [186]. This can be observed in Figure 1.12.

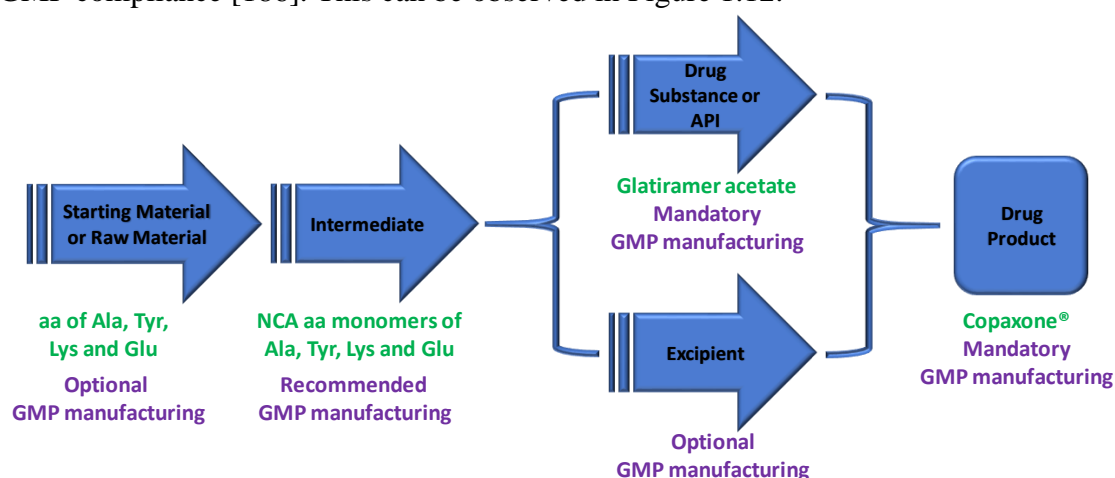


Figure 1.12. Scheme for drug product manufacturing with the example of Copaxone®.

4.4. CRITICAL ANALYTICAL METHODS TO ADDRESS QUALITY CONTROL OF PAA-BASED DRUGS

As stated, one of the desired goals in the development of drug substances and drug products, as well as excipients and starting materials, is to achieve a secure, robust, reproducible, scalable, and cost-efficient manufacturing process. To achieve the good translation of candidates “from bench to clinics” the CQAs for nanomaterials such as Mw, polydispersity, purity, identity, drug content, free drug content, and quantification of targeting units must be controlled along the manufacturing process through analytical characterization [86]. Importantly, analytics are not only used to characterize the products, but are also employed to determine the amount and identification of impurities, related degraded products, etc.

In 2015, Robert Luxenhofer, an important author in polymer chemistry specialized in the use of polypeptoids and poly(2-oxazoline)s, published an excellent article entitled *Polymers and nanomedicine: considerations on variability and reproducibility when combining complex systems*. In this article, Luxenhofer explains the importance of the statistical data in the reproducibility and batch to batch consistency in the manufacturing

process for polymers, and also for the analytical characterization techniques. Briefly, he explains that polymer synthesis should also be considered with systematic variability analysis, in particular in connection with downstream processes such as biological assays [187].

In the same article, Luxenhofer states that the reproducibility of scientific results is the fundamental basis of scientific methodology, and proposed two main questions: (i) what does the reproducibility results mean in the context of polymer science? and (ii) what should be reproduced, and how? [187]. Problems with batch-to-batch reproducibility (variation between different syntheses) and performance consistency of polymeric nanomaterials in biological assays are not unknown. This has also been addressed by researchers of the Nanotechnology Characterization Laboratory of the USA National Cancer Institute [188, 189].

One of the essential characteristics of polymer synthesis is that the polymer chains grow via a statistical process. For one, this leads to the situation that polymers underlie frequency distributions concerning their degree of polymerization (DP). A numerical value to describe the frequency distribution is the dispersity (\mathfrak{D}), formerly also polydispersity index (PDI) [52]. The PDI may be one of the most important defining properties of polymers, and it is obtained by dividing the weight-average molar mass (M_w) and the number-average molar mass (M_n) ($PDI = M_w/M_n$) [190]. For an ideal Poisson distribution, the dispersity can be approximated by $PDI = 1 + 1/DP$. In real life, we often consider that values of $PDI < 1.2$ or 1.3 represent well-defined polymers [187].

In 2011, four key players in polymer chemistry published an excellent review focused on overcoming the PEG addiction in drug delivery systems. Although this topic will be addressed in the Chapter II, the authors hold an interesting discussion over the PDI of the water-soluble HPMA polymer. They explain the importance of using PHPMA polymers with narrow M_w distributions focused on a PHPMA of 40 kDa theoretically. If the polymer shows a \mathfrak{D} of 1.04 to 1.20, this means that the majority of the population of the chain is between 35 – 40 kDa, but if the dispersity is 1.5, the major population is 20 – 60 kDa [52]. This is illustrated in the next figure adapted from the same review.

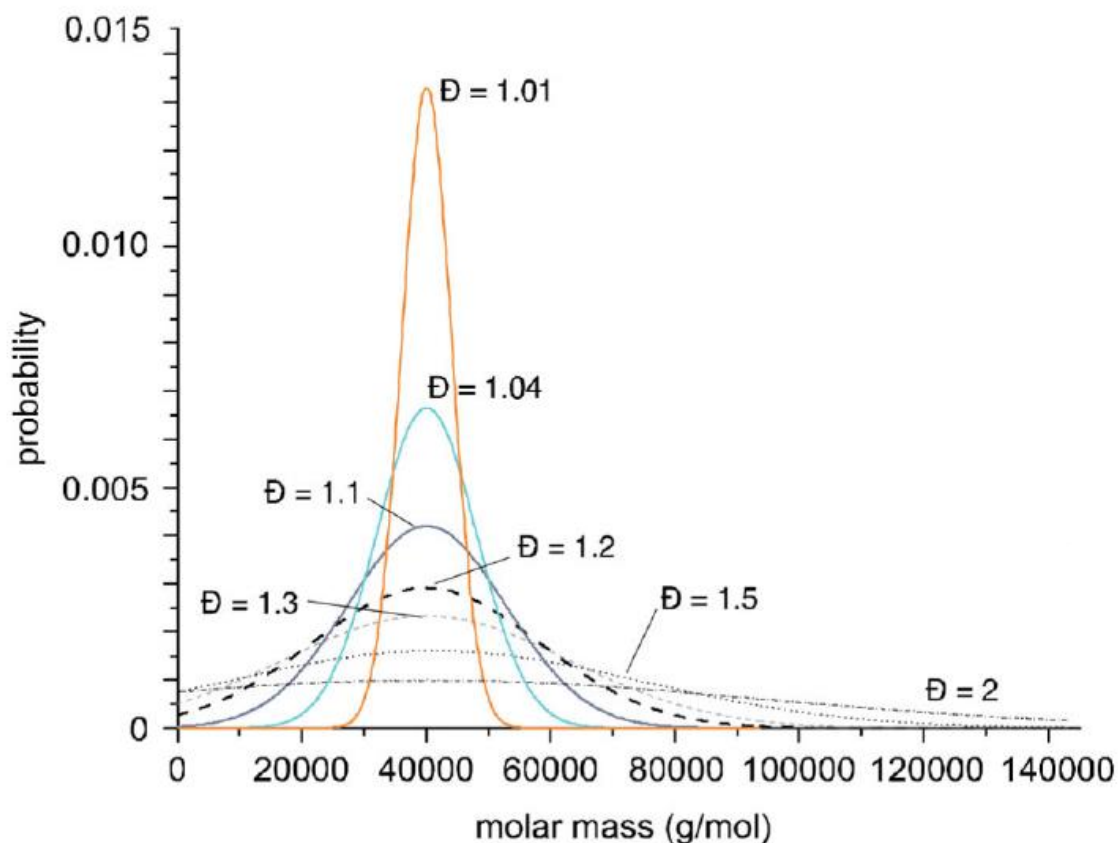


Figure 1.13. Representation of theoretical Gaussian distributions of PHPMA with a degree of polymerization of 300 ($M_w = 40$ kDa) with a variation in the dispersity from 1.01, 1.04, 1.1, 1.2, 1.5 to 2 [191].

SEC is the main technique used to obtain molecular weights (M_w or M_n) distributions and PDI. SEC techniques are fully developed and widely described to analyze plastic polymers, as well as being the main technique employed in the characterization of nanomedicines such as proteins, PEG, PEI or PLGA among others [192]. For these materials, columns, mobile phases, analytical methodologies and SEC methodologies are fully studied and developed. Furthermore, there is a vast variety of standards in the market available from different suppliers to perform column calibrations by SEC employing a Refraction Index (RI) or UV detector and the retention time. This allows the determination of M_w distributions of samples of the same material as the standards, simply by building a calibration curve with commercial standards of different M_w s and interpolating the retention time of the sample to determine the M_w [193]. Importantly, to make the calibration curve, the M_w employed is M_p , which is the molecular weight in the maximum of the peak and the M_w obtained is relative, not absolute. This kind of calibration is called Conventional Calibration.

However, PAA have only recently started their journey into the field of nanomedicine and the analytical techniques to analyze them are not fully developed. This fact, added to the low availability of standards with the same nature in the market, make M_w determination by SEC somewhat difficult. The main companies specialized in SEC

techniques are pioneers in Mw determination such as Malvern, Polymer Standard Solutions, Wyatt or Agilent among others, and offer their customers calibration curves of PEGs or PEIs to determine the Mw of PAA such as poly-L-glutamates, poly-L-lysines, poly-L-aspartics, etc., although this leads to an incorrect relative Mw. This is because if the standards are not of the same nature as the analyte, the interaction with the stationary phase in the SEC column will not be the same and the retention times will not be comparable. However, many researchers make this mistake.

In contrast, to the relative determination of Mw of polymers by column calibration, the use of Light Scattering (LS) detector, also called Multi Angle Laser Light Scattering (MALLS), offers the possibility to calculate the absolute value of Mw or Mn base on the relationship between the intensity of LS by a molecule and its molecular weight and size. These relationships are described by Rayleigh theory which states that the molecular weight of a molecule is proportional to the Rayleigh ratio of scattered [194]. The LS detector is composed mainly of a LASER and it is very sensitive to changes in the chromatographic system such as solvents, salts, temperature, or columns [195, 196].

For polymers small enough (less than 200 kDa approximately), P_{θ} (shape factor) equals to 1 and A_2 closes to 0. Thus, the Rayleigh equation is simplified, and the average molecular weight is dependent on the scattered light (area of light scattered under the polymer chromatographic peak), the concentration of the sample, and the dn/dc parameter which is the RI increment of the sample [197]. To determine the dn/dc , the RI area of the polymer peak is plotted versus the theoretical injected mass. Once the dn/dc value is known, it can be applied to calculate the concentration of the polymer, allowing to determine the polymer concentration in different media such as drug formulation. On the other hand, the PDI is determined by a complex algorithm based on the agreement between RI and LS elution profiles.

Luxenhofer closes his article with this excellent conclusion which fits perfectly into this thesis dissertation: *Polymer sciences and nanotechnology are fundamental building blocks of nanomedicine. Both typically suffer from synthetic variability and difficulties in reproducibility and scale-up. Although it cannot be and will never become the responsibility of academia to scale-up synthetic procedures and manufacturing, reproducibility lies at the core of academia. Since synthesis lies the foundation for any downstream processing and assays, we must take reproducibility and variability of polymer and nanomaterial synthesis more into account into the future. Such change will only be possible, if the community as a whole and/or the funding agencies require such change. I have outlined a simple and affordable strategy to do such, which could be easily implemented immediately. While such immediate implementation is probably unrealistic, I hope to at least induce a discussion on this important issue* [187].

The regulatory for analytical characterization techniques, the ICH Q2(R1) harmonized guideline “*Validation Of Analytical Procedures: Text And Methodology*” provides analytical researchers with an excellent guide to perform the analytical

development. This guideline explains that the objective of validation of an analytical procedure is to demonstrate that it is suitable for its intended purpose. The discussion of the validation of analytical procedures is directed to the four most common types of analytical procedures: (i) identification tests, (ii) quantitative tests to determine the content of impurities, (iii) limit tests for the control of impurities, and (iv) quantitative tests of the active moiety in samples of a drug substance or drug product, or other selected component(s) in the drug product. Furthermore, in the validation of the analytical technique the following parameters must be studied: (i) specificity, (ii) linearity, (iii) relative response factor of analyte or attribute, (iv) accuracy, (v) precision, (vi) sample stability, (vii) robustness, (viii) limit of quantification, (ix) limit of detection and (x) system suitability.

5. ADDRESSING CMC APPROACH FOR PAA-BASED MATERIALS

The PAA-based materials can be designed, modulated, and manufactured in order to drive solutions to treat diseases and to be employed in the preparation of drug products as starting materials, key intermediates, excipients, or even drug substances. Depending on their role in the drug product, the PAA-based materials can be developed and obtained in GMP compliance following the ICH Quality guidelines compliant with the specifications, parameters, and requirements of the regulatory agencies.

Our approach to address the CMC activities to develop a PAA-based material to be employed in a drug product is based on: (i) developing a manufacturing process robust, reproducible and scalable, (ii) developing the characterization techniques to analyze properly the defined CQA and (iii) being able to perform these activities within the quality assurance system complying with the GMP and ICH guidelines.

The main goal of a manufacturer in the drug product process development must be to execute the CMC activities properly to be able to generate the documental package that will be part of the dossier submitted to the regulatory agencies to obtain the authorization for the use of the drug product in humans for clinical trials and the market.

In the present thesis dissertation, we design a suitable strategy to address this challenge and bring disruptive novel therapies to have an impact on society. The main contribution of this work to the current state of the art of the PAA-based therapeutics is related to the optimization and development for (i) manufacturing process, (ii) analytical methodologies, (iii) design space, and (iv) submission of results to regulatory agencies under GMP standards that are addressed for poly-L-lysine.

6. REFERENCES

- [1] M. Khuphe, P.D. Thornton, Poly(amino acids), in: A. Parambath (Ed.), *Engineering of Biomaterials for Drug Delivery Systems: Beyond Polyethylene Glycol*, Woodhead Publ Ltd, Cambridge, 2018, pp. 199-228.
- [2] J. Huang, A. Heise, Stimuli responsive synthetic polypeptides derived from N-carboxyanhydride (NCA) polymerisation, *Chemical Society Reviews* 42(17) (2013) 7373-7390.

- [3] A. Lalatsa, A.G. Schatzlein, M. Mazza, B.H.L. Thi, I.F. Uchegbu, Amphiphilic poly(l-amino acids) - New materials for drug delivery, *Journal of Controlled Release* 161(2) (2012) 523-536.
- [4] <https://onlinesciencenotes.com/>.
- [5] D. Huesmann, K. Klinker, M. Barz, Orthogonally reactive amino acids and end groups in NCA polymerization, *Polymer Chemistry* 8(6) (2017) 957-971.
- [6] H. Lu, J. Wang, Z.Y. Song, L.C. Yin, Y.F. Zhang, H.Y. Tang, C.L. Tu, Y. Lin, J.J. Cheng, Recent advances in amino acid N-carboxyanhydrides and synthetic polypeptides: chemistry, self-assembly and biological applications, *Chemical Communications* 50(2) (2014) 139-155.
- [7] M. Barz, A. Duro-Castano, M.J. Vicent, A versatile post-polymerization modification method for polyglutamic acid: synthesis of orthogonal reactive polyglutamates and their use in "click chemistry", *Polymer Chemistry* 4(10) (2013) 2989-2994.
- [8] A. Duro-Castano, V.J. Nebot, A. Nino-Pariente, A. Arminan, J.J. Arroyo-Crespo, A. Paul, N. Feiner-Gracia, L. Albertazzi, M.J. Vicent, Capturing "Extraordinary" Soft-Assembled Charge-Like Polypeptides as a Strategy for Nanocarrier Design, *Advanced Materials* 29(39) (2017) 12.
- [9] Y. Ohya, S. Takeda, Y. Shibata, T. Ouchi, A. Kano, T. Iwata, S. Mochizuki, Y. Taniwaki, A. Maruyama, Evaluation of polyanion-coated biodegradable polymeric micelles as drug delivery vehicles, *Journal of Controlled Release* 155(1) (2011) 104-110.
- [10] C.G. Zhang, R.L. Zhang, Y. Zhu, W. Wei, Y. Gu, X.Y. Liu, Polymer vesicles prepared from the (L-phenylalanine ethyl ester)-modified hyaluronic acid, *Materials Letters* 164 (2016) 15-18.
- [11] G.S. Kwon, K. Kataoka, Block copolymer micelles as long-circulating drug vehicles, *Advanced Drug Delivery Reviews* 64 (2012) 237-245.
- [12] A. Birke, J. Ling, M. Barz, Polysarcosine-containing copolymers: Synthesis, characterization, self-assembly, and applications, *Progress in Polymer Science* 81 (2018) 163-208.
- [13] A. Carlsen, S. Lecommandoux, Self-assembly of polypeptide-based block copolymer amphiphiles, *Current Opinion in Colloid & Interface Science* 14(5) (2009) 329-339.
- [14] L.I.F. Moura, A. Malfanti, C. Peres, A.I. Matos, E. Guegain, V. Sainz, M. Zloh, M.J. Vicent, H.F. Florindo, Functionalized branched polymers: promising immunomodulatory tools for the treatment of cancer and immune disorders, *Materials Horizons* 6(10) (2019) 1956-1973.
- [15] A.R. Mazo, S. Allison-Logan, F. Karimi, N.J.A. Chan, W.L. Qiu, W. Duan, N.M. O'Brien-Simpson, G.G. Qiao, Ring opening polymerization of alpha-amino acids: advances in synthesis, architecture and applications of polypeptides and their hybrids, *Chemical Society Reviews* 49(14) (2020) 4737-4834.
- [16] M. Khuphe, B. Mukonoweshuro, A. Kazlauciuonas, P.D. Thornton, A vegetable oil-based organogel for use in pH-mediated drug delivery, *Soft Matter* 11(47) (2015) 9160-9167.
- [17] Y. Shen, X.H. Fu, W.X. Fu, Z.B. Li, Biodegradable stimuli-responsive polypeptide materials prepared by ring opening polymerization, *Chemical Society Reviews* 44(3) (2015) 612-622.
- [18] K. Wang, G.F. Luo, Y. Liu, C. Li, S.X. Cheng, R.X. Zhuo, X.Z. Zhang, Redox-sensitive shell cross-linked PEG-polypeptide hybrid micelles for controlled drug release, *Polymer Chemistry* 3(4) (2012) 1084-1090.
- [19] A. Duro-Castano, I. Conejos-Sanchez, M.J. Vicent, Peptide-Based Polymer Therapeutics, *Polymers* 6(2) (2014) 515-551.
- [20] H. Leuchs, Glycine-carbonic acid, *Berichte Der Deutschen Chemischen Gesellschaft* 39 (1906) 857-861.
- [21] J.J. Cheng, T.J. Deming, Synthesis of Polypeptides by Ring-Opening Polymerization of alpha-Amino Acid N-Carboxyanhydrides, *Peptide-Based Materials* 310 (2012) 1-26.
- [22] H.R. Kricheldorf, Polypeptides and 100 years of chemistry of alpha-amino acid N-carboxyanhydrides, *Angewandte Chemie-International Edition* 45(35) (2006) 5752-5784.
- [23] N. Hadjichristidis, H. Iatrou, M. Pitsikalis, G. Sakellariou, Synthesis of Well-Defined Polypeptide-Based Materials via the Ring-Opening Polymerization of alpha-Amino Acid N-Carboxyanhydrides, *Chemical Reviews* 109(11) (2009) 5528-5578.
- [24] T.J. Deming, Synthesis and Self-Assembly of Well-Defined Block Copolypeptides via Controlled NCA Polymerization, *Hierarchical Macromolecular Structures: 60 Years after the Staudinger Nobel Prize* 11 262 (2013) 1-37.

- [25] T.J. Deming, Facile synthesis of block copolypeptides of defined architecture, *Nature* 390(6658) (1997) 386-389.
- [26] O. Schafer, K. Klinker, L. Braun, D. Huesmann, J. Schultze, K. Koynov, M. Barz, Combining Orthogonal Reactive Groups in Block Copolymers for Functional Nanoparticle Synthesis in a Single Step, *ACS Macro Letters* 6(10) (2017) 1140-1145.
- [27] S.G. Waley, J. Watson, THE KINETICS OF THE POLYMERIZATION OF SARCOSINE CARBONIC ANHYDRIDE, *Proceedings of the Royal Society of London Series a-Mathematical and Physical Sciences* 199(1059) (1949) 499-517.
- [28] E. Peggion, M. Terbojevich, A. Cosani, Colombin.C, MECHANISM OF N-CARBOXYANHYDRIDE (NCA) POLYMERIZATION IN DIOXANE . INITIATION BY CARBON-14-LABELED AMINES, *Journal of the American Chemical Society* 88(15) (1966) 3630-+.
- [29] M. Goodman, J. Hutchison, MECHANISMS OF POLYMERIZATION OF N-UNSUBSTITUTED N-CARBOXYANHYDRIDES, *Journal of the American Chemical Society* 88(15) (1966) 3627-&.
- [30] G.J.M. Habraken, A. Heise, P.D. Thornton, Block Copolypeptides Prepared by N-Carboxyanhydride Ring-Opening Polymerization, *Macromolecular Rapid Communications* 33(4) (2012) 272-286.
- [31] D.G.H. Ballard, C.H. Bamford, REACTIONS OF N-CARBOXY-ALPHA-AMINO-ACID ANHYDRIDES CATALYSED BY TERTIARY BASES, *Journal of the Chemical Society (FEB)* (1956) 381-387.
- [32] E. Peggion, A. Cosani, A.M. Mattucci, E. Scoffone, POLYMERIZATION OF GAMMA-ETHYL-L-GLUTAMATE-N-CARBOXYANHYDRIDE INITIATED BY DI-N-BUTYL AND DI-ISOPROPYL AMINE, *Biopolymers* 2(1) (1964) 69-78.
- [33] D.G.H. Ballard, C.H. Bamford, THE POLYMERIZATION OF ALPHA-BENZYL-L-GLUTAMATE N-CARBOXY ANHYDRIDE, *Journal of the American Chemical Society* 79(9) (1957) 2336-2338.
- [34] P.D. Bartlett, D.C. Dittmer, A KINETIC STUDY OF THE LEUCHS ANHYDRIDES IN AQUEOUS SOLUTION .2, *Journal of the American Chemical Society* 79(9) (1957) 2159-2160.
- [35] M. Goodman, Hutchiso.J, PROPAGATION MECHANISM IN STRONG BASE INITIATED POLYMERIZATION OF ALPHA-AMINO ACID N-CARBOXYANHYDRIDES, *Journal of the American Chemical Society* 87(15) (1965) 3524-&.
- [36] C.H. Bamford, H. Block, INITIATION STEP IN POLYMERIZATION OF N-CARBOXY-ALPHA-AMINO-ACID ANHYDRIDES .1. CATALYSIS BY TERTIARY BASES, *Journal of the Chemical Society (NOV)* (1961) 4989-&.
- [37] C.H. Bamford, H. Block, INITIATION STEP IN POLYMERIZATION OF N-CARBOXY-ALPHA-AMINO-ACID ANHYDRIDES .2. EFFECTS RELATED TO STRUCTURE OF AMINE INITIATORS, *Journal of the Chemical Society (NOV)* (1961) 4992-&.
- [38] E. Katchalski, Y. Shalitin, M. Gehatia, THEORETICAL ANALYSIS OF THE POLYMERIZATION KINETICS OF N-CARBOXY-ALPHA-AMINO ACID ANHYDRIDES, *Journal of the American Chemical Society* 77(7) (1955) 1925-1934.
- [39] P. Doty, R.D. Lundberg, POLYPEPTIDES .10A. ADDITIONAL COMMENTS OF THE AMINE-INITIATED POLYMERIZATION, *Journal of the American Chemical Society* 79(9) (1957) 2338-2339.
- [40] R.D. Lundberg, P. Doty, POLYPEPTIDES .17. A STUDY OF THE KINETICS OF THE PRIMARY AMINE-INITIATED POLYMERIZATION OF N-CARBOXY-ANHYDRIDES WITH SPECIAL REFERENCE TO CONFIGURATIONAL AND STEREOCHEMICAL EFFECTS, *Journal of the American Chemical Society* 79(15) (1957) 3961-3972.
- [41] C. Gazon, P. Salas-Ambrosio, E. Ibarboure, A. Buol, E. Garanger, M.W. Grinstaff, S. Lecommandoux, C. Bonduelle, Aqueous Ring-Opening Polymerization Induced Self-Assembly (ROPISA) of N-carboxyanhydrides, *Angewandte Chemie-International Edition* 59(2) (2020) 622-626.
- [42] T. Aliferis, H. Iatrou, N. Hadjichristidis, Well-defined linear multiblock and branched polypeptides by linking chemistry, *Journal of Polymer Science Part a-Polymer Chemistry* 43(19) (2005) 4670-4673.

- [43] I. Dimitrov, H. Schlaad, Synthesis of nearly monodisperse polystyrene-polypeptide block copolymers via polymerisation of N-carboxyanhydrides, *Chemical Communications* (23) (2003) 2944-2945.
- [44] I. Conejos-Sanchez, A. Duro-Castano, A. Birke, M. Barz, M.J. Vicent, A controlled and versatile NCA polymerization method for the synthesis of polypeptides, *Polymer Chemistry* 4(11) (2013) 3182-3186.
- [45] W. Vayaboury, O. Giani, H. Cottet, A. Deratani, F. Schue, Living polymerization of alpha-amino acid N-carboxyanhydrides (NCA) upon decreasing the reaction temperature, *Macromolecular Rapid Communications* 25(13) (2004) 1221-1224.
- [46] H. Lu, J.J. Cheng, Hexamethyldisilazane-mediated controlled polymerization of alpha-Amino acid N-carboxyanhydrides, *Journal of the American Chemical Society* 129(46) (2007) 14114-+.
- [47] T.J. Deming, S.A. Curtin, Chain initiation efficiency in cobalt- and nickel-mediated polypeptide synthesis, *Journal of the American Chemical Society* 122(24) (2000) 5710-5717.
- [48] T.J. Deming, Living polymerization of alpha-amino acid-N-carboxyanhydrides, *Journal of Polymer Science Part a-Polymer Chemistry* 38(17) (2000) 3011-3018.
- [49] Y. Knobler, S. Bittner, M. Frankel, REACTION OF N-CARBOXY-ALPHA-AMINO-ACID ANHYDRIDES WITH HYDROCHLORIDES OF HYDROXYLAMINE O-ALKYLHYDROXYLAMINES + AMINES SYNTHESSES OF AMINO-HYDROXAMIC ACIDS AMIDO-OXY-PEPTIDES + ALPHA-AMINO-ACID AMIDES, *Journal of the Chemical Society (OCT)* (1964) 3941-&.
- [50] T. Aliferis, H. Iatrou, N. Hadjichristidis, Living polypeptides, *Biomacromolecules* 5(5) (2004) 1653-1656.
- [51] C.L. Chang, M.K. Leung, M.H. Yang, Alkyl and dialkylammonium tetrafluoroborate catalyzed cis-trans isomerization of 1,3,5-trimethyl-1,3,5-triphenylecylotrisiloxane, *Tetrahedron* 60(41) (2004) 9205-9212.
- [52] M. Barz, R. Luxenhofer, R. Zentel, M.J. Vicent, Overcoming the PEG-addiction: well-defined alternatives to PEG, from structure-property relationships to better defined therapeutics, *Polymer Chemistry* 2(9) (2011) 1900-1918.
- [53] J.V. Gonzalez-Aramundiz, M.V. Lozano, A. Sousa-Herves, E. Fernandez-Megia, N. Csaba, Polypeptides and polyaminoacids in drug delivery, *Expert Opinion on Drug Delivery* 9(2) (2012) 183-201.
- [54] O. Zagorodko, J.J. Arroyo-Crespo, V.J. Nebot, M.J. Vicent, Polypeptide-Based Conjugates as Therapeutics: Opportunities and Challenges, *Macromolecular Bioscience* 17(1) (2017).
- [55] M.A. Sheikh, Y.S. Malik, Z.K. Xing, Z.P. Guo, H.Y. Tian, X.J. Zhu, X.S. Chen, Polylysine-modified polyethylenimine (PEI-PLL) mediated VEGF gene delivery protects dopaminergic neurons in cell culture and in rat models of Parkinson's Disease (PD), *Acta Biomaterialia* 54 (2017) 58-68.
- [56] A. Duro-Castano, D. Moreira Leite, J. Forth, Y. Deng, D. Matias, C. Noble Jesus, G. Battaglia, Designing peptide nanoparticles for efficient brain delivery, *Advanced drug delivery reviews* 160 (2020) 52-77.
- [57] I. Tamai, A. Tsuji, Transporter-mediated permeation of drugs across the blood-brain barrier, *Journal of Pharmaceutical Sciences* 89(11) (2000) 1371-1388.
- [58] F. Rodriguez-Otormin, A. Duro-Castano, I. Conejos-Sanchez, M.J. Vicent, Envisioning the future of polymer therapeutics for brain disorders, *Wiley Interdisciplinary Reviews-Nanomedicine and Nanobiotechnology* 11(1) (2019).
- [59] L.A. Bareford, P.W. Swaan, Endocytic mechanisms for targeted drug delivery, *Advanced Drug Delivery Reviews* 59(8) (2007) 748-758.
- [60] A. Eldar-Boock, K. Miller, J. Sanchis, R. Lupu, M.J. Vicent, R. Satchi-Fainaro, Integrin-assisted drug delivery of nano-scaled polymer therapeutics bearing paclitaxel, *Biomaterials* 32(15) (2011) 3862-3874.
- [61] R. Duncan, S.C.W. Richardson, Endocytosis and Intracellular Trafficking as Gateways for Nanomedicine Delivery: Opportunities and Challenges, *Molecular Pharmaceutics* 9(9) (2012) 2380-2402.

- [62] S. Biswas, V.P. Torchilin, Nanopreparations for organelle-specific delivery in cancer, *Advanced Drug Delivery Reviews* 66 (2014) 26-41.
- [63] T. Melnyk, S. Dordevic, I. Conejos-Sanchez, M.J. Vicent, Therapeutic potential of polypeptide-based conjugates: Rational design and analytical tools that can boost clinical translation, *Advanced drug delivery reviews* 160 (2020) 136-169.
- [64] S.S. Nogueira, Polysarcosine-Functionalized Lipid Nanoparticles for Therapeutic mRNA Delivery, in: A. Schlegel (Ed.) *ACS Appl. Nano Mater.*, 2020, pp. 10634–10645.
- [65] M.P. Bevilacqua, D.J. Huang, B.D. Wall, S.J. Lane, C.K. Edwards, J.A. Hanson, D. Benitez, J.S. Solomkin, T.J. Deming, Amino Acid Block Copolymers with Broad Antimicrobial Activity and Barrier Properties, *Macromolecular Bioscience* 17(10) (2017) 9.
- [66] I. Dolz-Perez, M.A. Sallam, E. Masia, D. Morello-Bolomar, M.D.P. del Caz, P. Graff, D. Abdelmonsif, S. Hedtrich, V.J. Nebot, M.J. Vicent, Polypeptide-corticosteroid conjugates as a topical treatment approach to psoriasis, *Journal of Controlled Release* 318 (2020) 210-222.
- [67] E.J.L. Steen, J.T. Jorgensen, K. Johann, K. Norregaard, B. Sohr, D. Svatunek, A. Birke, V. Shalgunov, P.E. Edem, R. Rossin, C. Seidl, F. Schmid, M.S. Robillard, J.L. Kristensen, H. Mikula, M. Barz, A. Kjaer, M.M. Herth, Trans-Cyclooctene-Functionalized PeptoBrushes with Improved Reaction Kinetics of the Tetrazine Ligation for Pretargeted Nuclear Imaging, *Acs Nano* 14(1) (2020) 568-584.
- [68] R. Wang, B. Zhou, D.L. Xu, H. Xu, L. Liang, X.H. Feng, P.K. Ouyang, B. Chi, Antimicrobial and biocompatible epsilon-polylysine-gamma-poly(glutamic acid)-based hydrogel system for wound healing, *Journal of Bioactive and Compatible Polymers* 31(3) (2016) 242-259.
- [69] K. Jain, U. Gupta, N.K. Jain, Dendronized nanoconjugates of lysine and folate for treatment of cancer, *European Journal of Pharmaceutics and Biopharmaceutics* 87(3) (2014) 500-509.
- [70] M. Lee, J. Jeong, D. Kim, Intracellular Uptake and pH-Dependent Release of Doxorubicin from the Self-Assembled Micelles Based on Amphiphilic Polyaspartamide Graft Copolymers, *Biomacromolecules* 16(1) (2015) 136-144.
- [71] J.M. Qian, M.H. Xu, A.L. Suo, W.J. Xu, T. Liu, X.F. Liu, Y. Yao, H.J. Wang, Folate-decorated hydrophilic three-arm star-block terpolymer as a novel nanovehicle for targeted co-delivery of doxorubicin. and Bcl-2 siRNA in breast cancer therapy, *Acta Biomaterialia* 15 (2015) 102-116.
- [72] A. Sinaga, T.A. Hatton, K.C. Tam, Thermodynamics of micellization of beta-sheet forming poly(acrylic acid)-block-poly(l-valine) hybrids, *Journal of Physical Chemistry B* 112(37) (2008) 11542-11550.
- [73] S.H. Wibowo, A. Sulistio, E.H.H. Wong, A. Blencowe, G.G. Qiao, Functional and Well-Defined -Sheet-Assembled Porous Spherical Shells by Surface-Guided Peptide Formation, *Advanced Functional Materials* 25(21) (2015) 3147-3156.
- [74] S. Niimura, H. Kurosu, A. Shoji, Precise structural analysis of alpha-helical polypeptide by quantum-chemical calculation related to reciprocal side-chain combination of two L-phenylalanine residues, *Journal of Molecular Structure* 970(1-3) (2010) 96-100.
- [75] Y. Mochida, H. Cabral, Y. Miura, F. Albertini, S. Fukushima, K. Osada, N. Nishiyama, K. Kataoka, Bundled Assembly of Helical Nanostructures in Polymeric Micelles Loaded with Platinum Drugs Enhancing Therapeutic Efficiency against Pancreatic Tumor, *Acs Nano* 8(7) (2014) 6724-6738.
- [76] J.A. Champion, Y.K. Katare, S. Mitragotri, Particle shape: A new design parameter for micro- and nanoscale drug delivery carriers, *Journal of Controlled Release* 121(1-2) (2007) 3-9.
- [77] N.P. Truong, M.R. Whittaker, C.W. Mak, T.P. Davis, The importance of nanoparticle shape in cancer drug delivery, *Expert Opinion on Drug Delivery* 12(1) (2015) 129-142.
- [78] D. Paul, S. Achouri, Y.Z. Yoon, J. Herre, C.E. Bryant, P. Cicuta, Phagocytosis Dynamics Depends on Target Shape, *Biophysical Journal* 105(5) (2013) 1143-1150.
- [79] Y. Jia, S.N. Shmakov, E. Pinkhassik, Controlled Permeability in Porous Polymer Nanocapsules Enabling Size- and Charge-Selective SERS Nanoprobes, *Acs Applied Materials & Interfaces* 8(30) (2016) 19755-19763.
- [80] A. Duro-Castano, J. Movellan, M.J. Vicent, Smart branched polymer drug conjugates as nano-sized drug delivery systems, *Biomaterials Science* 3(10) (2015) 1321-1334.

- [81] H.L. Xu, Q. Yao, C.F. Cai, J.X. Gou, Y. Zhang, H.J. Zhong, X. Tang, Amphiphilic poly(amino acid) based micelles applied to drug delivery: The in vitro and in vivo challenges and the corresponding potential strategies, *Journal of Controlled Release* 199 (2015) 84-97.
- [82] R. Duncan, The dawning era of polymer therapeutics, *Nature Reviews Drug Discovery* 2(5) (2003) 347-360.
- [83] R. Duncan, M.J. Vicent, Polymer therapeutics-prospects for 21st century: The end of the beginning, *Advanced Drug Delivery Reviews* 65(1) (2013) 60-70.
- [84] P. Perdih, S. Cebasek, A. Mozir, E. Zagar, Post-Polymerization Modification of Poly(L-glutamic acid) with D-(+)-Glucosamine, *Molecules* 19(12) (2014) 19751-19768.
- [85] R. Herrendorff, P. Hanggi, H. Pfister, F. Yang, D. Demeestere, F. Hunziker, S. Frey, N. Schaeren-Wiemers, A.J. Steck, B. Ernst, Selective in vivo removal of pathogenic anti-MAG autoantibodies, an antigen-specific treatment option for anti-MAG neuropathy, *Proceedings of the National Academy of Sciences of the United States of America* 114(18) (2017) E3689-E3698.
- [86] A. Nino-Pariente, V.J. Nebot, M.J. Vicent, Relevant Physicochemical Descriptors of "Soft Nanomedicines" to Bypass Biological Barriers, *Current Pharmaceutical Design* 22(9) (2016) 1274-1291.
- [87] K. Knop, R. Hoogenboom, D. Fischer, U.S. Schubert, Poly(ethylene glycol) in Drug Delivery: Pros and Cons as Well as Potential Alternatives, *Angewandte Chemie-International Edition* 49(36) (2010) 6288-6308.
- [88] Y. Mochida, H. Cabral, K. Kataoka, Polymeric micelles for targeted tumor therapy of platinum anticancer drugs, *Expert Opinion on Drug Delivery* 14(12) (2017) 1423-1438.
- [89] H. Cabral, K. Miyata, K. Osada, K. Kataoka, Block Copolymer Micelles in Nanomedicine Applications, *Chemical Reviews* 118(14) (2018) 6844-6892.
- [90] N. Nishiyama, Y. Matsumura, K. Kataoka, Development of polymeric micelles for targeting intractable cancers, *Cancer Science* 107(7) (2016) 867-874.
- [91] H. Cabral, K. Kataoka, Progress of drug-loaded polymeric micelles into clinical studies, *Journal of Controlled Release* 190 (2014) 465-476.
- [92] R. Plummer, R.H. Wilson, H. Calvert, A.V. Boddy, M. Griffin, J. Sludden, M.J. Tilby, M. Eatock, D.G. Pearson, C.J. Ottley, Y. Matsumura, K. Kataoka, T. Nishiya, A Phase I clinical study of cisplatin-incorporated polymeric micelles (NC-6004) in patients with solid tumours, *British Journal of Cancer* 104(4) (2011) 593-598.
- [93] U. Lachelt, E. Wagner, Nucleic Acid Therapeutics Using Polyplexes: A Journey of 50 Years (and Beyond), *Chemical Reviews* 115(19) (2015) 11043-11078.
- [94] K. Tappertzhofen, S. Beck, E. Montermann, D. Huesmann, M. Barz, K. Koynov, M. Bros, R. Zentel, Bioreducible Poly-L-Lysine-Poly HEMA Block Copolymers Obtained by RAFT-Polymerization as Efficient Polyplex-Transfection Reagents, *Macromolecular Bioscience* 16(1) (2016) 106-120.
- [95] N.J. Baumhover, J.T. Duskey, S. Khargharia, C.W. White, S.T. Crowley, R.J. Allen, K.G. Rice, Structure Activity Relationship of PEGylated Polylysine Peptides as Scavenger Receptor Inhibitors for Non-Viral Gene Delivery, *Molecular Pharmaceutics* 12(12) (2015) 4321-4328.
- [96] K.M. Takeda, Y. Yamasaki, A. Dirisala, S. Ikeda, T.A. Tockary, K. Toh, K. Osada, K. Kataoka, Effect of shear stress on structure and function of polyplex micelles from poly(ethylene glycol)-poly(L-lysine) block copolymers as systemic gene delivery carrier, *Biomaterials* 126 (2017) 31-38.
- [97] A. Krivitsky, V. Krivitsky, D. Polyak, A. Scomparin, S. Eliyahu, H. Gibori, E. Yeini, E. Pisarevsky, R. Blau, R. Satchi-Fainaro, Molecular Weight-Dependent Activity of Aminated Poly(glutamates) as siRNA Nanocarriers, *Polymers* 10(5) (2018).
- [98] A. Nino-Pariente, A. Arminan, S. Reinhard, C. Scholz, E. Wagner, M.J. Vicent, Design of Poly-L-Glutamate-Based Complexes for pDNA Delivery, *Macromolecular Bioscience* 17(10) (2017).
- [99] L. Rodriguez-Arco, A. Poma, L. Ruiz-Perez, E. Scarpa, K. Ngamkham, G. Battaglia, Molecular bionics - engineering biomaterials at the molecular level using biological principles, *Biomaterials* 192 (2019) 26-50.
- [100] G.M. Whitesides, B. Grzybowski, Self-assembly at all scales, *Science* 295(5564) (2002) 2418-2421.

- [101] S.S. Song, A.X. Song, J.C. Hao, Self-assembled structures of amphiphiles regulated via implanting external stimuli, *Rsc Advances* 4(79) (2014) 41864-41875.
- [102] S. Xue, X.L. Gu, J. Zhang, H.L. Sun, C. Deng, Z.Y. Zhong, Construction of Small-Sized, Robust, and Reduction-Responsive Polypeptide Micelles for High Loading and Targeted Delivery of Chemotherapeutics, *Biomacromolecules* 19(8) (2018) 3586-3593.
- [103] G.H. Van Domeselaar, G.S. Kwon, L.C. Andrew, D.S. Wishart, Application of solid phase peptide synthesis to engineering PEO-peptide block copolymers for drug delivery, *Colloids and Surfaces B-Biointerfaces* 30(4) (2003) 323-334.
- [104] Y.P. Chan, R. Meyrueix, R. Kravtsoff, F. Nicolas, K. Lundstrom, Review on Medusa (R): a polymer-based sustained release technology for protein and peptide drugs, *Expert Opinion on Drug Delivery* 4(4) (2007) 441-451.
- [105] S.E. Barrett, R.S. Burke, M.T. Abrams, C. Bason, M. Busuek, E. Carlini, B.A. Carr, L.S. Crocker, H. Fan, R.M. Garbaccio, E.N. Guidry, J.H. Heo, B.J. Howell, E.A. Kemp, R.A. Kowtoniuk, A.H. Latham, A.M. Leone, M. Lyman, R.G. Parmar, M. Patel, S.Y. Pechenov, T. Pei, N.T. Pudvah, C. Raab, S. Riley, L. Sepp-Lorenzino, S. Smith, E.D. Soli, S. Staskiewicz, M. Stern, Q. Truong, M. Vavrek, J.H. Waldman, E.S. Walsh, J.M. Williams, S. Young, S.L. Colletti, Development of a liver-targeted siRNA delivery platform with a broad therapeutic window utilizing biodegradable polypeptide-based polymer conjugates, *Journal of Controlled Release* 183 (2014) 124-137.
- [106] D. Huesmann, A. Sevenich, B. Weber, M. Barz, A head-to-head comparison of poly(sarcosine) and poly(ethylene glycol) in peptidic, amphiphilic block copolymers, *Polymer* 67 (2015) 240-248.
- [107] L. Messenger, J. Gaitzsch, L. Chierico, G. Battaglia, Novel aspects of encapsulation and delivery using polymersomes, *Current Opinion in Pharmacology* 18 (2014) 104-111.
- [108] N. L'Amoreaux, A. Ali, S. Iqbal, J. Larsen, Persistent prolate polymersomes for enhanced co-delivery of hydrophilic and hydrophobic drugs, *Nanotechnology* 31(17) (2020).
- [109] B. Weber, C. Kappel, M. Scherer, M. Helm, M. Bros, S. Grabbe, M. Barz, PeptoSomes for Vaccination: Combining Antigen and Adjuvant in Polypept(o)ide-Based Polymersomes, *Macromolecular Bioscience* 17(10) (2017) 6.
- [110] P.J. Photos, L. Bacakova, B. Discher, F.S. Bates, D.E. Discher, Polymer vesicles in vivo: correlations with PEG molecular weight, *Journal of Controlled Release* 90(3) (2003) 323-334.
- [111] T.M. Allen, C. Hansen, F. Martin, C. Redemann, A. Yauyoung, LIPOSOMES CONTAINING SYNTHETIC LIPID DERIVATIVES OF POLY(ETHYLENE GLYCOL) SHOW PROLONGED CIRCULATION HALF-LIVES INVIVO, *Biochimica Et Biophysica Acta* 1066(1) (1991) 29-36.
- [112] M.C. Woodle, SURFACE-MODIFIED LIPOSOMES - ASSESSMENT AND CHARACTERIZATION FOR INCREASED STABILITY AND PROLONGED BLOOD-CIRCULATION, *Chemistry and Physics of Lipids* 64(1-3) (1993) 249-262.
- [113] M.C. Woodle, K.K. Matthay, M.S. Newman, J.E. Hidayat, L.R. Collins, C. Redemann, F.J. Martin, D. Papahadjopoulos, VERSATILITY IN LIPID COMPOSITIONS SHOWING PROLONGED CIRCULATION WITH STERICALLY STABILIZED LIPOSOMES, *Biochimica Et Biophysica Acta* 1105(2) (1992) 193-200.
- [114] M.D. Brown, A. Schatzlein, A. Brownlie, V. Jack, W. Wang, L. Tetley, A.I. Gray, I.F. Uchegbu, Preliminary characterization of novel amino acid based polymeric vesicles as gene and drug delivery agents, *Bioconjugate Chemistry* 11(6) (2000) 880-891.
- [115] E.P. Holowka, D.J. Pochan, T.J. Deming, Charged polypeptide vesicles with controllable diameter, *Journal of the American Chemical Society* 127(35) (2005) 12423-12428.
- [116] E.P. Holowka, V.Z. Sun, D.T. Kamei, T.J. Deming, Polyarginine segments in block copolypeptides drive both vesicular assembly and intracellular delivery, *Nature Materials* 6(1) (2007) 52-57.
- [117] E. Vlakh, A. Ananyan, N. Zashikhina, A. Hubina, A. Pogodaev, M. Volokitina, V. Sharoyko, T. Tennikova, Preparation, Characterization, and Biological Evaluation of Poly(Glutamic Acid)-b-Polyphenylalanine Polymersomes, *Polymers* 8(6) (2016).

- [118] M.S. Kim, K. Dayananda, E.Y. Choi, H.J. Park, J.S. Kim, D.S. Lee, Synthesis and characterization of poly(L-glutamic acid)-block-poly(L-phenylalanine), *Polymer* 50(10) (2009) 2252-2257.
- [119] J. Rodriguez-Hernandez, S. Lecommandoux, Reversible inside-out micellization of pH-responsive and water-soluble vesicles based on polypeptide diblock copolymers, *Journal of the American Chemical Society* 127(7) (2005) 2026-2027.
- [120] N.A. Peppas, P. Bures, W. Leobandung, H. Ichikawa, Hydrogels in pharmaceutical formulations, *European Journal of Pharmaceutics and Biopharmaceutics* 50(1) (2000) 27-46.
- [121] M. Guvendiren, H.D. Lu, J.A. Burdick, Shear-thinning hydrogels for biomedical applications, *Soft Matter* 8(2) (2012) 260-272.
- [122] H.F. Darge, A.T. Andrgie, H.C. Tsai, J.Y. Lai, Polysaccharide and polypeptide based injectable thermo-sensitive hydrogels for local biomedical applications, *International Journal of Biological Macromolecules* 133 (2019) 545-563.
- [123] X.F. Zhou, Z.B. Li, Advances and Biomedical Applications of Polypeptide Hydrogels Derived from alpha-Amino Acid N-Carboxyanhydride (NCA) Polymerizations, *Advanced Healthcare Materials* 7(15) (2018).
- [124] Y.T. Sun, T.J. Deming, Self-Healing Multiblock Copolypeptide Hydrogels via Polyion Complexation, *Acs Macro Letters* 8(5) (2019) 553-557.
- [125] H.J. Song, G. Yang, P.S. Huang, D.L. Kong, W.W. Wang, Self-assembled PEG-poly(L-valine) hydrogels as promising 3D cell culture scaffolds, *Journal of Materials Chemistry B* 5(9) (2017) 1724-1733.
- [126] O. Zagorodko, V.J. Nebot, M.J. Vicent, The generation of stabilized supramolecular nanorods from star-shaped polyglutamates, *Polymer Chemistry* 11(6) (2020) 1220-1229.
- [127] R. Otter, N.A. Henke, C. Berac, T. Bauer, M. Barz, S. Seiffert, P. Besenius, Secondary Structure-Driven Hydrogelation Using Foldable Telechelic Polymer-Peptide Conjugates, *Macromolecular Rapid Communications* 39(17) (2018).
- [128] S.J. Shirbin, F. Karimi, N.J.A. Chan, D.E. Heath, G.G. Qiao, Macroporous Hydrogels Composed Entirely of Synthetic Polypeptides: Biocompatible and Enzyme Biodegradable 3D Cellular Scaffolds, *Biomacromolecules* 17(9) (2016) 2981-2991.
- [129] M.T. Popescu, G. Lontos, A. Avgeropoulos, C. Tsitsilianis, Stimuli responsive fibrous hydrogels from hierarchical self-assembly of a triblock copolypeptide, *Soft Matter* 11(2) (2015) 331-342.
- [130] G.E. Negri, T.J. Deming, Triggered Copolypeptide Hydrogel Degradation Using Photolabile Lysine Protecting Groups, *Acs Macro Letters* 5(11) (2016) 1253-1256.
- [131] S.X. Lv, W.T. Song, Z.H. Tang, M.Q. Li, H.Y. Yu, H. Hong, X.S. Chen, Charge-Conversional PEG-Polypeptide Polyionic Complex Nanoparticles from Simple Blending of a Pair of Oppositely Charged Block Copolymers as an Intelligent Vehicle for Efficient Antitumor Drug Delivery, *Molecular Pharmaceutics* 11(5) (2014) 1562-1574.
- [132] C. Bonduelle, J. Huang, E. Ibarboure, A. Heise, S. Lecommandoux, Synthesis and self-assembly of "tree-like" amphiphilic glycopolypeptides, *Chemical Communications* 48(67) (2012) 8353-8355.
- [133] Y. Zhu, T. Akagi, M. Akashi, Self-Assembling Stereocomplex Nanoparticles by Enantiomeric Poly(g-glutamic acid)poly(lactide) Graft Copolymers as a Protein Delivery Carrier, *Macromolecular Bioscience* 14(4) (2014) 576-587.
- [134] T. Akagi, T. Kaneko, T. Kida, M. Akashi, Preparation and characterization of biodegradable nanoparticles based on poly(gamma-glutamic acid) with L-phenylalanine as a protein carrier, *Journal of Controlled Release* 108(2-3) (2005) 226-236.
- [135] A. Gonzalez-Paredes, D. Torres, M.J. Alonso, Polyarginine nanocapsules: A versatile nanocarrier with potential in transmucosal drug delivery, *International Journal of Pharmaceutics* 529(1-2) (2017) 474-485.
- [136] C. Tanford, *The Hydrophobic Effect: Formation of Micelles and Biological Membranes*, 1980.
- [137] A. Siew, H. Le, M. Thiovolet, P. Gellert, A. Schatzlein, I. Uchegbu, Enhanced Oral Absorption of Hydrophobic and Hydrophilic Drugs Using Quaternary Ammonium Palmitoyl Glycol Chitosan Nanoparticles, *Molecular Pharmaceutics* 9(1) (2012) 14-28.

- [138] L.X. Zhao, N.N. Li, K.M. Wang, C.H. Shi, L.L. Zhang, Y.X. Luan, A review of polypeptide-based polymersomes, *Biomaterials* 35(4) (2014) 1284-1301.
- [139] M. Byrne, R. Murphy, A. Kapetanakis, J. Ramsey, S.A. Cryan, A. Heise, Star-Shaped Polypeptides: Synthesis and Opportunities for Delivery of Therapeutics, *Macromolecular Rapid Communications* 36(21) (2015) 1862-1876.
- [140] B. Weinstock-Guttman, K.V. Nair, J.L. Glajch, T.C. Ganguly, D. Kantor, Two decades of glatiramer acetate: From initial discovery to the current development of generics, *Journal of the Neurological Sciences* 376 (2017) 255-259.
- [141] <https://www.copaxone.com/>.
- [142] <https://www.amicrobe.com/>.
- [143] N. Hegde, V. Velingkar, B. Prabhakar, An Update on Design and Pharmacology of Dendritic Poly(l-lysine), *International Journal of Peptide Research and Therapeutics* 25(4) (2019) 1539-1562.
- [144] <https://starpharma.com/vivagel>.
- [145] J.W. Singer, Paclitaxel poliglumex (XYOTAX (TM), CT-2103): A macromolecular taxane, *Journal of Controlled Release* 109(1-3) (2005) 120-126.
- [146] H. Mukai, T. Kogawa, N. Matsubara, Y. Naito, M. Sasaki, A. Hosono, A first-in-human Phase 1 study of epirubicin-conjugated polymer micelles (K-912/NC-6300) in patients with advanced or recurrent solid tumors, *Investigational New Drugs* 35(3) (2017) 307-314.
- [147] https://starpharma.com/drug_delivery.
- [148] G.M. Nicolle, E. Toth, H. Schmitt-Willich, B. Raduchel, A.E. Merbach, The impact of rigidity and water exchange on the relaxivity of a dendritic MRI contrast agent, *Chemistry-a European Journal* 8(5) (2002) 1040-1048.
- [149] P. Polcyn, M. Jurczak, A. Rajnisz, J. Solecka, Z. Urbanczyk-Lipkowska, Design of Antimicrobially Active Small Amphiphilic Peptide Dendrimers, *Molecules* 14(10) (2009) 3881-3905.
- [150] E.F. Jackson, E. Esparza-Coss, X.X. Wen, C.S. Ng, S.L. Daniel, R.E. Price, B. Rivera, C. Charnsangavej, J.G. Gelovani, C. Li, Magnetic resonance imaging of therapy-induced necrosis using gadolinium-chelated polyglutamic acids, *International Journal of Radiation Oncology Biology Physics* 68(3) (2007) 830-838.
- [151] Y. Matsumura, T. Hamaguchi, T. Ura, K. Muro, Y. Yamada, Y. Shimada, K. Shirao, T. Okusaka, H. Ueno, M. Ikeda, N. Watanabe, Phase I clinical trial and pharmacokinetic evaluation of NK911, a micelle-encapsulated doxorubicin, *British Journal of Cancer* 91(10) (2004) 1775-1781.
- [152] T. Hamaguchi, T. Doi, T. Eguchi-Nakajima, K. Kato, Y. Yamada, Y. Shimada, N. Fuse, A. Ohtsu, S. Matsumoto, M. Takanashi, Y. Matsumura, Phase I Study of NK012, a Novel SN-38-Incorporating Micellar Nanoparticle, in Adult Patients with Solid Tumors, *Clinical Cancer Research* 16(20) (2010) 5058-5066.
- [153] J. Homsy, G.R. Simon, C.R. Garrett, G. Springett, R. De Conti, A. Chiappori, P.N. Munster, M.K. Burton, S. Stromatt, C. Allievi, P. Angiulli, A. Eisenfeld, D.M. Sullivan, A.I. Daud, Phase I trial of poly-L-glutamate camptothecin (CT-2106) administered weekly in patients with advanced solid malignancies, *Clinical Cancer Research* 13(19) (2007) 5855-5861.
- [154] <https://clinicaltrials.gov/ct2/show/NCT00910741>.
- [155] <https://www.nanocarrier.co.jp/en/pipeline/>.
- [156] Y.C. Huang, Y.S. Yang, T.Y. Lai, J.S. Jan, Lysine-block-tyrosine block copolypeptides: Self-assembly, cross-linking, and conjugation of targeted ligand for drug encapsulation, *Polymer* 53(4) (2012) 913-922.
- [157] H. Iatrou, H. Frielinghaus, S. Hanski, N. Ferderigos, J. Ruokolainen, O. Ikkala, D. Richter, J. Mays, N. Hadjichristidis, Architecturally induced multiresponsive vesicles from well-defined polypeptides. Formation of gene vehicles, *Biomacromolecules* 8(7) (2007) 2173-2181.
- [158] C. Sanson, C. Schatz, J.F. Le Meins, A. Brulet, A. Soum, S. Lecommandoux, Biocompatible and Biodegradable Poly(trimethylene carbonate)-b-Poly (L-glutamic acid) Polymersomes: Size Control and Stability, *Langmuir* 26(4) (2010) 2751-2760.

- [159] J. Gaspard, J.A. Silas, D.F. Shantz, J.S. Jan, Supramolecular assembly of lysine-b-glycine block copolypeptides at different solution conditions, *Supramolecular Chemistry* 22(3) (2010) 178-185.
- [160] J.H. Tang, X.Q. Wang, T. Wang, F.H. Chen, J.P. Zhou, In vivo pharmacokinetics, biodistribution and antitumor effect of amphiphilic poly(L-amino acids) micelles loaded with a novel all-trans retinoic acid derivative, *European Journal of Pharmaceutical Sciences* 51 (2014) 157-164.
- [161] S.S. Desale, S.M. Cohen, Y. Zhao, A.V. Kabanov, T.K. Bronich, Biodegradable hybrid polymer micelles for combination drug therapy in ovarian cancer, *Journal of Controlled Release* 171(3) (2013) 339-348.
- [162] Z.C. Luo, P. Li, J.H. Deng, N.N. Gao, Y.J. Zhang, H. Pan, L.L. Liu, C. Wang, L.T. Cai, Y.F. Ma, Cationic polypeptide micelle-based antigen delivery system: A simple and robust adjuvant to improve vaccine efficacy, *Journal of Controlled Release* 170(2) (2013) 259-267.
- [163] C.H. Chen, M.L. Kuo, J.L. Wang, W.C. Liao, L.C. Chang, L.P. Chan, J. Lin, CCM-AMI, A POLYETHYLENE GLYCOL MICELLE WITH AMIFOSTINE, AS AN ACUTE RADIATION SYNDROME PROTECTANT IN C57BL/6 MICE, *Health Physics* 109(3) (2015) 242-248.
- [164] M.W. Konstan, P.B. Davis, J.S. Wagener, K.A. Hilliard, R.C. Stern, L.J.H. Milgram, T.H. Kowalczyk, S.L. Hyatt, T.L. Fink, C.R. Gedeon, S.M. Oette, J.M. Payne, O. Muhammad, A.G. Ziady, R.C. Moen, M.J. Cooper, Compacted DNA nanoparticles administered to the nasal mucosa of cystic fibrosis subjects are safe and demonstrate partial to complete cystic fibrosis transmembrane regulator reconstitution, *Human Gene Therapy* 15(12) (2004) 1255-1269.
- [165] C.H. Tung, S. Mueller, R. Weissleder, Novel branching membrane translocational peptide as gene delivery vector, *Bioorganic & Medicinal Chemistry* 10(11) (2002) 3609-3614.
- [166] H.K. Bayele, T. Sakthivel, M. O'Donnell, K.J. Pasi, A.F. Wilderspin, C.A. Lee, I. Toth, A.T. Florence, Versatile peptide dendrimers for nucleic acid delivery, *Journal of Pharmaceutical Sciences* 94(2) (2005) 446-457.
- [167] A. Shibata, S. Murata, S. Ueno, S.Q. Liu, S. Futaki, Y. Baba, Synthetic copoly(Lys/Phe) and poly(Lys) translocate through lipid bilayer membranes, *Biochimica Et Biophysica Acta-Biomembranes* 1616(2) (2003) 147-155.
- [168] D.J. Coles, S. Yang, A. Esposito, D. Mitchell, R.F. Minchin, I. Toth, The synthesis and characterisation of a novel dendritic system for gene delivery, *Tetrahedron* 63(49) (2007) 12207-12214.
- [169] <https://www.fda.gov/>.
- [170] C.A. Umscheid, D.J. Margolis, C.E. Grossman, Key Concepts of Clinical Trials: A Narrative Review, *Postgraduate Medicine* 123(5) (2011) 194-204.
- [171] J. Strovel, *Early Drug Discovery and Development Guidelines: For Academic Researchers, Collaborators, and Start-up Companies*, 2016.
- [172] ICH Q2(R1) Validation Of Analytical Procedures: Text And Methodology.
- [173] ICH Q6A Specifications: Test Procedures and Acceptance Criteria for New Drug Substances and New Drug Products: Chemical Substances.
- [174] R. Wahid, R. Holt, R. Hjorth, F.B. Scorza, Chemistry, manufacturing and control (CMC) and clinical trial technical support for influenza vaccine manufacturers, *Vaccine* 34(45) (2016) 5430-5435.
- [175] G. Akshatha, V.A. Narayanan, D.S. Sandeep, R.N. Charyulu, Chemistry, Manufacturing and Control (CMC) Evaluations of ANDA Submission in the USA, *Indian Journal of Pharmaceutical Education and Research* 53(3) (2019) 414-420.
- [176] N.S. Cauchon, S. Oghamian, S. Hassanpour, M. Abernathy, Innovation in Chemistry, Manufacturing, and Controls-A Regulatory Perspective From Industry, *Journal of Pharmaceutical Sciences* 108(7) (2019) 2207-2237.
- [177] M.Q. Picat, N. Houede, E. Chamorey, S. Mathoulin-Pelissier, Phase 0 exploratory clinical trials: literature review 2006-2009, *Bulletin Du Cancer* 98(7) (2011) 753-759.
- [178] <https://www.thebalance.com/pipelines-in-biotech-companies-375591>.
- [179] <https://rareisease.powellcenter.med.ufl.edu/clinical-trial/>.

- [180] https://www.hamarichemicals.com/wp/wp-content/themes/hamari_EN/products/img/znr01-02.png.
- [181] <https://www.gsk.com/en-gb/research-and-development/development/how-we-develop-new-medicines/>.
- [182] F. Towfic, J.M. Funt, K.D. Fowler, S. Bakshi, E. Blaugrund, M.N. Artyomov, M.R. Hayden, D. Ladkani, R. Schwartz, B. Zeskind, Comparing the Biological Impact of Glatiramer Acetate with the Biological Impact of a Generic, *Plos One* 9(1) (2014).
- [183] [https://www.nationalmssociety.org/About-the-Society/News/FDA-Approves-Two-New-Generic-Forms-of-Copaxone%C2%AE-\(G](https://www.nationalmssociety.org/About-the-Society/News/FDA-Approves-Two-New-Generic-Forms-of-Copaxone%C2%AE-(G).
- [184] J. Zhao, E.J. Koay, T.T. Li, X.X. Wen, C. Li, A hindsight reflection on the clinical studies of poly(L-glutamic acid)-paclitaxel, *Wiley Interdisciplinary Reviews-Nanomedicine and Nanobiotechnology* 10(3) (2018).
- [185] <https://www.ich.org/>.
- [186] ICH Q7 Good Manufacturing Practice Guide For Active Pharmaceutical Ingredients.
- [187] R. Luxenhofer, Polymers and nanomedicine: considerations on variability and reproducibility when combining complex systems, *Nanomedicine* 10(20) (2015) 3109-3119.
- [188] R.M. Crist, J.H. Grossman, A.K. Patri, S.T. Stern, M.A. Dobrovolskaia, P.P. Adisheshaiah, J.D. Clogston, S.E. McNeil, Common pitfalls in nanotechnology: lessons learned from NCI's Nanotechnology Characterization Laboratory, *Integrative Biology* 5(1) (2013) 66-73.
- [189] P.P. Adisheshaiah, J.B. Hall, S.E. McNeil, Nanomaterial standards for efficacy and toxicity assessment, *Wiley Interdisciplinary Reviews-Nanomedicine and Nanobiotechnology* 2(1) (2010) 99-112.
- [190] R.F.T. Stepto, Dispersity in polymer science (IUPAC Recommendation 2009) International union of Pure and Applied Chemistry, Polymer Division, Sub-Committee on Polymer Terminology, *Polymer International* 59(1) (2010) 23-24.
- [191] M. Talelli, M. Barz, C.J.F. Rijcken, F. Kiessling, W.E. Hennink, T. Lammers, Core-crosslinked polymeric micelles: Principles, preparation, biomedical applications and clinical translation, *Nano Today* 10(1) (2015) 93-117.
- [192] B.S. Kendrick, B.A. Kerwin, B.S. Chang, J.S. Philo, Online size-exclusion high-performance liquid chromatography light scattering and differential refractometry methods to determine degree of polymer conjugation to proteins and protein-protein or protein-ligand association states, *Analytical Biochemistry* 299(2) (2001) 136-146.
- [193] R. Garcia-Lopera, A. Codoner, M.C. Bano, C. Abad, A. Campos, Size-exclusion chromatographic determination of polymer molar mass averages using a fractal calibration, *Journal of Chromatographic Science* 43(5) (2005) 226-234.
- [194] <https://www.malvernpanalytical.com/en>.
- [195] A. Bisio, A. Mantegazza, D. Vecchiotti, D. Bensi, A. Coppa, G. Torri, S. Bertini, Determination of the Molecular Weight of Low-Molecular-Weight Heparins by Using High-Pressure Size Exclusion Chromatography on Line with a Triple Detector Array and Conventional Methods, *Molecules* 20(3) (2015) 5085-5098.
- [196] J.T. Oberlerchner, T. Rosenau, A. Potthast, Overview of Methods for the Direct Molar Mass Determination of Cellulose, *Molecules* 20(6) (2015) 10313-10341.
- [197] H.Y. Zhao, P.H. Brown, P. Schuck, On the Distribution of Protein Refractive Index Increments, *Biophysical Journal* 100(9) (2011) 2309-2317.

CHAPTER II: AMPHIPHILIC POLYAMINO ACID BASED MICELLES FOR DRUG DELIVERY

Some parts of this chapter has been censured in order to protect the “know-how” of the manufacturing process strategy and analytical techniques to produce and analyze Poly(Amino Acid) based materials at R&D level developed by Polypeptide Therapeutic Solutions S.L.

1. INTRODUCTION

1.1. BRIEF INTRODUCTION TO POLYMERIC MICELLES BASED ON APAA MATERIALS IN DRUG DELIVERY

1.1.1. BASIC CONCEPT OF APAA-BASED MICELLES

The International Union of Pure and Applied Chemistry (IUPAC) defines a micelle as “an aggregate of colloidal dimensions formed by surfactants in solutions, which exists in equilibrium with the molecules or ions from which they are formed”, and a polymeric micelle is defined as “a micelle formed by one or more block or graft copolymers in a selective solvent” [1]. In more detail, a polymeric micelle can be described as a nanoscopic core/shell structure formed by amphiphilic block copolymers containing two parts (i) **hydrophilic part** (also called water-soluble or polar part) and (ii) **hydrophobic part** (also denominated lipophilic, water-insoluble, or non-polar part). When the block copolymers are composed of amino acid monomers, the polymeric micelle can be named amphiphilic polyamino acid (APAA) micelle (see Figure 2.1). Both the inherent and modifiable properties of polymeric micelles make them particularly well-suited for drug delivery purposes [2]. Micelles are usually formed in aqueous media since the self-assembly is driven by the entropy gain associated with the dehydration of the hydrophobic moieties and the resultant hydrophobic associations [3], as described in the general introduction

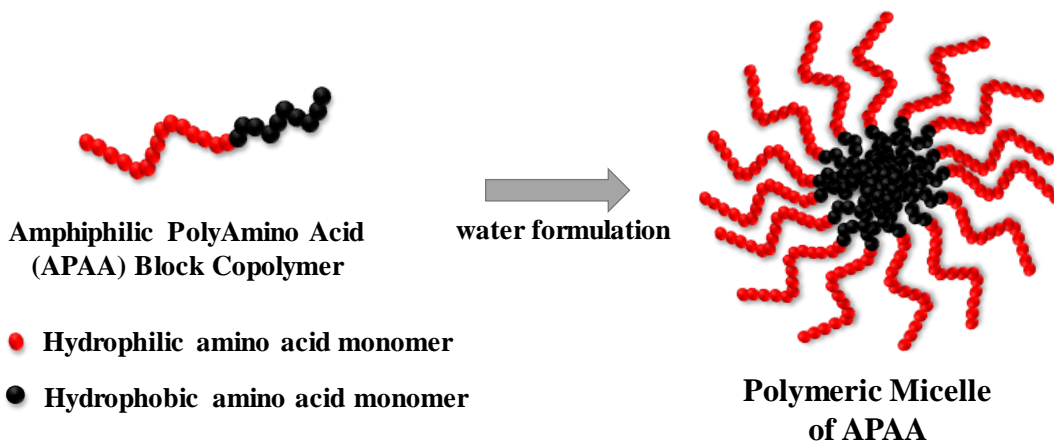


Figure 2.1. Polymeric Micelle based on Amphiphilic PolyAmino Acid (APAA) block copolymer composition.

1.1.2. API-APAA MICELLE INTERACTION: COVALENT AND NON-COVALENT

One of the main uses of the APAA-based micelles is as a vehicle to transport APIs for nanomedical applications [4], which means that APAA-based micelles are used commonly as a drug carrier in drug delivery. APIs can be incorporated within micellar

structures via covalent interactions or physical (non-covalent) interactions as described in the general introduction [2, 5]. Actives that are incorporated via chemical bond to the PAA, are considered NCEs and the formation of micelles is driven by the amphiphilicity as a result of the PAA-API construct rendering an APAA-based micellar system that is considered a drug substance [6]. The covalent conjugation of drugs to polymers or copolymers has been widely reported for various types of drugs. These covalent bonds are normally hydrolyzable amide/ester bonds [7], or stimulus-sensitive bonds such as pH-sensitive linkage, (Schiff base, azomethine or hydrazone bond), or enzyme-sensitive linkage [glycine-leucine-phenylalanine-glycine (GLFG) linker] [5].

On the other hand, if the API-carrier interaction is physical, the APAA-based micelle is considered as an excipient instead of a drug substance. This non-covalent interaction can be enabled via (i) hydrophobic interactions between hydrophobic blocks on the carrier with a hydrophobic API [5], (ii) electrostatic interactions using aa monomers with an electrostatic charge, such as Glu and Asp for negative charges [8, 9] or Lys, His, Arg [8, 9] and Orn for positive charges [10], and (iii) polymer-metal ion coordination [5].

Importantly, the APIs or drug substances within this approach are normally hydrophobic or lipophilic, so they can be included in the architecture of the hydrophobic part of the micelle for APAA-based micelles by chemical interactions. For physical interactions, the API is incorporated in the micellar core, retained by non-covalent forces yielding its encapsulation and transport. Some examples of this include doxorubicin, paclitaxel, rapamycin, resveratrol, vitamin E, and cisplatin among others [4, 5, 11].

1.2. DRUG DELIVERY APPLICATIONS OF APAA-BASED MICELLES AND THE IMPORTANCE OF PEG AND ITS ALTERNATIVES

Polymeric micelles are used to combat various ailments, including cancers, HIV/AIDS, malaria, multiple sclerosis, hypertension, infectious diseases, cardiovascular and metabolic diseases, immune disorders and many psychiatric disorders [6, 12-15]. See Table 1.1 in the general introduction to find examples.

To remark, polymeric micelles have also achieved breakthroughs in the clinics. APAA-based micelles have reached advanced clinical stages such as the NK105, a 85 nm PEG-b-poly(α,β -aspartic acid) micelle encapsulating Paclitaxel is in Phase III clinical trials for Gastric and breast cancer. Also, the NK012, a 20 nm PEG-b-poly(L-glutamic acid) of SN-38 is in Phase II for the treatment of Triple negative breast cancer. The NC-6300, a 60 nm PEG-b-poly(aspartatehydrazone) loaded Epirubicin is in Phase I for various solid tumors. And the NC-6004, a 20 nm PEG-block-poly(L-glutamic acid) Cisplatinmicelle is being studied in Phase III trials for pancreatic cancer [16].

As it can be seen in the clinical examples given above, Poly(ethylene glycol) (PEG), also called poly(ethylene oxide) (PEO), is the most widely-employed polymer in the hydrophilic water-soluble block in drug delivery [17]. Most conjugated drugs, as well

as liposomal and micellar formulations on the market or in advanced clinical trials, are PEG-containing products and these products are termed PEGylated products [18]. This means that these products have been approved by the health authorities such as FDA and EMA during the last 20 years. The fact that PEG is the main polymer employed in drug delivery is related to the multiple advantages of this material.

Ideally, a biodegradable polymer would be more beneficial in medical applications to avoid difficulties in achieving complete excretion, although other issues, such as the toxicity of degradation products and the limited shelf life, would need to be considered [17]. In general, polymers with low PDI are a basic requisite for pharmaceutical applications and for PEG polymers this is not a problem, given that the PEG manufacturing process is widely optimized to obtain Mw from 400 Da to 50 kDa with PDIs of below 1.1, or even 1.01 [17]. This is one of the main reasons, if not the most important reason, for the wide use of PEG, because of its commercial availability and sufficient quality for a wide range of molar masses with good PDI values [19]. However, it should be kept in mind that the excretion of the polymer is not directly dependent on the molar mass of the polymer, unless it is related to the hydrodynamic size, which is affected by the architecture of the vehicle in the drug delivery [17].

Scientists and researchers use PEG as the golden standard for hydrophilic segments in their drug delivery vehicles, since PEG gives supramolecular architectures a “conformational cloud”. This “conformational cloud” can be defined as a “cloak of invisibility”, and is generated by the highly flexible ethylene glycol chains, which have a large number of possible conformations. The higher rate of transition from one conformation to another means that the polymer exists statistically as a “conformational cloud” which prevents interactions with blood components, as well as protein interactions such as enzymatic degradation or opsonization followed by uptake by the RES [20]. This fact increases the circulation time of the drug vehicle and allows its accumulation in the target site of action. In addition, decreased interactions with the body means that the PEGylated products show less immunogenicity and antigenicity [17].

Furthermore, from a manufacturing point of view PEG shows high solubility in organic solvents and, therefore, end-group modifications are relatively easy. At the same time, PEG is soluble in water and when attached to hydrophobic drugs or carriers, the hydrophilicity of PEG increases their solubility in aqueous media, providing drugs with a greater physical and thermal stability as well as preventing or reducing aggregation of the drugs *in vivo* [17].

The success of PEG in drug-delivery applications also drives its use in other medical fields. Thus, PEG is used in blood and organ storage, where it reduces the aggregation of red blood cells and improves the blood compatibility of poly(vinyl chloride) bags [21]. PEG copolymers that are implanted as cardiovascular devices, such as stents, decrease thrombosis [22]. Furthermore, PEG is not only used in pharmaceutical

preparations as an excipient for parenteral, topical, nasal, and ocular applications, it is also used as the active principle ingredient in laxatives or cosmetics [17].

However, PEG also shows drawbacks in its uses [17]. There are many publications about the advantages and drawbacks of PEG, as well as its alternatives for drug delivery applications. In 2010, an extensive review called “*Poly(ethylene glycol) in Drug Delivery: Pros and Cons as Well as Potential Alternatives*” was published by Knop, Hoogenboom, Fischer and Schubert [17]. The following year, in 2011, Barz, Luxenhofer, Zentel and Vicent published an excellent review talking about overcoming the PEG-addiction, employing well-defined polymers as new alternatives to PEG [19]. In 2013 Hatakeyama et al reported the “*PEG dilemma*” for liposomes in gene delivery [23]. Zhang and co-workers in 2014 discussed this topic for therapeutic proteins [24]. Recently (2017), Fang et al wrote about the strategy for overcoming the “*PEG dilemma*” to achieve an efficient drug delivery system [25]. Finally, in 2020 Kozma, Shimizu, Ishida and Szebeni published a review about anti-PEG antibodies, explaining their properties, formation, testing, and role in adverse immune reactions for PEGylated nanobiopharmaceuticals materials [26].

The high use of PEG and PEGylated products in clinical trials and applications, as well as pharmaceutical research, not only provides new knowledge about the mechanism of the beneficial properties. It also increases the possibility to find potential undesired reactions [17]. The rise of anti-PEG antibodies, both in animal models and in patients, were observed in pre-clinical and clinical assays with different PEGylated drugs. These anti-drug antibodies may neutralize the therapeutic effect of the drug and thereby reduce its clinical efficacy. Furthermore, the mentioned anti-PEG antibodies may cause adverse immune effects. Specifically, an acceleration of the blood clearance of the PEGylated drug (ABC phenomenon), resulting in a loss of efficacy, and hypersensitivity reactions which can lead to anaphylactic shock, and even death [26].

The essence of the ABC phenomenon is based in the case of repeated dosis administration (e.g. injections) with PEGylated materials, the second and subsequent doses display progressively decreasing circulation time, and hence, reduced efficacy and PEG accumulation in the organism [26].

Hypersensitivity has been reported using PEG-based materials as an immunological response when the PEGylated products are applied by the three main administration pathways: (i) intravenous, (ii) oral, and (iii) dermal. Adverse side effects in the body can be driven by the polymer itself or by side products formed during synthesis that lead to hypersensitivity. Moreover, unexpected changes in pharmacokinetic behavior can occur with PEG-based drug delivery carriers [17].

In the last two decades, a multitude of new methods for controlled polymerization have been established, such as atom transfer radical polymerization (ATPR), reversible addition fragmentation chain transfer (RAFT) and nitroxide mediated polymerization

(NMP) [19], as well as the aforementioned ROP [12, 27]. This has allowed scientists to obtain a tremendous number of well-defined polymer architectures that can be used to compete with PEG in drug delivery [19]. Some examples are: (i) **glycopolymers**, such as poly(glycerol), (ii) **poly(2-oxazoline)s** [e.g. poly(2-methyl-2-oxazoline)], (iii) **vinyl polymers** involving the poly(meth)acrylates, also called poly(meth)acrylamides, such as poly(acrylamide), poly(vinylpyrrolidone) and the most important, poly(*N*-(2-hydroxypropyl) methacrylamide) (PHPMA) [17, 19], (iv) **polypeptides** or **PAA** fully described in this thesis work (e.g. PAsp, PGlu, PLys, PArg, PHis [12, 15, 19], and also poly-L-methionine sulfoxide (PMet(O)) [28-30] and glyco-poly-L-lysine [31, 32]; or (v) **polypeptoids** such as polysarcosine [33, 34].

Peptides and peptoids were not separated in early publications. In 1992, Bartlett defined peptoids as oligomers of *N*-substituted glycines, and later Zuckermann introduced the term polypeptoids for 30 – 36 units of peptoids, establishing the commonly accepted terminology [33]. Polysarcosine (PSar) is the simplest polypeptoid, and incidentally also shows the highest water solubility [34], making it a biodegradable alternative to PEG.

PSar polymers contain multiple units of the naturally occurring amino acid sarcosine (*N*-methyl glycine) which can be found in our muscles and other tissues in concentrations ranging from 0.6 to 2.6 $\mu\text{mol/L}$. Sarcosine is an intermediate in the natural glycine metabolism starting from choline and betaine, which provide methylation equivalents from dietary intake, especially from meat [33]. Although the first polysarcosine synthesis by Wesseley et al was reported almost a century ago [35], it is only recently that PSar has gained high attention and has been considered a potential alternative of PEG.

As a polymer, PSar shares certain properties of PEG, such as excellent solubility in water, protein resistance, low cellular toxicity, and a non-immunogenic character, but with the important exception that it is biocompatible and biodegradable since it's made up of endogenous monomers [33]. Regarding its manufacturing process, PSar can be obtained by several techniques just like other PAA such as biosynthesis, polycondensation, solid-phase peptide synthesis and of course by ROP of NCAs via NAM, with the last technique being the most employed [34].

In 2018 Birke, Ling and Braz published a very complete review regarding the use of polysarcosine in copolymers [33]. The authors explained the combination of PSar with polyethers, polyesters, polysaccharides, or with other polypeptoids as well as PAA in block or graft topologies. They also illustrated the self-assembly of the PSar-containing copolymers in micelles, vesicles, nanotubes, nanosheets and hydrogels, as well as their use as antifouling surfaces and in drug delivery, tumor imaging, gene therapy and targeted delivery. Regarding the biological data, the authors conclude that PSar has displayed comparable properties to PEG in biomedical applications. It can reduce protein adsorption on surfaces, may effectively prevent aggregation of nanoparticles in complex body fluids, and can shield sensitive bioactive agents from degradation. Although degradation and

metabolism of the polypeptoid are not yet understood, PSar seems to avoid acute immune responses and acute toxicity, which overall indicates that PSar may become more than a mere alternative to PEG [33].

In 2020, a very interesting article about polysarcosine-functionalized lipid nanoparticles for therapeutic mRNA delivery was published. The authors demonstrated how higher protein secretion with a reduced immunostimulatory response was observed when using PSar-lipid systems compared with PEG-lipids. Moreover, they illustrated how the PSar materials showed a lower proinflammatory cytokine secretion and reduced complement activation compared to PEGylated nanoparticles. The researchers described their PSar-based lipid nanoparticles as a safe and potent carrier for mRNA delivery, thus signifying an excellent basis for the development of PEG-free RNA therapeutics [36].

1.3. MICELLE FORMULATION

Polymeric micelles employed in drug delivery require loading with drug or API molecules. Most of the reported applications of polymeric micelles have focused on the delivery of hydrophobic drugs [5].

In 2005, Gaucher et al published an excellent review to prepare block copolymer micelles. Although they did not describe any APAA, the methodologies described can be applied to any kind of block copolymer. Depending on the physicochemical properties of the block copolymer, two main classes of drug-loading procedures can be applied. The first class, named the **direct solution or direct method**, involves the direct mixture of the block copolymer together with the drug in an aqueous solvent. This procedure is mostly employed for moderately hydrophobic copolymers. Sometimes this technique requires heating of the aqueous solution to promote micelle formation via the dehydration of the core-forming segments [37].

The second category is **drug-loading through organic solvents**. This procedure applies to amphiphilic copolymers which are not readily soluble in water, and for which an organic solvent common to both the copolymer and the drug (such as DMSO, DMF, acetonitrile, THF, acetone or dimethylacetamide) is needed. The mechanism by which micelle formation is induced depends on the solvent removal procedure. For water-miscible organic solvents, the copolymer-API mixture can be dialyzed against water, whereby slow removal of the organic phase triggers micellization. This method can be called **co-solvent**. Alternatively, the other method is the evaporation of the organic phase to yield a polymeric thin film where block copolymer–drug interactions are favored. Then, this film between block copolymer and API is dissolved in water yielding the micelles. This method can be named **thin-film**. Physical entrapment of a hydrophobic drug may be further achieved through an **oil-in-water (O/W) emulsion process** which involves the use of a non-water-miscible organic solvent (dichloromethane, ethyl acetate). Figure 2.2. illustrates these commonly employed drug incorporation methods [37].

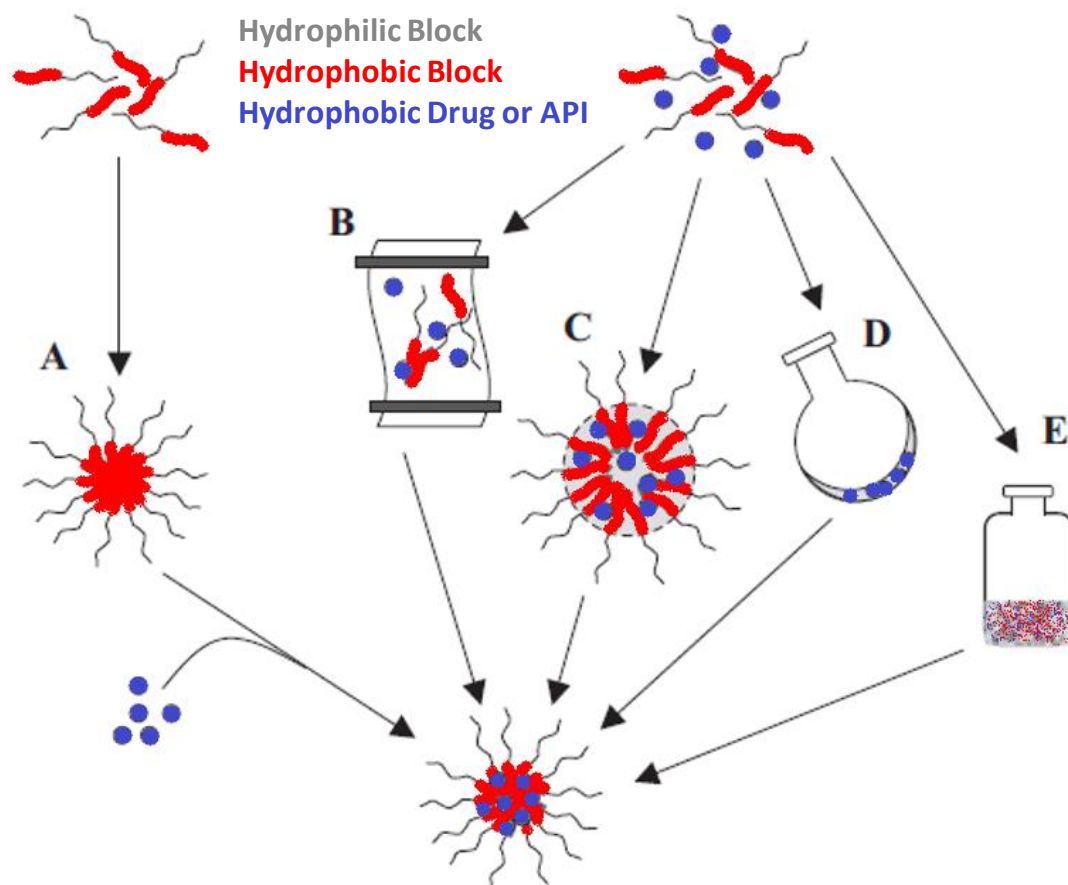


Figure 2.2. Common drug-loading procedures for block copolymer micelles: (A) direct method, (B) co-solvent, (C) O/W emulsion, (D) thin-film, and (E) freeze-drying. Figure adapted from Gaucher et al [37].

1.4. DESIGN OF APAA MICELLES IN THE PRESENT WORK

As described in the general introduction, the use of APAA produced by ROP of NCA aa monomers via NAM allows us to finetune and modulate certain properties to drive hydrophobic API/drug encapsulation in the polymeric micelles, facilitating delivery to the target body place. This is done by applying all the scientific knowledge previously described taking into account the *physico-chemical parameters* such as the **size** (small or large), **electrostatic charge** (positive, negative, neutral or zwitterionic), **conformation** (alpha-helix, beta-sheet, random coil, etc.), **geometry** (sphere, nanotube, etc.), **topology** (linear, star, graft or branched) and **monomer composition** (homo, random, or block), as well as the *structural elements* such as the **interaction between APAA and API** [chemical (covalent) or physical (non-covalent)] and the **supramolecular architecture of the micellar system** (classical, cross-linked, PIC or layer-by-layer).

1.4.1. APAA BLOCK COPOLYMERS COMPOSITION

It is well known that polymers can be classified according to several properties such as the number of monomers, their origin, the structure, the process to obtain them, etc. In agreement with what many researchers and scientists describe in the literature, the polymeric materials in the present work will be classified by the nature of the electrostatic

charge of the hydrophilic block [9], and the secondary structure of the hydrophobic block [38].

For the electrostatic charge of the hydrophilic block, 4 families are described: (i) **neutral** using polymers without an electrostatic charge (PEG [17, 19, 39] and PSar [33, 34]), (ii) **negative** using anionic aa (PGlu) [40], (iii) **positive** using cationic aa (POrn) [10, 41] and (iv) **zwitterionic** containing a mixture of aa with anionic and cationic (random copolymer of Glu and Orn). For positive electrostatic charges, PArg [42] and PLys [40] were also developed, but only as homo PAA, not in the APAA. The PLys materials have been fully studied in the Chapter IV. For neutral electrostatic charges, the development with PEG was carried out in the first place. These block copolymers were selected to study their micellar properties employing Dil as a hydrophobic API model. Many researchers classify PEG-b-PAA as APAA block copolymers [8, 37].

Regarding the composition of the hydrophobic block, it is classified based on the secondary structure that each aa can adopt in aqueous solution, generally an alpha-helix or a beta-sheet. For **alpha-helix** the selected aa are Phe [43, 44] and benzyl-protected Glu (abbreviated to PGlu(OBzl) or PBG) [45]. It is widely reported that these moieties adopt the alpha-helix conformation in aqueous solution [46, 47]. To get the **beta-sheet** secondary structure conformation in water solution, the selected aa is Val [48-52].

1.4.2. SYNTHETIC APPROACH

All this section has been removed (censored) in order to protect the know-how of the company.

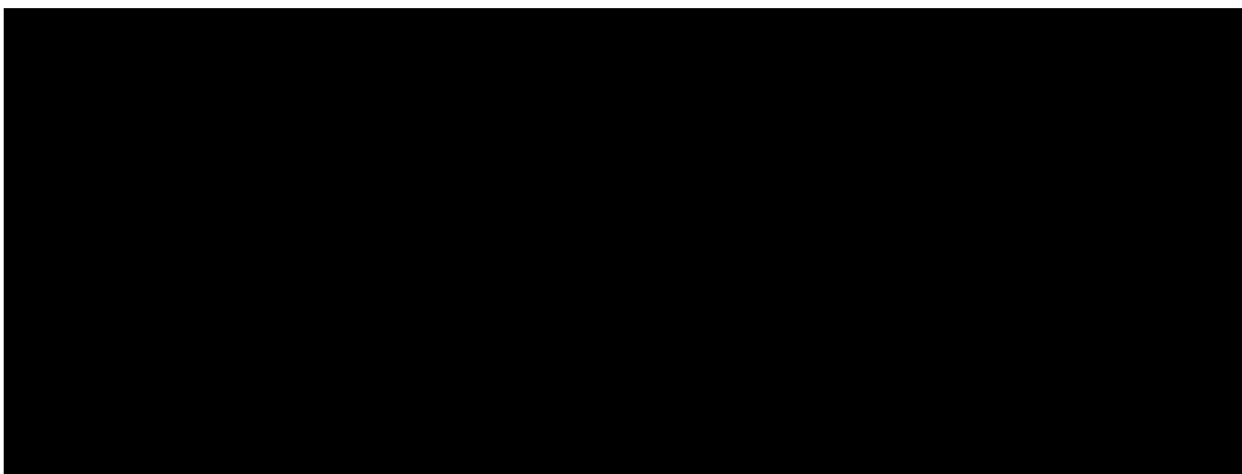


Figure 2.3. General synthetic approach to yield micelles of APAA.

1.5. EXPLORING OTHER KINDS OF POLYMERIC MICELLES: TOCOPHERSOLAN AND ITS BIODEGRADABLE ALTERNATIVE

Herein we have discussed polymeric micelles based on APAA materials and their derivatives with PEG and PSar. However, there are examples of other kinds of surfactants and micelles, for example micelles composed of amphiphiles containing a hydrophobic

tail and hydrophilic head which is the case of classical surfactants like sodium lauryl sulfate or sodium dodecyl sulfate [53]. As mentioned, PEG is the most hydrophilic polymer for this kind of material that can be used in drug delivery [54, 55]. One example of a Hydrophilic Polymer BioMolecule (HP-BM) is PEG-cholesterol. It is described that cholesterol-based PEGylated lipoplexes tend to accumulate mainly in hepatic tumors, and show great potential in gene therapy of liver diseases [55].

Another very interesting example of a well-known HP-BM PEGylated material is the D-alpha-tocopherol-poly(ethylene glycol)-succinate, also called **TPGS** or tocophersolan (see Figure 2.4). **TPGS** was invented by Eastman Kodak in 1950 [56], and is an amphiphilic polymer where the hydrophilic block is PEG, with neutral electrostatic nature, and the hydrophobic part is alpha-tocopherol, commonly called Vitamin E [57]. Alpha-tocopherol is a hydrophobic biomolecule that provides the lipophilic part of **TPGS** to grant its amphiphilic properties. The union between both products is achieved employing the succinate linker, a di-acid which is bonded to PEG at one end and to Vitamin E at the other, resulting in the conjugation from PEG to alpha-tocopherol. This process is widely described in literature [58].

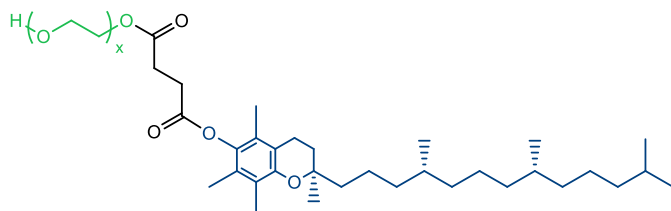
This hybrid compound has the properties of both components. On one hand, it is water soluble thanks to PEG. On the other hand, it has antioxidant properties and skin benefits due to the Vitamin E [59]. Therefore, this Vitamin E derivative was very important since it effectively provides with a form of water-soluble Vitamin E [57]. This product architecture extends the possible applications of Vitamin E in aqueous media such as serums or formulations, without needing to use extra excipients or additional products to help its solubility in water. Moreover, it is employed in the pharmaceutical field as an excipient in drug formulations [60] and also to generate pro-drugs and conjugates with doxorubicin or cisplatin [57]. Besides being used extensively in drug delivery systems, TPGS-based polymers can improve the drug encapsulation efficiency, intracellular uptake and therapeutic effect. Some examples include poly(lactic-co-glycolic acid) (PLGA)-TPGS or hyaluronic acid (HA)-TPGS [57].

The biological and physico-chemical properties of **TPGS** provide multiple advantages for its applications in drug delivery, like high biocompatibility, enhancement of drug solubility, improvement of drug permeation and selective antitumor activity. Especially, **TPGS** can inhibit the activity of ATP-dependent P-glycoprotein and act as a potent excipient for overcoming multidrug resistance in tumors [57]. Furthermore, its amphiphilic attributes such as hydrophilic-lipophilic (H-L) balance and relatively low Critical Aggregation Concentration (CAC), also called Critical Micelle Concentration (CMC) (0.02 %) make it a perfect molecule for drug delivery systems, including prodrugs, micelles, liposomes and nanoparticles [58, 61]. Importantly, **TPGS** is approved by the FDA [54]. In 2005, the FDA approved Tocosol® emulsion formulation of paclitaxel from Sonus Pharmaceuticals, Inc. Tocosol® was designed to treat nonsuperficial urothelial cancer. In this formulation, the **TPGS** is used to create the nanoparticles [61].

Taking into account the high range of applications for **TPGS** and its market niche in cosmetic [62], food [63] and pharmaceutical applications [58, 61], PTS has invested resources in the development of a biodegradable analog of **TPGS** based on PSar due to the drawbacks of PEG and the potential of PSar as an alternative as described above. Various researchers have directly compared PEG with PSar as a hydrophilic block in polymeric micelles. Specifically, in 2015 Huesmann and co-workers compared head-to-head PEG and PSar block copolymers with protected PAA Glu(OBzl) and PLys(Z) as the hydrophobic segment with the same DP. The authors found virtually the same CAC and the same Rh in aqueous solution by AFM and DLS for both PEG and PSar [64]. Furthermore, Chinese scientists have studied other biodegradable analogs to **TPGS** using hyaluronic acid instead of PEG [65]. Beyond micellar structures, in 2017 Heise and Lang found very similar results comparing PSar and PEG-based hydrogels [66]. Furthermore, in 2020 Japanese researchers reported interesting data about evading the ABC phenomenon employing a polysarcosine coating of liposome instead of PEG [67].

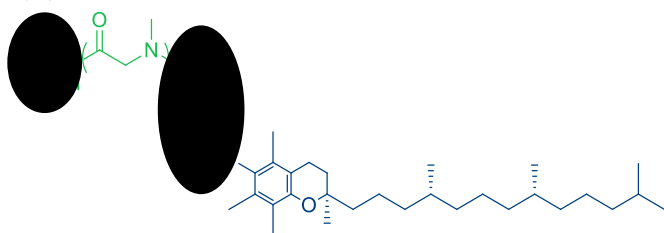
Comparing **TPGS** with its PSar-based analog fits perfectly within this thesis and within this chapter opening and exploring a new point for amphiphilic materials. This chapter contains the development and optimization of the manufacturing process of the **TPSS**, as well as the required analytical techniques (see Figure 2.4).

(A)



α -Tocopherol Poly(ethylene Glycol) Succinate (**TPGS**)

(B)



TPSS

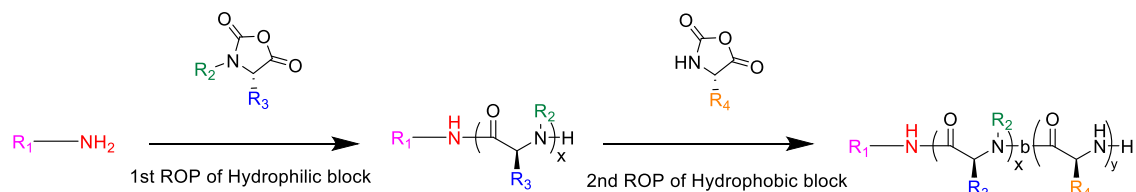
Figure 2.4. Nomenclature and chemical structures for (A) **TPGS** and (B) **TPSS**. Hydrophilic polymer (HP) and D-alpha-tocopherol BioMolecule (BM).

2. RESULTS AND DISCUSSION

In this chapter, the synthesis and development of several polymeric materials is explained within the POC stage, as well as the micellar properties for selected candidates. The selection of the APAA materials for the screening was made considering future scale-up processes. Moreover, a novel HP-BM material called **TPSS** was developed and compared with its commercial analog **TPGS** containing PEG instead of PSar.

2.1. DEVELOPMENT OF AMPHIPHILIC POLYAMINOACIDS (APAA) BY ROP OF NCAs THROUGH NAM

As stated in the introduction, the technology employed in the present thesis dissertation to achieve well defined PAA is the use of ROP techniques of NCAs monomers through NAM. The NCAs contain the protecting group of the residual chain commonly described in literature [12, 68-70]. The PAA selected for the hydrophilic part is obtained by ROP using the appropriate NCA. A schematic representation of this synthetic approach is shown below.



Scheme 2.1. General synthetic approach to yield PAA blocks through ROP of NCAs via NAM.

The PEG series was first developed using a 5kDa PEG (DP = 114) amine macroinitiator as the hydrophilic segment. To study the H-L balance, 3 ratios were prepared with DP 10, 20, and 40 for the hydrophobic block employing Glu(OBzl) and Phe as aa monomers. Analogously, these blocks also were prepared with a PSar of 100 units for the hydrophilic part. The APAA obtained for DP 20 and 40 of Phe showed bimodal distributions by SEC and low DP by NMR. For this reason, and also to simplify the number of compounds, the rest of the APAAs were designed only with a DP 10 for the hydrophobic chain. Regarding the length of the hydrophilic part, the DP selected was around 100 units for all materials to maintain consistency with the 114 PEG units. According to this architectural design, the development of hydrophilic blocks is first explained, followed by the amphiphilic PAA including the hydrophobic part.

All PAA and APAA synthesized were analyzed by NMR and, when possible, by SEC. For anionic, cationic and zwitterionic materials, the SEC analysis was found to be challenging. The nature of the mobile phase, in terms of solvent composition, ionic strength, and pH, as well as the stationary phase in the column all have a high impact on the sample elution, appropriate detection and analysis. Due to the high number of the synthesized materials, we only tested the routine base conditions for SEC, and when the samples were not soluble, they were analyzed only by NMR.

Below is a Table including all the APAA materials developed, synthesized and characterized. Moreover, in Figure 2.5, these block copolymers and the micellar structures can be observed, classified attending to their electrostatic charge and their secondary structure conformation as well as the DP for each block copolymer.

Table 2.1. Summary of block copolymers synthesized herein.

Short Name of Block Copolymer	Hydrophilic Electrostatic Charge	Hydrophobic Secondary Structure	aa for Hydrophilic Block	aa for Hydrophobic Block	DP of PAA for Hydrophilic Block	DP of PAA for Hydrophobic Block
PEG114-b-PCL (OP-D)10-20-40	N (4-1)	A1, I, II, V	EG*	CL (OP-D)	114	10-20-40

**AMPHIPHILIC POLYAMINO ACID
HYDROPHOBIC BLOCK**

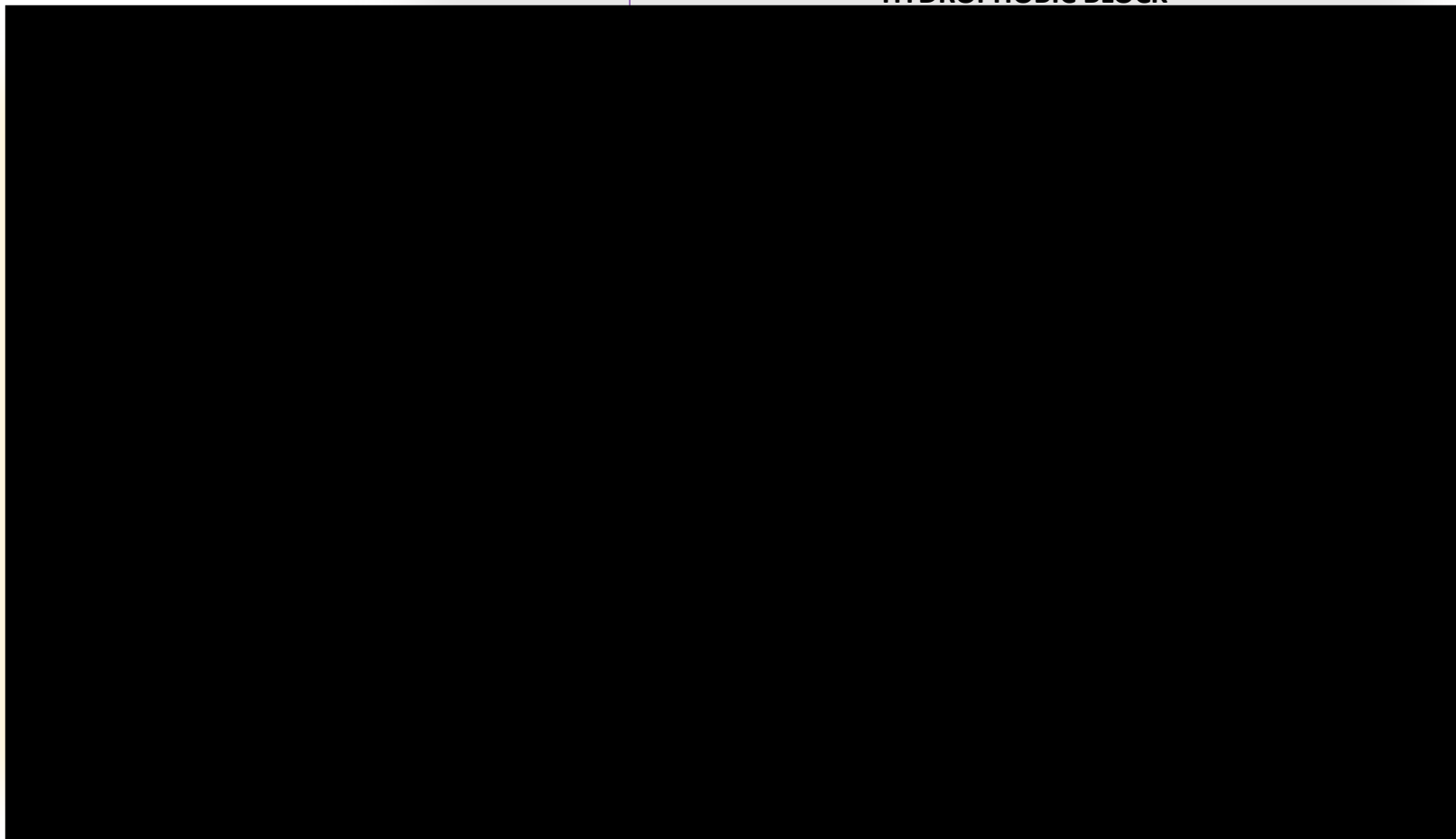


Figure 2.5. Summary of PAA, APAA and polymeric micelles synthesized containing the chemical structures and combined architectures.

2.1.1. HYDROPHILIC BLOCK DEVELOPMENT

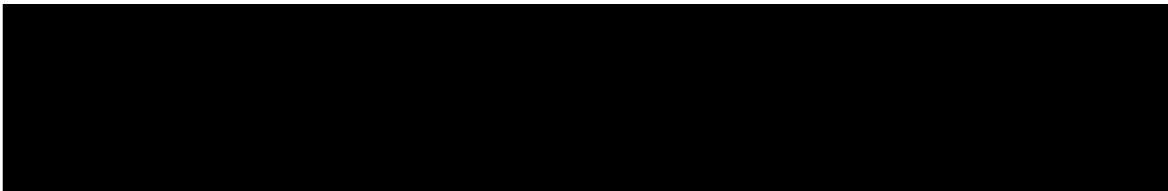
To build the APAA it is necessary to develop the hydrophilic and hydrophobic parts of the copolymer. First, the hydrophilic blocks were developed and classified attending to the nature of their electrostatic charge being 4: (i) **neutral**, (ii) **negative** (anionic), (iii) **positive** (cationic) and (iv) **zwitterionic** (a mixture of cationic and anionic).

PAA WITH NEUTRAL ELECTROSTATIC CHARGE

The polymers selected to use in the hydrophilic block of APAA with neutral electrostatic charge are PEG and PSar.

Poly(sarcosine) → PSar

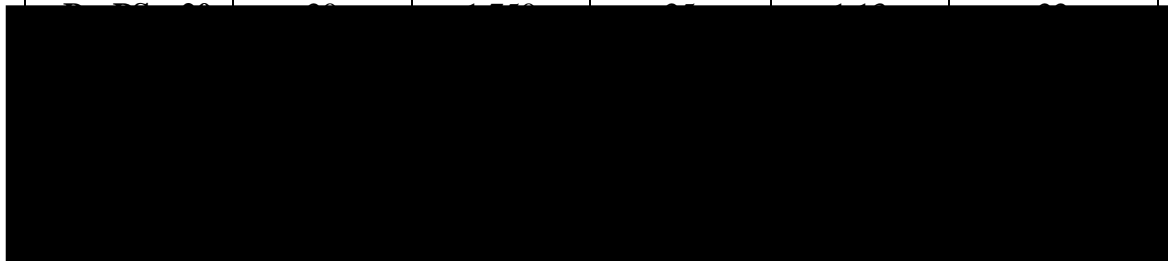
The synthesis of PSar is fully described and reported in the scientific literature [34]. Its uses in polymeric materials have been explored and developed in terms of block copolymers with polypeptoids, polypeptides, and polyesters, among others [33].



Scheme 2.2. General synthesis by ROP of NCA through NAM

Table 2.2. Results for series of PSar.

Product	Target DP	Mw (kDa) ^a	DP by Mw ^a	PDI ^a	DP by NMR ^b
---------	-----------	-----------------------	-----------------------	------------------	------------------------



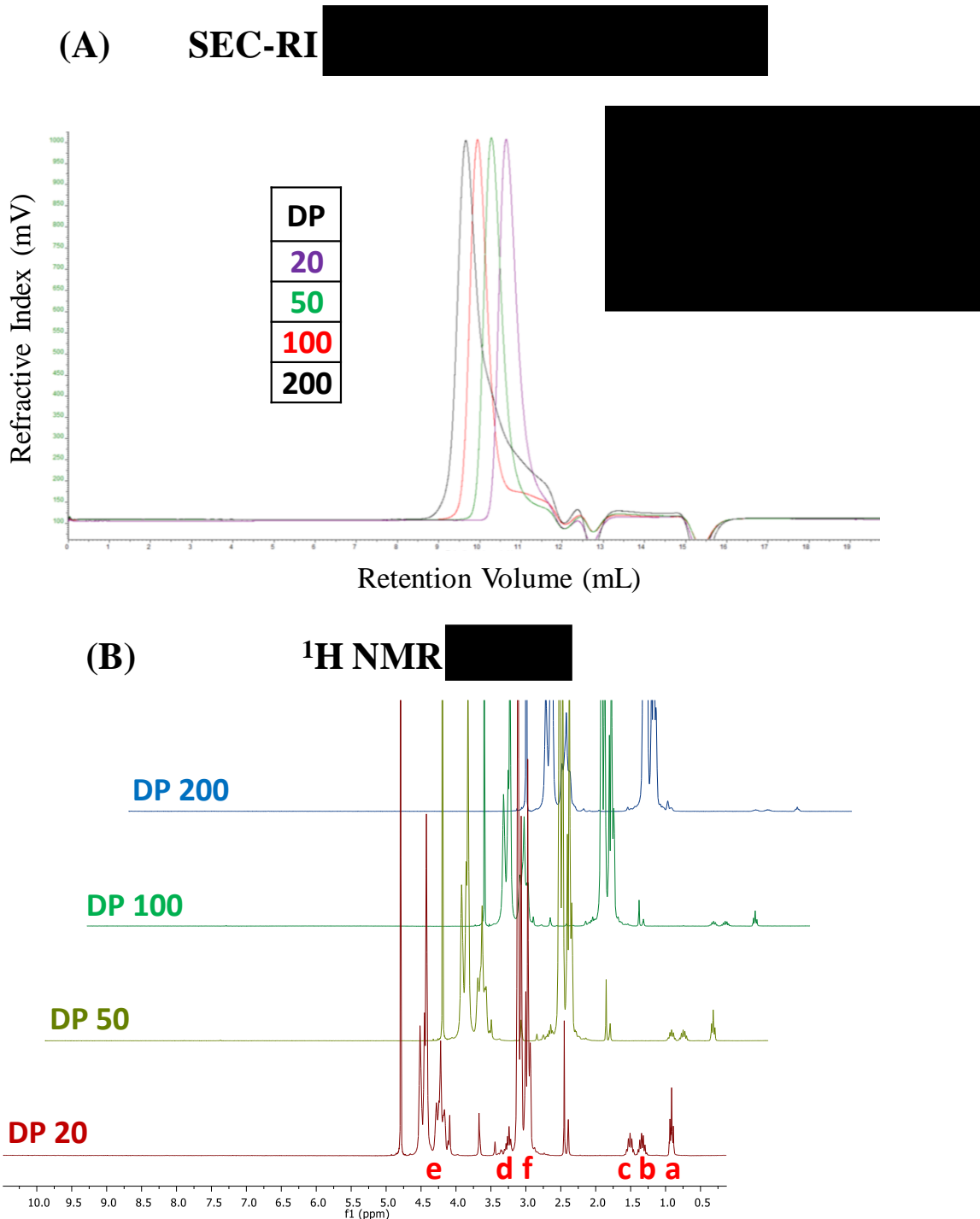


Figure 2.6. PSar series characterization (A) SEC. (B) ^1H NMR.

PAA WITH NEGATIVE ELECTROSTATIC CHARGE

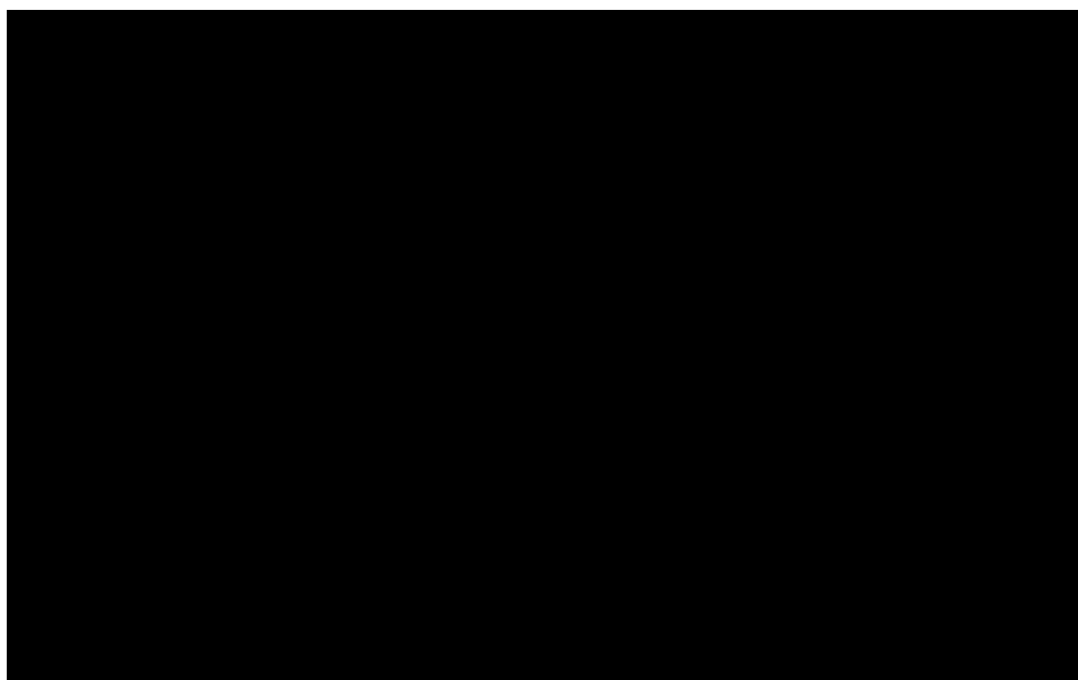
The selected aa to reach the PAA with a negative electrostatic charge is the L-glutamate.

Poly(L-glutamate) \rightarrow *PGlu*

Poly(L-glutamate) is a polyanion containing a negative electrostatic charge. This PAA is commonly used in its sodium salt form in biological assays due to its water solubility. The synthesis by ROP of NCAs and the applications of *PGlu* in the

nanomedicine field as a carrier for drug delivery are fully described and reported [71]. The fact that the residual chain is a carboxylic acid allows for varied chemical strategies to conjugate APIs to the polymer through chemical bonds such as amides or esters [72, 73].

The NCA monomers for glutamates required a protecting group for the carboxylic acid in the residual chain to avoid any interference in the polymerization. Normally, this protecting group is the –OBzl, and this is the group employed in this project. However, -OMe or -OtBu protecting group are also used [70]. The manufacturing process for PGlu has two steps: (i) polymerization and (ii) deprotection.



**Scheme 2.3. Polymerization: PGlu(OBzl) synthesis by ROP of NCA through NAM
Deprotection: PGlu(ONa) synthesis**

Table 2.3. Results for series of PGlu.

Product	Target DP	Protected Precursor PGlu(OBzl)				Sodium Salt form PGlu(ONa)	
		Mw (kDa) ^a	DP by Mw ^a	PDI ^a	DP by NMR ^b	Deprotection Yield by NMR ^c	DP by NMR ^c

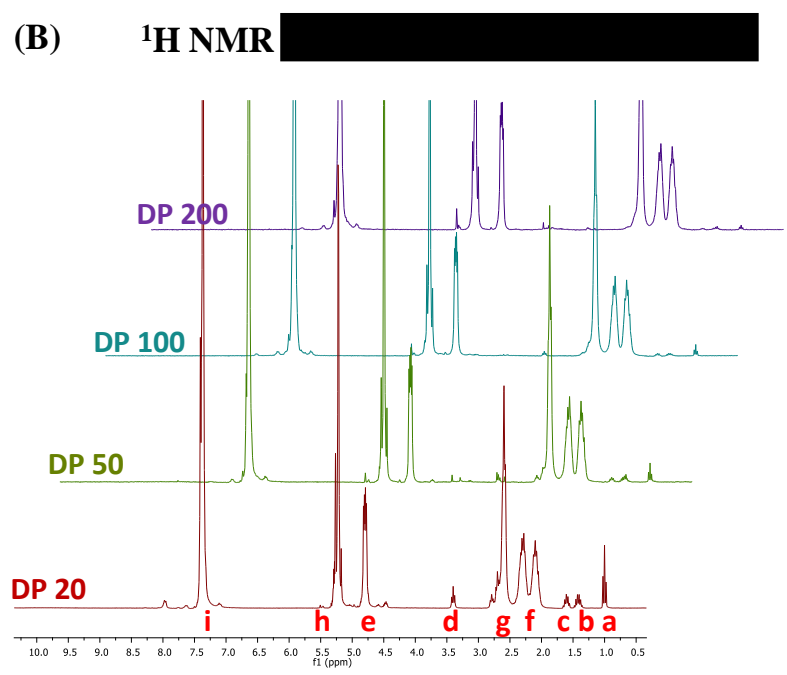
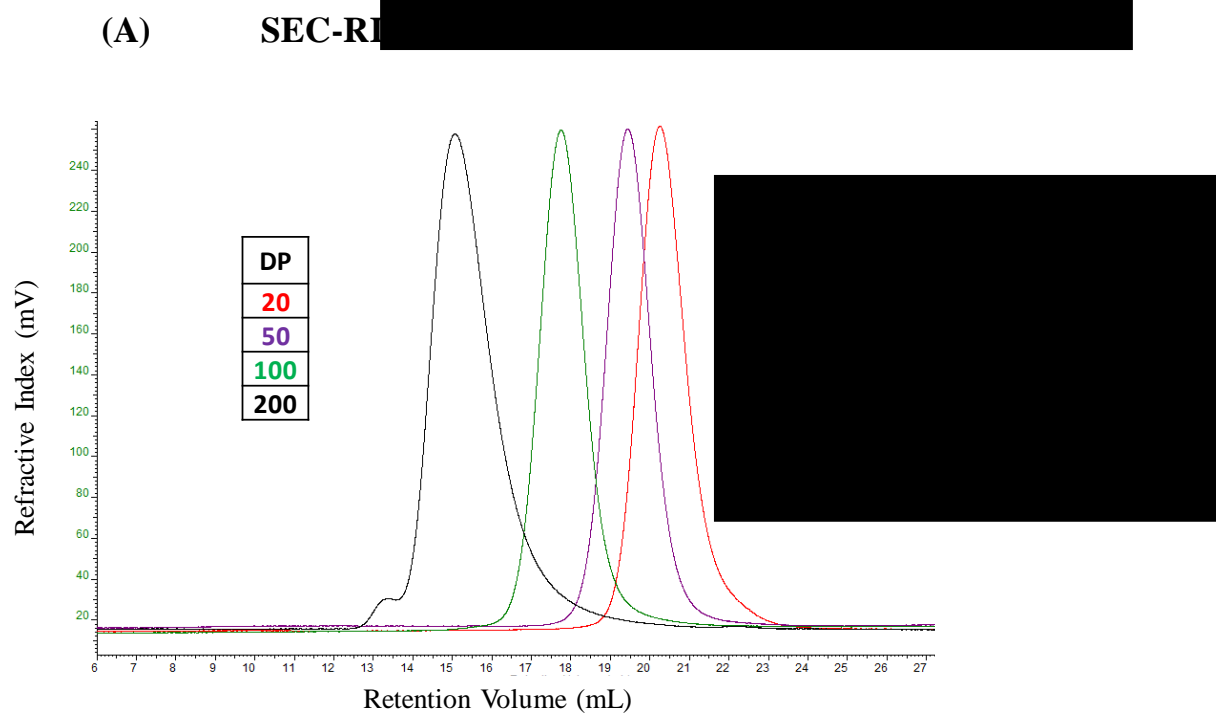


Figure 2.7. nBu-PGlu(OBzl) series characterization. (A) Overlap SEC-RI in DMF containing 0.1% of LiBr. (B) Overlap ¹H NMR in deuterated TFA (TFA-d₁) at 20 mg/mL.

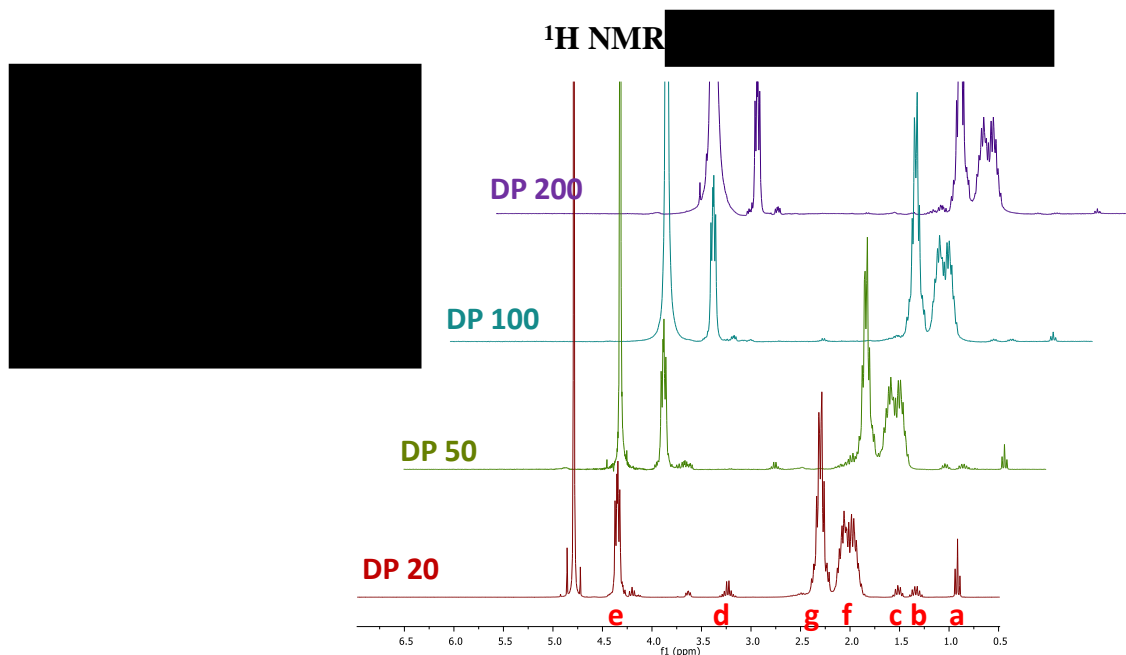


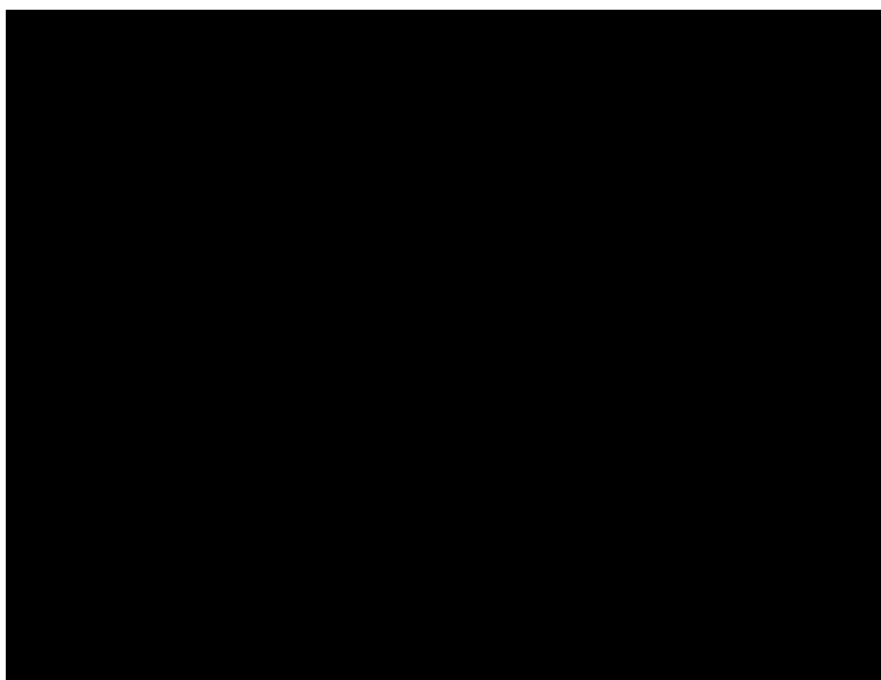
Figure 2.8. PGLu(ONa) series NMR characterization.

PAA WITH POSITIVE ELECTROSTATIC CHARGE

For the preparation of PAA with a positive electrostatic charge, several aa can be used, such as L-lysine (Lys), L-ornithine (Orn) or L-arginine (Arg). The first two present a primary amine in the residual chain, and Arg shows an inert guanidine group [12, 74]. In the present work, to produce the APAA we have selected POrn as the hydrophilic block with cationic nature, but the synthesis of PArg has also been explored and reported in this chapter due to their applications in drug delivery as previously mentioned. PLys is described in Chapter IV.

Poly(L-ornithine) → POrn

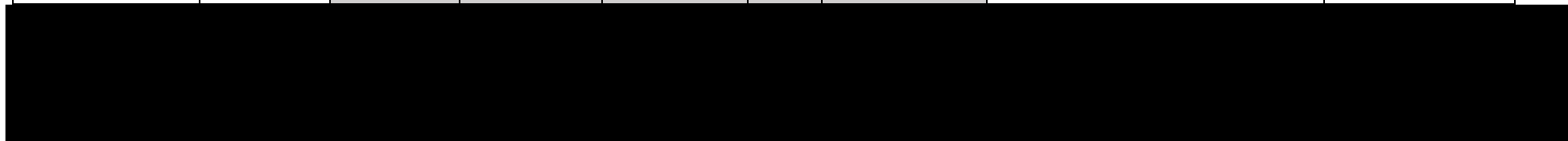
For the POrn we fixed the DP at 100 and we explored two L-Orn-NCA monomers. The synthetic route employed was based on that previously described for PSar and PGLu.



**Scheme 2.4. Polymerization: PO_{rn}(Z or Boc) synthesis by ROP of NCA through NAM
Deprotection: PO_{rn}(HBr) synthesis.**

Table 2.4. Results for POrn100.

Product	Target DP	Protecting Group	Protected Precursor POrn(Z or Boc)				Hydrobromic Salt form POrn(HBr)	
			Mw (kDa) ^a	DP by Mw ^a	PDI ^a	DP by NMR ^b	Deprotection Yield by NMR ^c	DP by NMR ^c



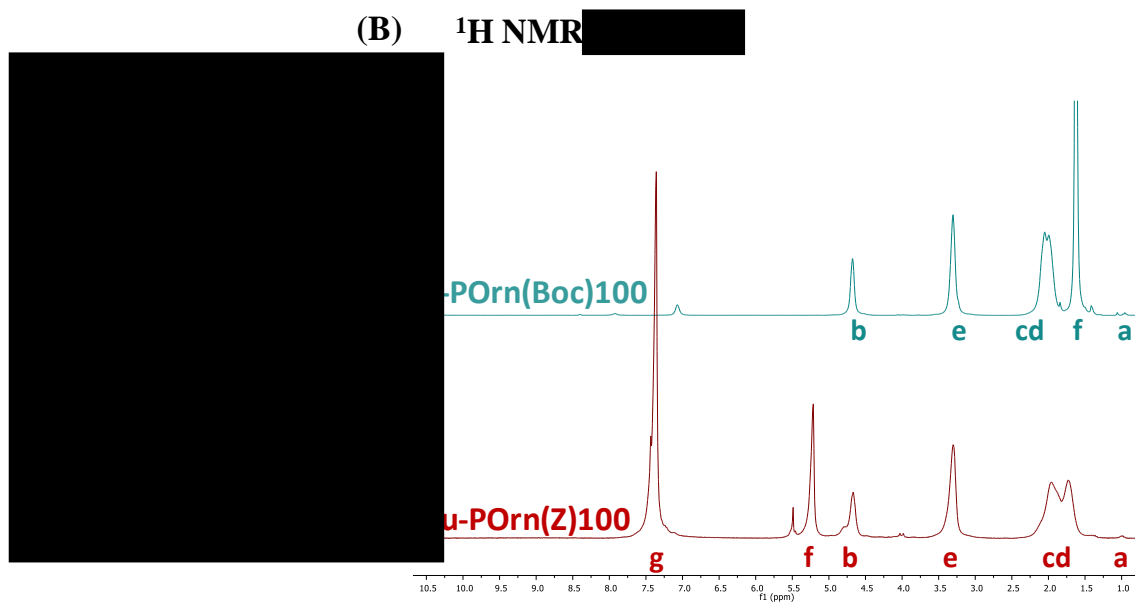
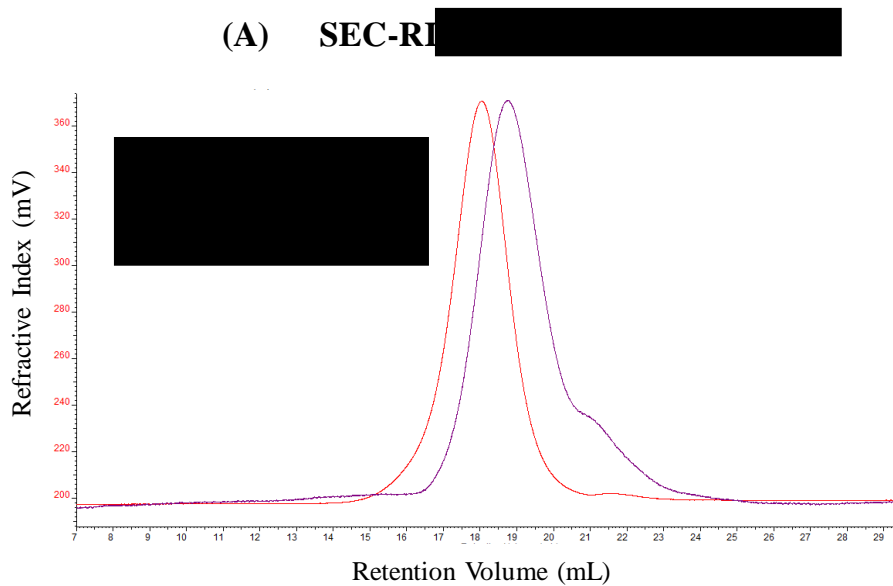


Figure 2.9. (A) Overlap SEC-RI in DMF containing 0.1% of LiBr. (B) Overlap ^1H NMR in deuterated TFA (TFA-d_1) at 20 mg/mL.

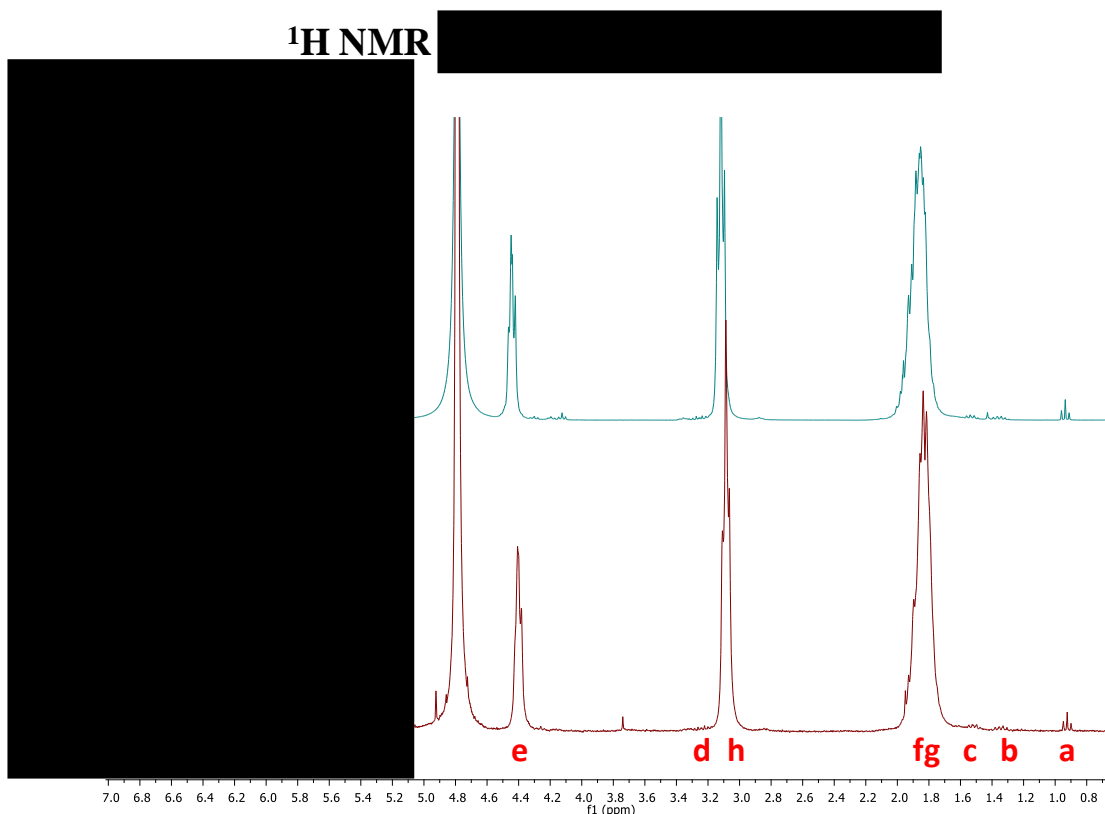
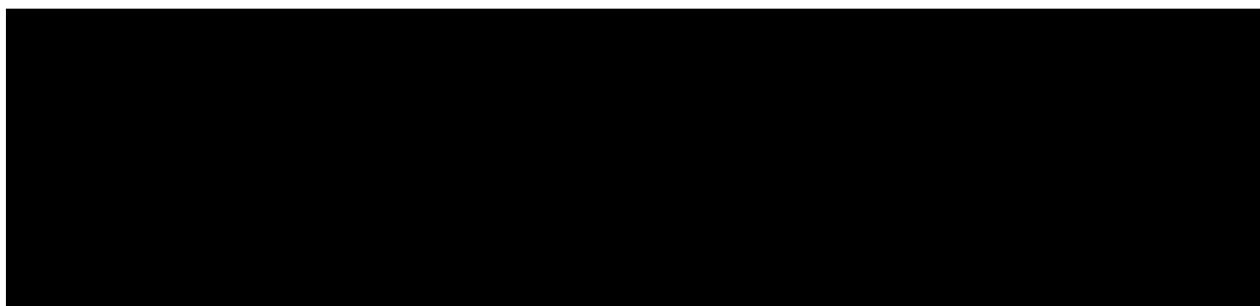


Figure 2.10. ¹H NMR in D₂O at 20 mg/mL for **nBu-POrn(HBr)100**.

Poly(L-arginine) → PArg

Once PO_{rn} was synthesized and optimized, the development of poly-L-arginine was also explored as another PAA containing a positive electrostatic charge. Although PArg is not used in the APAA design, PArg materials are very interesting for researchers in nanomedicine due to their uses and applications such as nanocapsule formation [75] or intracellular drug delivery [42].



Scheme 2.5. Synthetic scheme showing the guanidinzation of primary amines of PO_{rn} to yield the PArg.

NMR is a powerful tool to monitor the reaction and control the ratio between ornithine and arginine in the polycation.

Table 2.5. Results for PArg conversion from POrn.

Product	Triazole Equivalents	% Molar of Orn theoretical	% Molar of Arg theoretical	% Molar of Orn by NMR	% Molar of Arg by NMR
---------	-------------------------	----------------------------------	----------------------------------	-----------------------------------	--------------------------------

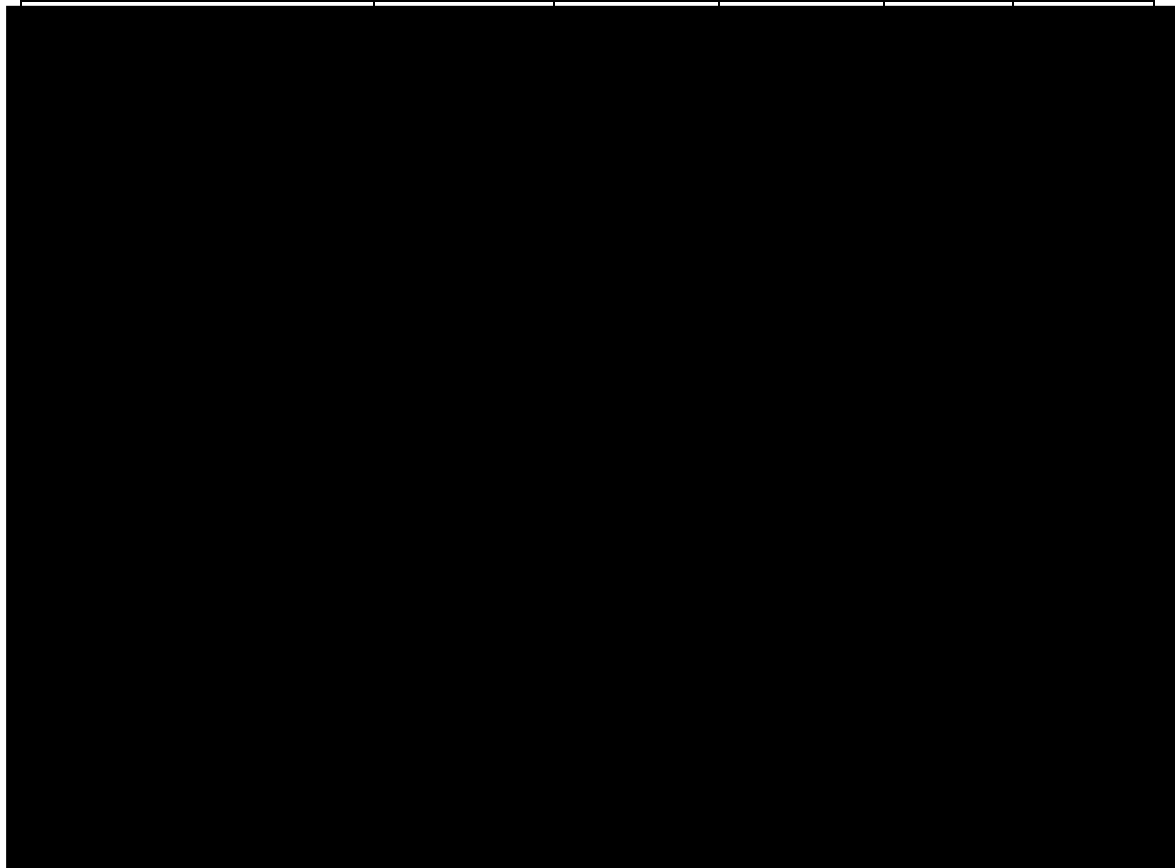


Figure 2.11. Overlap ¹H NMR

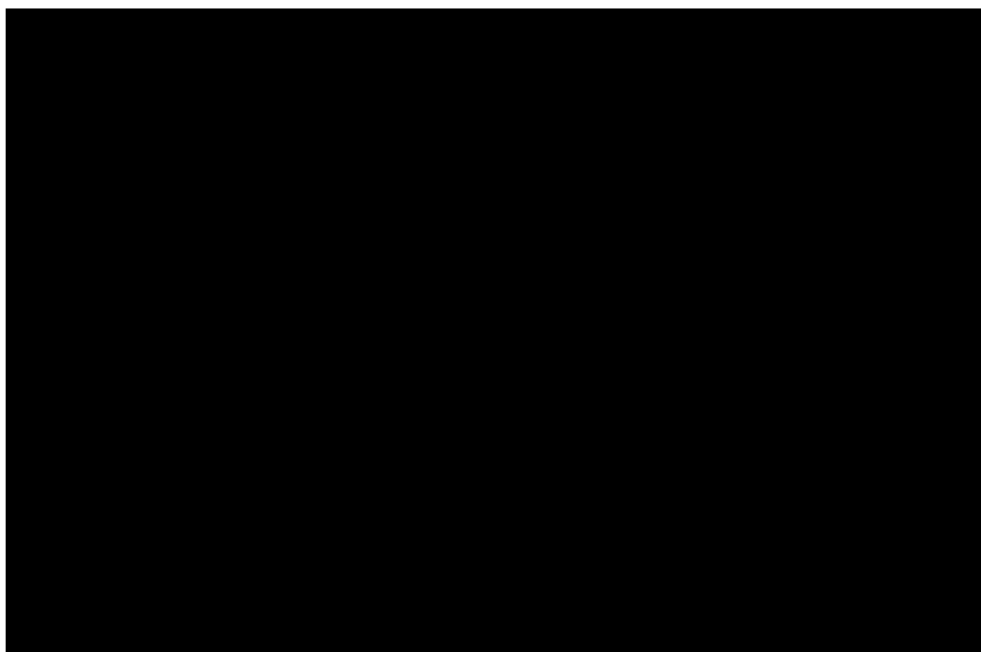
PAA WITH ZWITTERIONIC ELECTROSTATIC CHARGE

Zwitterionic block copolymers are widely employed in several applications such as pH-responsive vesicles [76]. Although this specific random copolymer between Glu and Orn is poorly described, zwitterionic PAA-based blocks of Glu and Lys are reported by the Lecommandoux group [76].

Poly(L-glutamate-co-L-ornithine) → P(Glu-co-Orn)

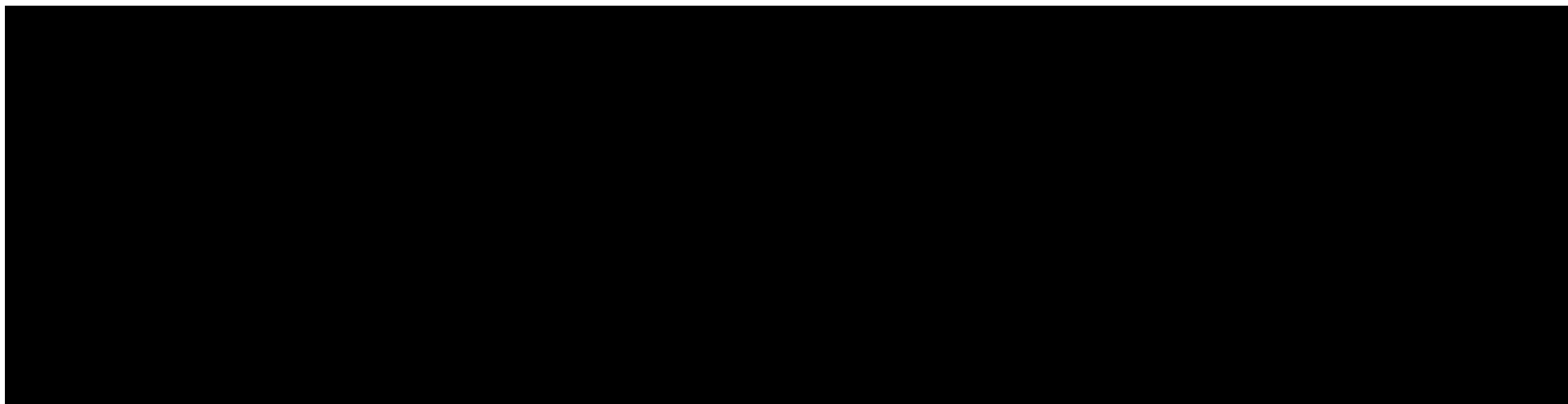
The selection of protecting groups for residual aa chains was a key part in the design and development of the random copolymer architecture, considering the molar ratio determination by NMR.

The synthetic strategy can be observed in scheme 2.6.

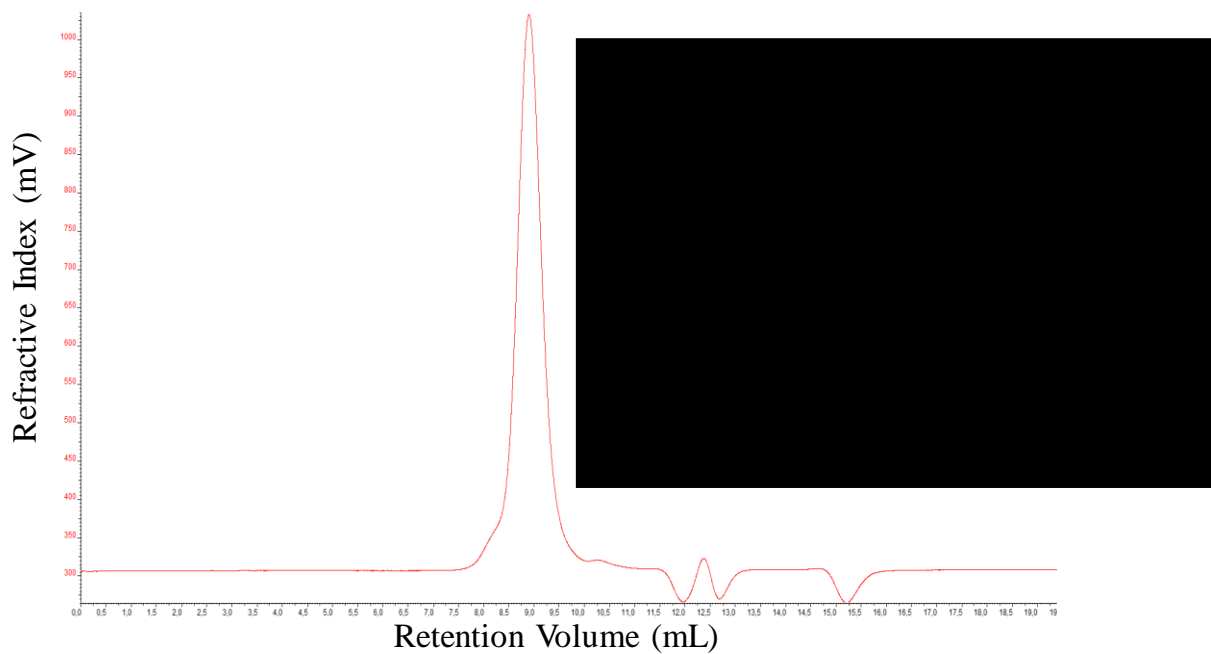


Scheme 2.6. Polymerization: P[Glu(OBzl)-co-Orn(Boc)] synthesis by ROP of NCA through NAM. **Deprotection: P[Glu(ONa)-co-Orn(HBr)]** synthesis

Table 2.6. Results for P[Glu-co-Orn]



(A) SEC-RI [REDACTED]



(B) ¹H NMR [REDACTED]

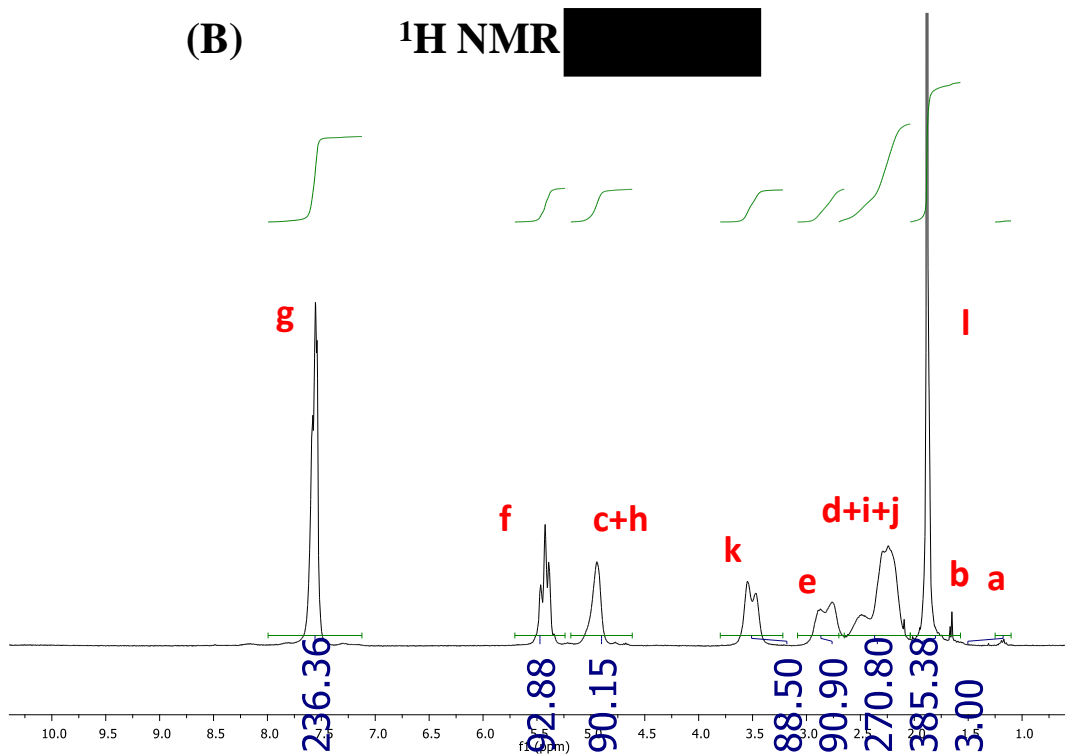


Figure 2.12. (1) SEC-RI. (2) ¹H NMR.

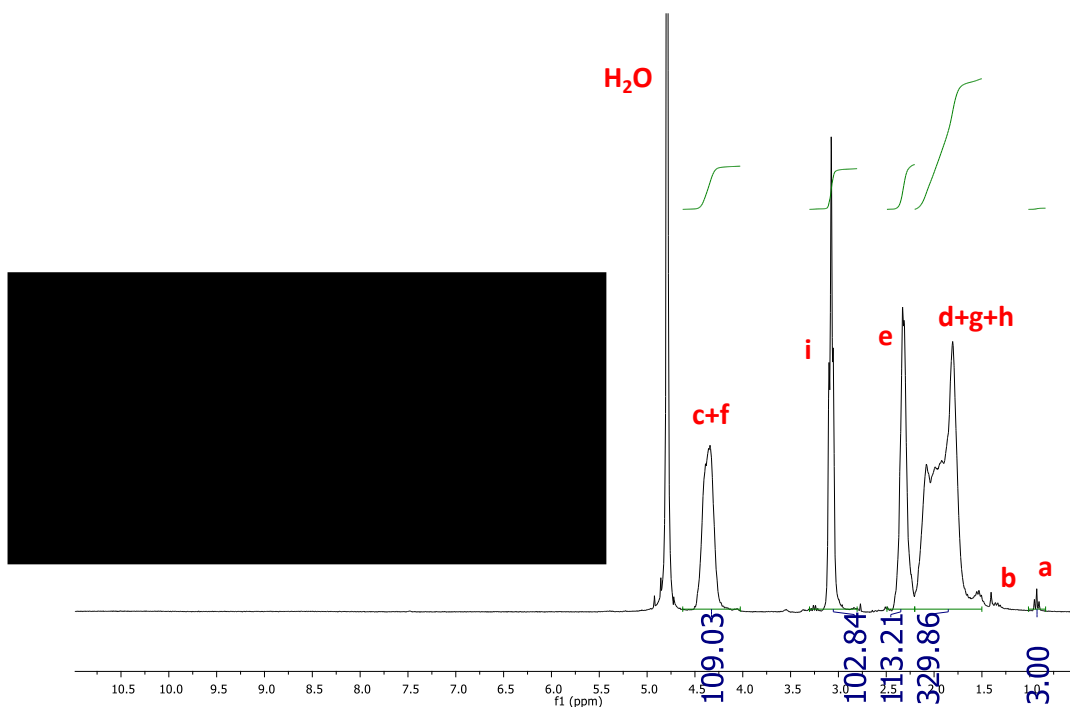


Figure 2.13. ^1H NMR

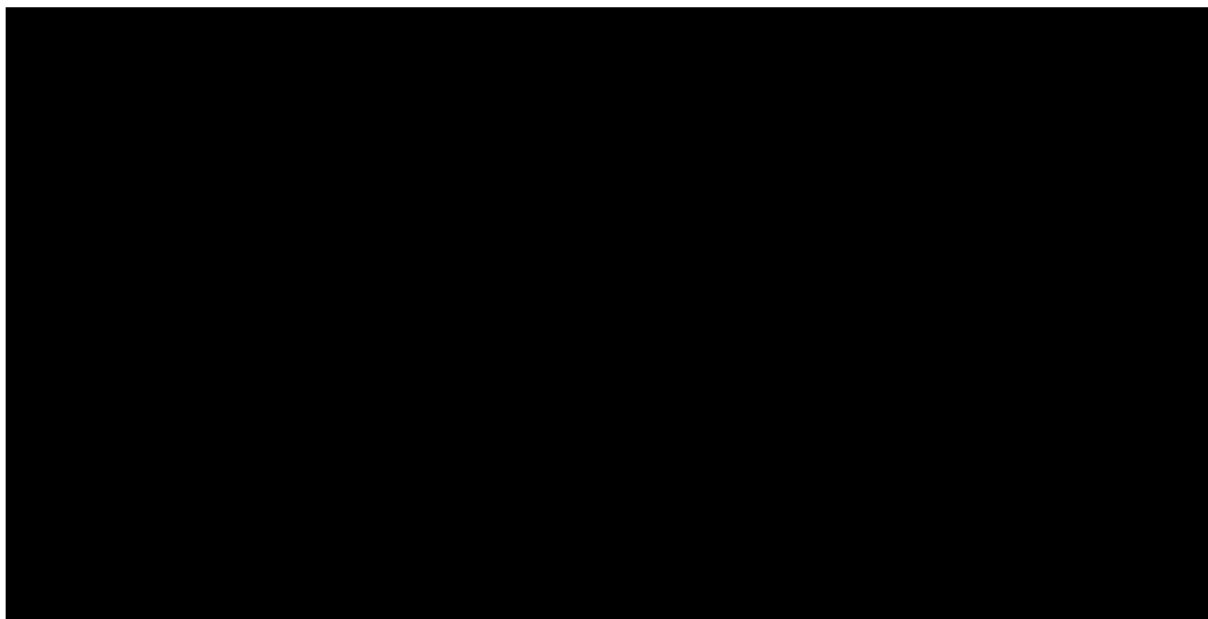
2.1.2. HYDROPHOBIC BLOCK DEVELOPMENT: APAAs WITH ALPHA HELIX AND BETA SHEET CONFORMATION

To achieve the synthesis of designed APAA materials, a polymerization optimization was first performed comparing PEG and PSar as hydrophilic segments. To construct the hydrophobic part in a alpha-helix conformation, the PGLu(OBzl) and PPhe were selected [12, 43-47]. Then, following with the alpha-helix conformation, the rest of the APAAs were synthesized using the Phe as aa. Finally, APAAs with beta-sheet conformation were prepared using PVal as the hydrophobic chain [48-52].

5 KDa PEG (114 units) was commercially available, but the rest of the hydrophilic blocks were prepared as previously described. To reach the APAA, the hydrophilic PAA was used as the initiator in its protected form to allow for orthogonal chemistry in the ROP reactions. The technology employed to yield the PAA previously described is perfectly suitable to achieve the APAAs via NAM, in which the initiator is incorporated into the final architecture of the resultant polymer. This methodology to build diblocks is widely reported in the scientific literature [38, 77].

METHODOLOGY OPTIMIZATION: SYNTHESIS OF SERIES FOR HYDROPHILIC PEG AND PSar BLOCKS WITH PGLu(OBzl) AND PPhe AS HYDROPHOBIC CHAIN

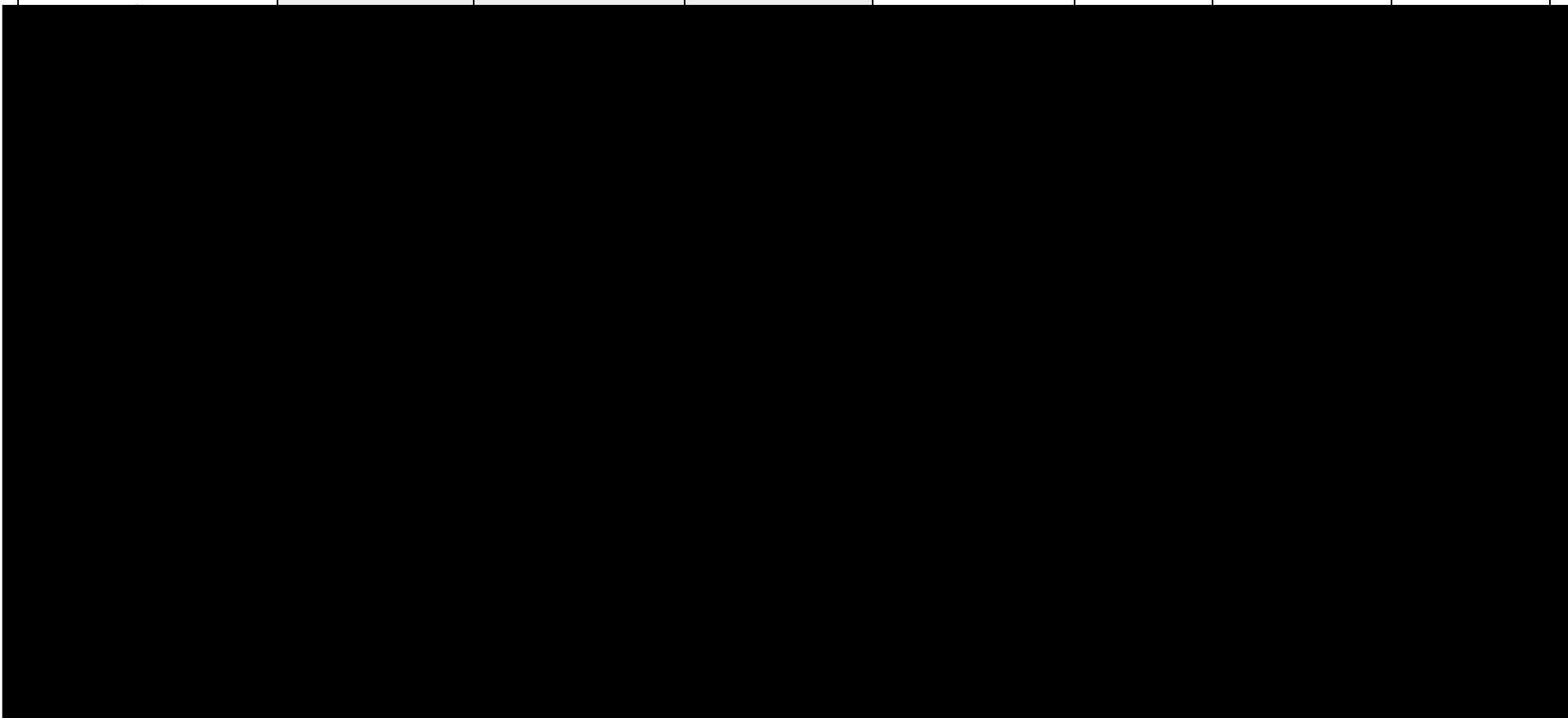
The first family developed was the APAA based on PEG as the hydrophilic block with PGLu(OBzl) and PPhe as hydrophobic blocks to yield the secondary structure of alpha-helix. The general reaction scheme to yield the PEG/PSar block PGLu(OBzl)/PPhe, their characterization through SEC and NMR and the obtained results can be seen below.



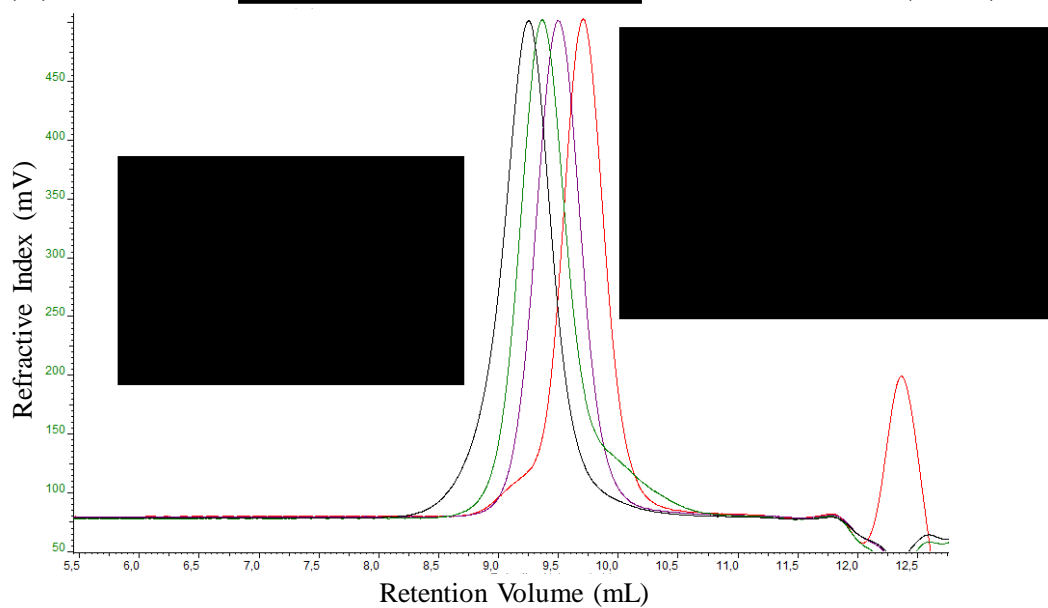
Scheme 2.7. General reaction scheme to yield the PEG and PSar series with hydrophobic blocks of PGlu(OBzl) and Phe .

Table 2.7. Results for PEG and PSar series with hydrophobic blocks of PGlu(OBzl) and Phe.

Short Name of Block Copolymer	Target			Block Copolymer			
	DP for Hydrophilic Block	DP for Hydrophobic Block	Theoretical Mw (kDa)	Mw (kDa) by SEC	PDI	DP for Hydrophilic Block by NMR	DP for Hydrophobic Block by NMR



(A) SEC-RI XXXXXXXXXX for PEG-b-PGlu(OBzl) series



(B) ^1H NMR in TFA- d_1 for PEG-b-PGlu(OBzl) series

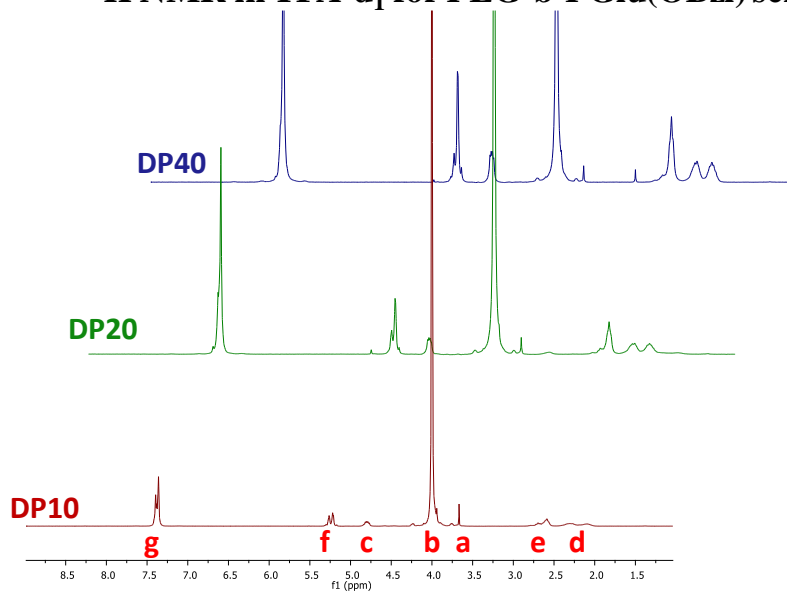
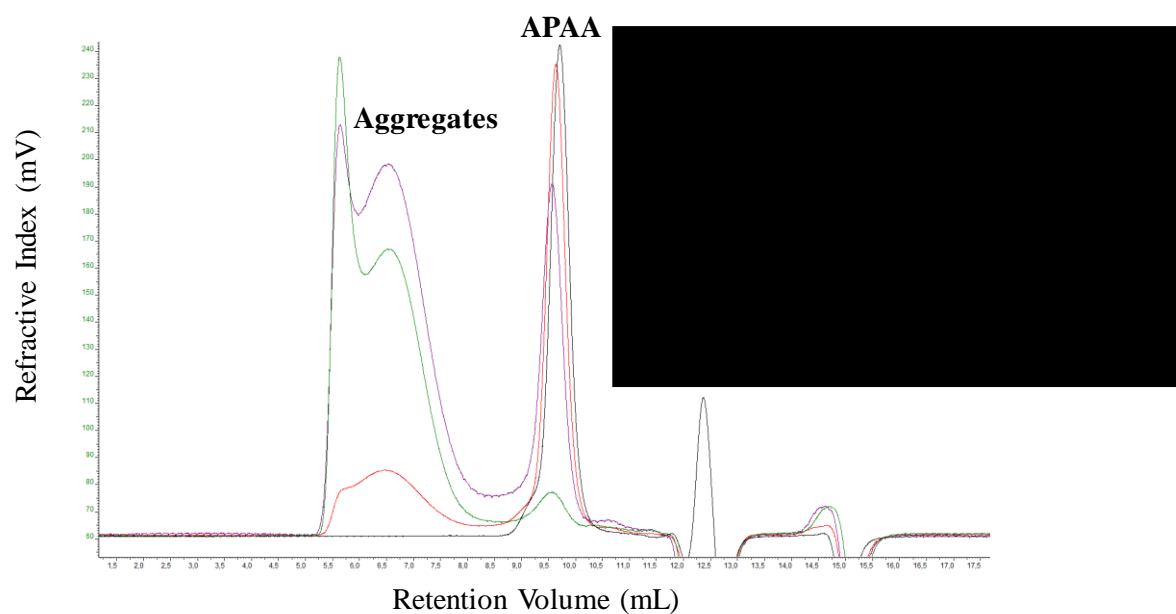


Figure 2.14. PEG-b-PGlu(OBzl) series characterization. (A) Overlap SEC-RI. (B) Overlap ^1H NMR.

(A) SEC-RI [REDACTED] for PEG-b-PPhe series



(B) ^1H NMR [REDACTED] PEG-b-PPhe series

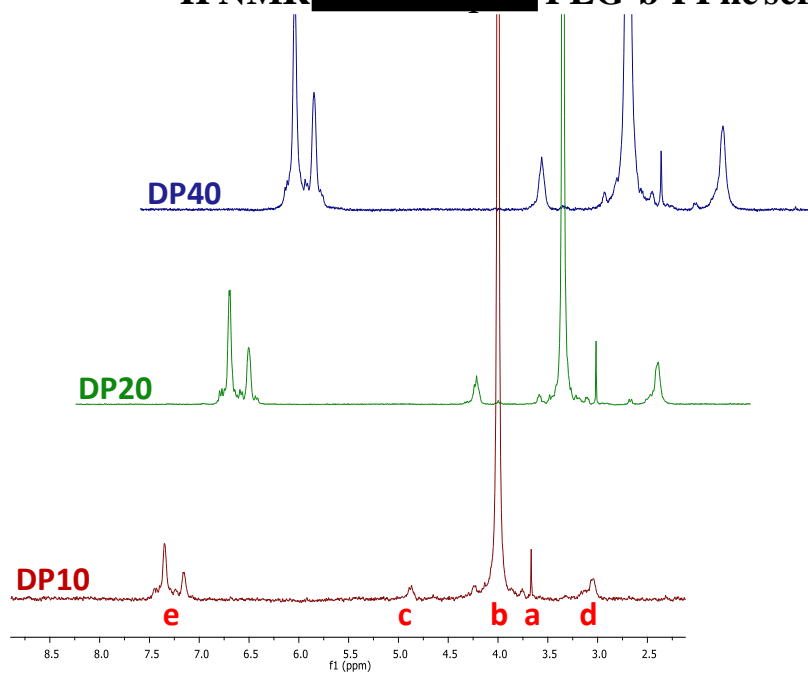
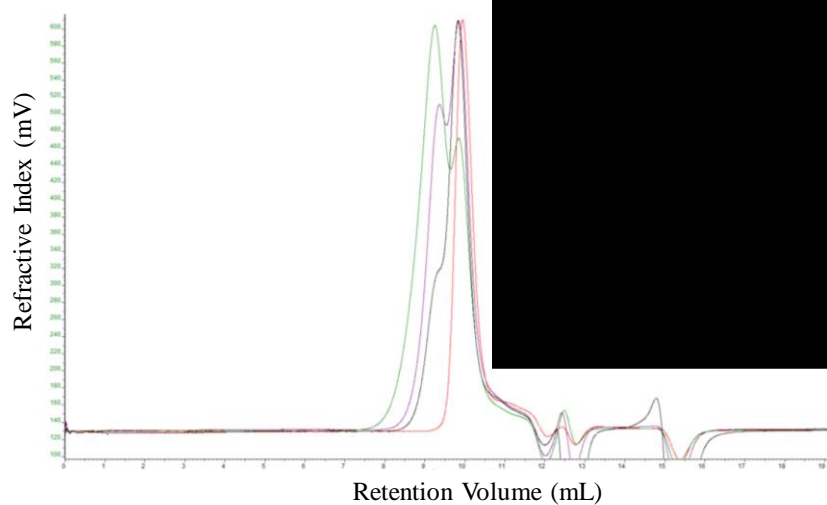


Figure 2.15. PEG-b-PPhe series characterization. (A) Overlap SEC-RI. (B) Overlap ^1H NMR

(A) SEC-RI



(B) ^1H NMR

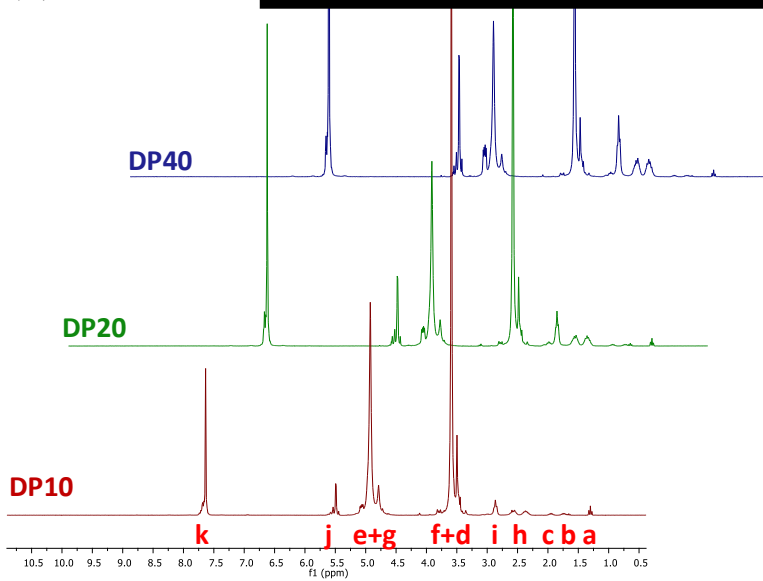


Figure 2.16. PSar-b-PGlu(OBzl) series characterization. (A) Overlap SEC-RI. (B) Overlap ^1H NMR.

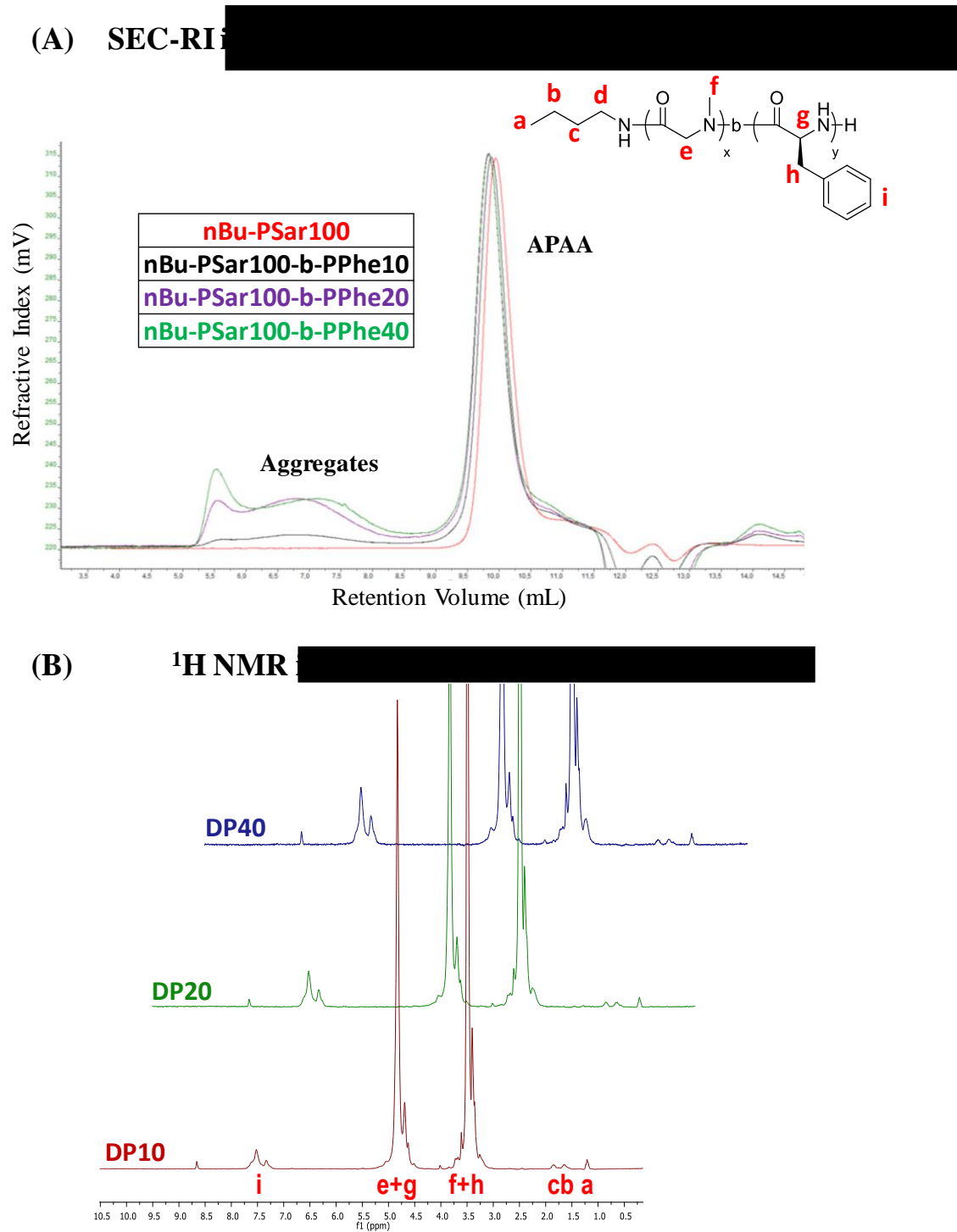


Figure 2.17. PSar-b-PPhe series characterization. (A) Overlap SEC-RI. (B) Overlap ^1H NMR.

As can be observed in Table 2.7 and Figure 2.14, **PEG-b-PGlu(OBzl)** diblock series are well defined in terms of Mw distributions. Results of DPs by NMR and SEC are very similar to theoretical values. Thus, the SEC and NMR analytical methodologies are appropriate to characterize these families of block copolymers.

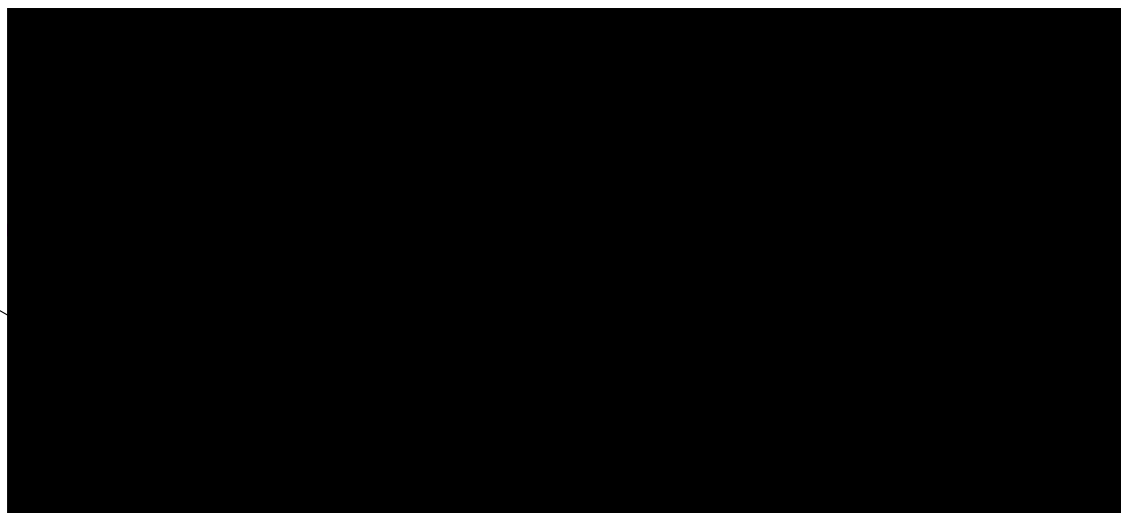
Similar results for PSar family were obtained, with a much more pronounced gel formation for Phe in the reaction media. In the **PSar-b-PGlu(OBzl)** series, Mw

distributions resulted in bimodal peaks for some DPs, but DP by Mw and NMR results were similar to target numbers (see Table 2.7 and Figure 2.15). Although the Mw values were similar to theoretical values for the **PSar-b-PPhe** series, the presence of aggregates in SEC elugrams and the low DPs obtained by NMR indicated that these block copolymers are not well defined.

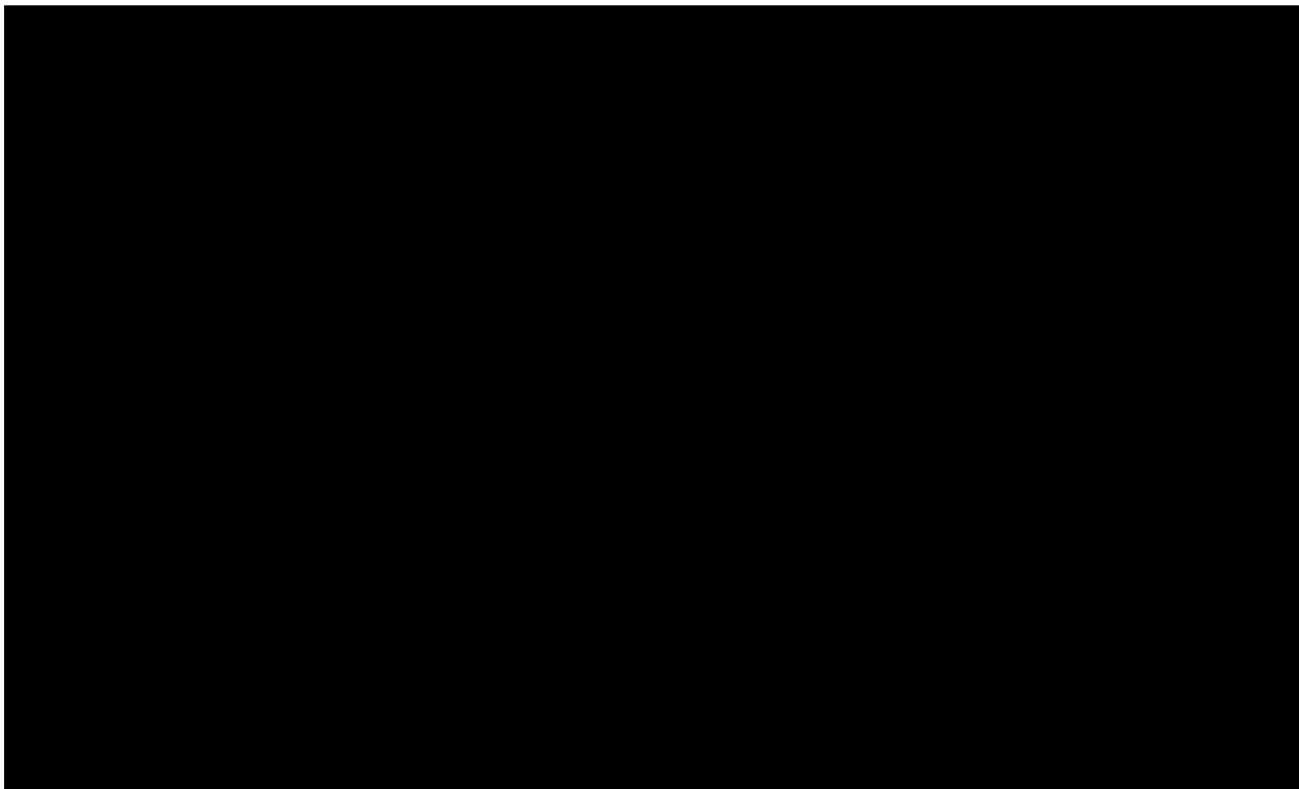
The fact that both materials containing a high DP failed, as well as **PSar100-b-PPhe20**, prompted us to redefine the architectures for this study fixing the DP value for the hydrophobic block at 10 units to have comparative materials.

HYDROPHOBIC BLOCK FOR ALPHA HELIX CONFORMATION → ***PAA_{Hydrophilic}-b-PPhe***

After the results obtained in the optimization, APAA architectures containing just 10 units of Phe as a hydrophobic block were synthesized as illustrated in Scheme 2.8. Characterization results by NMR and SEC can be found in Table 2.8. The **PEG114-b-PPhe10** and **PSar100-b-PPhe10** materials with neutral electrostatic charges were included in this discussion again for comparative purposes.



Scheme 2.8. Polymerization: Protected-PAA_{Hydrophilic}-b-PPhe



Scheme 2.9. Deprotection: PAA_{Hydrophilic}-b-PPhe general synthesis

Table 2.8. Characterization results for **PAA_{Hydrophilic}-b-PPhe**

Short Name of Block Copolymer	Hydrophilic Electrostatic Charge	Monomer for Hydrophilic Block	Target		Protected Precursors and Copolymers without Deprotection Step					Deprotected Product		
			DP for Hydrophilic Block	DP for Hydrophobic Block	Theoretical Mw (kDa)	Mw (kDa) by SEC	PDI	DP for Hydrophilic Block by NMR	DP for Hydrophobic Block by NMR	Deprotection Yield by NMR	DP for Hydrophilic Block by NMR	DP for Hydrophobic Block by BNR

SEC-RI [REDACTED] for PAA_{Hydrophilic}-b-PPhe

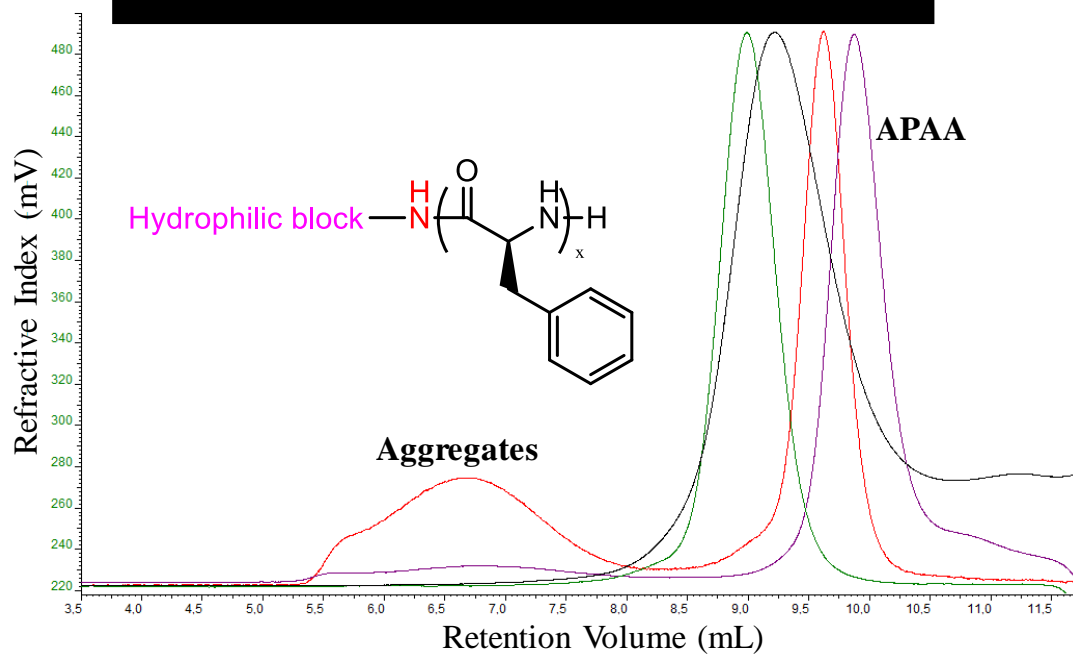


Figure 2.18. Overlap SEC-RI PAA_{Hydrophilic}-b-PPhe.

¹H NMR [REDACTED] for Protected-PAA_{Hydrophilic}-b-PPhe

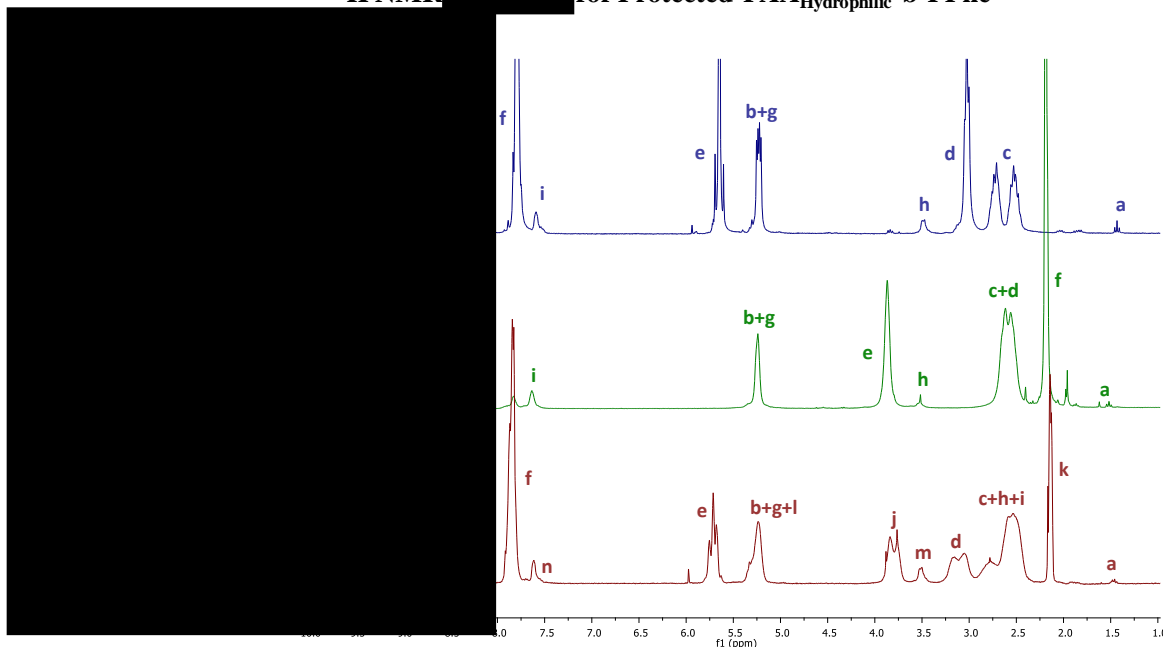


Figure 2.19. Overlap ¹H NMR.

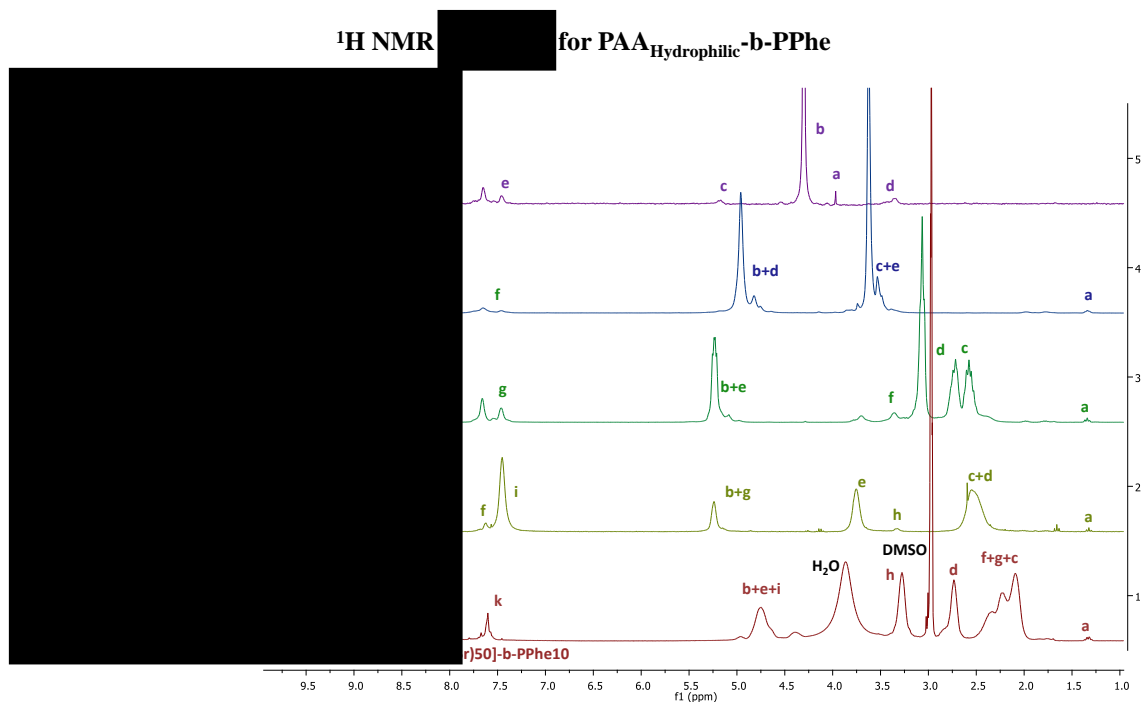
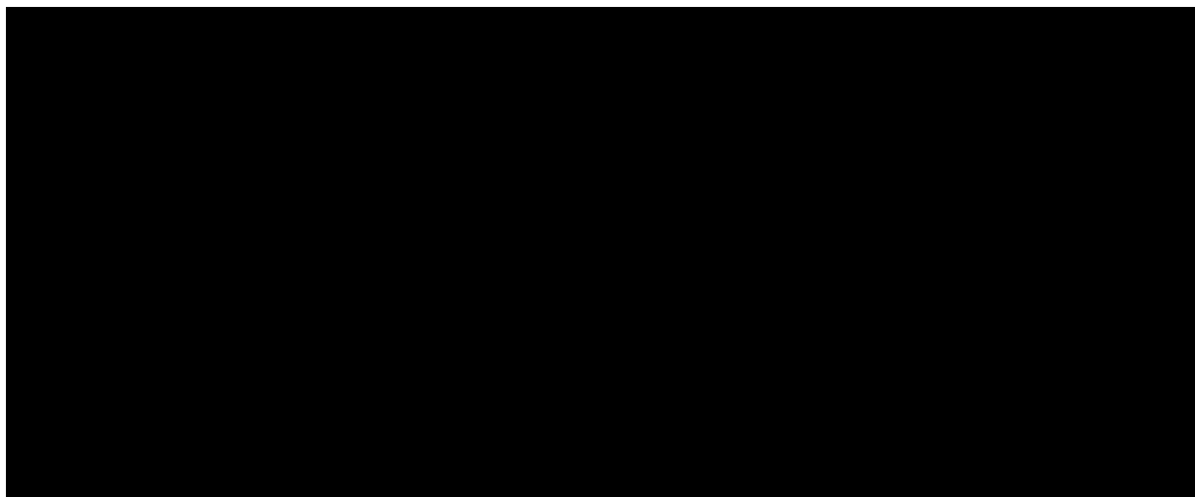


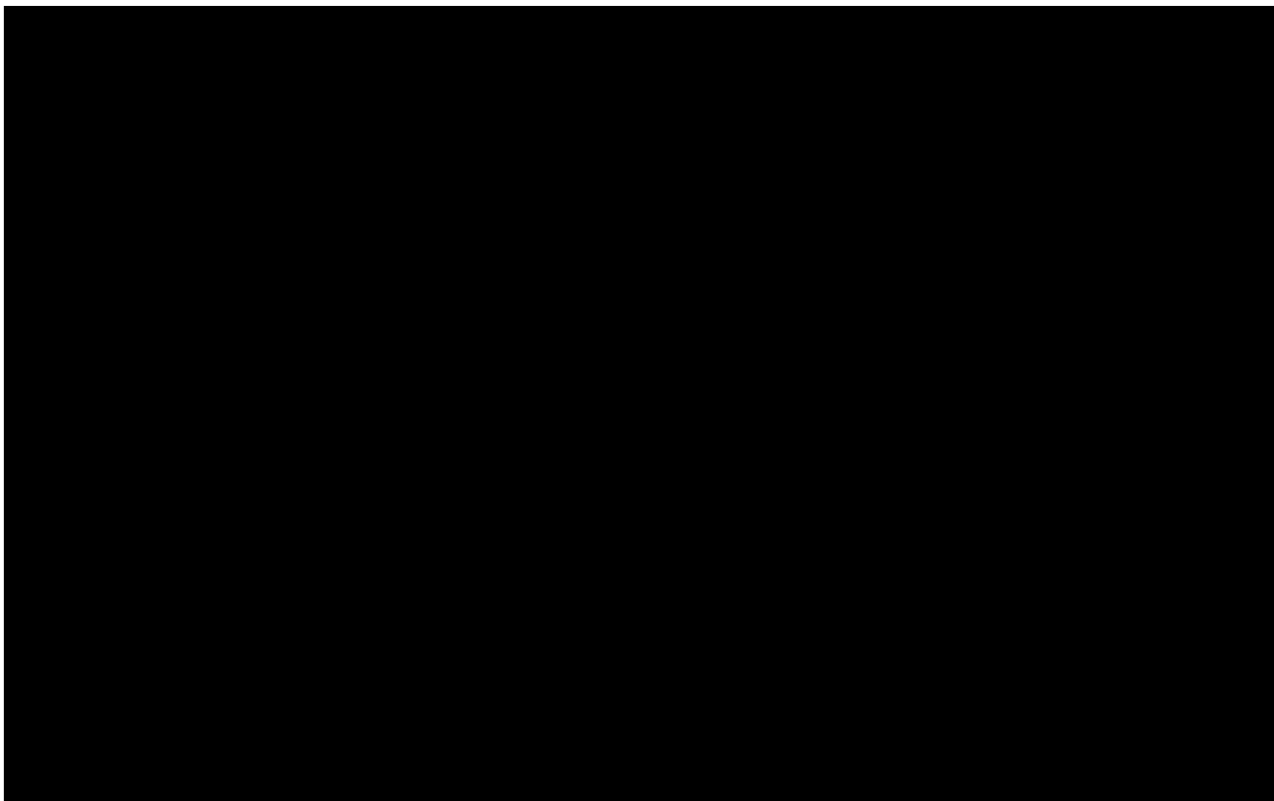
Figure 2.20. Overlap ¹H NMR

HYDROPHOBIC BLOCK FOR BETA SHEET CONFORMATION → PAA_{Hydrophilic}-b-PVal

As stated, for the beta-sheet secondary structure, L-valine was selected as aa. The synthetic approach to reach the APAAs containing PVal was the same as previously described for PPhe. The synthetic pathway is shown below, along with the characterization by SEC and NMR, and the results obtained.



Scheme 2.10. Polymerization: Protected-PAA_{Hydrophilic}-b-PVal general synthesis



Scheme 2.11. Deprotection: PAA_{Hydrophilic}-b-PVal general synthesis

Table 2.9. Characterization results for **PAA_{Hydrophilic}-b-PVal**

Short Name of Block Copolymer	Hydrophilic Electrostatic Charge	Monomer for Hydrophilic Block	Target		Protected Precursors and Copolymers without Deprotection Step					Deprotected Product		
			DP for Hydrophilic Block	DP for Hydrophobic Block	Theoretical Mw (kDa)	Mw (kDa) by SEC	PD I	DP for Hydrophilic Block by NMR	DP for Hydrophobic Block by NMR	Deprotection Yield by NMR	DP for Hydrophilic Block by NMR	DP for Hydrophobic Block by BNR

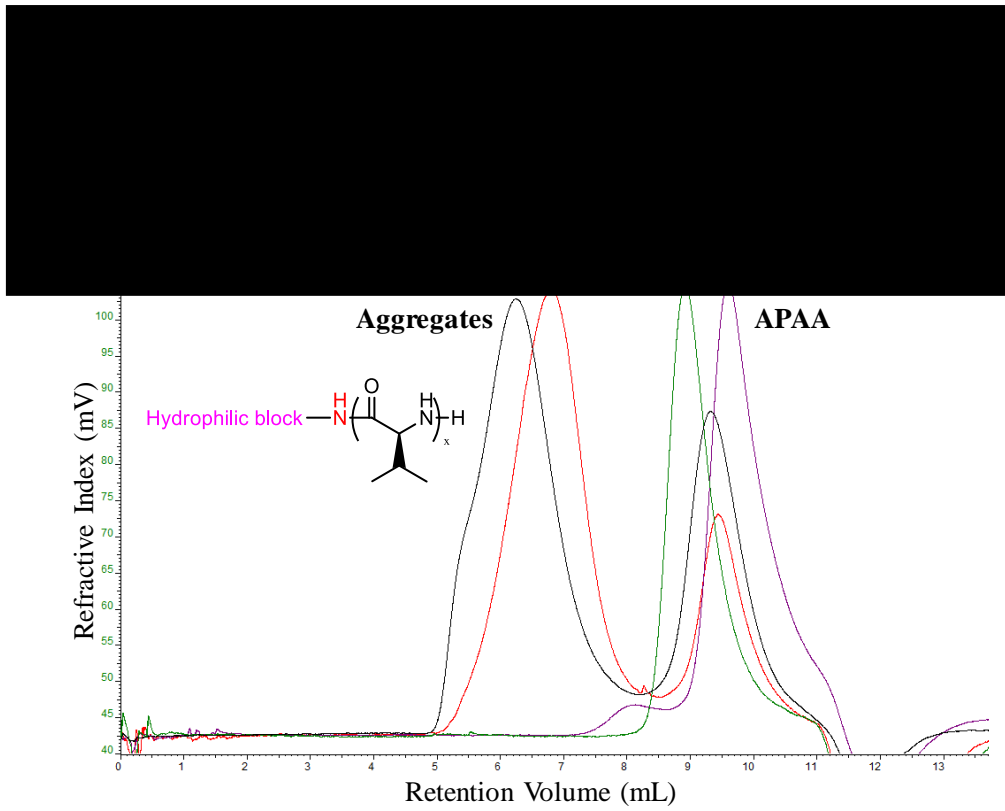


Figure 2.21. Overlap SEC-RI

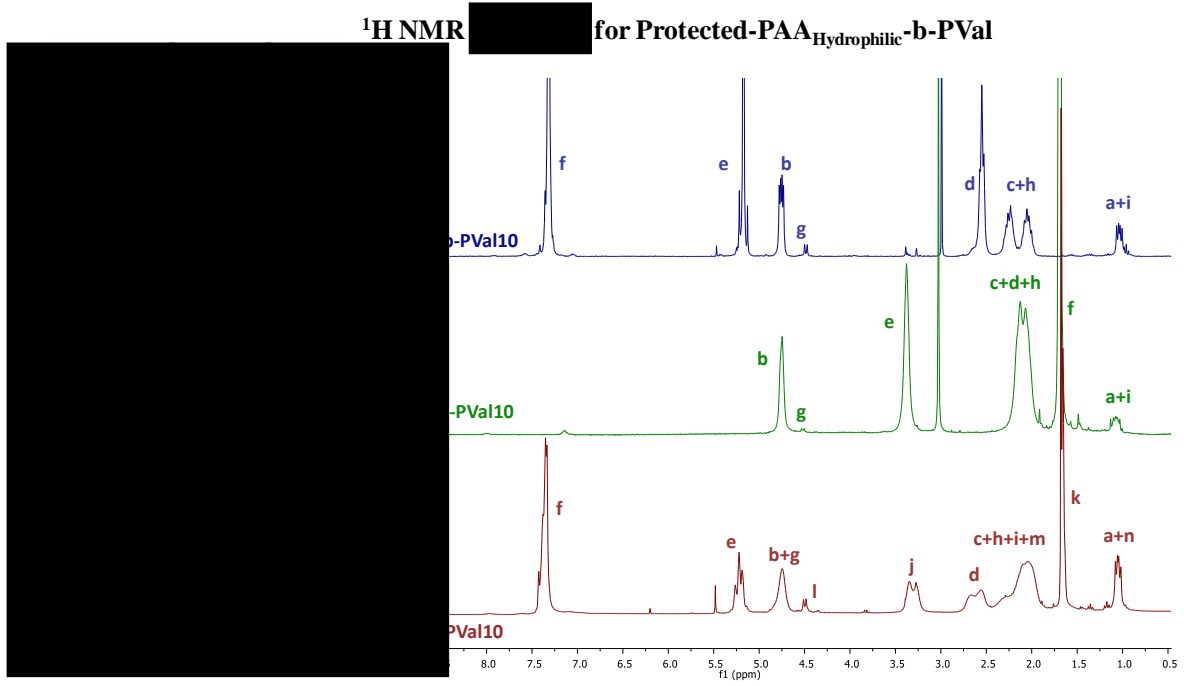


Figure 2.22. Overlap $^1\text{H NMR}$

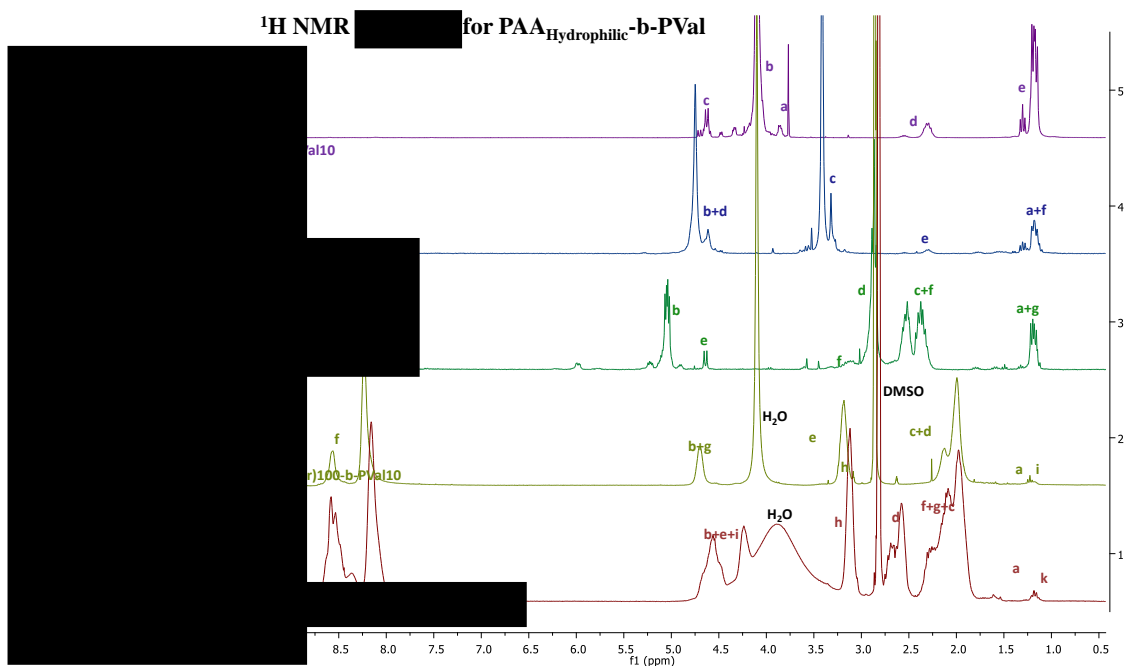


Figure 2.23. Overlap ^1H NMR

For APAAs containing PVal, the polymerization reactions were more complicated than for PPh. Practically all reactions turned cloudy after a few hours except for **PGlu(OBzl)100-b-PVal10**. This confirms that PVal gives rise to APAAs with lower solubility in the polymerization solvent than Phe chains. Results for PVal-based materials can be found in Table 2.9.

2.2. MICELLAR PROPERTIES CHARACTERIZATION FOR SELECTED CANDIDATES

After pre-screening 20 ACAA block copolymers and all the difficulties found in their synthesis and characterization, we decided to proceed with a small family of **PEG-b-PGlu(OBzl)** (or **PEG-PBG**) and **PEG-b-PPh** (or **PEG-PPh**) copolymers to compare the influence of the hydrophobic aa segments selected. This selection was made based on chemical feasibility, well-defined architecture, and ease of the physico-chemical characterization. To this end, the PEG and PSar copolymers of PBG and PPh complied with these criteria. Of note, the direct comparison of PEG vs. PSar materials is of great interest as discussed in the introductory section. Currently, only PEG-based micelles have been tested to develop micellar formulation processes and characterization techniques. This selection was also based on the fact that there are more data available for PEG-based micelles than PAA since PEG is the most widely-employed polymer as the hydrophilic segment [17, 19]. The characterization for the rest of ACAA-based micelles will be addressed in the future.

2.2.1. MICELLE FORMULATION

To study the self-assembly in aqueous media for selected APAAs based on PEG materials, micelles were obtained by the *co-solvent* method. This methodology consists in dissolving the PEG APAAs in THF followed by the addition of an excess of water to

performing the self-assembly into micellar structures. Next, the THF was removed by atmospheric evaporation at RT and micelles were obtained in solution. The formulation was allowed to equilibrate at room temperature for 24 hours, followed by centrifugation at 1000 rpm for 10 minutes and the supernatant was dialyzed against distilled water using a membrane with a MWCO of 1 kDa. Finally, the aqueous solution was freeze-dried to obtain the micelles in powder form, which were then redissolved in water to reach the micelle formulation. Figure 2.24 shows a representative scheme of the process to obtain empty and DiL loaded micelles of the selected APPAs.

In order to test the encapsulation capacity of hydrophobic molecules to improve their solubility in water, and to study the viability of selected APAs as carriers for those products, a DiL C18 fluorescent hydrophobic compound was selected as a hydrophobic model molecule to be representative of hydrophobic APIs thinking in the potential applications of these materials.. The high fluorescence and absorbance of this molecule facilitates its quantification by fluorescence or UV-Vis spectroscopy and analysis by Confocal Microscopy. The use of DiL C18 as a fluorophore for labeling micelles is reported in literature [78].

To obtain the DiL-labeled micelles, the micellar formulation was carried out following the same procedure described previously for empty micelles but including the DiL C18 in the THF solution together with the PEG-based APAs. The target amount of DiL loading was 1 % w/w and the synthetic scheme is shown in Figure 2.24 B .

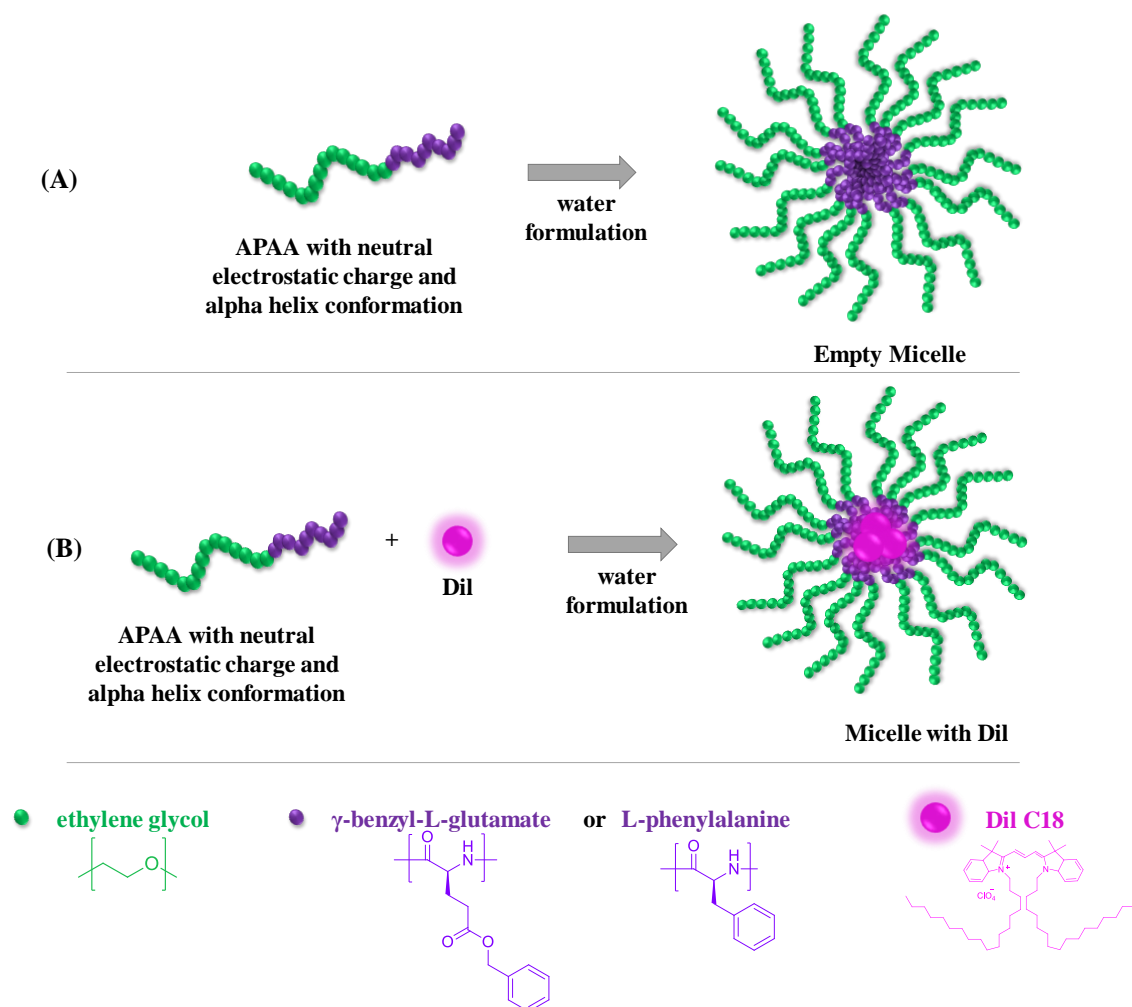


Figure 2.24. General scheme for micelle formulation. (1) Empty micelle formulation. (2) Dil encapsulation into the micelle.

2.2.2. PHYSICO-CHEMICAL CHARACTERIZATION

Block copolymer micelles with smaller Z potential average, hydrodynamic diameter, and a narrow polydispersity index were obtained by the co-solvent method [37] (Figure 2.24, Table 2.10), allowing for the encapsulation of the fluorescent dye Dil as a model hydrophobic API. The diblock copolymers to be incorporated within the hybrid material as polymeric micelles were preselected based on their micellar formulation stability. All micellar formulations at 10 mg/mL were evaluated for their stability, and it was found that those produced with larger polypeptide blocks (PEG-PPhe40 and **PEG-PBG40**) precipitated within a few hours when standing at room temperature, possibly due to an imbalance of the hydrophilic and hydrophobic ratio. For this reason, **PEG-PBG10**, **PEG-PBG20**, **PEG-PPhe10** and **PEG-PPhe20** were chosen for further evaluation.

Table 2.10. Characteristics of micelles formed by block copolymers with and without encapsulated dye.

Block Copolymer	E.E ^a	Dil Loading ^a	CAC ^b	Conc.	Size, I ^c	Size, N ^d	PDI	Z potential
	%	% w/w	mg/ml	mg/mL	nm	nm		mV
PEG-PBG10	---	---	0.04	10 ^e	28/317	16	0.316	-0.695
				5	30	16	0.251	-0.111
				1 ^e	22/312	12	0.312	7.243
PEG-PBG10 + Dil	114 f	1.14 f	---	10 ^e	32/173	15	0.420	-0.781
				5 ^e	33/179	17	0.373	0.230
				1 ^e	35/248	18	0.338	2.040
PEG-PBG20	---	---	0.01	10	30	18	0.149	-0.269
				5	32	19	0.130	-0.157
				1	33	20	0.152	-0.039
PEG-PBG20 + Dil	105 f	1.05 f	---	10	32	19	0.164	0.184
				5	34	20	0.127	0.384
				1	36	19	0.254	0.771
PEG-PPhe10	---	---	0.008	10	164	25	0.363	0.052
				5	137	31	0.279	0.481
				1	110	27	0.246	1.867
PEG-PPhe10 + Dil	47	0.47	---	10	166	30	0.322	0.390
				5	145	30	0.297	1.103
				1	108	28	0.261	3.36
PEG-PPhe20	---	---	<0.004	10	143	28	0.409	2.443
				5	128	30	0.282	3.207
				1	103	21	0.232	5.143
PEG-PPhe20 + Dil	58	0.58	---	10 ^e	77/403	30	0.466	2.683
				5 ^e	79/330	34	0.388	3.170
				1	107	26	0.317	5.110

E.E = Encapsulation efficiency. ^a Determined by UV-Vis. ^b Critical micelle concentration determined by fluorescence using pyrene as a hydrophobic probe (see Figure 2.25) ^c Hydrodynamic diameter by Intensity. ^d Hydrodynamic diameter by number. ^e Bimodal size distribution by intensity. **f** PEG-PBG was found to be highly hygroscopic, deviation in the weighed mass leads to E.E. > 100%.

PEG-PBG copolymers showed a CAC higher than the analogous Phe derivatives (Figure 2.25A). This suggested that PEG-PPhe copolymers had a more compact behavior in aqueous solution, likely due to the highly hydrophobic nature of phenylalanine. TEM observations showed that the micelles, in general, were mainly spherical with diameters of homogeneous size in good agreement with DLS data (Figure 2.25B and 2.25D). The fact that GPC analysis revealed strong aggregation for Phe-based block copolymers, their low CMC values and the low encapsulation efficiency, drove us to study in more detail the stability of these assemblies by looking at the secondary structure. Circular dichroism (CD) was employed to evaluate the secondary structure of the polypeptidic block within the micellar core. As shown in Figure 2.25C, micellar aqueous solutions of block copolymers showed the typical alpha-helix conformation that would be expected for PPhe

and PBG homopolymers, with a pronounced negative band for larger DPs and Phe copolymers. Previously reported data from CD studies with a Phe-arginine peptide showed a similar negative band over 200 nm [79]. This negative band for Phe derivatives was also observed for PEG-PGlu-PPhe triblocks at pH 4.5 in aqueous solutions [80], in good agreement with our results with micelles containing Phe residues. Interestingly, not only the intensity but also the shape of the characteristic alpha-helix band changed from PPhe to PBG blocks, pointing to a structurally different arrangement of side-chain groups. With a similar system to ours (PEG 5KDa and 4 Phe units) Castelletto et al. obtained well defined fibrils by self-assembly due to the π - π^* interactions [81], so it is clear that Phe derivatives tend to form strong self-assembly aggregates [82] promoting in our case a much more rigid inner core, which was probably closely packed at lower CAC values. This had some practical consequences, since the encapsulation efficiency with phenylalanine-derived block copolymers was much lower compared with PBG derivatives (47-58 % vs 105-114 %, respectively).

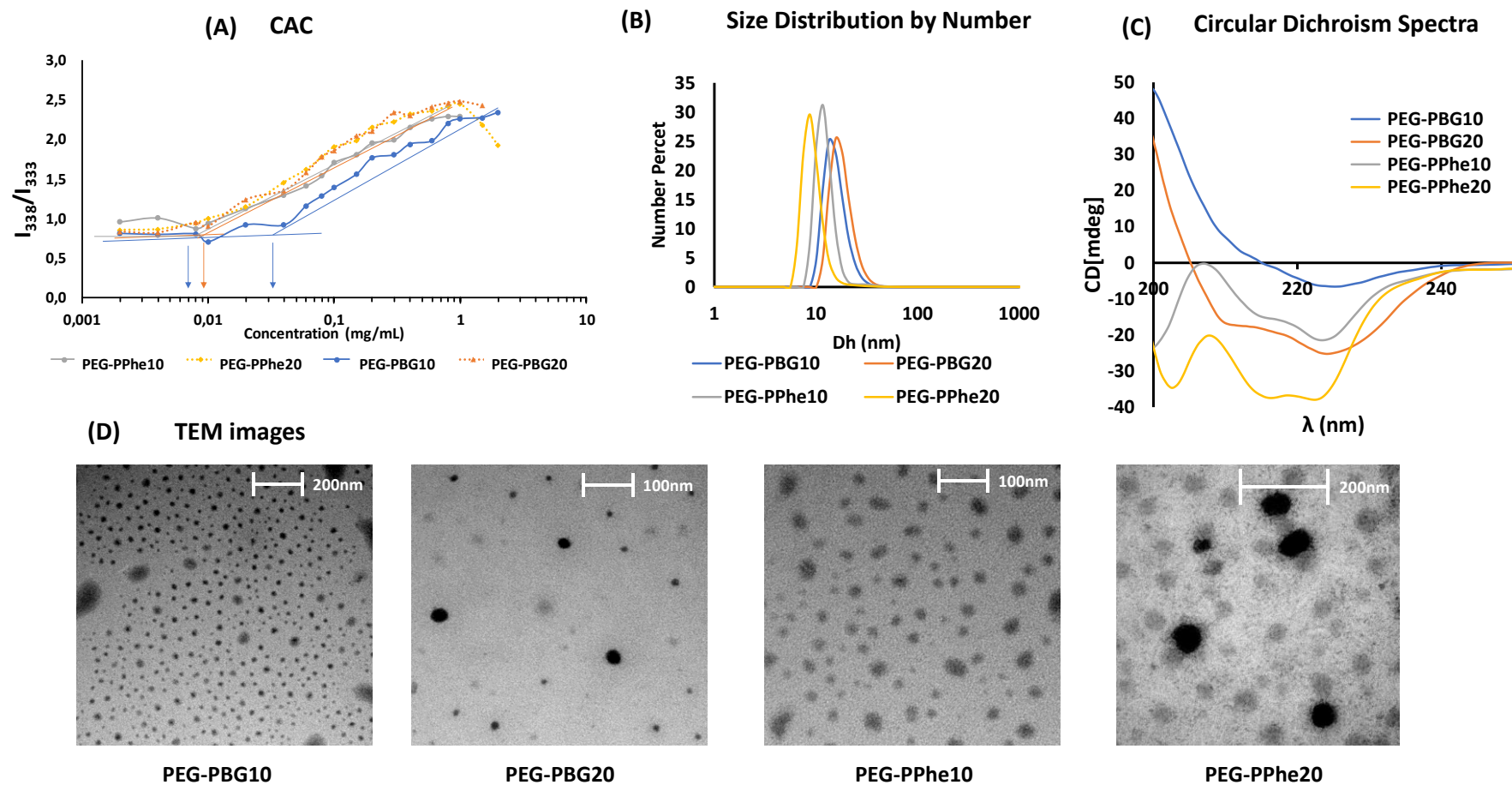


Figure 2.25. (A) Critical Aggregation Concentration (CAC) obtained for aqueous micellar formulations increasing their concentration employing pyrene assay published elsewhere [64, 83]. CAC measurements were performed using a fluorimeter employing an intensity ratio I_{338}/I_{333} . (B) Circular dichroism spectra for micellar solutions at 0.5 mg/mL of block copolymers in water. (C) Size distribution by number obtained from DLS measurements at 10 mg/mL of deblock copolymers micelles formulations. (D) TEM images of aqueous micellar formulations at 2 mg/mL block copolymers.

In terms of sizing studies by dynamic light scattering, all the formulated micelles showed a similar mean size distribution (Dh) ranging from 12-30 nm with no significant variation with concentration (1-10 mg/mL), in good agreement with reported values for similar amphiphilic block copolymers [84, 85] (Figure 2.25B). For z-potential, both benzylglutamate and phenylalanine-based copolymers display a small absolute value close to 0 (Table 2.10).

After the excellent results obtained for hydrophobic API model encapsulation, these 4 micelles have been studied for skin delivery and the results are shown in Chapter III.

2.3. POLYMERIC MICELLES CONTAINING AN ACTIVE HYDROPHOBIC MOLECULE

All this section has been removed (censored) since the TPSS synthesis, characterization and applications will be patented in the future.

3. CONCLUSIONS

Summarizing the described results, the NCA of alpha-amino acid monomers are excellent starting materials to obtain PAA and APAA by ROP using the NAM techniques. The methodology described in the literature has been adapted to obtain well-defined homo and random PAA and APAA with narrow Mw distributions, low PDI and good stoichiometric correlation values between the initiator and aa monomer(s), demonstrating its high versatility to achieve different architectures. Moreover, hydrolysis techniques to remove the protecting groups to reach the functionalized amino acid have been implemented successfully yielding a high percent (> 99 %) of hydrolysis. All homo and random PAA (18 compounds) were achieved without complications for different DPs for PSar, PGlu and POrn, PArg and P(Glu-co-Orn)]. For APAA (20 compounds), in terms of electrostatic charge in the hydrophilic block, we found that this technology works better for neutral (PEG, PSar) and anionic (PGlu) PAA, than cationic (POrn) or zwitterionic [P(Glu-co-Orn)] materials. Regarding the secondary structure conformation for hydrophobic segments, APAA containing Glu(OBzl) and Phe to achieve the alpha-helix conformation showed fewer problems to manufacture than the APAA containing PVal to reach the beta-sheet conformation. The poor solubility in common solvents of PVal combined by cationic and zwitterionic segments rendered their synthesis and proper characterization very difficult. Importantly, the secondary structure conformation of beta-sheet of APAA containing PVal was not confirmed by CD. We designed the architectures of these materials based on the data published [48-52].

On the other hand, **TPSS**, a new biodegradable amphiphilic HP-BM material was developed and properly characterized by comparison with the commercially available PEGylated version (**TPGS**), finding similar results for Mw distributions and

PDI by SEC and MALDI-TOF MS, diffusion coefficients by DOSY NMR, and vitamin E loading by NMR.

These results drive us to select the **PEG-PBG** and **PEG-PPhe** APAA series as well as **TPGS** and **TPSS**, to study their self-assembling properties in micellar structures to encapsulate a hydrophobic fluorophore as a hydrophobic API model. Encapsulation efficiency, fluorophore load, secondary conformational structure, CAC, and morphology were determined for the micelles finding promising results compared with values reported in literature. Moreover, size and Z potential were determined for micellar formulations prepared by different methodologies.

Results allow us to conclude that polymeric micelles prepared with APAA as well as HP-BM obtained by ROP of NCAs via NAM are excellent and versatile candidates to encapsulate hydrophobic drugs or APIs to be applied in the drug delivery field.

4. MATERIALS AND METHODS

4.1. MATERIALS

All chemicals were reagent grade, obtained from Sigma-Aldrich and used without further purification unless otherwise indicated. MeO-PEG-NH₂ (Mw = 5 kDa, 114 ethylene glycol units) was supplied for Rapp Polymere. Dil stain (1,1'-dioctadecyl-3,3,3',3'-tetramethylindocarbocyanine perchlorate (Dil; DilC18(3))) was purchased in Thermo Fisher Scientific. Pyrene was obtained from Fluka Analytical. Anhydrous DMF and DMSO were purchased from Scharlab. Ultrapure water (MilliQ) also called distilled water, with a resistivity of 18 MΩ.cm was used in all aqueous preparations. Deuterated trifluoroacetic acid (TFA-d₁), chloroform-d₁, dimethylsulfoxide-d₆, acetonitrile-d₃, acetone-d₆, *N,N*-dimethylformamide-d₇ and deuterium oxide (D₂O) were purchased from Deutero GmbH. Dialysis was performed in a Millipore ultrafiltration device fitted with a 1, 3, 10 or 30 kDa MWCO regenerated cellulose membrane (Vivaspin®) for mg scale. For 1 to 20 grams, dialysis was carried out using the Slide-A-Lyzer™ dialysis flasks, of 2 kDa of MWCO of 250 mL from Thermo Fisher Scientific.

4.2. METHODS

4.2.1. SYNTHETIC METHODS

All this section has been removed (censored) in order to protect the know-how of the company.

4.2.2. ANALYTICAL METHODS

NMR spectroscopy

NMR spectra were recorded at 27 °C (300 K) on a 300 Ultrashield™ from Bruker (Billerica MA, USA). Data were processed with the software Topspin (Bruker GmbH, Karlsruhe, Germany). Samples were prepared at a concentration of 20 - 10 mg/mL approx. in the required solvent.

Diffusion Experiments

Pulsed-field gradient NMR spectroscopy was used to measure translational diffusion by fitting the integrals or intensities of the NMR signals to the Stejskal–Tanner [86] equation: $I = I_0 \exp[-D\gamma^2 g^2 \delta^2 (\Delta - \delta / 3)]$ where I is the observed intensity, I_0 the reference intensity (unattenuated signal intensity), D the diffusion coefficient, γ the gyromagnetic ratio of the observed nucleus, g the gradient strength, δ the length of the gradient, and Δ the diffusion time. Two-dimensional diffusion-ordered NMR spectroscopy (DOSY) was performed with a stimulated echo sequence using bipolar gradient pulses. The lengths of delays were held constant at $\Delta = 100$ ms, and 32 spectra of 64 scans each were acquired with the strength of the diffusion gradient varying between 5 % and 95 %. The lengths of the diffusion gradient and the stimulated echo were optimized for each sample. Typical values were $\delta = 5$ ms for the analysis of physical mixture species and cross-linked materials at 15 mg/mL. Moreover, the hydrodynamic radius (R_h) in nm through diffusion coefficient was obtained employing the Stokes-Einstein equation. $R_h = (KB \cdot T) / (6\pi \cdot \eta \cdot D)$ where KB is the Boltzmann constant ($1.3806488 \cdot 10^{-23} \text{ m}^2 \cdot \text{Kg} / \text{s}^2 \cdot \text{K}$), T is the temperature (K) and η is the dynamic viscosity ($1.095 \cdot 10^{-3} \text{ Kg} / \text{m} \cdot \text{s}$ for D_2O at 298.15 K and 0.1 MPa) [73].

Matrix-assisted laser desorption/ionization time of flight mass spectroscopy (MALDI-TOF MS)

The matrix material used was DCTB in methanol (10 mg/mL). KTFA in water (5 mM) was added as a cationic ionization reagent. The polymer sample was dissolved in methanol (100 ng/ml), to which the matrix material and the ionization reagent were added (1:10:1), and the mixture was placed on the target plate. The resulting mixture was analyzed in a 5800 MALDI-TOF MS (ABSciex) in a mass range of 700 - 4000 m/z in reflector positive mode. Previously, the plate was calibrated with 1 μL the TOF calibration mixture (ABSciex), in 13 positions.

Circular Dichroism spectroscopy (CD)

CD Spectroscopy was performed with a J-815 CD Spectrometer (JASCO Corporation) using a Peltier thermostated cell holder (PTC-423, JASCO Corporation) with a recirculating cooler (JULABO F250, JASCO Corporation). A nitrogen flow (~2.7 L/min) was led through the spectrometer and controlled with a nitrogen flow monitor (Afriso Euro-Index). The samples were dissolved under different conditions (MilliQ water, SDS solutions or MilliQ water HFIP mixtures at different concentrations). Samples were measured repeatedly ($n = 3$) in a quartz cuvette with $d = 0.1$ cm.

Size Distribution

Dynamic Light Scattering (DLS) measurements were performed using a Malvern Zetasizer NanoZS instrument, equipped with a 532 nm laser at a fixed scattering angle of 173 °. Polymer solutions were prepared under different conditions (MilliQ or KCl 1 mM at different concentrations and temperatures), solutions were sonicated for 10 min and allowed to age for the required time, filtered through a 0.45 µm cellulose membrane filter and measured. Size distribution was measured (diameter, nm) for each polymer per triplicate with $n > 3$ measurements, automatic optimization of beam focusing and attenuation was applied for each sample.

Z-Potential measurements

Z-potential measurements were performed at 20 °C using a Malvern Zetasizer NanoZS instrument, equipped with a 532 nm laser using disposable folded capillary cells, provided by Malvern Instruments Ltd. (Worcestershire, UK). Polymer solutions were prepared in 1 mM KCl in MilliQ water. The solutions were filtered through a 0.45 µm cellulose membrane filter. Z-potential was measured for each sample per triplicate with $n > 3$ measurements.

Critical Aggregation Concentration (CAC) determination

CAC determination was carried out through fluorescence experiments performed using a JASCO FP-6500 spectrofluorometer at 25 °C with 1 cm quartz cells and pyrene assay was performed as published elsewhere [73]. In brief, several solutions of the compounds are prepared to cover a wide range of polymer concentrations (from 2 - 0.004 mg/mL) to which a volume of the pyrene stock solution (0.02 mg/mL) in acetone was added to reach a final pyrene concentration of $6 \cdot 10^{-7}$ mg/mL. Then, all solutions are placed in vials and are incubated in an oven at 37 °C for 2 hours to evaporate the acetone. After storing the samples for 24 hours, measurements were carried out. Each excitation spectra is recorded from 300 to 360 nm with an emission wavelength of 390 nm. The excitation and emission band slits are 5 and 2.5 nm respectively. Finally, data were expressed by plotting the intensity ratio I_{338}/I_{333} against the polymer concentration in order to determine the CAC value.

Quantification of Dil loading

Dye loading was determined by UV-Vis measurements UV-VIS using JASCO V-630 spectrophotometer at 25 °C with 1.0 cm matched quartz cells and with a spectral bandwidth of 0.5 nm. Dye loading was determined by recording the absorbance band at 548 nm using a calibration curve in MeOH.

Transmission Electron Microscopy

TEM images were recorded in a transmission electron microscope EM 410, Philips operating at 60-80 kV. Samples of block copolypeptides (1-2 mg/mL) were applied directly onto carbon film on 200 mesh copper grids. Excess of the sample was carefully removed by capillarity, and the grids were immediately stained with one drop of 0.1 % phosphotungstic acid for 30 seconds. Excess stain was removed by capillary action.

5. REFERENCES

- [1] M. Talelli, M. Barz, C.J.F. Rijcken, F. Kiessling, W.E. Hennink, T. Lammers, Core-crosslinked polymeric micelles: Principles, preparation, biomedical applications and clinical translation, *Nano Today* 10(1) (2015) 93-117.
- [2] S.R. Croy, G.S. Kwon, Polymeric micelles for drug delivery, *Current Pharmaceutical Design* 12(36) (2006) 4669-4684.
- [3] C. Tanford, *The Hydrophobic Effect: Formation of Micelles and Biological Membranes*, 1980.
- [4] A. Lalatsa, A.G. Schatzlein, M. Mazza, B.H.L. Thi, I.F. Uchegbu, Amphiphilic poly(l-amino acids) - New materials for drug delivery, *Journal of Controlled Release* 161(2) (2012) 523-536.
- [5] H.L. Xu, Q. Yao, C.F. Cai, J.X. Gou, Y. Zhang, H.J. Zhong, X. Tang, Amphiphilic poly(amino acid) based micelles applied to drug delivery: The in vitro and in vivo challenges and the corresponding potential strategies, *Journal of Controlled Release* 199 (2015) 84-97.
- [6] A. Duro-Castano, I. Conejos-Sanchez, M.J. Vicent, Peptide-Based Polymer Therapeutics, *Polymers* 6(2) (2014) 515-551.
- [7] I. Dolz-Perez, M.A. Sallam, E. Masia, D. Morello-Bolumar, M.D.P. del Caz, P. Graff, D. Abdelmonsif, S. Hedtrich, V.J. Nebot, M.J. Vicent, Polypeptide-corticosteroid conjugates as a topical treatment approach to psoriasis, *Journal of Controlled Release* 318 (2020) 210-222.
- [8] J. Huang, A. Heise, Stimuli responsive synthetic polypeptides derived from N-carboxyanhydride (NCA) polymerisation, *Chemical Society Reviews* 42(17) (2013) 7373-7390.
- [9] W.K. Hu, M. Ying, S.M. Zhang, J.L. Wang, Poly(amino acid)-Based Carrier for Drug Delivery Systems, *Journal of Biomedical Nanotechnology* 14(8D) (2018) 1359-1374.
- [10] S.E. Barrett, R.S. Burke, M.T. Abrams, C. Bason, M. Busuek, E. Carlini, B.A. Carr, L.S. Crocker, H. Fan, R.M. Garbaccio, E.N. Guidry, J.H. Heo, B.J. Howell, E.A. Kemp, R.A. Kowtoniuk, A.H. Latham, A.M. Leone, M. Lyman, R.G. Parmar, M. Patel, S.Y. Pechenov, T. Pei, N.T. Pudvah, C. Raab, S. Riley, L. Sepp-Lorenzino, S. Smith, E.D. Soli, S. Staskiewicz, M. Stern, Q. Truong, M. Vavrek, J.H. Waldman, E.S. Walsh, J.M. Williams, S. Young, S.L. Colletti, Development of a liver-targeted siRNA delivery platform with a broad therapeutic window utilizing biodegradable polypeptide-based polymer conjugates, *Journal of Controlled Release* 183 (2014) 124-137.
- [11] D. Skoulas, P. Christakopoulos, D. Stavroulaki, K. Santorinaios, V. Athanasiou, H. Iatrou, Micelles Formed by Polypeptide Containing Polymers Synthesized Via N-Carboxy Anhydrides and Their Application for Cancer Treatment, *Polymers* 9(6) (2017).
- [12] A.R. Mazo, S. Allison-Logan, F. Karimi, N.J.A. Chan, W.L. Qiu, W. Duan, N.M. O'Brien-Simpson, G.G. Qiao, Ring opening polymerization of alpha-amino acids: advances in synthesis, architecture and applications of polypeptides and their hybrids, *Chemical Society Reviews* 49(14) (2020) 4737-4834.
- [13] P. Mi, K. Miyata, K. Kataoka, H. Cabral, Clinical Translation of Self-Assembled Cancer Nanomedicines, *Advanced Therapeutics* (2020).
- [14] R. Thipparaboina, R.B. Chavan, D. Kumar, S. Modugula, N.R. Shastri, Micellar carriers for the delivery of multiple therapeutic agents, *Colloids and Surfaces B-Biointerfaces* 135 (2015) 291-308.

- [15] T. Melnyk, S. Dordevic, I. Conejos-Sanchez, M.J. Vicent, Therapeutic potential of polypeptide-based conjugates: Rational design and analytical tools that can boost clinical translation, *Advanced drug delivery reviews* 160 (2020) 136-169.
- [16] Y. Matsumura, K. Kataoka, Preclinical and clinical studies of anticancer agent-incorporating polymer micelles, *Cancer Science* 100(4) (2009) 572-579.
- [17] K. Knop, R. Hoogenboom, D. Fischer, U.S. Schubert, Poly(ethylene glycol) in Drug Delivery: Pros and Cons as Well as Potential Alternatives, *Angewandte Chemie-International Edition* 49(36) (2010) 6288-6308.
- [18] G. Pasut, F.M. Veronese, Polymer-drug conjugation, recent achievements and general strategies, *Progress in Polymer Science* 32(8-9) (2007) 933-961.
- [19] M. Barz, R. Luxenhofer, R. Zentel, M.J. Vicent, Overcoming the PEG-addiction: well-defined alternatives to PEG, from structure-property relationships to better defined therapeutics, *Polymer Chemistry* 2(9) (2011) 1900-1918.
- [20] K.D. Hinds, Protein conjugation, cross-linking, and PEGylation, *Biomaterials for Delivery and Targeting of Proteins and Nucleic Acids* (2005) 119-185.
- [21] S. Reichert, M. Calderon, K. Licha, R. Haag, Multivalent Dendritic Architectures for Theranostics, *Multifunctional Nanoparticles for Drug Delivery Applications: Imaging, Targeting, and Delivery* (2012) 315-344.
- [22] L.J. Suggs, J.L. West, A.G. Mikos, Platelet adhesion on a bioresorbable poly(propylene fumarate-co-ethylene glycol) copolymer, *Biomaterials* 20(7) (1999) 683-690.
- [23] H. Hatakeyama, H. Akita, H. Harashima, The Polyethyleneglycol Dilemma: Advantage and Disadvantage of PEGylation of Liposomes for Systemic Genes and Nucleic Acids Delivery to Tumors, *Biological & Pharmaceutical Bulletin* 36(6) (2013) 892-899.
- [24] F. Zhang, M.R. Liu, H.T. Wan, Discussion about Several Potential Drawbacks of PEGylated Therapeutic Proteins, *Biological & Pharmaceutical Bulletin* 37(3) (2014) 335-339.
- [25] Y. Fang, J.X. Xue, S. Gao, A.Q. Lu, D.J. Yang, H. Jiang, Y. He, K. Shi, Cleavable PEGylation: a strategy for overcoming the "PEG dilemma" in efficient drug delivery, *Drug Delivery* 24(2) (2017) 22-32.
- [26] G.T. Kozma, T. Shimizu, T. Ishida, J. Szebeni, Anti-PEG antibodies: Properties, formation, testing and role in adverse immune reactions to PEGylated nanobiopharmaceuticals, *Advanced drug delivery reviews* 154-155 (2020) 163-175.
- [27] T.J. Deming, Methodologies for preparation of synthetic block copolypeptides: materials with future promise in drug delivery, *Advanced Drug Delivery Reviews* 54(8) (2002) 1145-1155.
- [28] I. Captain, T.J. Deming, Methionine Sulfoxide and Phosphonate Containing Double Hydrophilic Block Copolypeptides and Their Mineralization of Calcium Carbonate, *Journal of Polymer Science Part a-Polymer Chemistry* 54(23) (2016) 3707-3712.
- [29] R. Petitdemange, E. Garanger, L. Bataille, W. Dieryck, K. Bathany, B. Garbay, T.J. Deming, S. Lecommandoux, Selective Tuning of Elastin-like Polypeptide Properties via Methionine/Oxidation, *Biomacromolecules* 18(2) (2017) 544-550.
- [30] A.L. Wollenberg, T.M. O'Shea, J.H. Kim, A. Czechanski, L.G. Reinholdt, M.V. Sofroniew, T.J. Deming, Injectable polypeptide hydrogels via methionine modification for neural stem cell delivery, *Biomaterials* 178 (2018) 527-545.
- [31] J.R. Kramer, A.R. Rodriguez, U.-J. Choe, D.T. Kamei, T.J. Deming, Glycopolypeptide conformations in bioactive block copolymer assemblies influence their nanoscale morphology, *Soft Matter* 9(12) (2013) 3389-3395.

- [32] J.R. Kramer, T.J. Deming, Glycopolypeptides via Living Polymerization of Glycosylated-L-lysine N-Carboxyanhydrides, *Journal of the American Chemical Society* 132(42) (2010) 15068-15071.
- [33] A. Birke, J. Ling, M. Barz, Polysarcosine-containing copolymers: Synthesis, characterization, self-assembly, and applications, *Progress in Polymer Science* 81 (2018) 163-208.
- [34] N. Gangloff, J. Ulbricht, T. Lorson, H. Schlaad, R. Luxenhofer, Peptoids and Polypeptoids at the Frontier of Supra- and Macromolecular Engineering, *Chemical Reviews* 116(4) (2016) 1753-1802.
- [35] F. Sigmund, F. Wessely, Research on the alpha-amino-Nu-carbonic acid anhydrides. II, *Hoppe-Seylers Zeitschrift Fur Physiologische Chemie* 157(1/3) (1926) 91-105.
- [36] S.S. Nogueira, Polysarcosine-Functionalized Lipid Nanoparticles for Therapeutic mRNA Delivery, in: A. Schlegel (Ed.) *ACS Appl. Nano Mater.*, ACS Appl. Nano Mater., 2020, pp. 10634–10645.
- [37] G. Gaucher, M.H. Dufresne, V.P. Sant, N. Kang, D. Maysinger, J.C. Leroux, Block copolymer micelles: preparation, characterization and application in drug delivery, *Journal of Controlled Release* 109(1-3) (2005) 169-188.
- [38] J.J. Cheng, T.J. Deming, Synthesis of Polypeptides by Ring-Opening Polymerization of alpha-Amino Acid N-Carboxyanhydrides, *Peptide-Based Materials* 310 (2012) 1-26.
- [39] G.H. Van Domeselaar, G.S. Kwon, L.C. Andrew, D.S. Wishart, Application of solid phase peptide synthesis to engineering PEO-peptide block copolymers for drug delivery, *Colloids and Surfaces B-Biointerfaces* 30(4) (2003) 323-334.
- [40] I.L. Shih, Y.T. Van, M.H. Shen, Biomedical applications of chemically and microbiologically synthesized poly(glutamic acid) and poly(lysine), *Mini-Reviews in Medicinal Chemistry* 4(2) (2004) 179-188.
- [41] A. Mann, M.A. Khan, V. Shukla, M. Ganguli, Atomic force microscopy reveals the assembly of potential DNA "nanocarriers" by poly-L-ornithine, *Biophysical Chemistry* 129(2-3) (2007) 126-136.
- [42] E.P. Holowka, V.Z. Sun, D.T. Kamei, T.J. Deming, Polyarginine segments in block copolypeptides drive both vesicular assembly and intracellular delivery, *Nature Materials* 6(1) (2007) 52-57.
- [43] O. Zagorodko, J.J. Arroyo-Crespo, V.J. Nebot, M.J. Vicent, Polypeptide-Based Conjugates as Therapeutics: Opportunities and Challenges, *Macromolecular Bioscience* 17(1) (2017).
- [44] S. Niimura, H. Kurosu, A. Shoji, Precise structural analysis of alpha-helical polypeptide by quantum-chemical calculation related to reciprocal side-chain combination of two L-phenylalanine residues, *Journal of Molecular Structure* 970(1-3) (2010) 96-100.
- [45] Z.Y. Song, H.L. Fu, J. Wang, J.S. Hui, T.R. Xue, L.A. Pacheco, H.Y. Yan, R. Baumgartner, Z.Y. Wang, Y.C. Xia, X.F. Wang, L.C. Yin, C.Y. Chen, J. Rodriguez-Lopez, A.L. Ferguson, Y. Lin, J.J. Cheng, Synthesis of polypeptides via bioinspired polymerization of in situ purified N-carboxyanhydrides, *Proceedings of the National Academy of Sciences of the United States of America* 116(22) (2019) 10658-10663.
- [46] G. Le Fer, D. Portes, G. Goudounet, J.-M. Guigner, E. Garanger, S. Lecommandoux, Design and self-assembly of PBLG-b-ELP hybrid diblock copolymers based on synthetic and elastin-like polypeptides, *Organic & Biomolecular Chemistry* 15(47) (2017) 10095-10104.
- [47] Z. Song, Z. Han, S. Lv, C. Chen, L. Chen, L. Yin, J. Cheng, Synthetic polypeptides: from polymer design to supramolecular assembly and biomedical application, *Chemical Society Reviews* 46(21) (2017) 6570-6599.

- [48] S.H. Wibowo, A. Sulistio, E.H.H. Wong, A. Blencowe, G.G. Qiao, Functional and Well-Defined -Sheet-Assembled Porous Spherical Shells by Surface-Guided Peptide Formation, *Advanced Functional Materials* 25(21) (2015) 3147-3156.
- [49] A. Sinaga, T.A. Hatton, K.C. Tam, Thermodynamics of micellization of beta-sheet forming poly(acrylic acid)-block-poly(L-valine) hybrids, *Journal of Physical Chemistry B* 112(37) (2008) 11542-11550.
- [50] H.J. Song, G. Yang, P.S. Huang, D.L. Kong, W.W. Wang, Self-assembled PEG-poly(L-valine) hydrogels as promising 3D cell culture scaffolds, *Journal of Materials Chemistry B* 5(9) (2017) 1724-1733.
- [51] H.Y. Zhu, M. Zhu, S.R. Shuai, C. Zhao, Y. Liu, X.H. Li, Z.K. Rao, Y. Li, J.Y. Hao, Effect of polypeptide block length on nano-assembly morphology and thermo-sensitivity of methyl poly (ethylene glycol)-poly (L-valine) copolymer aqueous solutions, *Journal of Sol-Gel Science and Technology* 92(3) (2019) 618-627.
- [52] A. Sinaga, P. Ravi, T.A. Hatton, K.C. Tam, Synthesis of poly(acrylic acid)-block-poly(L-valine) hybrid through combined atom transfer radical polymerization, click chemistry, and nickel-catalyzed ring opening polymerization methods, *Journal of Polymer Science Part a-Polymer Chemistry* 45(13) (2007) 2646-2656.
- [53] F.I. El-Dossoki, E.A. Gomaa, O.K. Hamza, Solvation thermodynamic parameters for sodium dodecyl sulfate (SDS) and sodium lauryl ether sulfate (SLES) surfactants in aqueous and alcoholic-aqueous solvents, *Sn Applied Sciences* 1(8) (2019).
- [54] S. Tan, C. Zou, W. Zhang, M. Yin, X. Gao, Q. Tang, Recent developments in D-alpha-tocopheryl polyethylene glycol-succinate-based nanomedicine for cancer therapy (vol 24, 1406561, 2017), *Drug Delivery* 24(1) (2017).
- [55] A.S. Nosova, O.O. Koloskova, A.A. Nikonova, V.A. Simonova, V.V. Smirnov, D. Kudlay, M.R. Khaitov, Diversity of PEGylation methods of liposomes and their influence on RNA delivery, *Medchemcomm* 10(3) (2019) 369-377.
- [56] <https://www.pharmtech.com/view/using-tocophersolan-drug-delivery>.
- [57] C.L. Yang, T.T. Wu, Y. Qi, Z.P. Zhang, Recent Advances in the Application of Vitamin E TPGS for Drug Delivery, *Theranostics* 8(2) (2018) 464-485.
- [58] Z.P. Zhang, S.W. Tan, S.S. Feng, Vitamin E TPGS as a molecular biomaterial for drug delivery, *Biomaterials* 33(19) (2012) 4889-4906.
- [59] N. Duhem, F. Danhier, V. Preat, Vitamin E-based nanomedicines for anti-cancer drug delivery, *Journal of Controlled Release* 182 (2014) 33-44.
- [60] S. Rathod, P. Bahadur, S. Tiwari, Nanocarriers based on vitamin E-TPGS: Design principle and molecular insights into improving the efficacy of anticancer drugs, *International journal of pharmaceutics* 592 (2021) 120045-120045.
- [61] Y. Guo, J. Luo, S. Tan, B.O. Otieno, Z. Zhang, The applications of Vitamin E TPGS in drug delivery, *European Journal of Pharmaceutical Sciences* 49(2) (2013) 175-186.
- [62] A.H. Nada, A.A. Zaghoul, M.M. Hedaya, I.S. Khattab, Development of novel formulations to enhance in vivo transdermal permeation of tocopherol, *Acta Pharmaceutica* 64(3) (2014) 299-309.
- [63] H. Singh, J. Singh, S.K. Singh, N. Singh, S. Paul, H.S. Sohal, U. Gupta, S.K. Jain, Vitamin E TPGS based palatable, oxidatively and physically stable emulsion of microalgae DHA oil for infants, children and food fortification, *Journal of Dispersion Science and Technology* 41(11) (2020) 1674-1689.
- [64] D. Huesmann, A. Sevenich, B. Weber, M. Barz, A head-to-head comparison of poly(sarcosine) and poly(ethylene glycol) in peptidic, amphiphilic block copolymers, *Polymer* 67 (2015) 240-248.

- [65] D. Liang, A.-t. Wang, Z.-z. Yang, Y.-j. Liu, X.-r. Qi, Enhance Cancer Cell Recognition and Overcome Drug Resistance Using Hyaluronic Acid and alpha-Tocopheryl Succinate Based Multifunctional Nanoparticles, *Molecular Pharmaceutics* 12(6) (2015) 2189-2202.
- [66] Y. Xiao, J.Q. Wang, J. Zhang, A. Heise, M.D. Lang, Synthesis and gelation of copolypept(o)ides with random and block structure, *Biopolymers* 107(10) (2017) 9.
- [67] K. Son, M. Ueda, K. Taguchi, T. Maruyama, S. Takeoka, Y. Ito, Evasion of the accelerated blood clearance phenomenon by polysarcosine coating of liposomes, *Journal of Controlled Release* 322 (2020) 209-216.
- [68] O. Schafer, K. Klinker, L. Braun, D. Huesmann, J. Schultze, K. Koynov, M. Barz, Combining Orthogonal Reactive Groups in Block Copolymers for Functional Nanoparticle Synthesis in a Single Step, *Acs Macro Letters* 6(10) (2017) 1140-1145.
- [69] D. Huesmann, K. Klinker, M. Barz, Orthogonally reactive amino acids and end groups in NCA polymerization, *Polymer Chemistry* 8(6) (2017) 957-971.
- [70] A. Isidro-Llobet, M. Alvarez, F. Albericio, Amino Acid-Protecting Groups, *Chemical Reviews* 109(6) (2009) 2455-2504.
- [71] I. Conejos-Sanchez, A. Duro-Castano, A. Birke, M. Barz, M.J. Vicent, A controlled and versatile NCA polymerization method for the synthesis of polypeptides, *Polymer Chemistry* 4(11) (2013) 3182-3186.
- [72] M. Barz, A. Duro-Castano, M.J. Vicent, A versatile post-polymerization modification method for polyglutamic acid: synthesis of orthogonal reactive polyglutamates and their use in "click chemistry", *Polymer Chemistry* 4(10) (2013) 2989-2994.
- [73] A. Duro-Castano, V.J. Nebot, A. Nino-Pariente, A. Arminan, J.J. Arroyo-Crespo, A. Paul, N. Feiner-Gracia, L. Albertazzi, M.J. Vicent, Capturing "Extraordinary" Soft-Assembled Charge-Like Polypeptides as a Strategy for Nanocarrier Design, *Advanced Materials* 29(39) (2017) 12.
- [74] H.Y. Yu, Z.H. Tang, D.W. Zhang, W.T. Song, T.C. Duan, J.K. Gu, X.S. Chen, Poly(ornithine-co-arginine-co-glycine-co-aspartic Acid): Preparation via NCA Polymerization and its Potential as a Polymeric Tumor-Penetrating Agent, *Macromolecular Bioscience* 15(6) (2015) 829-838.
- [75] A. Gonzalez-Paredes, D. Torres, M.J. Alonso, Polyarginine nanocapsules: A versatile nanocarrier with potential in transmucosal drug delivery, *International Journal of Pharmaceutics* 529(1-2) (2017) 474-485.
- [76] J. Rodriguez-Hernandez, S. Lecommandoux, Reversible inside-out micellization of pH-responsive and water-soluble vesicles based on polypeptide diblock copolymers, *Journal of the American Chemical Society* 127(7) (2005) 2026-2027.
- [77] T.J. Deming, Synthesis and Self-Assembly of Well-Defined Block Copolypeptides via Controlled NCA Polymerization, *Hierarchical Macromolecular Structures: 60 Years after the Staudinger Nobel Prize* 1-37 (2013) 1-37.
- [78] F.K.M. Chan, R.M. Siegel, D. Zacharias, R. Swofford, K.L. Holmes, R.Y. Tsien, M.J. Lenardo, Fluorescence resonance energy transfer analysis of cell surface receptor interactions and signaling using spectral variants of the green fluorescent protein, *Cytometry* 44(4) (2001) 361-368.
- [79] C.C. Decandio, E.R. Silva, I.W. Hamley, V. Castelletto, M.S. Liberato, V.X. Oliveira, C.L.P. Oliveira, W.A. Alves, Self-Assembly of a Designed Alternating Arginine/Phenylalanine Oligopeptide, *Langmuir* 31(15) (2015) 4513-4523.
- [80] X.Z. Liu, R.R. Fan, B.T. Lu, Y. Le, Polypeptides Micelles Composed of Methoxy-Poly(Ethylene Glycol)-Poly(L-Glutamic Acid)-Poly(L-Phenylalanine) Triblock Polymer for Sustained Drug Delivery, *Pharmaceutics* 10(4) (2018) 14.

- [81] V. Castelletto, I.W. Hamley, Self assembly of a model amphiphilic phenylalanine peptide/polyethylene glycol block copolymer in aqueous solution, *Biophysical Chemistry* 141(2-3) (2009) 169-174.
- [82] M. Reches, E. Gazit, Casting metal nanowires within discrete self-assembled peptide nanotubes, *Science* 300(5619) (2003) 625-627.
- [83] J. Aguiar, P. Carpena, J.A. Molina-Bolivar, C.C. Ruiz, On the determination of the critical micelle concentration by the pyrene 1 : 3 ratio method, *Journal of Colloid and Interface Science* 258(1) (2003) 116-122.
- [84] K. Prompruk, T. Govender, S. Zhang, C.D. Xiong, S. Stolnik, Synthesis of a novel PEG-block-poly(aspartic acid-stat-phenylalanine) copolymer shows potential for formation of a micellar drug carrier, *International Journal of Pharmaceutics* 297(1-2) (2005) 242-253.
- [85] Z. Ahmad, Z.H. Tang, A. Shah, S.X. Lv, D.W. Zhang, Y. Zhang, X.S. Chen, Cisplatin Loaded Methoxy Poly (ethylene glycol)-block-Poly (L-glutamic acid-co-L-Phenylalanine) Nanoparticles against Human Breast Cancer Cell, *Macromolecular Bioscience* 14(9) (2014) 1337-1345.
- [86] W. Fieber, A. Herrmann, L. Ouali, M.I. Velazco, G. Kreutzer, H.A. Klok, C. Ternat, C.J.G. Plummer, J.A.E. Manson, H. Sommer, NMR diffusion and relaxation studies of the encapsulation of fragrances by amphiphilic multiarm star block copolymers, *Macromolecules* 40(15) (2007) 5372-5378.

**CHAPTER III: DEVELOPMENT
OF A HYALURONATE-
POLYGLUTAMATE CROSS-
POLYMER AS PERMEATION
ENHANCER IN SKIN
DELIVERY APPROACHES**

The *in vitro* and *ex vivo* experiments of this chapter were performed by **Irene Dolz Perez**, who also presented part of these results in her thesis dissertation.

1. INTRODUCTION

The skin is the largest and most visible organ in the body, with an average surface area of 1.5 – 2 m², and represents the first barrier between the external environment and the interior of the human body [1]. The skin is a membranous, flexible, and protective cover formed by two principal layers: (i) an external, non-vascularized tissue layer (containing the stratum corneum and epidermis), and (ii) an internal, vascularized tissue layer (the dermis) [2]. The skin plays various roles, including temperature regulation, electrolyte balance control, and protection from microorganisms, chemical agents, physical injury, and ultraviolet radiation [3]. While these characteristics provide the human body with excellent protection, the various skin layers also function as barriers to the passage of therapeutic agents into the human body.

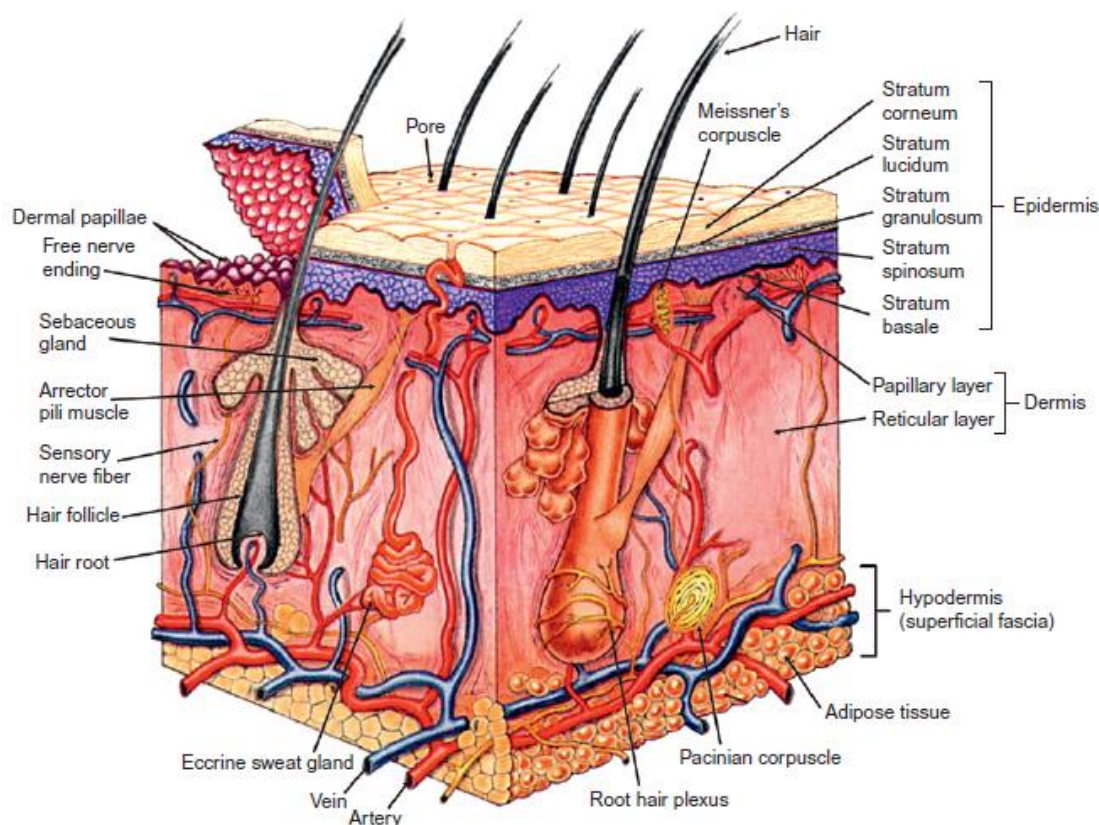


Figure 3.1. Schematic compounds and layers of the human skin. Image adapted from Shah et al [4].

Delivery through the skin offers a comfortable and non-invasive route for the administration of active pharmaceutical ingredients (APIs) that avoids the need for trained personnel and potential risks associated with hypodermic injections or oral administration [5]. Multiple nanosized platforms have been investigated to facilitate the topical delivery of APIs – strategies include liposomes (classical lipids), acrosomes (archaeobacterial lipids), lipoplexes (cationic lipid-DNA complex), proliposomes (dry,

free-flowing particles), cubosomes (particles of bicontinuous cubic liquid crystalline phase), ufasomes (lipids that attach to the skin surface), and niosomes (non-ionic surfactant and cholesterol-based lipids) [4], as well as other supramolecular architectures such as micelles, nanoparticles, emulsions, and hydrogels [3].

Recent strategies for the topical administration of APIs to specific skin layers have explored the potential of polymeric formulations of drugs as emulsions, creams, gels, hydrogels, transdermal patches, and wound dressings, and the application of polymers as penetration enhancers [6]. Among the currently studied polymer for skin delivery applications [6-8] selected polysaccharides and polyaminoacid could offer advantages over the other due to their multivalency and biodegradability [9-11].

Polysaccharides include naturally occurring polymers produced by algae (e.g., alginate), plants (e.g., cellulose), microbes (e.g., dextran), and animals (e.g., hyaluronic acid) [12]. Hyaluronic acid (HA, also called hyaluronan), a natural heteropolysaccharide with a linear structure discovered by Meyer and Palmer in 1934, contains alternating D-glucuronic acid and N-acetyl-D-glucosamide residues [13]. While the human body contains an average of 15 g of HA, the skin makes up approximately one-third of this total [14]. Thanks to its versatile properties, including biocompatibility, non-immunogenicity, biodegradability, and viscoelasticity, HA is an ideal biomaterial for cosmetic, medical, and pharmaceutical applications, which include the facilitation of drug delivery through the skin [15]. Examples include the implementation of HA to create a gel form of diclofenac (Solaraze®) for the topical treatment of actinic keratoses [16], and the formulation of HA microparticle-organogels for the topical delivery of caffeine [17, 18].

Compared to polysaccharides, there exist few examples of polypeptides in drug delivery through the skin. However, Ben-Zur and Goldman reported that gamma-poly-L-glutamic acid (γ -PGlu) could significantly improve skin moisturization and elasticity compared to hyaluronic acid and soluble collagen [19]. Significantly, PGlu inhibits hyaluronidase, the enzyme that degrades HA in the skin connective tissue, leading to enhanced hydration and elasticity [20]. Interestingly, antimicrobial and biocompatible crosslinked polyion complex hydrogels comprising γ -PGlu and epsilon-poly-L-lysine have been used to accelerate wound healing [11], while the antimicrobial and barrier properties of amphiphilic diblock copolymers of alpha-poly-L-lysine and poly-L-leucine have been explored for topical applications [21]. Amphiphilic micelles composed of PEG-based polypeptides are also widely employed to encapsulate hydrophobic drugs or APIs in aqueous solution [22], enhance transdermal delivery [5], and treat conditions such as psoriasis [23, 24].

Considering the reported evidence, we hypothesized that a combination of HA and different manners of polypeptides would be beneficial in skin delivery applications, not only as a penetration enhancer but also to achieve a long-term effect after topical administration. Herein, we describe the development of a biodegradable cross-polymer

composed of HA and alpha-PGlu crosslinked with L-lysine (**HA-CP**). We demonstrate its use as a platform for skin delivery and its enhanced properties compared to conventional linear HA of similar Mw, such as an increased resistance to hyaluronidases (HAase) and increased skin permeation. Furthermore, our novel platform allows both hydrophilic and hydrophobic APIs to reach the epidermis, after being previously encapsulated in amphiphilic poly(amino acid) (APAA) block copolymer micelle and also in Hydrophilic Polymer with a BioMolecule (HP-BM) micelles previously described in this thesis dissertation.

2. RESULTS AND DISCUSSION

Below is shown a general scheme for the work performed summarizing the human skin permeation enhancement of the APAA micelles formulated in the **HA-CP** compared with water and linear HA formulations.

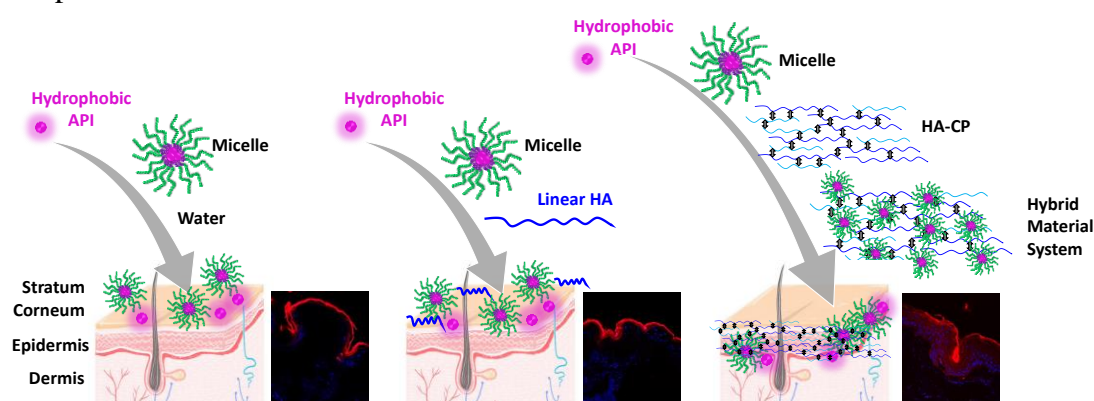


Figure 3.2. Schematic representation for skin delivery platforms developed being: (i) hydrophobic API into micelle applied in water, (ii) hydrophobic API into micelle applied in linear hyaluronic acid and (iii) hydrophobic API into micelle applied in HA-CP matrix yielding the Hybrid Material System. In the skin scheme is shown the Confocal Microscopy images obtained reaching the stratum corneum layer for two first systems and epidermis layer accumulation for Hybrid Material System.

2.1. SYNTHESIS AND CHARACTERIZATION OF A NEW HYBRID BIOMATERIAL

A novel hybrid biomaterial composed of a crosslinked hydrogel made of HA and polypeptides (**HA-CP**) capable of incorporating API-loaded polymeric micelles has been developed to be used as an API penetration enhancer in topical administrations (Scheme 3.1D). To achieve such hybrid materials three major steps have been followed: (i) synthesis of **HA-CP** (Scheme 3.1A), (ii) synthesis of polymeric micelles (Scheme 3.1C), and (iii) a final formulation of the hybrid system in aqueous media (Scheme 3.1D).

2.1.1. SYNTHESIS AND CHARACTERIZATION OF HYALURONATE-POLYGLUTAMATE CROSS-POLYMER (HA-CP)

The cross-linking of hyaluronic acid can be achieved by several methods, such as the Schiff-base reaction, Diels-Alder click cross-linking, thermo-response, ionic-cross-linking, amide or ester formation, supramolecular-cross-linking and photo-cross-linking[25]. Our hyaluronate-polyglutamate cross-polymer (**HA-CP**) was obtained through conventional amidation reactions via the activation of the carboxylic acid groups of HA and PGlu using DMTMMCl as coupling agent[26] and employing Lys primary amines as nucleophiles in a statistical crosslinking reaction (see Scheme 3.1A). The **HA-CP** cross-linking reaction was carried out under optimized experimental conditions to enhance the nucleophilicity of α and ϵ amines of Lysine (pH modulation of activation and coupling steps), the stoichiometry of the coupling agent (DMTMM). For this purpose, ^1H NMR analysis and TNBSA assay provided insight into the reaction progression, allowing us to identify the best reaction conditions [(i) activation pH \sim 7, (ii) coupling pH \sim 8, and (iii) 20 eq of DMTMMCl to Lys], yielding a product of 150 kDa after purification by dialysis (see M&M sections and Supporting Information for more details). Importantly, the starting HA employed was 50 kDa and by means of the present technology, the Mw increased over 3 times. Results can be observed in Table 3.1.

^1H NMR and DOSY NMR spectroscopy, SEC-RI-MALS, intrinsic viscosity and free amine quantification via TNBSA assay were all employed to study the crosslinking reaction and to characterize the final cross-polymer (Table 3.1, Figure 3.2).

Table 3.1. Physicochemical Characterization.

Compound	Diffusion Coefficient ($\text{m}^2 \text{s}^{-1}$)			Hydrodynamic Radius (nm)			Mw (KDa) by SEC	PDI by SEC	Mw (KDa) by intrinsic viscosity
	HA	PGlu	Lys	HA	PGlu	Lys			
HA	$1.8 \cdot 10^{-11}$ *	-	-	11.1	-	-	49.1	1.12	67
PGlu	-	$7.4 \cdot 10^{-11}$ *	-	-	2.7	-	18.9	1.37	-
Lys	-	-	$5.1 \cdot 10^{-10}$ *	-	-	0.4	-	-	-
Physical Mixture	$1.9 \cdot 10^{-11}$		$1.6 \cdot 10^{-9}$	10.4		0.1	-	-	-
HA-CP	$1.1 \cdot 10^{-11}$		**	17.9		**	145.2	1.86	114

*Values determined at 15 mg/mL. **Signals for Lys in HA-CP were not used for DOSY NMR calculations due to their very low intensity.

As observed in Figure 3.2A and 3.2B, the ^1H NMR spectra of cross-polymer confirmed the presence of HA and PGlu in the dialysis-purified cross-polymer. Lysine signals could be also identified at low intensity ratio due to the composition of **HA-CP** (\sim 1 % wt. Lys). Figure 3.2C shows a differential pulsed gradient spin of Diffusion-Ordered Spectroscopy (DOSY) NMR comparison between the physical mixture and the **HA-CP**, confirming the crosslinking and the absence of free components in **HA-CP** ($D = 1.9 \cdot 10^{-11} \text{ m}^2 \text{ s}^{-1}$ for the physical mixture vs. $1.1 \cdot 10^{-11} \text{ m}^2 \text{ s}^{-1}$ for **HA-CP**) (Table 3.1). The

Rh values obtained for HA and PGlu cross-polymer components experienced around a two-fold increase from the physical mixture compared to the **HA-CP** (10.4 nm vs. 17.9 nm, respectively), in agreement with an efficient cross-linking reaction with a moderate cross-linking degree, as expected from the Lys ratio in the reaction. This data was reinforced by SEC studies (Figure 3.2D) showing a lower retention time for **HA-CP** compared to HA with absolute Mw values being 3-fold higher upon crosslinking (145 vs 49 kDa, respectively) (Table 3.1) [13].

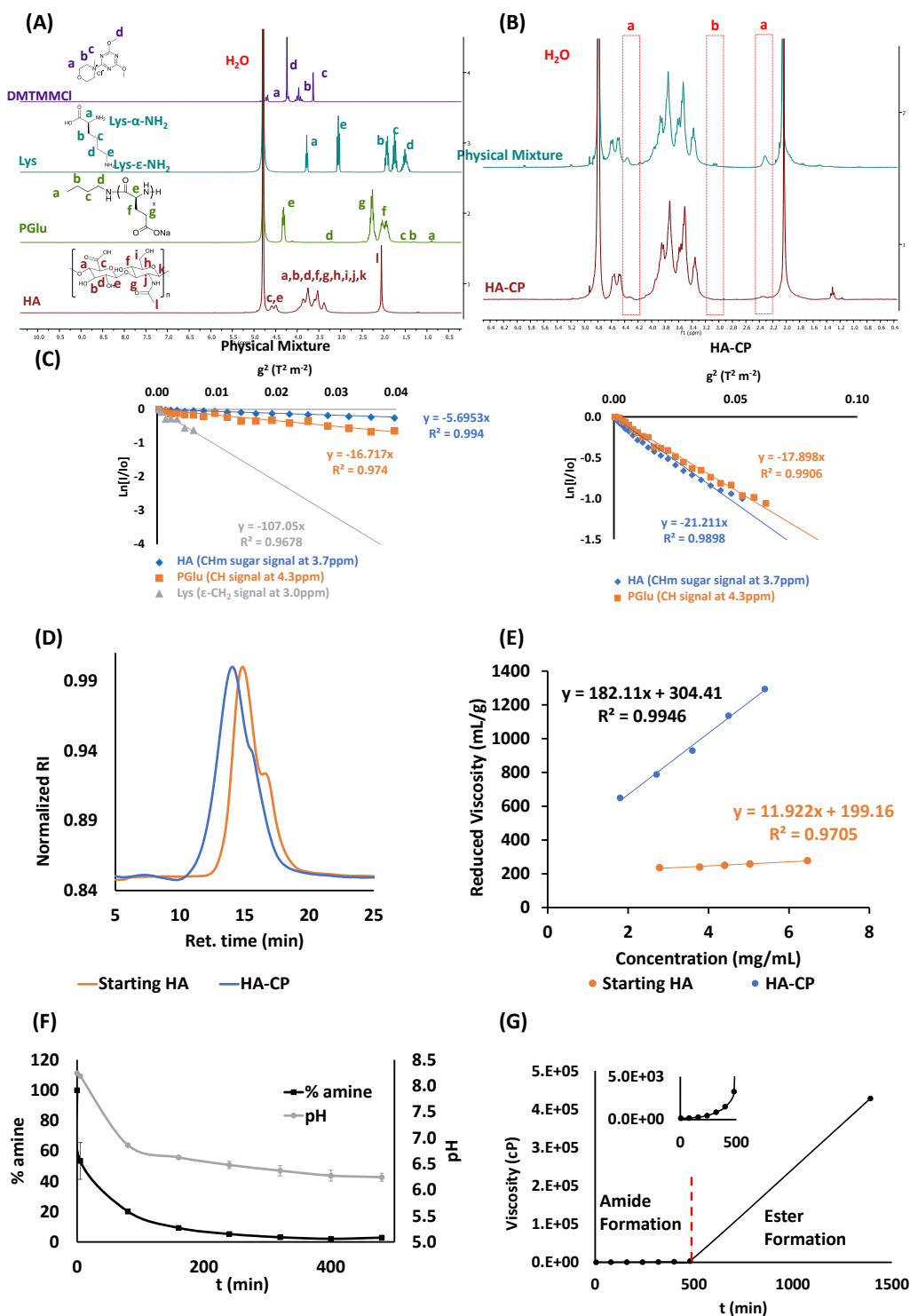


Figure 3.2. ¹H NMR studies: (A) ¹H NMR spectra in D₂O for starting materials with assigned protons. (B) ¹H NMR spectra in D₂O for **HA-CP** and physical mixture showing PGlu

signals in **HA-CP a**: Signal for PGlu; **b**: Signals for Lys in **HA-CP** were not used for DOSY NMR studies due to their very low intensity. **DOSY NMR studies (C)** Schematic representation of DOSY-NMR array data treated according to the Stejskal-Tanner equation to compare the diffusion decay of HA, PGlu, and Lys moieties. **Mw calculation (D)** SEC-RI elugram for **HA-CP** and starting HA in aqueous media NaNO₃ 100 mM at pH 5 (5 mM of PB) showing higher Mw distributions for **HA-CP** material instead of linear starting HA. **(E)** Graphic representation of reduced viscosity at different concentrations of HA-based materials to reach the average Mw. **Cross-linked reaction monitoring: (F)** % of free amine determined by TNBSA assay in the cross-linked reaction media vs pH. **(G)** Viscosity in cP for cross-linked reaction media showing an exponential increase during the first 500 minutes and very high viscosity increases after lysine consumption.

To further ratify such differences, the intrinsic viscosity was also used to determine the Mw distribution (Figure 3.2E) using the Mark-Howink-Sakurada equation (see Supporting Information (SI)), again showing similar results (Table 3.1).

In an attempt to optimize the reaction conditions for future large-scale manufacturing possibilities in mind, reaction monitoring strategies were implemented to better understand reaction kinetics. First, a colorimetric TNBSA assay was used to measure the free amine consumption with time (Figure 3.2F), determining amidation reaction completion after 400 minutes. This amine consumption was accompanied with a gradual drop in the pH that reached a plateau after the same amount of time (400 min) and remained stable at pH = 6.4 over time. Finally, simultaneous viscosity monitoring showed gradual increasing values as the reaction proceeded and, upon free amine consumption, a sharp increase after 500 minutes was observed (Figure 3.2G), suggesting that the cross-linking reaction proceeds beyond the consumption of free amines and pointing to the formation of ester bonds between hydroxyl groups of HA and carboxylates on both polymers [25, 27], an undesired side-reaction. Therefore, the ideal reaction end-timepoint was established at 400 min.

2.1.2. HA-CP SHOWS ENHANCED STABILITY IN THE PRESENCE OF HYALURONIDASE

Hyaluronidase (HAase) is an endogenous enzyme that can be encountered in many places of the human body, including the skin, that degrades HA to promote tissue renewal [28]. To study the behavior in terms of biological degradation of **HA-CP** vs. the parent HA, we performed stability experiments in presence of HAase to monitor changes in the Mw distribution. Among the techniques available to study HA degradation, (i.e. colorimetry, viscosity, electrophoresis, SEC, or mass spectrometry) [28], we selected SEC containing RI and MALS detectors due to its robustness, reproducibility, and consistency in Mw determination. HAase concentration was fixed as 5 U/mL to mimic human skin conditions [29, 30] (Figure 3.3).

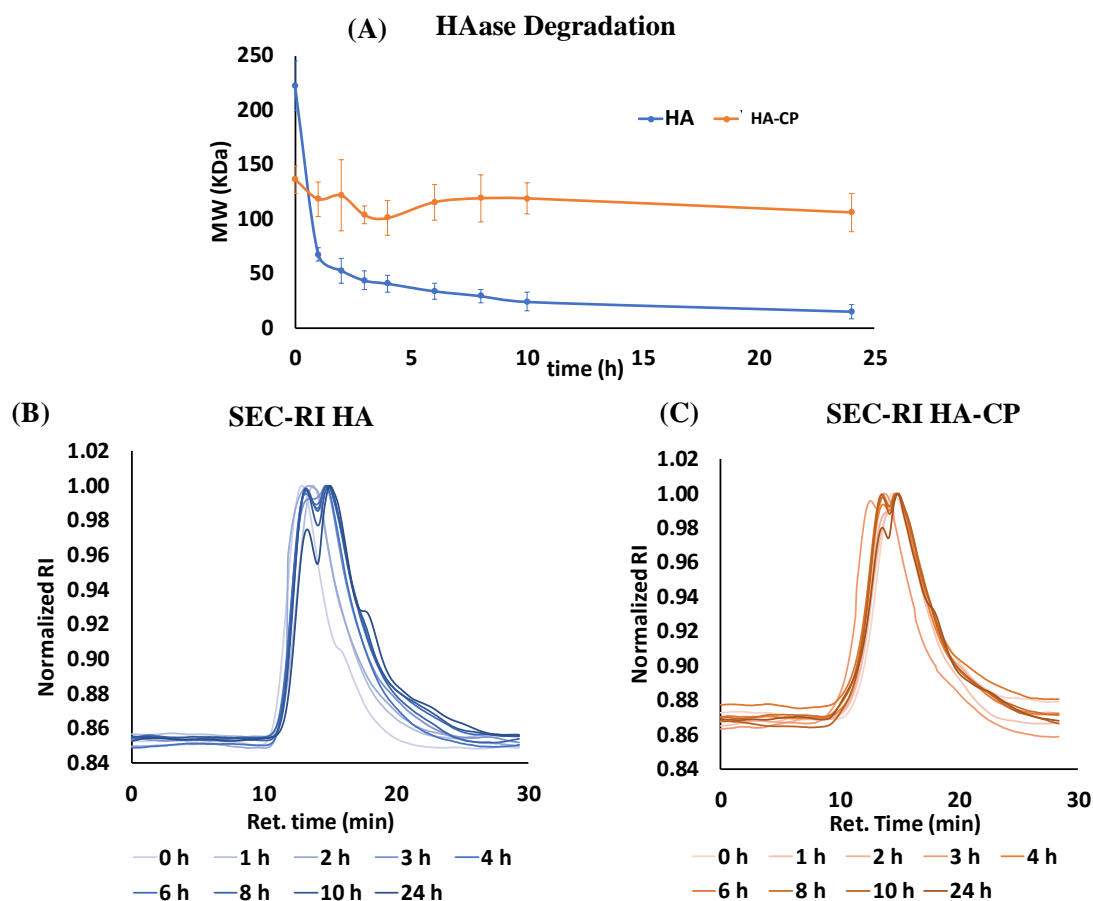


Figure 3.3. (A) Graphical representation of HAase degradation showing Mw obtained by SEC of cross-linked **HA-CP** and linear HA over time. (B) SEC-RI elugram for linear HA. (C) SEC-RI elugram for **HA-CP**. SEC conditions employed were: NaNO₃ 100 mM at pH 5 using PB 5 mM in presence of Bovine testicular HAase at 5 U/mL.

The results obtained by SEC, showed a much faster degradation for linear HA compared to our cross-linked **HA-CP** (Figure 3.3A). This effect can be explained by the different architecture of HA-based materials. The cross-linked conformation was more resistant to HAase activity most likely due to the diminished accessibility to HA chains within **HA-CP**. Due to HA degradation, bimodal Mw distribution peaks appeared with the kinetic degradation progression (Figure 3.3B-C). At the concentrations used, no direct inhibition of HAase by PGA or **HA-CP** was observed (data not shown).

2.1.3. TOWARDS THE DESIGN OF A HYBRID SYSTEM WITH CAPABILITY TO DELIVER HYDROPHILIC AS WELL AS HYDROPHOBIC APIs

In order to secure a highly efficient and versatile encapsulation of **HA-CP**, different APAA capable of encapsulating hydrophobic APIs yielding polymeric micelles were also synthesized and fully characterized. Block copolymers were based on PEG of 5 kDa as the hydrophilic part, used as a macroinitiator of ROP with L-phenylalanine (Phe) or benzyl-L-glutamate (BG) NCAs as previously described [31-33]; reaching different

degrees of polymerization (DP = 10, 20 and 40) and finally yielding a family of 6 APAA (PEG-PBG10-40 and PEG-PPhe10-40).

Block copolymer micelles with smaller Z potential average, hydrodynamic diameter, and a narrow polydispersity index were obtained by the co-solvent method [34] (see Chapter II for more detail), allowing for the encapsulation of the fluorescent dye Dil as a model hydrophobic API. The diblock copolymers to be incorporated within the hybrid material as polymeric micelles were preselected based on their micellar formulation stability. All micellar formulations at 10 mg/mL were evaluated for their stability, and it was found that those produced with larger polypeptide blocks (PEG-PPhe40 and PEG-PBG40) precipitated within a few hours when standing at room temperature, possibly due to an imbalance of the hydrophilic and hydrophobic ratio. For this reason, PEG-PBG10, PEG-PBG20, PEG-PPhe10 and PEG-PPhe20 were chosen for further evaluation. The synthesis and characterization for these APAA-based micelles is fully described in the previous chapter.

2.1.4. INTEGRATION OF THE HYBRID MATERIAL: HA-CP AND APAA BLOCK COPOLYMER MICELLES

With all the individual components ready, the desired hybrid systems composed of a **HA-CP** matrix with embedded APAA micelles were obtained, ready to test for use as penetration enhancers for hydrophobic APIs after topical administration (Scheme 3.2D). Each micelle was dissolved at 10 mg/mL in a **HA-CP** matrix solution at 1 % wt. The four resultant formulations of hybrid materials were stable with time and characterized in terms of morphology by TEM (Figure 3.4). Micelle solutions embedded into **HA-CP** with short amino acid backbone (10 units) showed spheres by TEM (Figure 3.4). We did not find any structure or morphological organization for both HA-based materials (see SI, Figure 3.11).

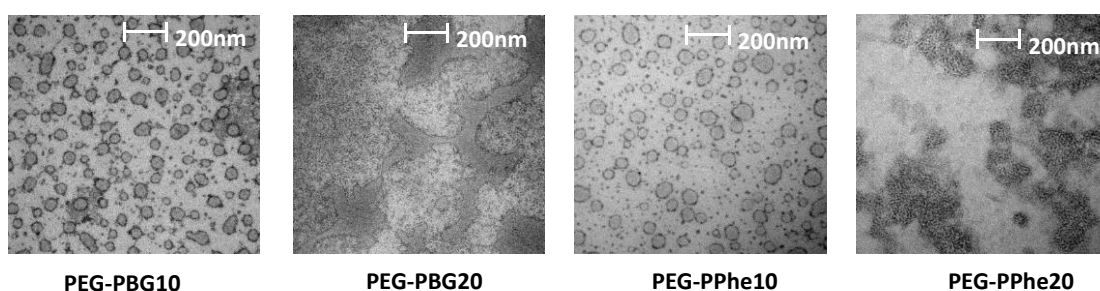


Figure 3.4. TEM images of aqueous micellar formulations at 10mg/mL block copolymers into **HA-CP** at 1%.

2.2. HA-CP CROSS-POLYMER-BASED MATERIALS AS SAFE PENETRATION ENHANCERS FOR TOPICAL ADMINISTRATION

2.2.1. ASSESSMENT OF HA-CP AND HYBRID SYSTEM SKIN PERMEATION PERFORMANCE BASED IN AMPHIPHILIC POLYAMINO ACID MICELLES

Linear HA and **HA-CP** were labelled with Cy5.5 (see Table 3.3 and Figure 3.12 in the SI section), and in parallel Dil was encapsulated in the APAA micelles as previously described in the previous chapter and its fluorescence intensity quantification used to monitor skin permeation, within the skin as well as in the Franz diffusion cell receptor chamber at different time-points. We employed benzoic acid as a positive permeation control and receptor chamber samples were analyzed by HPLC (see supporting Figure 3.13) [35].

According to skin permeation data obtained by confocal microscopy, the fluorescence emitted by Cy5.5 conjugated to both HA-based material formulations, provided direct evidence of percutaneous permeation (Figure 3.5). Skin images, as well as fluorescence quantification by means of ImageJ software, showed a greater **HA-CP** accumulation in the epidermis layer than in the stratum corneum, in direct contrast to that observed for HA (Figure 3.5A-B), demonstrating a greater skin permeation capability for our cross-linked **HA-CP**. Conventional linear HA images showed that HA was mainly accumulated in the stratum corneum as previously reported [36]. This result could be explained due to the greater skin bioavailability of **HA-CP** as shown in the stability studies in presence of HAase (Figure 3.3). No fluorescence signal was detected in either the dermis layer or the receptor chamber (see supporting Figure 3.14).

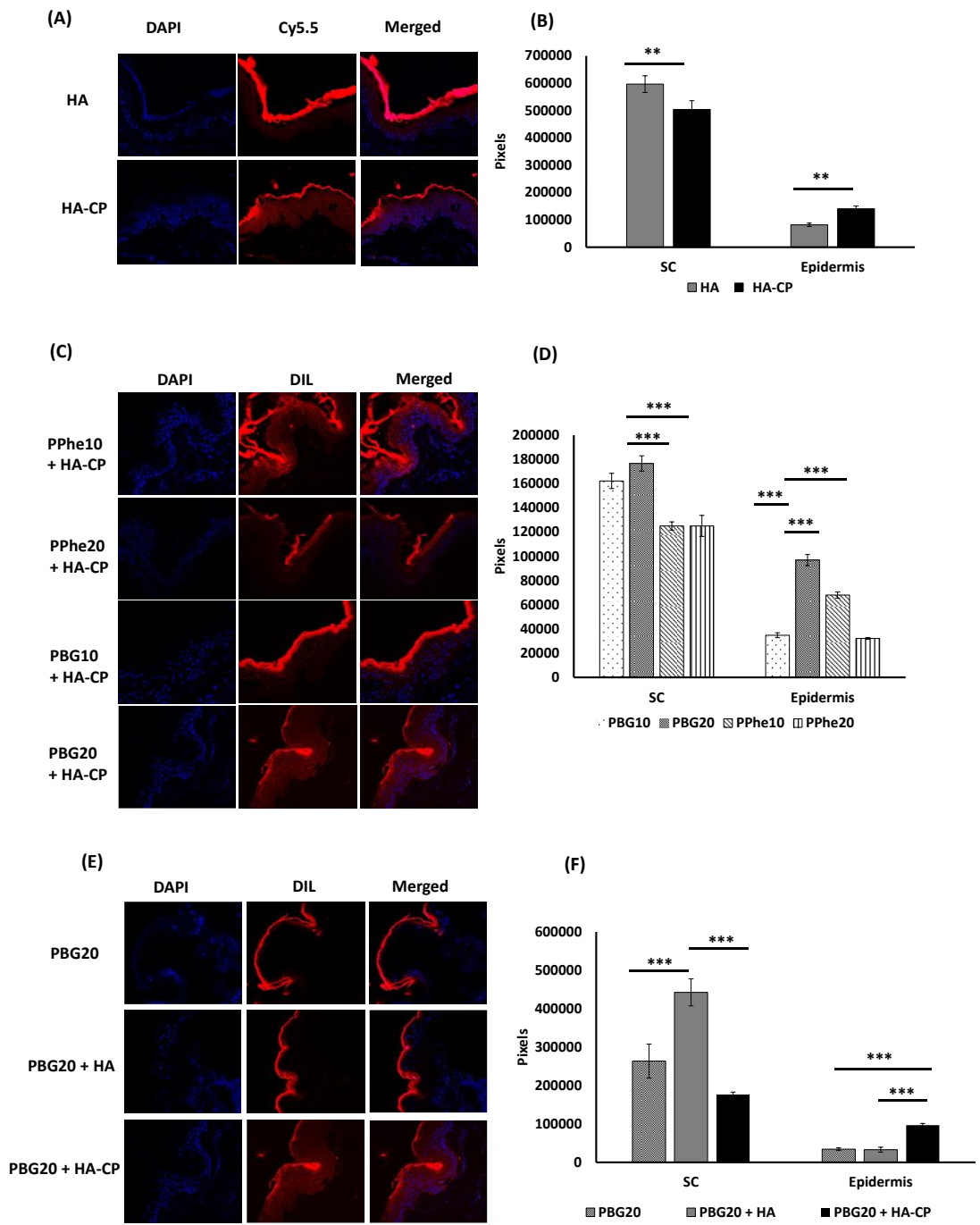


Figure 3.5. (A-B) Permeation studies of HA-Cy5.5 and HA-CP-Cy5.5 at 1 %. (A) Confocal microscopy images of Cy5.5-labeled HA and HA-CP after 8 hours of permeation using Franz diffusion cells. HA-CP was mainly accumulated in the epidermis. (B) Cy5.5 fluorescence intensity quantification by ImageJ suggests that HA-CP was able to penetrate significantly more than HA into the epidermis. (C-D) Permeation studies of the polypeptide-based micelles formulated in HA-CP (1 %). (C) Confocal microscopy images of Dil-labelled micelles formulated in HA-CP after 8 h of permeation using Franz diffusion cells. PEG-PBG20 was mainly accumulated in the epidermis. (D) Dil fluorescence intensity quantification by ImageJ suggests that PEG-PBG20 was able to penetrate significantly into the epidermis. (E-F) Permeation studies of PEG-PBG20 alone in water, applied in HA (1 %) and HA-CP (1 %). (E) Confocal microscopy images of Dil-labelled micelle PEG-PBG20 after 8 h of permeation using Franz diffusion cells. (F) Dil fluorescence intensity quantification by ImageJ. The original magnification displayed in

each image was 40x. (***) $p < 0.001$ indicates statistically significant differences after ANOVA analyses followed Bonferroni's post hoc tests). Data expressed as mean \pm SEM.

A similar trend was observed with the final hybrid material containing Dil encapsulated APAA micelles (Figure 3.5C-F). Results showed that all micelles formulated in **HA-CP** were able to reach the epidermis, with the greatest permeation up to the epidermis observed with PEG-PBG20 and PEG-PPhe10 (Figure 3.5D). However, the PEG-PBG20 micelle was selected to follow the study due to its higher encapsulation capacity and easier synthesis. The PEG-PBG20 permeation effect was more pronounced than expected when it was embedded in **HA-CP** in comparison with linear HA, or water as the control vehicle (Figure 3.5D-E). This can be attributed to the high resistance to HAase degradation of the **HA-CP** compared to the lineal HA.

2.2.2. SAFETY EVALUATION IN VITRO, EX VIVO AND IN VIVO AFTER TOPICAL ADMINISTRATION

Firstly, cell viability experiments against the two main skin cell lines, human keratinocytes (HaCaT cells) and fibroblasts [37], were performed with the individual components of the hybrid materials by MTS assay, showing the absence of toxicity up to the concentrations tested (Figure 3.15). However, due to the intrinsic viscosity of the synthesized **HA-CP**, bi-dimensional cultures were not the most adequate model and therefore, a human skin organotypic (hSOC) culture derived from healthy donor samples (from Hospital La Fe, Valencia after informed consent) was used [38]. The use of a human skin organotypic *ex vivo* culture represents an advantage for preclinical evaluation of topical delivery formulations since it not only offers more reliable results, but also provides an improvement of the 3Rs concept [39], diminishing the use of animal models [38, 40, 41]. The established human skin organotypic culture showed adequate cell viability up to 11 days, with values remaining constant until day 4 in culture media (see Figure 3.16) [41]. Hematoxylin-Eosin (H&E) staining revealed that there were no skin alterations, and the different skin layers were similar to the control at day 0. Additionally, the Ki67 marker (proliferation marker) was present at each time-point taken until day 11 in culture, suggesting that the keratinocytes were alive and able to proliferate. Ck5/6 was a marker for basal cells in the epidermis (Ck5 presents an important role giving stability to the epidermis, and Ck6 was considered as hyperproliferative cytokines) [42]. This marker represented another indication that the morphology of the skin was maintained with the cells still alive and capable to proliferate. The tissue viability was studied after 24, 48 and 72 hours of three selected formulations: (i) PEG-PBG20 in water, (ii) PEG-PBG20 applied in linear HA and (iii) PEG-PBG20 applied in **HA-CP**.

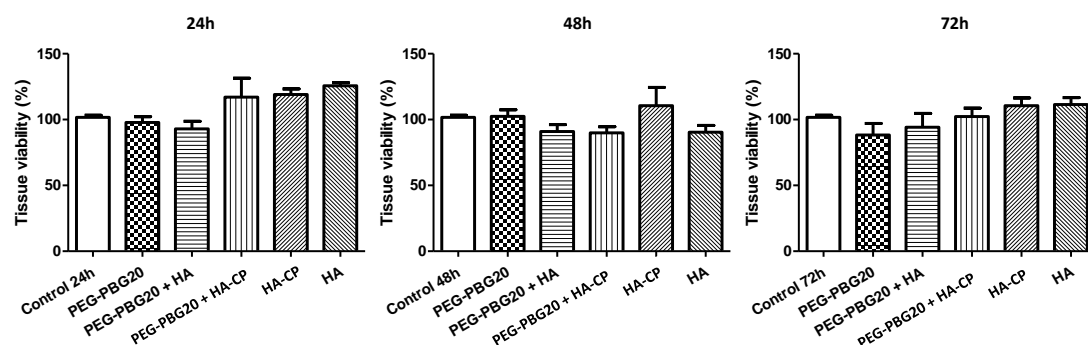


Figure 3.6. Tissue viability in hSOC after 24, 48 and 72 hours of treatment with **HA-CP**, HA, PEG-PBG20 and their combination.

The results shown in Figure 3.6 indicate that all the treatments maintain tissue viability at the concentration tested (10 mg/mL). Interestingly, our novel cross-polymer improved tissue viability at all times, with an increase even higher than HA at 48 hours. This phenomenon may be due to the increased hydration of the skin when our material was applied, since the degradation of the HA present in the **HA-CP** was slower than linear HA.

To finalize the safety evaluation of the synthesized **HA-CP** material, its irritant effect was also evaluated in a rabbit model. Repeated vaginal exposure for 5 days of albino rabbits to the **HA-CP** 1% solution revealed that **HA-CP** biomaterials do not have a vaginal irritant effect (including possible exudation, erythema, and edema features), obtaining a vaginal irritation index of 0 when tested according to the cited guidelines (Experimental section, Table 3.4 and Figure 3.17).

2.2.3. ASSESSMENT OF HA-CP AND HYBRID SYSTEM SKIN PERMEATION PERFORMANCE BASED IN HYDROPHILIC POLYMER WITH BIOMOLECULE MICELLES

Based on the obtained results for the **HA-CP** with the APAA-based micelles, we decided to study also for dermal applications both Hydrophilic Polymer with BioMolecule (HP-BM) based micelles materials: **TPGS** and **TPSS**. For this, the cell viability was tested in the first place (Figure 3.7) comparing the HP-BM materials with the free Vitamin E. Then, each HP-BM containing the Dil was formulated in the **HA-CP** matrix solution and the human skin permeation studies were carried out (Figure 3.8).

Both formulations **HA-CP** with **TPGS+Dil** and **HA-CP** with **TPSS+Dil** were analyzed in the same manner that **HA-CP** with APAA micelles containing Dil. Confocal Microscopy and pixels quantification by ImageJ results can be found in Figure 3.8. Images of Confocal Microscopy shown how the Dil accumulation in the epidermis layer is higher when it was applied in the **TPSS** micelle than **TPGS**. By pixels quantification using the ImageJ can be observed how both systems are accumulated mainly in the stratum corneum, but the **TPSS** micelle shows higher accumulation in the epidermis layer than the **TPGS** Dil micelle. In any case, we did not find Dil in the receptor chamber.

These preliminary results can be used as Proof of Concept to invert resources exploring the use of the PSar-based materials for skin delivery applications.

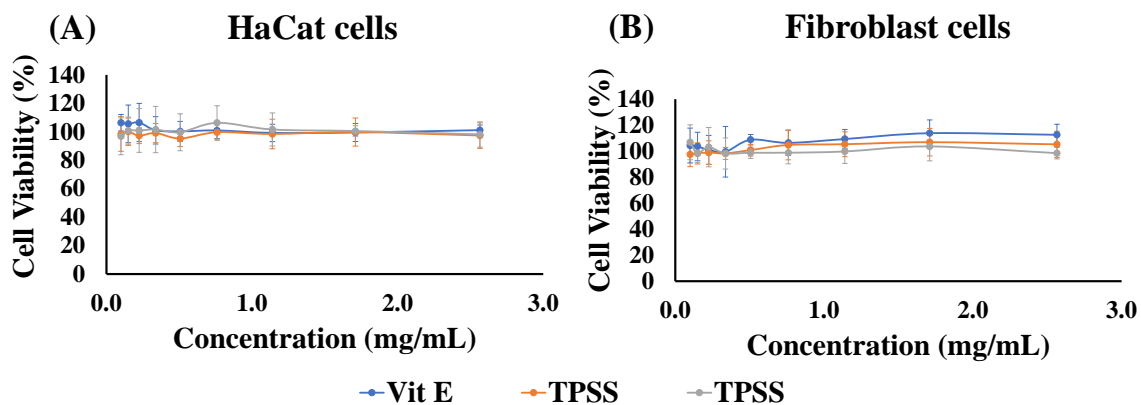


Figure 3.7. Cell viability by MTS assay: (A) Vit E and HP-BM in HaCat cells and (B) Vit E and HP-BM in Fibroblast cells. All of them after 72 hours of treatment (n = 3).

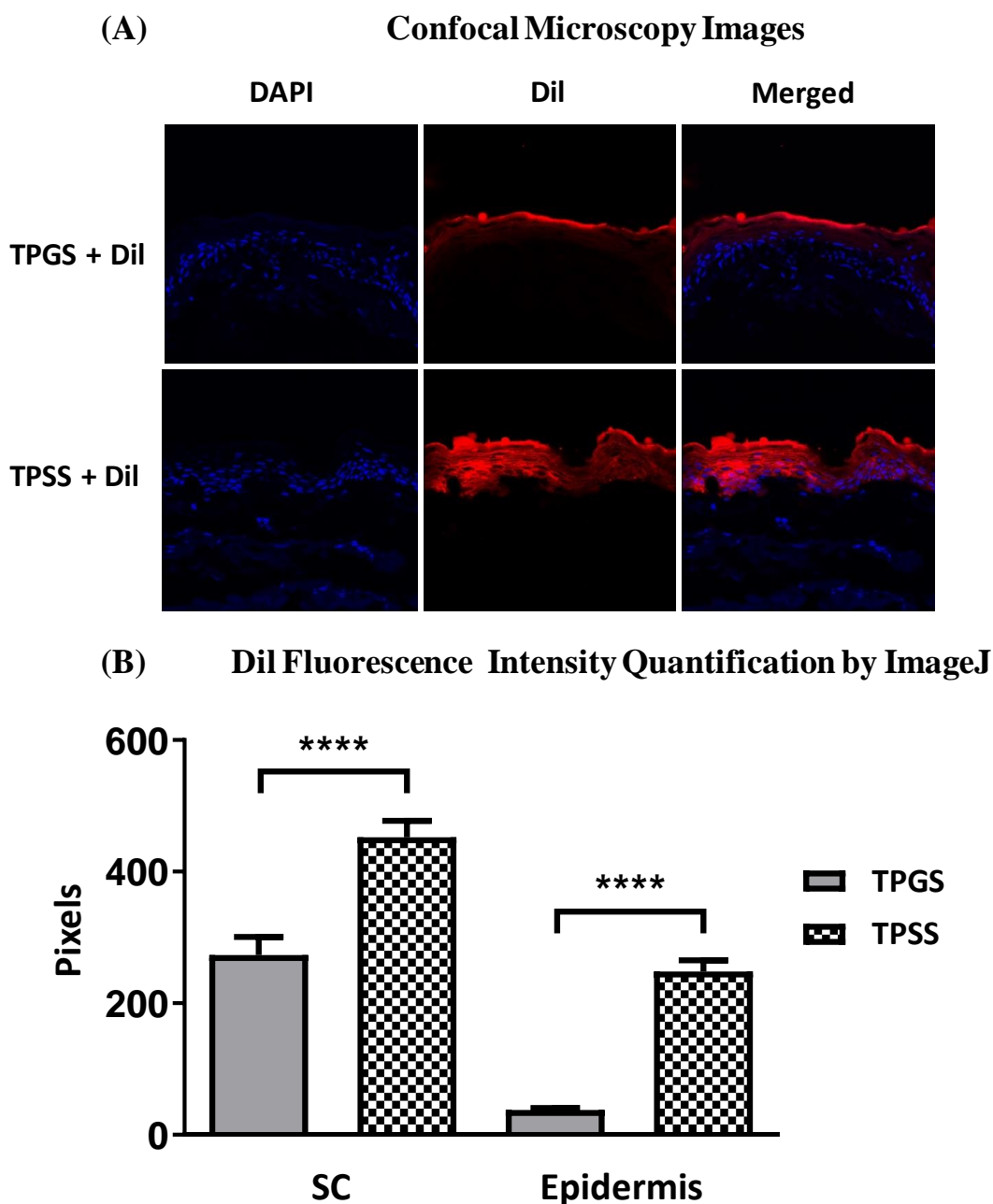


Figure 3.8. Permeation studies of **TPGS+Dil** and **TPSS+Dil** micelles at 10 mg/mL applied in **HA-CP** (1 %). (A) Confocal microscopy images of Dil-labelled micelles of **TPGS** and **TPSS** after 8 h of permeation using Franz Diffusion Cells. (B) Dil fluorescence intensity quantification by ImageJ. The original magnification displayed in each image was 40x. The asterisks indicate statistically significant differences after ANOVA analyses followed Bonferroni's post hoc tests. mean \pm SEM.

3. CONCLUSION

Herein we have described a hybrid polymeric topical delivery platform to allow skin permeation of API of different nature. This hybrid platform is composed by a polypeptide crosslinked Hyaluronan (**HA-CP**) with capability to directly include either hydrophilic API or hydrophobic APIs previously encapsulated in rationally designed polypeptide-based polymeric micelles. Polypeptide micelles have been fully

characterized (Mw distribution by SEC, DP by NMR, hydrodynamic radius by DLS, secondary structure stability by CD, etc.) and different solution conformation were observed mainly due to the strong self-assembly behaviour when Phe residues are present. A fluorophore as hydrophobic API model has been encapsulated obtaining good encapsulation yields, reproducibility and stability. These polypeptide micelles present intrinsic permeation capacity through the human skin, but importantly, this permeation can be enhanced in the presence of a cross-polymer, **HA-CP**.

The **HA-CP** synthesis was successfully achieved thanks to the previous optimization carried out for the simplified PGLu-Lys-PGLu system without HA. Moreover, the development of characterization techniques (NMR, SEC, intrinsic viscosity, free amine quantification, and pH monitoring) was key to controlling the cross-linking reaction. The **HA-CP** dermal properties were studied through *in vitro* and *ex vivo* assays, revealing substantial improvements over a lineal HA with similar Mw in terms of resistance to HAase degradation and intrinsic human skin permeation capability. Also, its excellent skin compatibility observed by hSOC and *in vitro* cell viability assays, as well as the *in vivo* rabbit model, all confirm its safety and excellent potential for topical applications. Due to the three-dimensional cross-linked network and the specific composition of **HA-CP**, this material represents an excellent skin administration platform for APIs embedded into hydrogel matrix. The APAA-based PEG-PBG20 and PEG-PPhel0 micelles showed the highest accumulation in the epidermis layer compared to the other studied micelles. However, the PEG-PBG20 micelle was selected due to follow the study due to its higher encapsulation capacity and easier synthesis. Thus, the combination of these two soft mater systems, namely, polypeptidic micelles embedded within a polypeptide-based cross-polymer hydrogel network (**HA-CP + PEG-PBG20**), present many possibilities to offer a novel and effective therapy to treat skin diseases.

Moreover, the **HA-CP** novel material also was able to form a hybrid carrier with HP-BM-based micelles of **TPGS** and **TPSS** materials. This small Proof of Concept is an evidence of the potential for polysarcosine materials to be used in skin drug delivery, since the TPSS showed higher accumulation in the deeper layer than the PEGylated material.

These excellent skin properties and part of this Thesis dissertation are the scientific ground underlying the use of the **HA-CP** as an ingredient in cosmetic products currently marketed under the name of **Biomimetic PBT** [43]. Currently, the HA-CP is being produced at 25 Kg scale.

4. MATERIALS AND METHODS

4.1. MATERIALS

All chemicals were reagent grade, obtained from Sigma-Aldrich and used without further purification, unless otherwise indicated. Sodium hyaluronate PrimalHyal300 (Mw = 200 kDa) was supplied by Comercial Química Massó S.A. and sodium hyaluronate

“AURORA” (Mw = 50 kDa) by Principium S.A. Dil stain (1,1'-dioctadecyl-3,3,3',3'-tetramethylindocarbocyanine perchlorate (Dil; DiI18(3))) and TNBSA reagents were purchased from Thermo Fisher Scientific. Cyanine 5.5 amine dye fluorophore was purchased from Lumiprobe GmbH. Bovine testicular hyaluronidase (HAase) (Type IV-S) with a specific activity of 999 units per milligram was obtained from Sigma Aldrich. HAase was weighed before each experiment because the activity in the frozen solution did not remain constant [28]. Pyrene was obtained from Fluka Analytical. Human immortalized non-tumorigenic keratinocyte cell line (HaCaT) was supplied by CLS Cell Lines Service (Eppelheim, Germany) and fibroblasts were supplied by Hospital La Fe (Valencia, Spain). High glucose DMEM Glutamax and Dulbecco's Modified Eagle's Medium-high glucose were purchased from Fisher and Sigma-Aldrich respectively. Phosphate buffer saline (PBS) and fetal bovine serum (FBS) Medium 200 were provided from Gibco. (3-(4,5-dimethylthiazol-2-yl)-5-(3-carboxymethoxyphenyl)-2-(4-sulfophenyl)-2H-tetrazolium) (MTS) was supplied by Promega (Sp). All solvents were of analytical grade and were dried and freshly distilled. Ultrapure water (MilliQ) with a resistivity of 18 M Ω .cm was used in all aqueous preparations. Deuterated trifluoroacetic acid (TFA-d₁), chloroform-d₁, acetone-d₆ and deuterium oxide (D₂O) were purchased from Deutero GmbH. Dialysis was performed in a Millipore ultrafiltration device fitted with a 1, 3, 10 or 30 kDa MWCO regenerated cellulose membrane (Vivaspin®).

4.2.METHODS

4.2.1. SYNTHETIC METHODS

Synthesis of 4-(4,6-dimethoxy-1,3,5-triazin-2-yl)-4-methylmorpholinium chloride → DMTMMC1

This coupling reagent was prepared according to synthetic procedures described in the literature [44]. Yield: 80%. ¹H NMR (300 MHz, D₂O) δ 4.70 (d, J = 11.4 Hz, 2H), 4.22 (d, J = 8.7 Hz, 8H), 4.06 – 3.87 (m, 4H), 3.63 (s, 3H).

Synthesis of cross-linked poly-L-glutamate → PGlu-Lys-PGlu

Cross-linked poly-L-glutamate was obtained by peptidic amide bond formation between carboxylic acid glutamate groups and both amines of L-lysine (Lys) using DMTMMC1 as the coupling reagent [26]. Three solutions were prepared in parallel: (A) Sodium poly-L-glutamate (100 mg, 0.66 mmol, 1 eq) was dissolved in distilled water. (B) DMTMMC1 (0.5 and 5 eq) was dissolved in distilled water. (C) L-lysine hydrochloride salt (30 mg, 0.16 mmol, 0.25 eq) was dissolved in distilled water. Solution B was then added to A, and the pH was adjusted to 7 with a few microliters of NaOH 1 M. The solution was stirred for 15 minutes. After that, solution C was added, and the pH was adjusted to 8.5 with a few microliters of NaOH 1 M. The reaction was carried out overnight at room temperature. Then, the product was purified by dialysis using a Vivaspin® centrifugal concentrators containing a MWCO membrane of 3 kDa. The product was washed first with phosphate buffer (PB) 5 mM at pH 7.5, and then with

distilled water. The solution was freeze-dried, and a white powder was obtained (80% yield).

Synthesis of cross-linked hyaluronic acid with poly-L-glutamate → HA-CP.

HA-CP was synthesized following the procedure described for PGlu-Lys-PGlu including hyaluronic acid (HA) “AURORA” (Mw = 50 kDa). Four solutions were prepared in parallel: (A) Sodium hyaluronate (100 mg, 0.249 mmol, 1 eq) was dissolved in distilled water. (B) Sodium poly-L-glutamate (2.6 mg, 0.017 mmol, 0.07 eq) was dissolved in distilled water. (C) DMTMMCl (44 mg, 0.159 mmol, 0.6 eq to total carboxylic acids) was dissolved in distilled water. (D) L-lysine hydrochloride salt (1.5 mg, 0.008 mmol, 0.03 eq to total carboxylic acids) was dissolved in distilled water. Solution B was added to A, and then, solution C was added with stirring and the pH was adjusted to 7 with a few microliters of NaOH 1 M. The solution was stirred for 15 minutes. After this time, solution D was added, and the pH was adjusted to 8.5 with a few more microliters of NaOH 1 M. The reaction was carried out overnight at room temperature. The product was then purified by dialysis using a Vivaspin® centrifugal concentrators containing a MWCO membrane of 30 kDa, first washing with 5 mM phosphate buffer (PB) at pH 7.5 and then with distilled water. The solution was lyophilized, and a white powder was obtained (70% yield).

Synthesis of fluorescent labeling of HA-CP containing Cyanine5.5 → HA-CP-Cy5.5

The fluorescent hydrogel was obtained through DMTMMCl promoted coupling between the carboxylic acid groups in HA and the amine present in Cyanine 5.5. **HA-CP** (100 mg; 0.249 mmol, 1 eq) was dissolved in distilled water. In parallel, coupling reagent DMTMMCl (3.4 mg; 0.012 mmol; 0.05 eq), was dissolved in water. The DMTMMCl solution was added to the **HA-CP** solution and the pH was adjusted to 7 with a few microliters of NaOH 1 M. The activation of the carboxylic acid groups with DMTMMCl was allowed to proceed for 30 minutes. After that, a solution of Cyanine 5.5 amine (1.8 mg; 0.003 mmol; 0.01 eq) that had been previously prepared in a water:DMSO (1:1) mixture was added and the pH was adjusted to 8.5 with a few microliters of NaOH 1 M. The resultant blue solution of the conjugation reaction was allowed to proceed for 72 hours at room temperature. Then, the product was purified by dialysis using a Vivaspin® centrifugal concentrators containing a MWCO membrane of 30 kDa. The product was first washed with phosphate buffer (PB) 5 mM at pH 7.5, and then with distilled water. The solution was freeze-dried, and a blue powder was obtained (60% yield).

Synthesis of fluorescent labelled hyaluronic acid containing Cyanine5.5 → HA-Cy5.5

Fluorescent HA was obtained through the same procedure described previously for HA-CP-Cy5.5 using a PrimalHyal300 HA (Mw = 200 kDa) (60% yield).

4.2.2. ANALYTICAL METHODS

NMR spectroscopy.

NMR spectra were recorded at 27 °C (300 K) on a 300 Ultrashield™ from Bruker (Billerica MA, USA). Data were processed with the software Topspin (Bruker GmbH, Karlsruhe, Germany). Samples were prepared at a concentration of 10 mg/mL approx. in the required solvent.

Diffusion Experiments (300MHz NMR).

Pulsed field gradient NMR spectroscopy was used to measure translational diffusion by fitting the integrals or intensities of the NMR signals to the Stejskal–Tanner [45] equation: $I = I_0 \exp[-D\gamma^2 g^2 \delta^2 (\Delta - \delta / 3)]$ where I is the observed intensity, I_0 the reference intensity (unattenuated signal intensity), D the diffusion coefficient, γ the gyromagnetic ratio of the observed nucleus, g the gradient strength, δ the length of the gradient, and Δ the diffusion time. Two-dimensional diffusion-ordered NMR spectroscopy (DOSY) was performed with a stimulated echo sequence using bipolar gradient pulses. The lengths of delays were held constant at $\Delta = 100$ ms, and 32 spectra of 64 scans each were acquired with the strength of the diffusion gradient varying between 5 % and 95 %. The lengths of the diffusion gradient and the stimulated echo were optimized for each sample. Typical values were $\delta = 5$ ms for the analysis of physical mixture species and cross-linked materials at 15 mg/mL. Moreover, the hydrodynamic radius (R_h) in nm through diffusion coefficient was obtained employing the Stokes-Einstein equation. $R_h = (K_B \cdot T) / (6\pi \cdot \eta \cdot D)$ where K_B is the Boltzmann constant ($1.3806488 \cdot 10^{-23}$ m²·Kg/s²·K), T is the temperature (K) and η is the dynamic viscosity ($1.095 \cdot 10^{-3}$ Kg/m·s for D₂O at 298.15 K and 0.1 MPa) [46].

Gel Permeation Chromatography (GPC) in aqueous media.

For SEC measurements in aqueous media containing 150 mM of NaNO₃, 5 mM of phosphate buffer (PB) at pH 5 and 0.005 % (w/w) sodium azide as an additive were performed in an AF2000 system from Postnova Analytics (Landsberg, Germany). The system was configured to work on SEC mode with an isocratic pump (PN1130) an autosampler (PN5300), a refractive index (RI, PN3150), 21 angle-multi angle light scattering (MALS, PN3621) and an ultraviolet-visible (UV-VIS) (PN3211) detector. A working flow rate of 0.8 mL/min at 30 °C was employed with one TSKgel G6000PWXL column. Refractive index (RI) and Multi Angle Light Scattering (MALS) were used for detection and Mw determination, calibration of both RI and MALS detectors was achieved with well-defined Pullulan (50 kDa), and validation with polymethacrylic acid sodium salt (62.5 kDa PMASS) standards, purchased from Polymer Standards Service (PSS)/Mainz Germany. dn/dc values for sodium hyaluronates cross-linked were determined from recovered mass assuming 95-100 % recovery from the chromatographic column and found to be within 0.094 – 0.150 mL/g. 30 μ L of a polymer solution of 3.75 mg/mL were injected each time. For linear sodium hyaluronates, 0.150 mL/g was used as the dn/dc according to that reported in literature [28]. Mw values were obtained employing Zimm-Stockmayer equation in SEC software [13].

Hyaluronidase degradation studies by Gel Permeation Chromatography (GPC) in aqueous media.

Hyaluronic acid-based materials were degraded by hyaluronidase at 37 °C employing the thermal conditioning autosampler of AF2000 system from Postnova Analytics (Landsberg, Germany). Aqueous GPC measurements were carried out as described above. The concentration of HA materials was 3.75 mg/mL and that of HAase was 5 U/mL. Mw distribution values were achieved per triplicate and the graphic in Figure 3.3 shows the average and their standard deviations.

Amine quantification by TNBSA assay.

The method was adapted from Thermo Fisher Scientific public protocol. 0.01% (w/v) solution of TNBSA was prepared using a 0.1 M sodium bicarbonate buffer at pH 8.5 as a diluent. It was prepared fresh for each measurement. The calibration curve was built with L-lysine from 10 to 250 µM. **HA-CP** aliquots were taken at different times and diluted in the sodium bicarbonate buffer until the measurement concentration. The amine amount was obtained employing interpolation in the calibration curve. Measurements were performed with a UV-Vis spectrophotometer plate reader for 96 well plates SpectroStar^{NANO} from Biogen at 335 nm.

Dil quantification in Franz cell diffusion experiments by HPLC.

High performance liquid chromatography (HPLC) analyses to evaluate the Dil content in the receptor chamber from permeation studies, were carried out on a system consisting of an Agilent 1260 Infinity II Quaternary Pump solvent delivery module, a G7115A Diode Array Detector WR (Santa Clara, CA, USA), an InfinityLab Poroshell 120 C18 RP-HPLC column (EC-C18, 4.6 x 100 mm, 4 µm) (Santa Clara, CA, USA) and an Open Lab (Agilent) workstation. The composition of the mobile phase was MeOH:THF (8:2) with a flow rate of 1.0 mL/min and a column temperature of 25 °C. The injected sample volume was 10 µL at a concentration of 0.1 mg/mL for micelles and Dil standard. The dye was monitored at 552 nm (absorbance wavelength of Dil dye).

Cy5.5 quantification in Franz cell diffusion experiments by HPLC.

HPLC analyses to evaluate the Cy5.5 content in the receptor chamber from permeation studies of HA-Cy5.5 and HA-CP-Cy5.5, were carried out on a system consisting of an Agilent 1260 Infinity II Quaternary Pump solvent delivery module, a G7115A Diode Array Detector WR (Santa Clara, CA, USA), an InfinityLab Poroshell 120 C18 RP-HPLC column (EC-C18, 4.6 x 100 mm, 4 µm) (Santa Clara, CA, USA) and an Open Lab (Agilent) workstation. The composition of the mobile phase was MeOH:THF (6:4) with a flow rate of 1.0 mL/min and a column temperature of 35 °C. The injected sample volume was 10 µL at a concentration of 0.1 mg/mL for the Cy5.5 standard. The dye was monitored at 680 nm (Absorbance wavelength of Cy5.5 dye).

Viscosity measurements.

Viscosity values were obtained using a Fungilab rotational viscosimeter Visco Smart LT20 composed by (i) viscometer head, (ii) AMP adapter for small samples and (iii) a spindle. The concentration of hydrogel in aqueous solution was 3.4% wt. The employed temperature was 25 °C. The starting rpm were fixed at 100 until system

stabilization. Then, rpm values were varied until reaching a % of the base scale 40 ± 3 %. When the % was stable to 40, the value was obtained as long as the stable values were constant ± 10 cP.

Determination of MW by intrinsic viscosity.

The desired amount of at least 6 samples in the range of 1 to 10 mg/mL of HA or **HA-CP**, was weighed and dissolved in 8 mL (the minimum amount of sample required for measuring inside the viscometer) with NaCl 0.2 M to screen the charges of the HA and obtain an extended conformation of HA and **HA-CP** in solution. The dynamic viscosity for all samples was recorded at 25 °C for 5 minutes. The % base scale was set between 60% to 15% varying the rpm. Then intrinsic viscosity was calculated applying the Mark-Howink-Sakurada equation plotting the reduced viscosity vs concentration [47].

Quantification of Cyanine 5.5 loading.

Dye loading was determined by UV-Vis measurements UV-VIS using JASCO V-630 spectrophotometer at 25 °C with 1.0 cm matched quartz cells and with a spectral bandwidth of 0.5 nm. Dye loading was determined by recording the absorbance band at 676 nm using a calibration curve in water containing 0.001 % of DMSO to improve the Cyanine 5.5 solubility.

Transmission electron microscopy (TEM).

TEM images were recorded in a transmission electron microscope EM 410, Philips operating at 60-80 kV. Samples of block copolypeptides (1-2 mg/mL) were applied directly onto carbon film on 200 mesh copper grids. Any excess sample was carefully removed by capillarity, and the grids were immediately stained with one drop of 0.1 % phosphotungstic acid for 30 seconds. Excess stain was removed by capillary action.

4.2.3. BIOLOGICAL EVALUATION METHODS

Cell viability studies in vitro.

To carry out the cytotoxicity studies *in vitro* two cell lines were used: human immortalized non-tumorigenic keratinocyte cell line (HaCaT) was supplied by CLS Cell Lines Service (Eppelheim, Germany) and primary culture of human fibroblasts was kindly donated by Hospital La Fe (Valencia, Spain).

The culture media used were high glucose DMEM Glutamax (Fisher, Spain) for HaCaT cells and Dulbecco's Modified Eagle's Medium-high glucose (Sigma-Aldrich Chemical Co., Spain) for fibroblasts cells, and both were supplemented with 2% penicillin/streptomycin and 50mL of fetal bovine serum (FBS) in a humidified incubator (Hucoa-Erlöss S.A., Spain) 5% CO₂ and 37 °C.

50 µL of cells were seeded in 96-well plates at a concentration of 4000 cells/well in the case of HaCaT cells and 2000 cells/well for fibroblast cells. After 24 hours, 50 µL of each treatment were added reaching a final volume of 100 µL in the well. All the treatments were filtered before adding to the well (pore size 0.45 µm). Cells were

incubated with samples or controls for 72 hours and then the MTS assay was performed. For that, 20 μ L of the solution of Phenazine Methosulfate Minimum 90% (PMS, Sigma, Spain) and 3-(4,5-dimethylthiazol-2-yl)-5-(3-carboxymethylphenyl)-2-(4-sulfophenyl)-2H tetrazolium) (MTS, Promega, Spain) were added, with a dilution of 1:20 respectively. After 3 hours of incubation, the absorbance was read at 490 nm using a Victor2Wallac™ plate reader. The concentrations tested ranged from 0.5 to 0.029 mg/mL for PEG-PPhe10, PEG-PPhe20, PEG-PBG10, PEG-PBG20, PEG-PBG40.

DEVELOPMENT OF HUMAN SKIN EX VIVO MODEL (hOSEC: HUMAN ORGANOTYPIC SKIN EXPLANT CULTURE)

Breast skin samples were obtained from healthy women undergoing plastic surgery after written informed consent. The skin was cut to approximately 1cm² and placed in 6-well plates, so that the dermal side was in the Dulbecco's modified Eagle medium (DMEM) supplemented with 50 mL fetal bovine serum, 5.5mL penicillin/streptomycin and amphotericin B, and the epidermis was exposed to the air. After each time-point (1, 4, 7, 11 days) in culture media, the skin samples were washed twice with PBS-BSA 0.1% (PBS supplemented with Bovine Serum Albumin (BSA)) and kept in 4% paraformaldehyde (PFA) for 24 hours at room temperature. Then, the samples were washed with 30% sucrose in PBS solution, and incubated in this solution for 24 hours at 4 °C. Finally, the skin samples were washed twice with PBS and preserved in a cryopreservation solution (40 % PB 0.1M, 30 % ethylene glycol and 30 % glycerol) at 4 °C.

MTT assay for tissue viability

The skin organ culture was incubated at 37 °C under 5% CO₂ for 11 days, and the medium was changed every day. The tissue viability after 1, 4, 7, and 11 days was evaluated by MTT assay. The skin pieces were washed twice with PBS and were introduced into 4 mL of MTT solution (2 mg/mL) at 37 °C. The MTT assay is a colorimetric assay for assessing cell metabolic activity. NAD(P)H-dependent cellular oxidoreductase enzymes reflect the number of viable cells present. These enzymes are capable of reducing the tetrazolium dye MTT 3-(4,5-dimethylthiazol-2-yl)-2,5-diphenyltetrazolium bromide to insoluble formazan (Sigma, Spain). After 4 hours of incubation, the skin samples were washed twice with PBS and introduced into 4 mL of DMSO, to extract the formazan from the skin. After 15 hours of extraction, the absorbance was read at 490nm using Victor2Wallac™ plate reader.

Histological Analysis and Imaging

The tissue samples were processed for histological analysis. For this, skin pieces preserved in the cryopreservation solution were washed with PBS and shaken 3 times. Common dehydration and paraffin-inclusion procedures were carried out leading to blocks that were sliced into 4- μ m sections. To include the sample in paraffin, previous dehydration of the sample through 2 min incubation in an increasing degree of alcohol solutions (30%, 50%, 70%, 96% and 99.9 %) was performed, followed by two xylol

washes of 1min to finally include the sample in paraffin. Then, the paraffin block was cut into 5µm and set up in SuperFrost plus glass slide for hematoxylin-eosin staining. To this end, the tissue slides were previously deparaffinized with xylene and then rehydrated with a decreasing battery of ethanol solutions (99.9%, 96%, 70%) and water 5min, followed by Dako hematoxylin staining for 2.5 min. Skin samples were then washed with DEM water (1.5 min bath), blueing buffer (1 min) and water (1.5 min). Then, tissue slides were incubated 2 min in lithium carbonate and HCl 0.25% in ethanol 70%, to remove the excess of hematoxylin staining. Following this, tissue slides were incubated with Dako Eosin for 2 min. Finally, dehydration was performed by washing with 96% ethanol (30 s) and 99.9% ethanol (2.5 min). Hematoxylin-Eosin (H-E) staining and immunostaining (Ki67 and Ck5/6) were performed as required (Dako Autostainer 48, US) and the slides were finally assembled with Eukitt. Tissue slides were observed under the microscope and those of interest were scanned with a Panoramic 250 Flash III slide scanner and processed with CaseViewer software (both from (3DHISTECH Ltd, Budapest, Hungary).

Evaluation of tissue viability with block copolymer treatment in hSOC by MTT assay

Skin pieces were incubated at 37 °C under 5% CO₂ for 72 hours. The toxicity of 3µL of PEG-PBG20 (10 mg/mL) alone, in HA (1%), in a HA-CP (1%) and the vehicles HA and HA-CP applied in the SC, was evaluated after 24, 48 and 72 hours of treatment. The tissue viability after each treatment was evaluated by MTT assay. The skin pieces were washed twice with PBS and were introduced into 4 mL of MTT solution (2 mg/mL). After 4 hours of incubation at 37 °C, the skin samples were washed twice with PBS and introduced into 4 mL of DMSO, to extract the formazan from the skin. After 15 hours of extraction, the absorbance was read at 490 nm using Victor2Wallac™ plate reader.

Cell viability on Human Organotypic Skin Explant Culture (hOSEC)

Breast skin samples were obtained from healthy women undergoing plastic surgery after written informed consent (Hospital La Fe, Valencia, Spain) and immediately processed and cultured in culture media as previously reported [48]. The tissue viability was monitored after 1, 4, 7, 11 days by MTT assay (see Supporting Information for further details).

Tissue viability studies of selected materials were also performed as follows. Skin pieces were incubated at 37 °C under 5 % CO₂ for 72 hours. The tissue viability of samples with: (i) 3µL of PEG-PBG20 (10 mg/mL) in water, (ii) in HA (1 % wt.) and (iii) in HA-CP (1 % wt.) were carefully applied on the skin stratum corneum (SC), was evaluated after 24, 48 and 72 hours by MTT assay. After treatment, the skin pieces were washed twice with PBS and introduced in 4 mL of an MTT solution (2 mg/mL). After 4 hours of incubation at 37 °C, the skin samples were washed twice with PBS and introduced into 4 mL of DMSO, to extract the formazan from the skin. After 15 hours of extraction, the absorbance was read at 490 nm using Victor2Wallac™ plate reader.

The tissue samples were then processed for histological analysis. Hematoxylin-Eosin (H-E) staining and immunostaining (Ki67 and Ck5/6) were performed as required (Dako

Autostainer 48, US) and the slides were finally assembled with Eukitt. Tissue slides were observed under the microscope and those of interest were scanned with a Panoramic 250 Flash III slide scanner and processed with CaseViewer software (both from (3DHISTECH Ltd, Budapest, Hungary) (see SI for further details).

EX VIVO HUMAN SKIN PERMEATION STUDIES BY FRANZ DIFFUSION CELLS.

Ex vivo human skin permeation studies using Franz Diffusion Cells.

Breast skin samples were obtained from healthy women undergoing plastic surgery (age range 30-60 years) after written informed consent (La Fe Hospital, Valencia). Immediately after excision, the subcutaneous fatty tissue was carefully removed using a scalpel. The skin was cut into 4x4 cm pieces, wrapped in aluminium foil and stored at -20 °C until use. To reduce inter-individual variability and afford a better comparison of results, skin from only one donor was used in all experiments. Before starting the experiment, the skin was allowed to warm to room temperature [48].

All skin permeation studies employed the modified Franz diffusion cell (Logan Instruments Corp., USA) with a diffusional area of 0.95 cm² following a previously described protocol [35, 49, 50]. In summary, the skin was carefully fixed between the donor and the receptor chamber, so that the stratum corneum was facing upwards. The receptor chamber was filled with 8 mL of PBS 0.01 M pH = 7.4 with great care to avoid trapping air beneath the membrane, and stirred with a magnetic stirrer bar at 600 rpm with a thermostatted temperature of 37 °C. After an equilibration time of 30 minutes, 100 µL of each of the tested formulations was introduced into the donor compartment using a standard pipette. A fixed concentration of the formulations was used in all cases (10 mg/mL of block copolymer carrier). The donor compartment was then sealed with Parafilm® and aluminium foil. The experiment was run for 8 hours. Samples from the receptor chamber were taken at 0, 4 and 8 hours and 2mL of the sample taken was immediately refilled with fresh solution. Dil and/or Cy5.5 from the samples taken was quantified by HPLC (see Supporting Information)

After the 8 hours time point, the skin samples were gently rinsed with PBS-BSA 0.1% (PBS supplemented with Bovine Serum Albumin (BSA)) and kept in 4 % paraformaldehyde (PFA) for 24 hours at room temperature. Then, the samples were washed with 30 % sucrose in PBS solution for 24 hours at 4 °C. Finally, the skin samples were washed twice with PBS and preserved in a cryopreservation solution (40 % PB 0.1 M, 30 % ethylene glycol and 30 % glycerol) at 4 °C until used.

Confocal Laser Scanning Microscopy.

The skin permeation was evaluated by confocal fluorescence microscopy. Skin samples were washed 3 times with PBS pH 7.4 and shaking to remove the cryopreservation solution. A cryostat (Leica Cryostat CM 3050S, Wetzlar, Germany) was used to prepare the vertical cross-sections of skin. Nine to twelve vertical sections of each

sample with a thickness of 5 μm were obtained and stored at 4 °C. The slices were placed on glass slides, fixed with formalin and stained by 6-diamidino-2-phenylindole (DAPI) to stain cell nuclei. Then, images were captured with an inverted DM IRE2 microscope equipped with a λ -blue 40x oil immersion objective and handled with a TCS SP2 system, equipped with an Acoustic Optical Beam Splitter (AOBS). Dil C18(3) was excited at 549 nm, Cy5.5 at 675 nm and DAPI at 405 nm. Images were captured at an 8-bit greyscale and processed with LCS software (version 2.5.1347a, Leica Germany) containing multicolour, macro and 3D components. Control tissue that followed the same incubation time with MilliQ H₂O was also analyzed to establish the autofluorescence. Image J was the software used for image analysis (see Supporting Information for further details).

Fluorescence intensity qualification by Image J.

Dil intensity in the different skin layers was quantified 5 times per sample using ImageJ software. The control intensity was subtracted.

Dil quantification in Franz diffusion cell experiments by HPLC.

High performance liquid chromatography (HPLC) analyses to evaluate the Dil content in the receptor chamber from permeation studies, were carried out on a system consisting of an Agilent 1260 Infinity II Quaternary Pump solvent delivery module, a G7115A Diode Array Detector WR (Santa Clara, CA, USA), an InfinityLab Poroshell 120 C18 RP-HPLC column (EC-C18, 4.6 x 100 mm, 4 μm) (Santa Clara, CA, USA) and an Open Lab (Agilent) workstation. The composition of the mobile phase was MeOH:THF (8:2) with a flow rate of 1.0 mL/min and a column temperature of 25 °C. The injected sample volume was 10 μL at a concentration of 0.1 mg/mL for micelles and Dil standard. The dye was monitored at 552 nm (absorbance wavelength of Dil dye).

Cy5.5 quantification in Frank diffusion cell experiments by HPLC.

HPLC analyses to evaluate the Cy5.5 content in the receptor chamber from permeation studies of HA-Cy5.5 and HA-CP-Cy5.5, were carried out on a system consisting of an Agilent 1260 Infinity II Quaternary Pump solvent delivery module, a G7115A Diode Array Detector WR (Santa Clara, CA, USA), an InfinityLab Poroshell 120 C18 RP-HPLC column (EC-C18, 4.6 x 100 mm, 4 μm) (Santa Clara, CA, USA) and an Open Lab (Agilent) workstation. The composition of the mobile phase was MeOH:THF (6:4) with a flow rate of 1.0 mL/min and a column temperature of 35 °C. The injected sample volume was 10 μL at a concentration of 0.1 mg/mL for the Cy5.5 standard. The dye was monitored at 680 nm (absorbance wavelength of Cy5.5 dye).

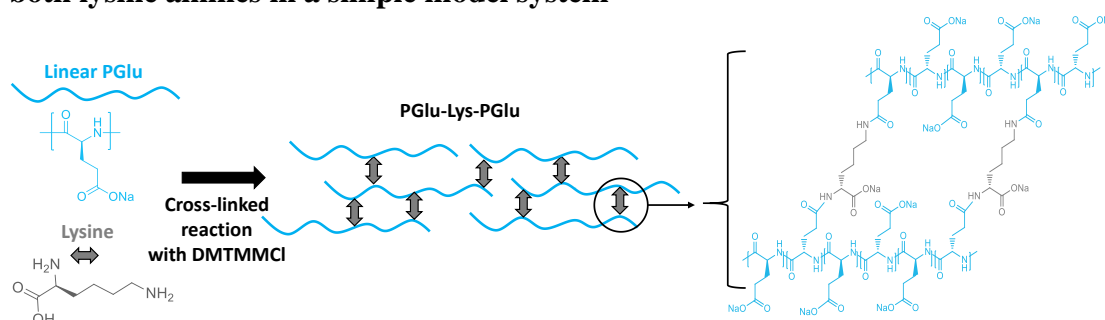
IN VIVO ACUTE VAGINAL IRRITATION TEST IN RABBIT MODEL

Animal experiments using albino rabbits (New Zealand breed) were performed in the Instituto Valenciano de Microbiología (Valencia, Spain) following the guidelines UNE-EN-ISO 10993-10: 2013), and certified by AENOR (Spanish Association for Standardization and Certification). The animals were split into representative groups (n=3 per group). To perform the study, 1 ml of the HA-CP solution was applied to the vaginal area of the rabbits during 5 days (24, 48, 72, 96 and 120 hours), and animals treated with

1ml of NaCl solution were used as negative controls. At each time-point, the irritation of the area was evaluated using an irritation index (0: None, 1 to 4: Minimum, 5 to 8: Mild, 9 to 11: Moderate, and 12 to 16: Intense).

5. SUPPORTING INFORMATION

Synthesis optimization of experimental conditions for nucleophilic reactivity of both lysine amines in a simple model system



Scheme 3.2. Synthetic scheme for polyglutamate cross-linked employing Lys as a simple model system.

Optimization of this methodology was performed in the first place with a simple model system composed of PGlu and Lys called PGlu-Lys-PGlu, without HA (Scheme 3.2). ¹H NMR was used to characterize the reactivity of lysine amino groups by monitoring the chemical shifts of chiral and epsilon protons near the two reactive amines (see Figure 3.9A and 3.9B). Different equivalents of DMTMMCl (20 and 2 eq) and pH values for peptidic coupling were tested. The results (Table 3.2) showed that lysine best reacted through two amines when the pH activation value was around 7, the coupling pH was close to 8 and when 20 eq of DMTMMCl were added. These results were compared with a physical mixture which contained the same ratio of PGlu and Lys (without DMTMMCl). With 2 eq of DMTMMCl to Lys, only the ε-NH₂ showed a new amide bond formation by NMR. Besides, the coupling pH was also fixed at 11 to have both amines in their basic forms (table S1), but after purification the corresponding signals for Lys were not detectable by NMR (Figure 3.9). This was attributed to the instability of the adduct between carboxylic glutamate groups and DMTMM in aqueous solution at pH 11 [51]. In addition to proton NMR assays, bidimensional DOSY NMR studies were carried out to determine the profile of diffusion decay for PGlu and Lys employing the Stejskal–Tanner equation [45, 46]. As can be seen, the diffusion decay for PGlu in the physical mixture differed considerably from Lys. However, as we expected, diffusion decay for the Lys moiety was very close to PGlu in the cross-linked materials. This suggested that PGlu and Lys move together in the media and, as such, are joined covalently. Thus, the conditions for the crosslinking reaction were established as: (i) activation pH ~ 7, (ii) coupling pH ~ 8 and (iii) 20 eq of DMTMMCl to Lys.

Table 3.2. Optimization of the nucleophilic reactivity for both amines of lysine.

Compound	Activation pH	Coupling pH	Eq DMTMMCl to PGlu	Eq Lys to PGlu	Eq DMTMMCl to Lys	Lys- α -NH ₂ conjugation	Lys- ϵ -NH ₂ conjugation
Physical Mixture	-	-	-	0.25	-	-	-
PGlu-Lys-PGlu (1)	6.89	8.16	0.5	0.25	2	17%	66%
PGlu-Lys-PGlu (2)	11.03	11.03	0.5	0.25	2	*	*
PGlu-Lys-PGlu (3)	7.32	8.15	5.0	0.25	20	79%	95%

*No signals for lysine were found in ¹H-NMR spectra.

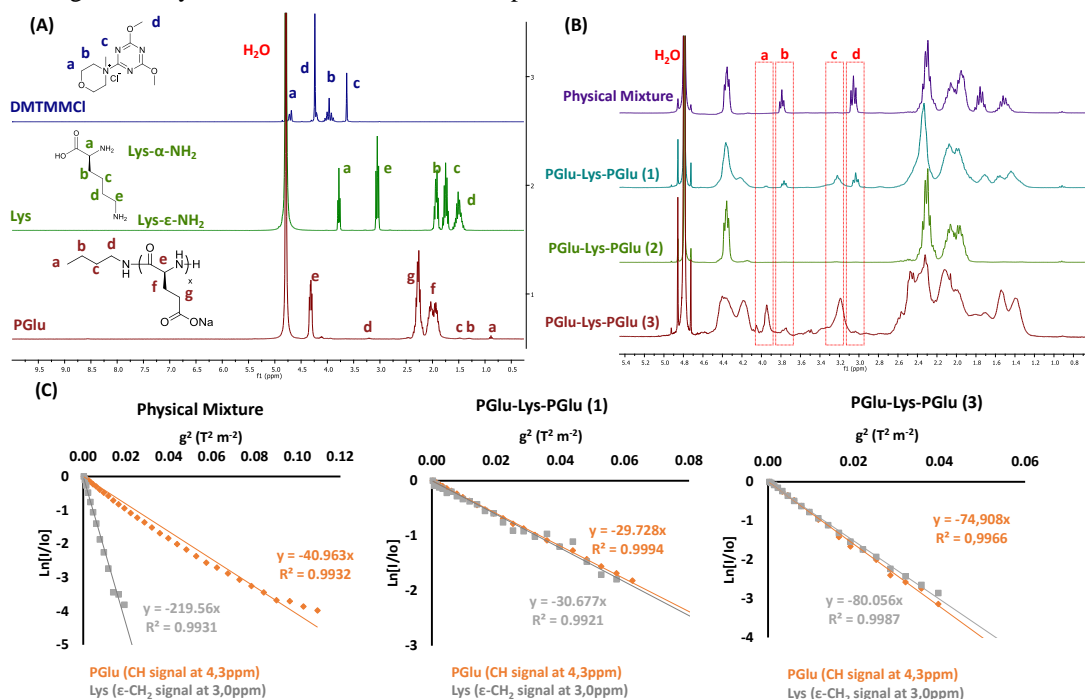


Figure 3.9. NMR studies: (A) ¹H-NMR spectra in D₂O for starting materials with assigned protons. (B) ¹H-NMR spectra in D₂O for simple model system PGlu-Lys-PGlu showing new signals for CH- α -NH₂ and CH₂- ϵ -NH₂ with a new chemical shift indicative of a new amide bond. **a**: Signal for CH of α -NH₂ conjugated as amide; **b**: Signal for CH of α -NH₂ as free amine; **c**: Signal for CH₂ of ϵ -NH₂ conjugated as amide; **d**: Signal for CH₂ of ϵ -NH₂ as free amine. The % of conjugation for each amine of Lys was obtained between the relation **a** & **b** for ϵ -NH₂ and **c** & **d** for α -NH₂. (C) Schematic representation of DOSY-NMR array data treatment according to the Stejskal-Tanner equation to compare the diffusion decay of PGlu and Lys moieties. Proton signals from DOSY-NMR data treatment were CH at 4.3 ppm for Glu and ϵ -CH₂ at 3.0 ppm for Lys.

HA-CP characterization by DOSY-NMR and TEM.

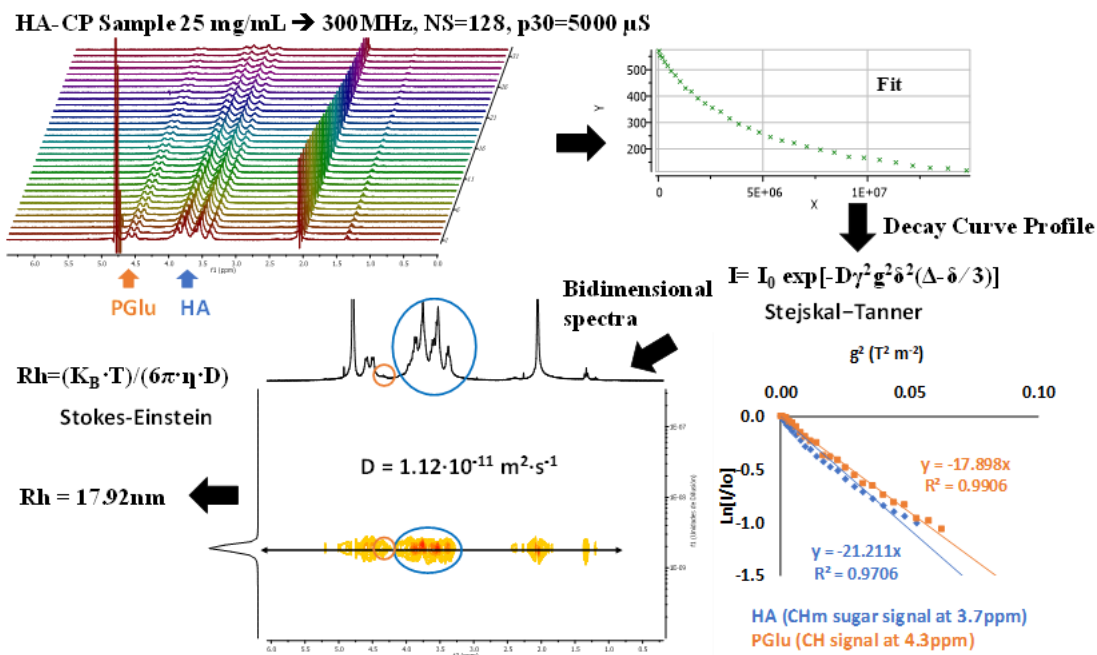


Figure 3.10. Schematic pathway to obtain diffusion decay curve, DC ($\text{m}^2 \cdot \text{S}^{-1}$) and Rh (nm) for HA-CP.

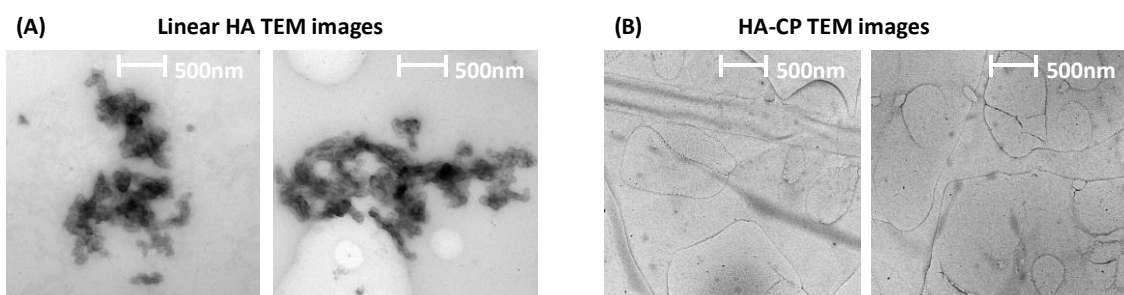


Figure 3.11. (A) TEM images for linear HA solution at 1%. (B) TEM images for HA-CP at 1%.

Ex vivo human skin permeation: Franz diffusion cell experiments

To gain a greater knowledge about **HA-CP** intrinsic permeation characteristics, a **HA-CP** fluorophore label conjugate was prepared by employing Cyanine 5.5 as the fluorophore dye (HA-CP-Cy5.5). To compare the permeation properties of our novel cross-polymer with conventional HA, a second label conjugate was prepared employing the linear HA with a similar Mw distribution (200 kDa). The synthetic strategy to yield these fluorophore materials was based on peptidic coupling, through DMTMMCl carboxylic acid group activation followed by nucleophilic attack from the Cyanine 5.5 amine resulting in the formation of a new amide bond. In order to compare the skin permeation, both labelled materials were characterized by UV-Vis to determine the % of dye and by SEC using the RI, MALS and UV detectors to determine their Mw distributions. SEC results showed that the dye was conjugated successfully to both HA-

based materials. SEC traces recovered from RI and UV detectors, showed a perfect correlation in terms of retention times. This can be attributed to the covalent union between the carboxylic HA moiety and Cy5.5. Regarding the dye loading, **HA-CP** showed a better conjugation efficiency (0.63 % molar dye) than linear HA (0.43 % molar dye), although the target was 1 % molar dye both cases (see Table 3.3 and Figure 3.12). The resulting fluorescent products were employed for skin permeation studies.

Table 3.3. Results of Cy5.5 loading and Mw distributions

Compound	% w/w Cy5.5*	% molar Cy5.5*	Conjugation efficiency*	Mw (KDa) by SEC	PDI by SEC
HA-CP-Cy5.5	1.18	0.63	63%	145.2	1.863
HA-Cy5.5	0.81	0.43	43%	205.5	1.442

*Data obtained by UV-Vis spectroscopy measured at 676 nm.

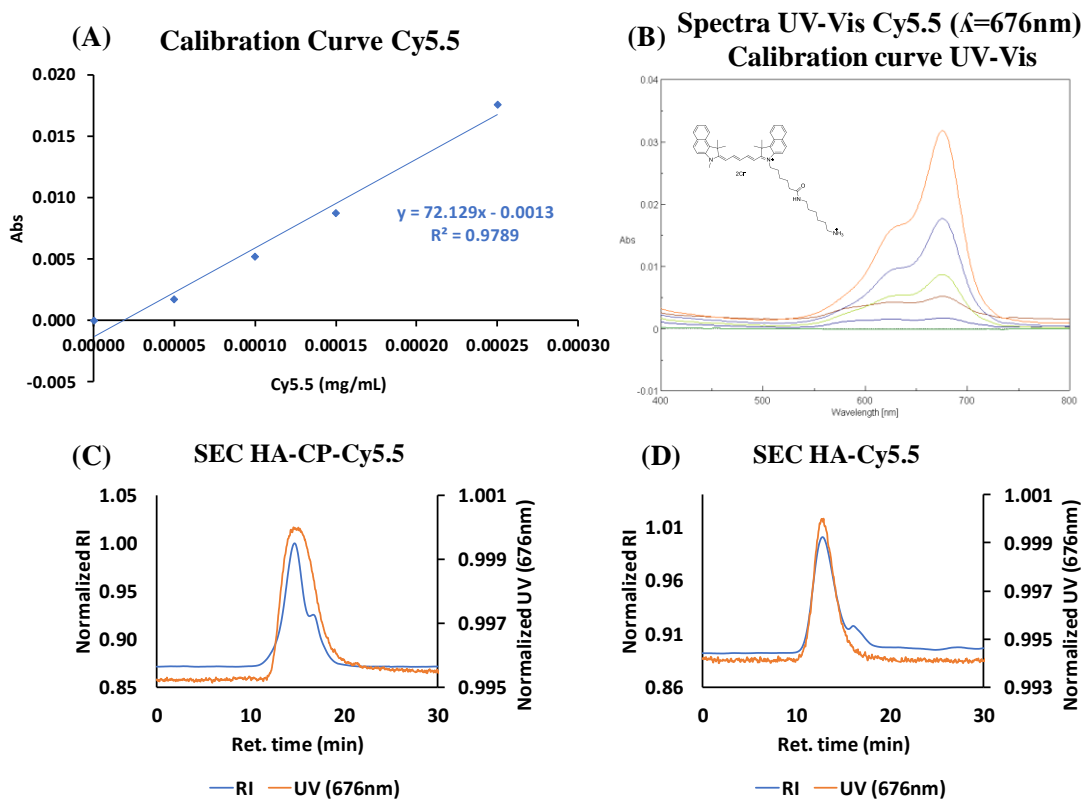


Figure 3.12. (A) Calibration curve of Cy5.5 in water obtained by absorbance spectroscopy measured at 676 nm. (B) Absorbance spectra of calibration curve of Cy5.5 in water and the molecular structure of cyanine 5.5 amines. (C) SEC-RI-UV for HA-CP-Cy5.5. (D) SEC-RI-UV for HA-Cy5.5. SEC-RI-UV chromatograms were achieved at 3.75 mg/mL in NaNO₃ 150 mM at pH 5 adjusted with PB 5 mM.

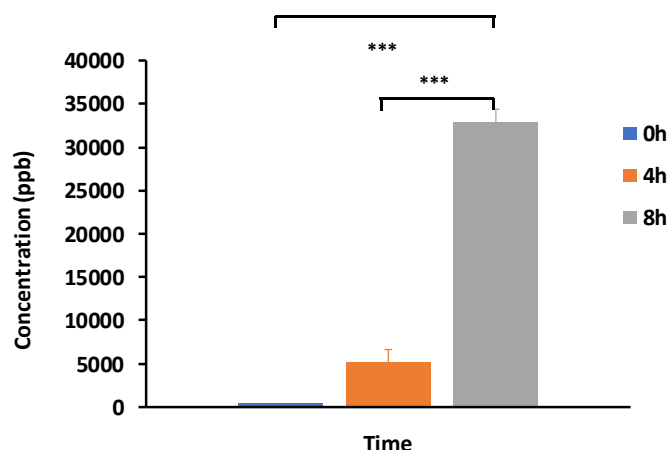


Figure 3.13. The concentration of benzoic acid in the receptor chamber of Franz diffusion cell experiments analyzed by HPLC at 8 hours showing how benzoic acid reached the receptor chamber, giving direct information that it was capable to reach the bloodstream. This experiment was performed to obtain a positive API control in the bloodstream, to optimize the Franz diffusion cell technique and its analysis by HPLC.

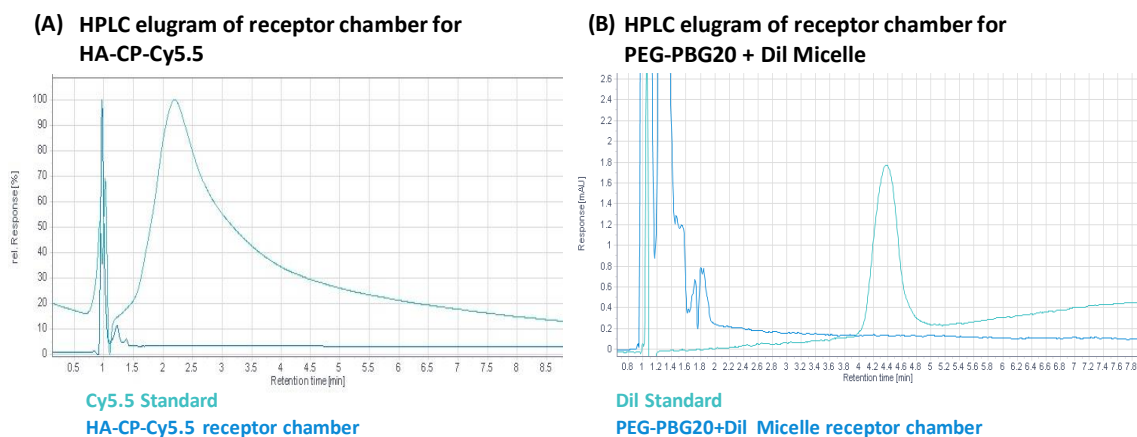


Figure 3.14. Examples of two HPLC chromatograms of receptor chamber solution of Franz diffusion cell experiments at 8 hours showing how neither system reached the receptor chamber and giving direct information that they were not capable to reach the bloodstream. **(A)** Example for HA-Cy5.5. For HA-CP-Cy5.5 was found the same results. **(B)** Example of PEG-PBG20 with Dil micelle. For PEG -PBG10, PEG-PPhe10 and PEG -PPhe20 Dil micelles were found the same results.

Cell Viability of HA-based materials and APAA

Cell viability assays were carried out for linear HA, **HA-CP**, and the 4 selected micelles to determine the toxicity of each block copolymer in the two main skin cells: (i) HaCaT in the representation of human keratinocytes and (ii) fibroblasts [37].

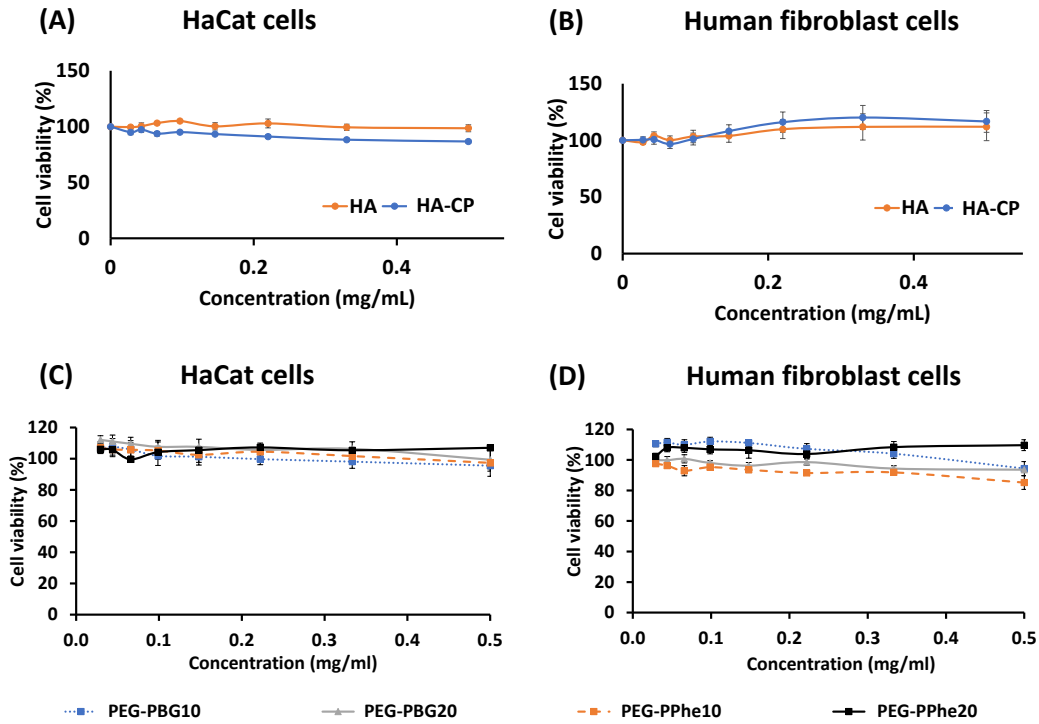


Figure 3.15. Cell viability by MTS assay of HA-based materials in (A) HaCaT cells and (B) human fibroblasts cells and APAA in (C) HaCaT cells and (D) human fibroblasts cells after 72 h of treatment (n = 3).

Human Skin Organ Culture (hSOC)

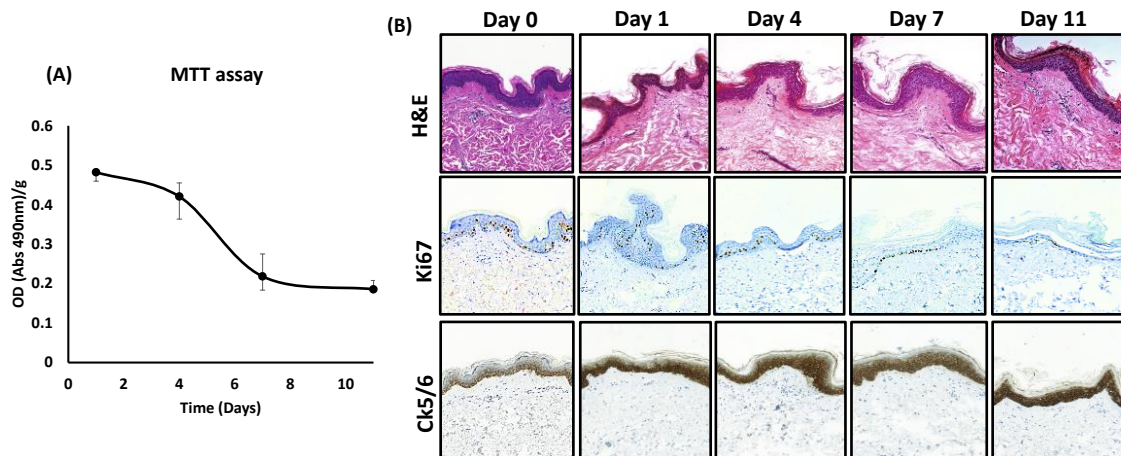


Figure 3.16. (A) Tissue viability after 11 days in culture media by MTT assay. (B) HE-stained images (first row) of representative skin sections showing intact skin structure. Immunohistochemical staining of skin for Ki67 (second row) and Ck5/6 (third row), demonstrating the proliferative capacity of keratinocytes (10x magnification).

***In vivo* acute vaginal irritation test in rabbit model.**

Table 3.4. Daily macroscopic evaluation of vaginal and perineal appearance in the animals after the application of **HA-CP** solution during 5 days.

Signs	Hours	Animal 1	Animal 2	Animal 3
Exudation	24	0	0	0
	48	0	0	0
	72	0	0	0
	96	0	0	0
	120	0	0	0
Erythema	24	0	0	0
	48	0	0	0
	72	0	0	0
	96	0	0	0
	120	0	0	0
Edema	24	0	0	0
	48	0	0	0
	72	0	0	0
	96	0	0	0
	120	0	0	0

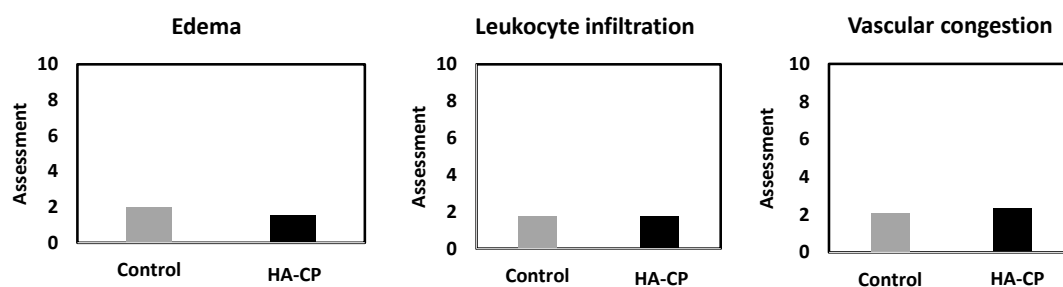


Figure 3.17. Assessment result of Control and **HA-CP** in vaginal irritation test in rabbit model showing the non-irritation effect of **HA-CP**.

6. REFERENCES

- [1] C. Pegoraro, S. MacNeil, G. Battaglia, Transdermal drug delivery: from micro to nano, *Nanoscale* 4(6) (2012) 1881-1894.
- [2] N.G. Kotla, B. Chandrasekar, P. Rooney, G. Sivaraman, A. Larranaga, K.V. Krishna, A. Pandit, Y. Rochev, Biomimetic Lipid-Based Nanosystems for Enhanced Dermal Delivery of Drugs and Bioactive Agents, *Acs Biomaterials Science & Engineering* 3(7) (2017) 1262-1272.
- [3] X.L. Zhou, Y. Hao, L.P. Yuan, S. Pradhan, K. Shrestha, O. Pradhan, H.J. Liu, W. Li, Nanoformulations for transdermal drug delivery: A review, *Chinese Chemical Letters* 29(12) (2018) 1713-1724.
- [4] S. Jain, N. Patel, M.K. Shah, P. Khatri, N. Vora, Recent Advances in Lipid-Based Vesicles and Particulate Carriers for Topical and Transdermal Application, *Journal of Pharmaceutical Sciences* 106(2) (2017) 423-445.
- [5] K.A. Kosakowska, B.K. Casey, S.L. Kurtz, L.B. Lawson, S.M. Grayson, Evaluation of Amphiphilic Star/Linear-Dendritic Polymer Reverse Micelles for Transdermal Drug Delivery: Directing Carrier Properties by Tailoring Core versus Peripheral Branching, *Biomacromolecules* 19(8) (2018) 3163-3176.
- [6] C. Valenta, B.G. Auner, The use of polymers for dermal and transdermal delivery, *European Journal of Pharmaceutics and Biopharmaceutics* 58(2) (2004) 279-289.

- [7] S.A. Castleberry, M.A. Quadir, M. Abu Sharkh, K.E. Shopsowitz, P.T. Hammond, Polymer conjugated retinoids for controlled transdermal delivery, *Journal of Controlled Release* 262 (2017) 1-9.
- [8] A.B. Kutikov, J. Song, Biodegradable PEG-Based Amphiphilic Block Copolymers for Tissue Engineering Applications, *ACS Biomaterials Science & Engineering* 1(7) (2015) 463-480.
- [9] R. Gul, N. Ahmed, K.U. Shah, G.M. Khan, A.U. Rehman, Functionalised nanostructures for transdermal delivery of drug cargos, *Journal of Drug Targeting* 26(2) (2018) 110-122.
- [10] M.C.G. Pella, M.K. Lima-Tenorio, E.T.T. Neto, M.R. Guilherme, E.C. Muniz, A.F. Rubira, Chitosan-based hydrogels: From preparation to biomedical applications, *Carbohydrate Polymers* 196 (2018) 233-245.
- [11] R. Wang, B. Zhou, D.L. Xu, H. Xu, L. Liang, X.H. Feng, P.K. Ouyang, B. Chi, Antimicrobial and biocompatible epsilon-polylysine-gamma-poly(glutamic acid)-based hydrogel system for wound healing, *Journal of Bioactive and Compatible Polymers* 31(3) (2016) 242-259.
- [12] Q. Li, Y.M. Niu, P.F. Xing, C.M. Wang, Bioactive polysaccharides from natural resources including Chinese medicinal herbs on tissue repair, *Chinese Medicine* 13 (2018) 11.
- [13] C. Guarise, M. Pavan, L. Pirrone, D. Renier, SEC determination of cross-link efficiency in hyaluronan fillers, *Carbohydrate Polymers* 88(2) (2012) 428-434.
- [14] M. Essendoubi, C. Gobinet, R. Reynaud, J.F. Angiboust, M. Manfait, O. Piot, Human skin penetration of hyaluronic acid of different molecular weights as probed by Raman spectroscopy, *Skin Research and Technology* 22(1) (2016) 55-62.
- [15] S. Berko, M. Maroda, M. Bodnar, G. Eros, P. Hartmann, K. Szentner, P. Szabo-Revesz, L. Kemeny, J. Borbely, E. Csanyi, Advantages of cross-linked versus linear hyaluronic acid for semisolid skin delivery systems, *European Polymer Journal* 49(9) (2013) 2511-2517.
- [16] Y. Zeng, L. Zhu, Q. Han, W. Liu, X.J. Mao, Y.Q. Li, N.Z. Yu, S.Y. Feng, Q.Y.E. Fu, X.J. Wang, Y.N. Du, R.C. Zhao, Preformed gelatin microcryogels as injectable cell carriers for enhanced skin wound healing, *Acta Biomaterialia* 25 (2015) 291-303.
- [17] E.E. Simsolo, I. Eroglu, S.T. Tanriverdi, O. Ozer, Formulation and Evaluation of Organogels Containing Hyaluronan Microparticles for Topical Delivery of Caffeine, *Aaps Pharmscitech* 19(3) (2018) 1367-1376.
- [18] X.B. Ma, T.T. Xu, W. Chen, H.Y. Qin, B. Chi, Z.W. Ye, Injectable hydrogels based on the hyaluronic acid and poly (gamma-glutamic acid) for controlled protein delivery, *Carbohydrate Polymers* 179 (2018) 100-109.
- [19] A. Ogunleye, A. Bhat, V.U. Irorere, D. Hill, C. Williams, I. Radecka, Poly-gamma-glutamic acid: production, properties and applications, *Microbiology-Sgm* 161 (2015) 1-17.
- [20] I. Bajaj, R. Singhal, Poly (glutamic acid) - An emerging biopolymer of commercial interest, *Bioresource Technology* 102(10) (2011) 5551-5561.
- [21] M.P. Bevilacqua, D.J. Huang, B.D. Wall, S.J. Lane, C.K. Edwards, J.A. Hanson, D. Benitez, J.S. Solomkin, T.J. Deming, Amino Acid Block Copolymers with Broad Antimicrobial Activity and Barrier Properties, *Macromolecular Bioscience* 17(10) (2017) 9.
- [22] V. Castelletto, I.W. Hamley, Self assembly of a model amphiphilic phenylalanine peptide/polyethylene glycol block copolymer in aqueous solution, *Biophysical Chemistry* 141(2-3) (2009) 169-174.
- [23] M. Lapteva, V. Santer, K. Mondon, I. Patmanidis, G. Chiriano, L. Scapozza, R. Gurny, M. Moller, Y.N. Kalia, Targeted cutaneous delivery of ciclosporin A using micellar nanocarriers and the possible role of inter-cluster regions as molecular transport pathways, *Journal of Controlled Release* 196 (2014) 9-18.
- [24] M. Lapteva, K. Mondon, M. Moller, R. Gurny, Y.N. Kalia, Polymeric Micelle Nanocarriers for the Cutaneous Delivery of Tacrolimus: A Targeted Approach for the Treatment of Psoriasis, *Molecular Pharmaceutics* 11(9) (2014) 2989-3001.
- [25] S. Khunmanee, Y. Jeong, H. Park, Crosslinking method of hyaluronic-based hydrogel for biomedical applications, *Journal of Tissue Engineering* 8 (2017) 16.
- [26] M. Barz, A. Duro-Castano, M.J. Vicent, A versatile post-polymerization modification method for polyglutamic acid: synthesis of orthogonal reactive polyglutamates and their use in "click chemistry", *Polymer Chemistry* 4(10) (2013) 2989-2994.

- [27] S. Pluda, M. Pavan, D. Galesso, C. Guarise, Hyaluronic acid auto-crosslinked polymer (ACP): Reaction monitoring, process investigation and hyaluronidase stability, *Carbohydrate Research* 433 (2016) 47-53.
- [28] F. Tranchepain, B. Deschrevel, M.N. Courel, N. Levasseur, D. Le Cerf, C. Loutelier-Bourhis, J.C. Vincent, A complete set of hyaluronan fragments obtained from hydrolysis catalyzed by hyaluronidase: Application to studies of hyaluronan mass distribution by simple HPLC devices, *Analytical Biochemistry* 348(2) (2006) 232-242.
- [29] B.A. Buhren, H. Schrumpf, K. Gorges, O. Reiners, E. Bolke, J.W. Fischer, B. Homey, P.A. Gerber, Dose- and time-dependent effects of hyaluronidase on structural cells and the extracellular matrix of the skin, *European Journal of Medical Research* 25(1) (2020).
- [30] B.A. Buhren, H. Schrumpf, N.P. Hoff, E. Bolke, S. Hilton, P.A. Gerber, Hyaluronidase: from clinical applications to molecular and cellular mechanisms, *European Journal of Medical Research* 21 (2016).
- [31] D. Huesmann, A. Sevenich, B. Weber, M. Barz, A head-to-head comparison of poly(sarcosine) and poly(ethylene glycol) in peptidic, amphiphilic block copolymers, *Polymer* 67 (2015) 240-248.
- [32] J.J. Cheng, T.J. Deming, Synthesis of Polypeptides by Ring-Opening Polymerization of alpha-Amino Acid N-Carboxyanhydrides, *Peptide-Based Materials* 310 (2012) 1-26.
- [33] A.V. Hubina, A.A. Pogodaev, V.V. Sharoyko, E.G. Vlakh, T.B. Tennikova, Self-assembled spin-labeled nanoparticles based on poly(amino acids), *Reactive & Functional Polymers* 100 (2016) 173-180.
- [34] G. Gaucher, M.H. Dufresne, V.P. Sant, N. Kang, D. Maysinger, J.C. Leroux, Block copolymer micelles: preparation, characterization and application in drug delivery, *Journal of Controlled Release* 109(1-3) (2005) 169-188.
- [35] L. Bartosova, J. Bajgar, Transdermal Drug Delivery In Vitro Using Diffusion Cells, *Current Medicinal Chemistry* 19(27) (2012) 4671-4677.
- [36] M. Kong, X.G. Chen, D.K. Kweon, H.J. Park, Investigations on skin permeation of hyaluronic acid based nanoemulsion as transdermal carrier, *Carbohydrate Polymers* 86(2) (2011) 837-843.
- [37] A.M. Wojtowicz, S. Oliveira, M.W. Carlson, A. Zawadzka, C.F. Rousseau, D. Baksh, The importance of both fibroblasts and keratinocytes in a bilayered living cellular construct used in wound healing, *Wound Repair and Regeneration* 22(2) (2014) 246-255.
- [38] T.A. Andrade, A.F. Aguiar, F.A. Guedes, M.N. Leite, G.F. Caetano, E.B. Coelho, P.K. Das, M.A. Frade, Ex vivo model of human skin (hOSEC) as alternative to animal use for cosmetic tests, 4th International Conference on Tissue Engineering, Icte2015, an Eccomas Thematic Conference 110 (2015) 67-73.
- [39] <https://www.nc3rs.org.uk/the-3rs>.
- [40] G.P. Sidgwick, D. McGeorge, A. Bayat, Functional testing of topical skin formulations using an optimised ex vivo skin organ culture model, *Archives of Dermatological Research* 308(5) (2016) 297-308.
- [41] C. Gelis, S. Girard, A. Mavon, M. Delverdier, N. Paillous, P. Vicendo, Assessment of the skin photoprotective capacities of an organo-mineral broad-spectrum sunblock on two ex vivo skin models, *Photodermatology Photoimmunology & Photomedicine* 19(5) (2003) 242-253.
- [42] P. Aquino, Citoqueratinas en dermatología, *Dermatol Rev Mex.* 52(6) (2008) 254-262.
- [43] <https://www.biomimeticdermocosmetics.com/en/>.
- [44] M. Kunishima, C. Kawachi, J. Morita, K. Terao, F. Iwasaki, S. Tani, 4-(4,6-dimethoxy-1,3,5-triazin-2-yl)-4-methyl-morpholinium chloride: An efficient condensing agent leading to the formation of amides and esters, *Tetrahedron* 55(46) (1999) 13159-13170.
- [45] W. Fieber, A. Herrmann, L. Ouali, M.I. Velazco, G. Kreutzer, H.A. Klok, C. Ternat, C.J.G. Plummer, J.A.E. Manson, H. Sommer, NMR diffusion and relaxation studies of the encapsulation of fragrances by amphiphilic multiarm star block copolymers, *Macromolecules* 40(15) (2007) 5372-5378.
- [46] A. Duro-Castano, V.J. Nebot, A. Nino-Pariente, A. Arminan, J.J. Arroyo-Crespo, A. Paul, N. Feiner-Gracia, L. Albertazzi, M.J. Vicent, Capturing "Extraordinary" Soft-Assembled Charge-Like Polypeptides as a Strategy for Nanocarrier Design, *Advanced Materials* 29(39) (2017) 12.

- [47] D. Lath, K. Csomorova, G. Kollarikova, M. Stankovska, L. Soltes, Molar mass-intrinsic viscosity relationship of high-molar-mass hyaluronans: Involvement of shear rate, *Chemical Papers* 59(5-6) (2005) 291-293.
- [48] I. Dolz-Perez, M.A. Sallam, E. Masia, D. Morello-Bolumar, M.D.P. del Caz, P. Graff, D. Abdelmonsif, S. Hedtrich, V.J. Nebot, M.J. Vicent, Polypeptide-corticosteroid conjugates as a topical treatment approach to psoriasis, *Journal of Controlled Release* 318 (2020) 210-222.
- [49] A.H. Nada, A.A. Zaghoul, M.M. Hedaya, I.S. Khattab, Development of novel formulations to enhance in vivo transdermal permeation of tocopherol, *Acta Pharmaceutica* 64(3) (2014) 299-309.
- [50] S.F. Ng, J.J. Rouse, F.D. Sanderson, V. Meidan, G.M. Eccleston, Validation of a Static Franz Diffusion Cell System for In Vitro Permeation Studies, *Aaps Pharmscitech* 11(3) (2010) 1432-1441.
- [51] J.M. Pelet, D. Putnam, An In-Depth Analysis of Polymer-Analogous Conjugation using DMTMM, *Bioconjugate Chemistry* 22(3) (2011) 329-337.

**CHAPTER IV:
MANUFACTURING PROCESS
DEVELOPMENT FOR ALPHA
POLY-L-LYSINES UNDER
DRUG SUBSTANCE QUALITY
GRADE IN GOOD
MANUFACTURING PRACTICE
COMPLIANCE**

Some parts of this chapter has been censured in order to protect the “know-how” of the manufacturing process strategy and analytical techniques to produce and analyze Poly(Amino Acid) based materials under Good Manufacturing Practices compliance developed by Polypeptide Therapeutic Solutions S.L.

1. INTRODUCTION

As mentioned in the general introduction, the main Poly(Amino Acid) (PAA) or polypeptide employed in the biomedical field is poly-L-lysine (PLys). In recent years, the publication numbers containing PLys materials have increased (see Figure 4.1) compared with the second PAA most used, poly-L-glutamic acid (PGlu).

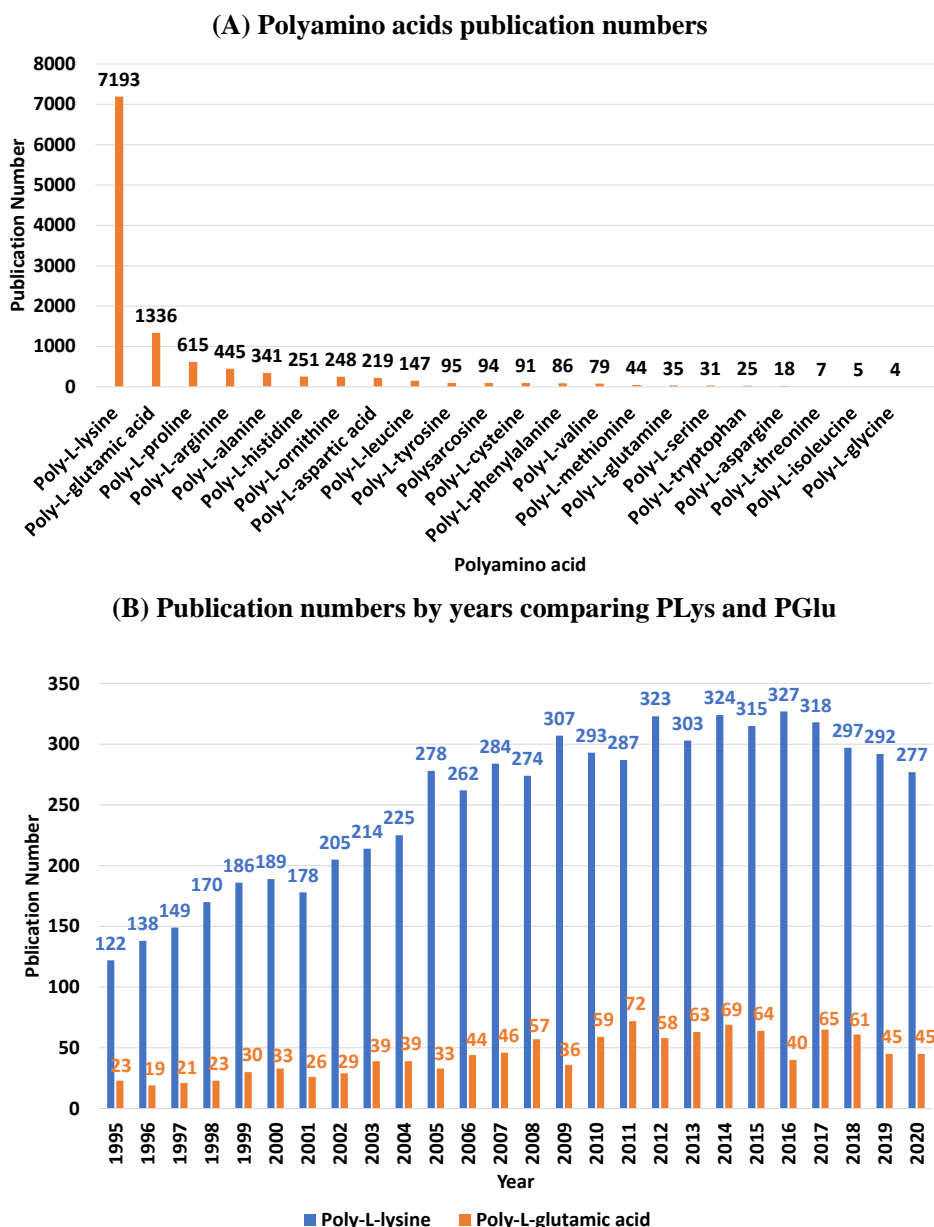


Figure 4.1. (A) Polyamino acid publication numbers and (B) Publication numbers by year comparing PLys and PGlu. Both graphics are based on data until December 2020 in the Web of Science database by keywords same as in the introduction.

Taking this into account, the present chapter is based on the manufacturing process development of PLys materials implemented at PTS SL by applying the quality grade of drug substance following the ICH Q11 harmonized guideline “*Development And Manufacture Of Drug Substances (Chemical Entities And Biotechnological/Biological Entities)*” to enable the Good Manufacturing Practices (GMP) production.

1.1. POLY-L-LYSINE

It is difficult to establish the first time that a poly-L-lysine was obtained. The vast majority of scientists indicate that the first poly-L-lysine was an epsilon-poly-L-lysine (ϵ -PLys), that was accidentally discovered by Shima and Sakai in 1977 as an extracellular material produced by the filamentous bacterium *Streptomyces albulus ssp. lysinopolymerus* strain 346 as a result of screening for a Dragendorff's positive substance [1-4]. However, it has also been described that PLys and other polycations such as poly(vinylamine), were first used for DNA complexation in the 1950s [5]. For example, an article from 1948 by Katchalski, Grossfeld and Frankel describes the synthesis of alpha-poly-L-lysine (α -PLys) by polycondensation of the L-Lys(Z)-NCA monomer [6].

Chemically, ϵ -PLys and α -PLys are structural isomers that differ only in the amide bond. For ϵ -PLys, the amide bond is formed between the alpha carboxylic acid and the amine in epsilon position, and the functional amine in the residual chain is the alpha. In contrast, in α -PLys the amide bond is between the alpha carboxylic acid and the alpha amine, and the functional amine in the residual chain is the epsilon position (see Figure 4.2).

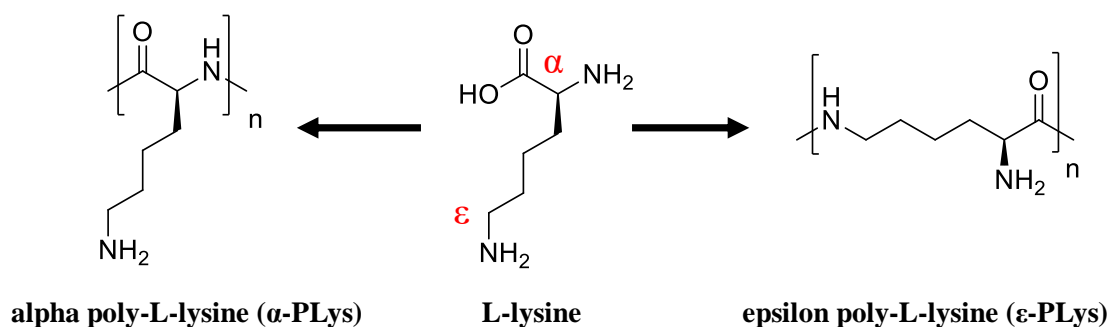


Figure 4.2. Chemical structures of alpha-poly-L-lysine (α -PLys), L-lysine and epsilon-poly-L-lysine (ϵ -PLys).

The main uses of ϵ -PLys are as an antimicrobial agent, and a preservative in the food industry. Since ϵ -PLys is a natural substance that can be mass produced by the metabolism of *Streptomyces albus*, it has been used as a food preservative in Japan, South Korea, the United States, and other countries [5]. This antimicrobial effect is due to its cationic surfactant properties, based on the positively charged amine group in water, allowing a wide antimicrobial activity against yeast, fungi, gram-positive and gram-negative bacteria [2]. ϵ -PLys can also be used for medical applications. For example, in 2012 Shukla and co-workers published an excellent review illustrating the uses of ϵ -PLys as a drug carrier, as a nanoparticle, as a gene carrier, as liposomes, as interferon inducer,

as lipase inhibitor, and as a hydrogel as well as a coating material [2].

On the other hand, α -PLys is applied mainly in the medical field [2, 5]. As previously mentioned, it can be used to form polymeric micelles [7], polymersomes (vesicles) [8], polymer-drug conjugated [9], polyplexes [10], hydrogels [11, 12] and nanoparticles [13]. Structurally, α -PLys can also be found as a homopolymer [9], as the hydrophilic block in amphiphilic PAA block copolymers [14], with PEG [15] or PSar [16], or amphiphilic copolymers with other polymers such as poly-L-lactide [17]. Additionally, there are reported examples with dendrimers of PLys that found their way to advanced clinical trials with the DEP® Technology developed by Starpharma [18] or even up to market approval as device with VivaGel®, currently used as virucide for topical administration [19].

Of course, these materials behave differently depending on the chemical structure of the PLys backbone. Recently (2018) Kim et al reported a comparison of ϵ -PLys and α -PLys in terms of their physicochemical, colloidal, and biological characteristics in terms of gene delivery applications. The authors concluded that ϵ -PLys showed less cytotoxicity and a greater proton buffering capacity for endosomal release than α -PLys. They also mentioned that ϵ -PLys/DNA polyplexes presented higher nucleus preference than their α -PLys counterparts. However, ϵ -PLys had a weaker affinity for DNA than α -PLys, leading to the formation of larger, less compact ϵ -PLys/DNA complexes with successively faster decomplexation [5].

It is important to note that within the scope of this thesis dissertation, we will focus on alpha-PAA, and therefore from now on PLys will refer exclusively to α -PLys.

1.2. GOOD MANUFACTURING PRACTICES AND MANUFACTURING PROCESS DEVELOPMENT

As mentioned, the vast majority of examples for PLys materials are in the POC stage [20]. However, there are several PLys compounds in preclinical trials such as PLys-mimHMK1 [9] or PLys-b-PLeu copolymer [14], clinical trials [19], and others on the market like the VivaGel® [21], as above-mentioned. Contrary to the R&D stage in academia (universities or research institutes), private companies rarely share their *know-how* on the manufacturing process, analytical methodologies, facilities, suppliers, quality controls, etc. in scientific journals or databases.

Fortunately, the ICH Quality guidelines show manufacturers, engineers and scientists how they can develop the production of a drug substance and a drug product with good practices to gain approval from health authorities. Having said that, when the product is an excipient or a key starting material, there are no specific guidelines to address its manufacturing process. In our case, the present chapter is focused on developing a manufacturing process for PLys starting materials or key intermediates to obtain drug substances. As there are no guidelines or documents to describe the rules for developing a manufacturing process guaranteeing that health authorities will agree on the approach, we decided to apply the highest quality grade to our PLys materials, and therefore we developed the process, analytical methods and control strategy on the basis of the drug substance grade. Therefore, the ICH Q11 “*Development And Manufacture Of*

Drug Substances (Chemical Entities And Biotechnological/Biological Entities)” and ICH Q7 “*Good Manufacturing Practice Guide for Active Pharmaceutical Ingredients*” harmonized guidelines have been followed.

ICH Q11 harmonized guideline describes approaches to developing and understanding the manufacturing process of a drug substance. It addresses aspects of development and manufacture that pertain to a drug substance, including steps designed to reduce impurities. In addition, ICH Q11 provides further clarification on the principles and concepts described in ICH Guidelines on Pharmaceutical Development (Q8), Quality Risk Management (Q9), and Pharmaceutical Quality System (Q10) as they pertain to the development and manufacture of a drug substance. Other guidelines are also recommended to properly develop the new drug substances or APIs, such as Validation of Analytical Procedures (Q2R1), Impurities in New Drug Substances (Q3AR2), Guideline For Elemental Impurities (Q3D), and Test Procedures and Acceptance Criteria for New Drug Substances and New Drug Products: Chemical Substances (Q6A) [22].

In the present chapter, we address some of the key aspects of manufacturing process development that are required at the current stage of development for poly-L-lysine related pharmaceutical products being developed at our site. These include:

Manufacturing process development:

According to ICH Q11, the manufacturing process development is a course to establish a commercial manufacturing process capable of producing a drug substance of the intended quality. The resulting process must be reproducible allowing the drug substance to be obtained with batch-to-batch consistency. For this, there are two different approaches: (i) **traditional** and (ii) **enhanced**. In the **traditional approach**, the setpoints and operating ranges for process parameters are defined, and the drug substance control strategy is typically based on the demonstration of process reproducibility and testing to meet established acceptance criteria. In the **enhanced approach**, risk management and scientific knowledge are used more extensively to identify and understand process parameters and unit operations that impact the Critical Quality Attributes (CQAs). Thus, the development of the appropriate control strategies applicable throughout the lifecycle of the drug substance must be carried out [22]. In this work, the **enhanced approach** has been adapted to PLys materials.

A CQA is a physical, chemical, biological, or microbiological property or characteristic that should be within an appropriate limit, range, or distribution to ensure the desired product quality. To guide the process development, the potential drug substance CQAs are employed. Drug substance CQAs typically include properties or characteristics that affect identity, purity, biological activity, as well as the stability. When the physical properties are a key part of the drug product manufacture or performance, these can be designated as CQAs. Impurities represent an important class of potential drug substance CQAs since they can potentially have an impact on drug product safety. For chemical entities, impurities can include organic impurities (including potentially mutagenic impurities), inorganic impurities e.g., metal residues, and residual solvents [22].

To properly address the manufacturing process development, the risk assessment

can be carried out during development to identify parts of the process that can impact the potential CQAs. Using the enhanced approach, the determination of appropriate material specifications and process parameter ranges could be addressed as follows:

- Identify potential sources of process variability.
- Identify the material attributes and process parameters that can have the greatest impact on drug substance quality.
- Design and conduct studies (e.g., mechanistic and/or kinetic evaluations, multivariate design of experiments, simulations, modeling) to identify and confirm the links and relationships of material attributes and process parameters to drug substance CQAs.
- Analyze and assess data to establish appropriate ranges, including the establishment of design space if desired [22].

Selection of starting materials and source materials:

As can be imagined, the selection of raw materials and their suppliers is a key part of the manufacturing process. The raw materials can be classified according to their role in the manufacturing process, i.e. starting materials, reagents, solvents, etc. Starting materials are incorporated as a significant structural fragment into the structure of the drug substance. “Significant structural fragment” in this context is intended to distinguish starting materials from reagents, solvents, or other raw materials. Other commonly-used chemical materials used to create salts, esters, or other simple derivatives should simply be considered as reagents [22]. To select the suppliers and the starting materials, it is important to define the CQAs and their quality level to be applied in the Drug Substance synthesis. Moreover, it is recommended to establish the acceptance criteria for the quality level of the CQAs. The selection of the supplier must be based on its manufacturing capability, the batch-to-batch consistency securing the quality levels for the CQAs, cost-efficiency of the process, availability, prices, etc.

Control strategy:

The control strategy can be defined as a set of controls to ensure the process is performed in a reproducible manner and that the CQAs are within the target quality standards. The ICH guidelines indicate that the control strategy should include the following points:

- Controls on material attributes (including raw materials, starting materials, intermediates, reagents, primary packaging materials for the drug substance, etc.).
- Controls implicit in the design of the manufacturing process.
- In-process controls development.
- Controls on drug substance [22].

Submission of manufacturing process development & related information:

There is no Common Technical Document (CTD) format to perform the submission of the results [22], although the package documentation should contain (i) the Quality Risk Management, (ii) the Process Development, (iii) the definition and rationale for CQAs, (iv) the Design Space, (v) the Control Strategy, and (vi) the analytical methodologies. This part is very important, because it is the report of the results obtained

in the previous sections. Here, the CMC package documentation is generated to support and defend the new drug substance with the health regulatory authorities. As commented previously, this chapter can be considered as a part of the CMC section inside the CTD.

1.3. AIMS AND APPROACH

According to the FDA website, the steps to scale-up a drug substance are the (i) proof of concept (POC), (ii) prototype, (iii) pilot, and (iv) production [23]. These steps are described below, adapting the scale-up process to our PLys materials including the scale, the purpose, and the quality grade. For this, it can be established that for the POC and the prototype, the quality level is R&D. For pilot, there is a scale-up process involving different quality grades such as R&D, preclinical and GMP. The production stage (commercial batches) is outside of the scope of this chapter. This can be observed in Figure 4.5. The guidelines provide a solid ground for pharmaceutical development; however, the progressive implementation of GMP requirements during clinical development may vary on a project-by-project basis. To that aim, the Manufacturing Process Development & Robustness is assessed based on a Quality by Design approach by defining the Critical Quality attributes defined by the downstream processing of the materials (CQAs translated into the Certificate of analysis), knowledge, identification, risk assessment & monitoring of the Critical Process Parameters (CPPs) affecting CQAs through appropriate In-Process Controls (IPCs), and finally establishing a Normal Operating Range (NOR) of the process for the Proven Acceptable Range (PAR) defined for each CPP. An accepted approach to illustrate all parameters that might affect the CQAs of a drug substance is the use of the ISHIKAWA diagram (Figure 4.3). This outlines the different steps in the manufacturing process, determining where quality control issues may arise and defining the resources and action plans to be established [24].

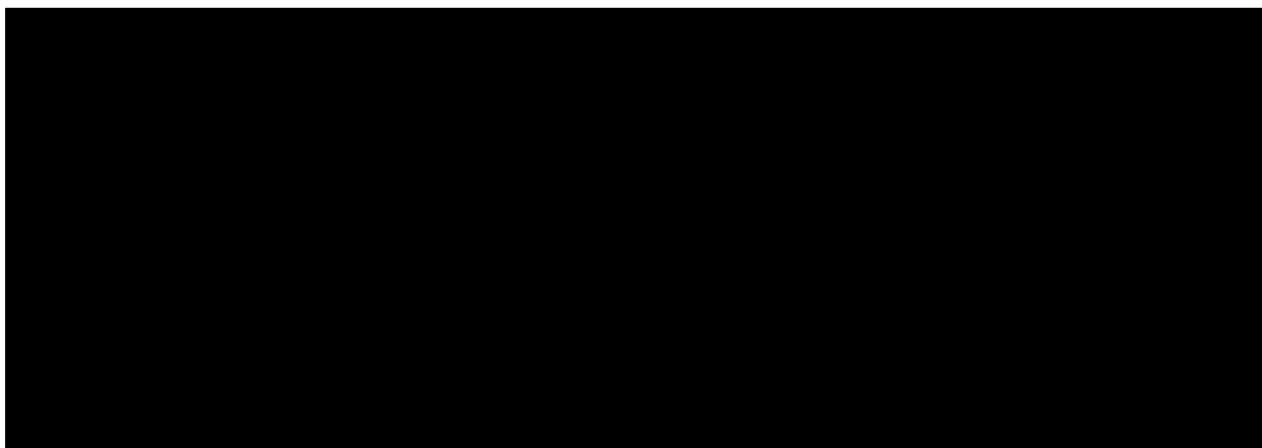


Figure 4.3. ISHIKAWA diagram. Identification of internal and external factors affecting the CQAs. Adapted from [24].

As highlighted in Figure 4.3, the present chapter is focused on the development of sections 2, 4 and 6. Sections 1, 3, 5 & 7 are highly related to the GMP compliant Quality System and are summarized in Figure 4.4. These will not be further discussed in the present chapter, with the exception of storage and shelf-life.

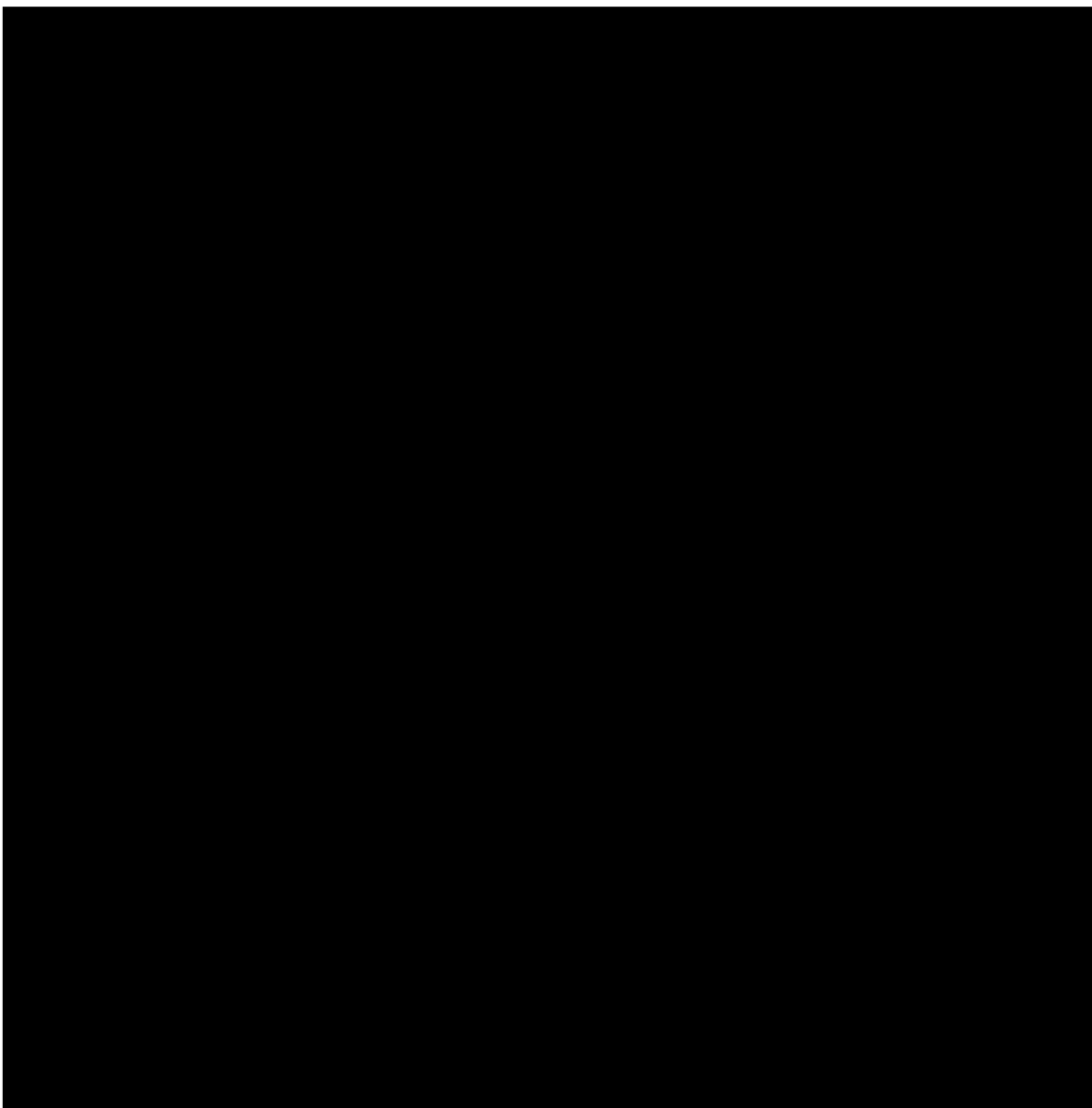


Figure 4.4. GMP Quality System in terms of Personnel, Environment, Equipment and Material Transfer.

In practice the Manufacturing Process development has been developed at each step of the scale-up as follows:

Proof of Concept (POC) is a demonstration to verify that certain concepts or theories have the potential for real-world application. Normally, the quality grade is an R&D feasibility study, and the product amounts are a few grams.

Process Optimization is the step when the Proven Acceptable Range (PAR) studies are performed, stressing the Critical Process Parameters (CPPs) to obtain a comfortable range of operation to meet CQAs. Also, the kinetics are determined in this stage to reach a high efficiency in the manufacturing process. This optimization is also performed in the R&D environment, increasing the scale up to 20 – 30 grams.

Pilot Batches are performed to obtain information about the process in a relevant production environment at a scale ranging from 100 – 2000 grams, and to verify the optimized process performance. Here, the operations are done inside of the normal

Operating Range established in the PAR of CPPs, and allows the verification of process suitability at a relevant set-up and scale. During the execution of these processes, analytical methods are refined for IPCs and release items. Also, the purification process is refined and the impurities identified and controlled by establishing the appropriate control strategy. These batches can be considered as prototypes, and if adequate control over bioburden and endotoxins is considered, the material can be employed for GLP Toxicological studies.

GMP Engineering Batches are run at large scale (> 2 Kg) inside a GMP compliant facility, and represent the first time that the process is transferred to a GMP environment. All Standard Operating Procedures (SOPs), including process and analytical methods, are generated as a first draft version. These batches allow the verification and optimization of the developed process and analytical methods at the GMP production plant. The obtained product could be employed for GLP toxicology or even clinical trials in humans, if no major deviations from the manufacturing guide arise.

GMP clinical batches: at this stage the product is produced according to all developed procedures under GMP standards. No major changes on the process are applied other than modifications to scale, small operational optimizations or equipment adaptations. These batches are aimed at use in clinical trials, and represent an historical ground that should allow the validation of the manufacturing processes towards commercial production.

GMP Commercial Batches: are performed when the product is on the market, in commercial phases, and the manufacturing process and analytical methods are validated, and a fully compliant stability program has been conducted for at least three representative batches. Market authorization is required from the regulatory authorities.

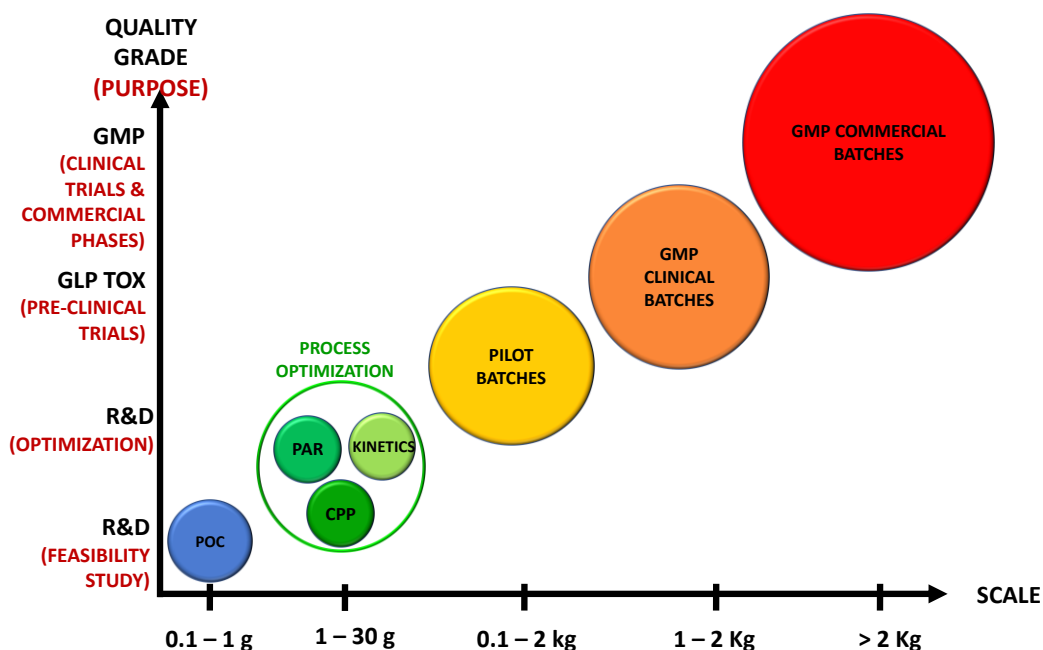


Figure 4.5. Adapted scale-up process for PLys materials including the scale amount, the purpose and the quality grade.

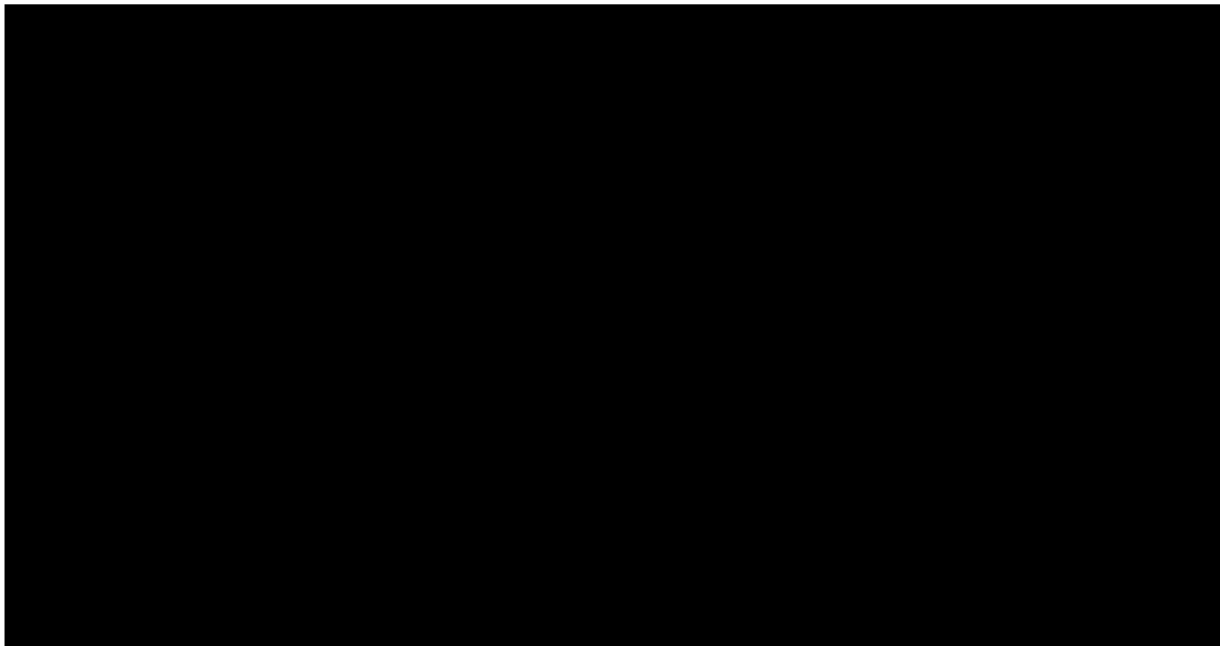


Figure 4.6. Examples of set-ups for R&D Development.

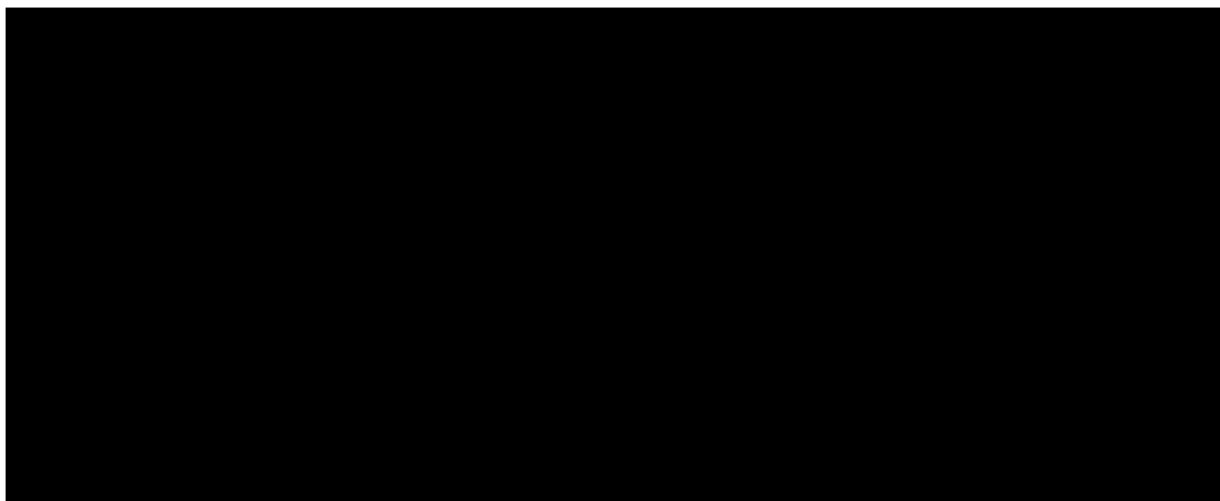


Figure 4.7. Examples of set-ups for Pilot Plants.

This chapter is possibly the most important in the present industrial thesis dissertation since it aims to show how to develop an appropriate process, analytical methods and control strategy to develop PAA materials to be used in clinical trials, and potentially to reach market authorization. As previously mentioned, there are no sections in either the United States Pharmacopeia (USP) or the European Pharmacopoeia dedicated to these materials, which are not commodities. Therefore, this work has been dedicated to developing, to our best knowledge, an unprecedented deep understanding of PLys synthesis, its physico-chemical characterization, analytical methods and control strategy as well as a complete understanding of the regulatory standards that need to be addressed to efficiently develop poly-L-lysine based drugs.

2. RESULTS & DISCUSSION

Process and analytics are developed side-by-side, with a devoted team of 3-4 people with complementary skills in polymer chemistry, organic synthesis, process development, analytical chemistry and quality control.

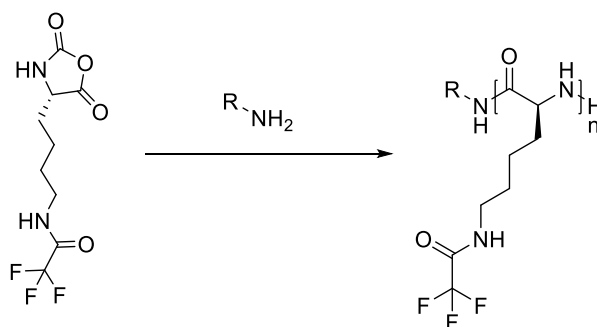
2.1. MANUFACTURING PROCESS DEVELOPMENT

As illustrative examples of alpha poly-L-lysine manufacturing process development, two PLys materials are fully described in the present chapter: (i) **HL50** and (ii) **ML400**. The initiators and Mw are not explained.

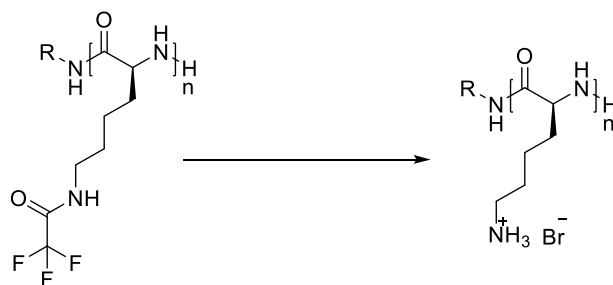
The manufacturing process for the polymerization, deprotection and purification steps for **HL50** and **ML400** are fully optimized, developed and explained in the following pages. The **HL50-P** and **ML400-P** nomenclature makes reference to protected PLysTFA.

2.1.1. SYNTHETIC ROUTE

The manufacturing process for these PLys materials follows the same synthetic route as most other PAA described in the present thesis, based on two main steps: (i) polymerization and (ii) deprotection.



Scheme 4.1. General synthesis for protected PLys.



Scheme 4.2. General reaction scheme for PLysTFA deprotection.

2.1.2. PRELIMINARY PROCESS WORKFLOW & CRITICAL PROCESS PARAMETERS.

As a starting point for the development of the manufacturing process, figures 4.8 and 4.9 show the preliminary process workflow based on background state-of-the-art and our know-how. In Figure 1, the manufacturing process is described in the form of a flow diagram with sequential procedure narrative for each process. Of note, the work-flow diagrams for each step are valid for both PLys examples **HL50** and **ML400**.

These are the CPPs for polymerization and deprotection steps that will be studied and verified in detail throughout the next sections.



Figure 4.8. Preliminary work-flow diagram for the polymerization step.

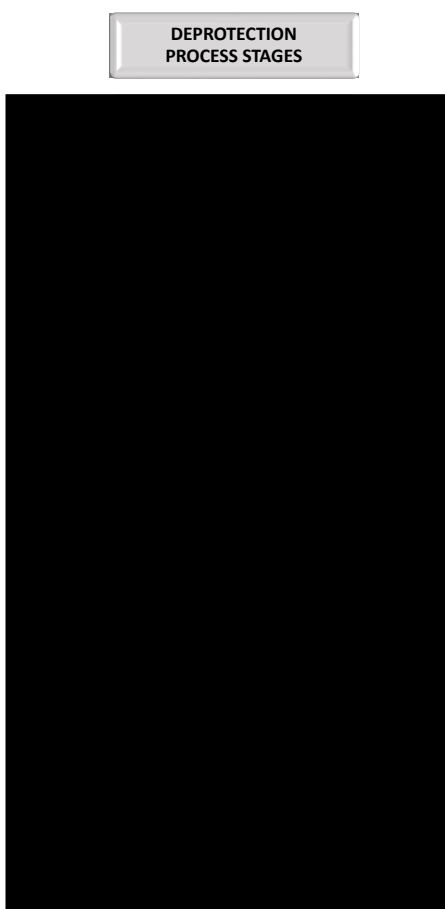


Figure 4.9. Preliminary work-flow diagram for the deprotection step.

2.1.3. CRITICAL QUALITY ATTRIBUTES (CQAs) OF POLY-L-LYSINE HYDROBROMIDE

Each of the physical, chemical, biological or microbiological properties of PLys can be considered a CQA according to ICH Q11 harmonized guideline. To appropriately develop the manufacturing process, we need to understand how the CPPs impact each CQA for PLys, which can be defined in 4 main categories: (i) Physical & Chemical data (appearance, colour and solubility), (ii) Analytical quality (Identity, purity, Mw, PDI, Degree of polymerization, Counterion content and enantiomeric excess), (iii) Impurities (raw materials, process related, volatile, degradation products, microbiological or elemental). The most critical attributes of PLys are those related to its analytical quality, given that if one parameter is outside the desirable range, the performance of the final drug substance could be altered and there would be no possibility to reprocess the PLys products, resulting in a product that is Outside Of Specifications (OOS). The rest of the attributes are mainly impurities coming from reagents, raw materials, process related, degradation products, microbiological or elemental. The limits established for the impurities are based on either ICH, or pharmacopeia monographies and usually need to account for the final drug product dosage and administration route. Impurities are controlled throughout the process and the workflow usually includes reprocessing steps to reduce the impurities below the established limit.

Table 4.2 illustrates the previously established CQAs and limits translated into the Certificate of Analysis (CoA) for poly-L-lysine after the manufacturing process development work that will be discussed in this chapter. The limits are established preliminarily, based on background and know-how with regulatory agencies.

Table 4.2. Preliminary Limits for CQA in our poly-L-lysine hydrobromide salt final products.

Attribute	Limits for HP50	Limits for MP400
<u>Physical & Chemical Data</u>		
Appearance		
Color		
<u>Analytical Quality</u>		
Identity by NMR		
Purity by SEC (in anhydrous basis)		
Molecular Weight (Da) (Mw) by SEC		
Polydispersity Index (Mw/Mn) by SEC		
Degree of Polymerization by SEC		
Enantiomeric excess (L-form) by CC		
<u>Impurities</u>		
<u>Microbiological data</u>		
Endotoxin (EU/g)		
Total Aerobic Microbial Count (CFU/g)		
Total Yeasts and Molds Count (CFU/g)		

As stated previously, having the impurities under control is a very important part of the manufacturing process development from both a chemical and safety point of view. According to ICH Q3A(R2) harmonized guideline “*Impurities in New Drug Substances*”, impurities can be classified into organic impurities, inorganic impurities, and residual solvents.

Endotoxins are lipopolysaccharides, with a complex structure exhibiting amphiphilic characteristics, consisting of three different regions: (i) a non-polar lipid, (ii) a core polysaccharide and (iii) a long-chain polysaccharide. Endotoxins are heat-stable toxins present in the outer cell walls of Gram-negative bacteria. When cell membranes are disrupted, due to cell death or during downstream processing, endotoxins are released. Endotoxin contamination of pharmaceutical products represents a major problem, especially when the medication is applied intravenously. When endotoxins reach the bloodstream, they can cause adverse effects such as fever, vasodilatation, diarrhea, blood coagulation, chills, headache, malaise, yawns, impaired hepatic and endocrine systems, and even death. Endotoxins are relatively insensitive to pH changes and resistant to heat and bactericidal substances, making the sterilization of solutions, glassware and laboratory equipment very difficult [25]. For these reasons, the design and control of the working space is a very important parameter to control the endotoxin level in the final product.

Elemental impurities are analyzed and their limits are established according to ICH Q3D harmonized guideline “*Guideline for Elemental Impurities*”. Elemental impurities in drug products may arise from several sources; they may be residual catalysts that were added intentionally in the synthesis, or they may be present as impurities (e.g. through interactions with processing equipment or container/closure systems, or by being present in components of the drug product). Since elemental impurities at higher concentrations can be toxic, their levels in the drug product should be controlled within acceptable limits.

2.1.4. SELECTION OF RAW MATERIALS

For the industrial manufacturing process of PLys at a large scale, the supplier for each raw material involved was selected carefully in terms of price, their capability of large-scale production, the product’s quality, impurities profile, reproducibility, and specific documentation and quality system management to support the traceability of their RM, process and QC. Table 4.3 shows the Raw Materials (RM) selected.

Table 4.3. Raw Materials selected for the manufacturing process for **HL50** and **ML400**.

Compound	Supplier	Purpose	Critical Parameter	Process Stage
Compound 1	PMC-ISOCHEM	N/A	N/A	Polymerization
Compound 2	Sigma Aldrich	N/A	N/A	Polymerization
Compound 3	Scharlab S.L.	N/A	N/A	Polymerization
Compound 4	Scharlab S.L.	N/A	N/A	Polymerization precipitation
Compound 5	Scharlab S.L.	N/A	N/A	Polymerization precipitation
Compound 6	Scharlab S.L.	N/A	N/A	Deprotection
Compound 7	Scharlab S.L.	N/A	N/A	Deprotection
Compound 8	Scharlab S.L.	N/A	N/A	Deprotection
Compound 9	Scharlab S.L.	N/A	N/A	Acidification
Compound 10	Scharlab S.L.	N/A	N/A	Deprotection precipitation

2.1.5. PROCESS DEVELOPMENT

PROOF OF CONCEPT (POC)

To assess the feasibility of the process conditions at this POC stage, critical CQAs were established on the basis of their connection to architectural and chemical characteristics of the polymer.

Polymerization was performed by ROP of NCAs via NAM following Scheme 4.1. After that, the product was precipitated in several solvents commonly employed for other protected PAA in which PLysTFA is not soluble, such as diethyl ether, *n*-hexane or water [26].

Once the intermediate PLysTFA was isolated, SEC-RI-MALS and NMR analysis were performed to characterize the materials. Figure 4.10 shows SEC elugrams with both the RI and MALS (7 angles) detectors in DMF with narrow peaks for **HL50-P** and **ML400-P**. See the quantitative results by SEC-RI-MALS and NMR in Table 4.

As stated at the beginning of this section, deprotection optimization was carried out for **HL50** and applied directly for **ML400**. The deprotection step of **HL50** was performed following the synthetic route previously illustrated in Scheme 4.2. The elugrams and NMR spectra for the physico-chemical characterization can be found below. The qualitative results have been censured.

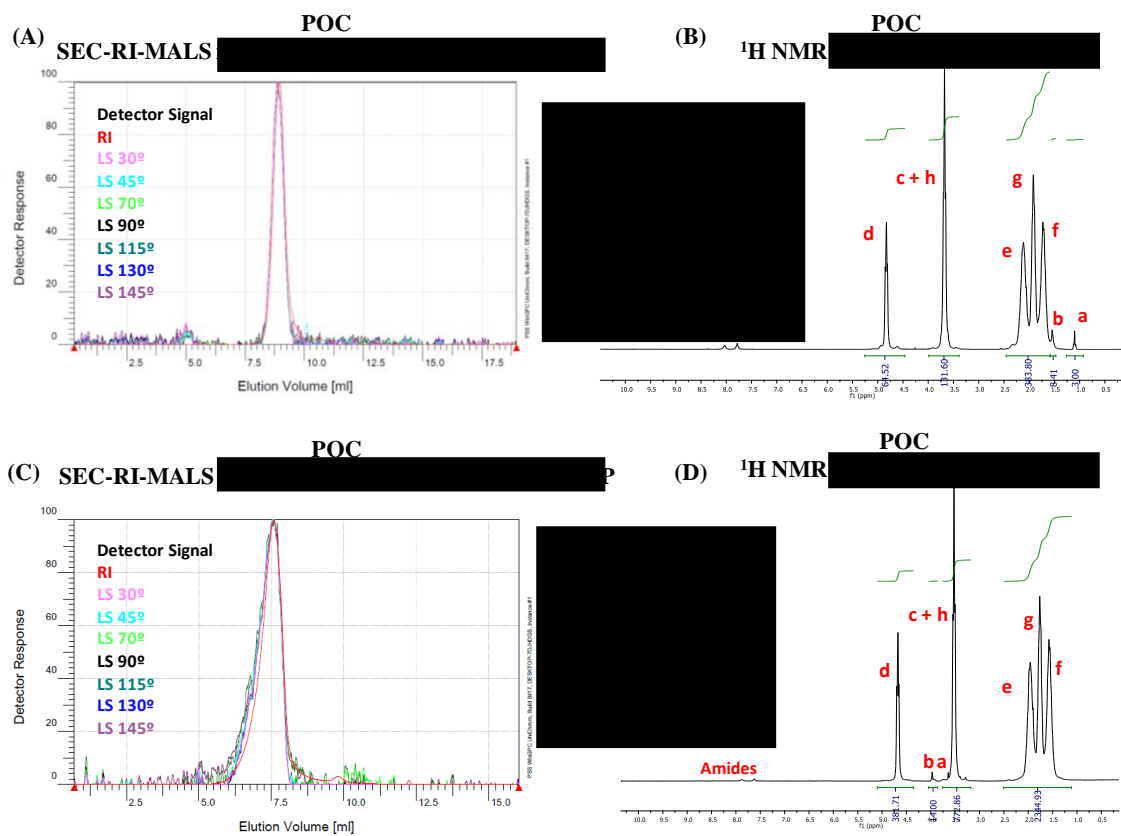


Figure 4.10. HL50-P characterization. (A) SEC-RI-MALS. (B) ^1H NMR. ML400-P characterization. (C) SEC-RI-MALS. (D) ^1H NMR.

Table 4.5. Deprotection optimization for **HL50**.

Trial Number	Deprotector Reagent	Equivalents to TFA group	Temperature	Deprotection Percent by NMR	Specific Rotation ($^{\circ} \cdot \text{m} \cdot \text{g}^{-1} \cdot \text{dm}^{-1}$)
1	Compound 1	N/A	N/A	80%	N/A
2	Compound 1	N/A	N/A	83%	N/A
3	Compound 2	N/A	N/A	100%	N/A
4	Compound 2	N/A	N/A	100%	N/A
5	Compound 3	N/A	N/A	100%	N/A
6	Compound 1	N/A	N/A	100%	N/A

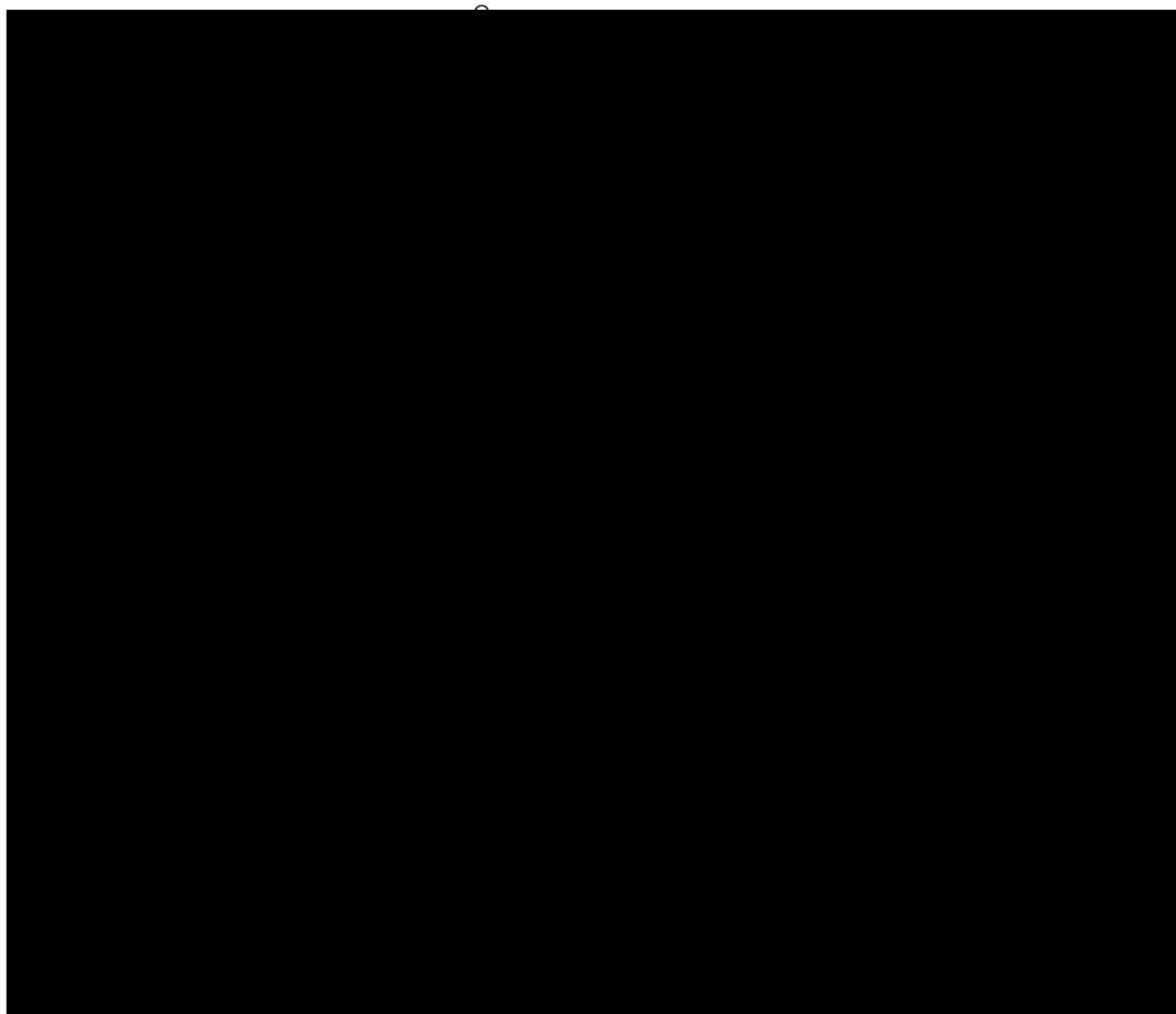


Figure 4.11. Deprotection optimization of **HL50** by ^1H NMR.

As seen in Table 4.5 and Figure 4.11, for Compound 1 an incomplete hydrolysis of TFA groups was found by NMR. Compounds 2 and 3 yielded the complete hydrolysis with no impact on the stereochemistry of alpha carbon. Compound 3 was selected due to its subproducts.

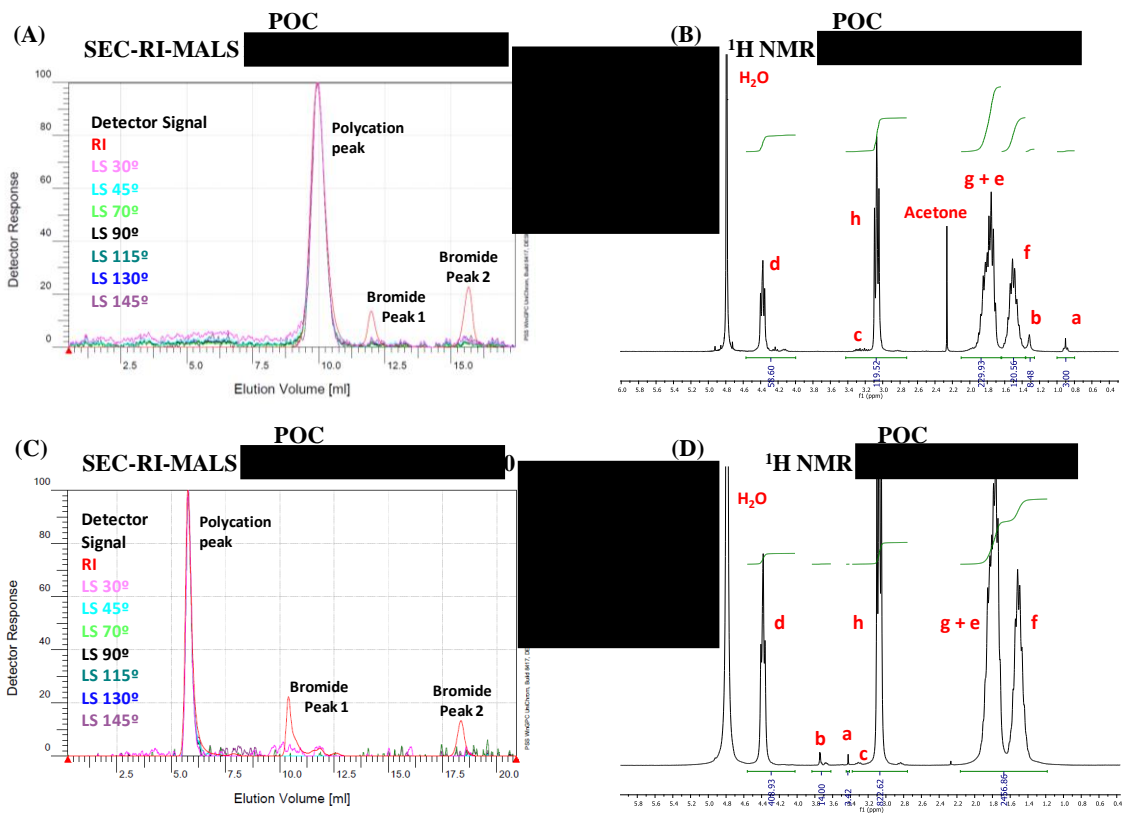


Figure 4.12. HL50 characterization. (A) SEC-RI-MALS. (B) ^1H NMR. ML400 characterization. (C) SEC-RI-MALS. (D) ^1H NMR.

Table 4.6. Results for POC of **HL50** and **ML400**.

Product	Target	Protected PLysTFA	Deprotected PLysHBr
HL50	[Redacted]		
ML400			

The DP values obtained by SEC-RI-MALS and by NMR for **ML400** are in good agreement with the target values. However, the DP for **HL50** is slightly higher by SEC and NMR with respect to the desired values. These slight deviations, as well as the elimination of solvents and other impurities during the purification process, were adjusted and optimized in the next stages of manufacturing process development. From now on, for SEC elugrams only the polymer peaks (not bromide peaks) and the RI signal detector (not MALS detector) will be shown. Similarly, only the region of interest (0.5 to 6.0 ppm) will be illustrated in ^1H NMR spectra.

As seen in Table 4.7, in terms of Mw distributions, DP, PDI and molar ratio between lysine and initiator, the Proof of Concept synthesis for both PLys materials was carried out successfully at a scale of 1 gram of NCA. The preliminary process parameters are established to move into the next developmental stage.

PROCESS OPTIMIZATION - KINETIC STUDY

To perform the kinetic study of the polymerization process for **HL50**, 4 experiments were carried out combining two concentrations and two target DPs at a scale of 10g NCA. The kinetics were monitored by SEC.

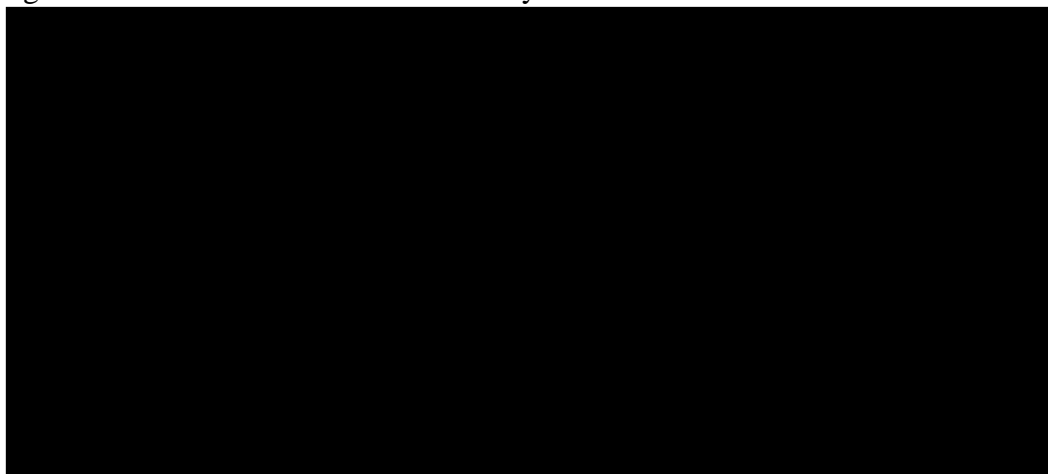


Figure 4.13. Graphic representation of DP determined by Mw (SEC-RI-MALS) in the polymerization kinetics assays for **HL50-P**.

Kinetic results show that for diluted polymerizations experimental DPs are similar to targeted DPs with a much slower reaction progression. However, for the more concentrated polymerization, the reaction was complete earlier. Since SEC elugrams were directly measured in the reaction media on the PLysTFA precursor, a more accurate Mw estimation is required to establish the correlation from precursor to final PLys specifications. The 4 batches were therefore processed to yield the crude solid, and results are shown in Table 4.7. Moreover, a fast and reliable IPC to monitor polymerization progression by SEC was established. By means of this IPC, the peak of NCA can be observed as well as a broad peak at the time zero of millions of Da.

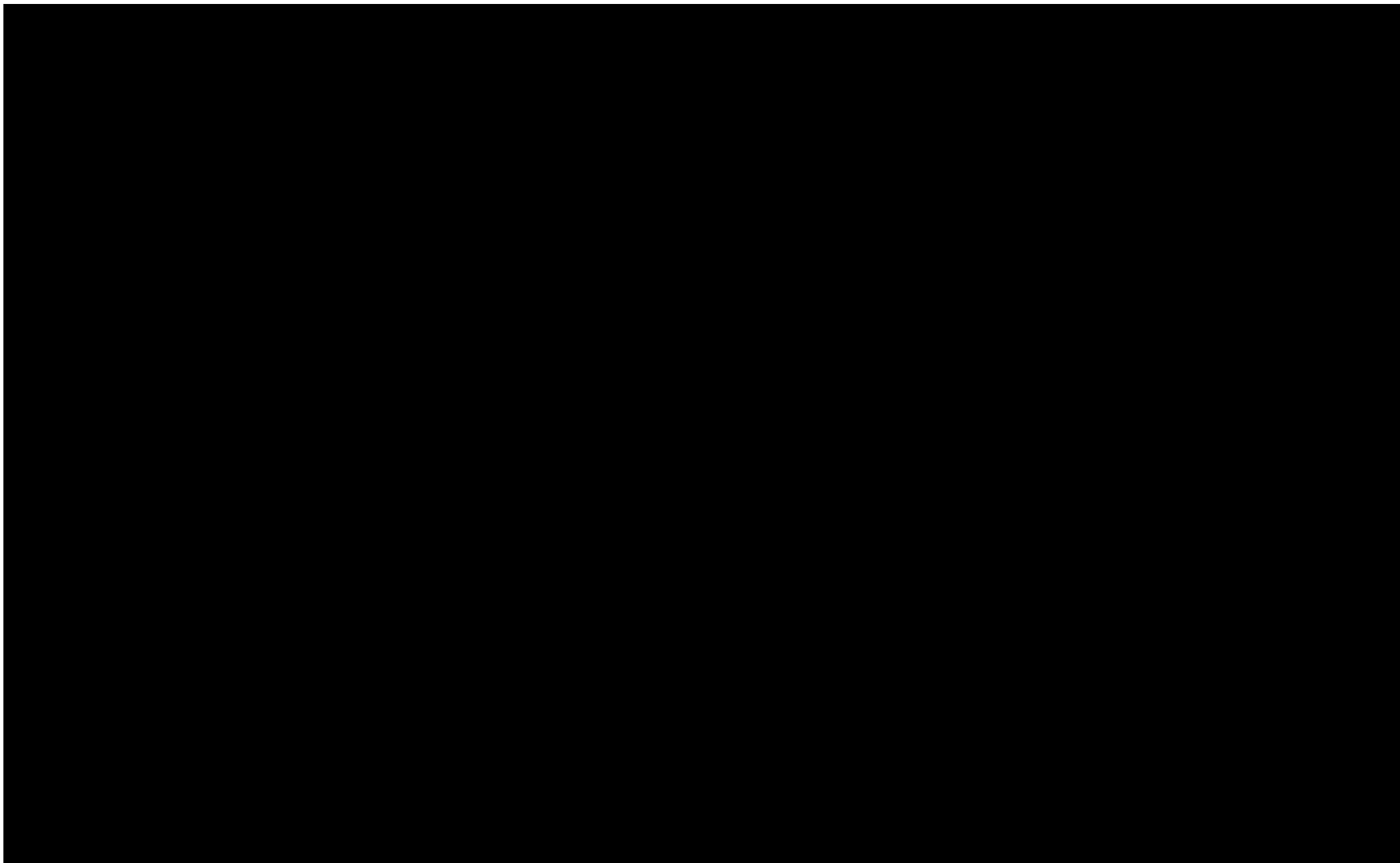


Figure 4.14. Overlapped SEC-RI elugrams of polymerization kinetics for **HL50-P**.

Table 4.7. Results of **HL50** for DP and concentration optimization

Trial Number	Target	Protected HL50-P	Deprotected HL50
1	[REDACTED]		
2			
3			
4			

Analogous to **HL50**, the polymerization kinetics for **ML400** were studied at the scale of 100g NCA.

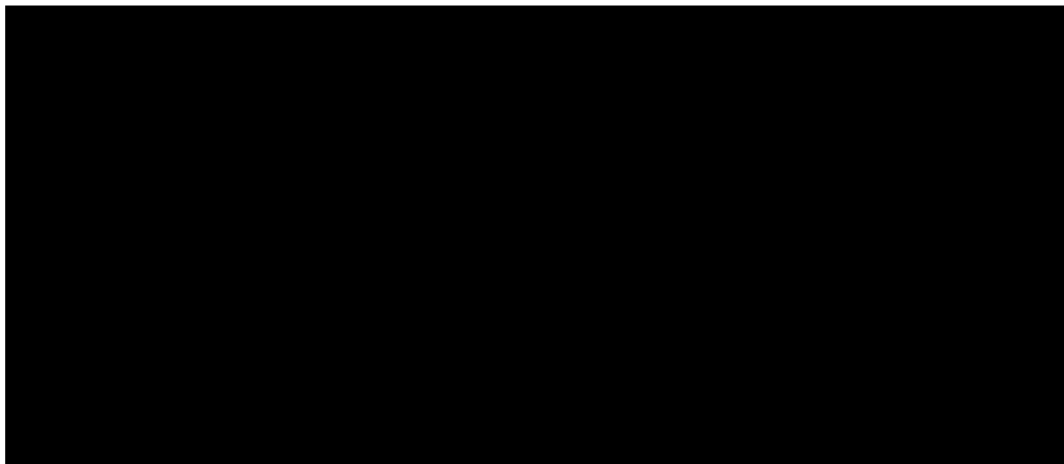


Figure 4.15. Graphic representation of DP determined by absolute Mw (SEC-RI-MALS) in the polymerization kinetics for **ML400-P** with 100g NCA.

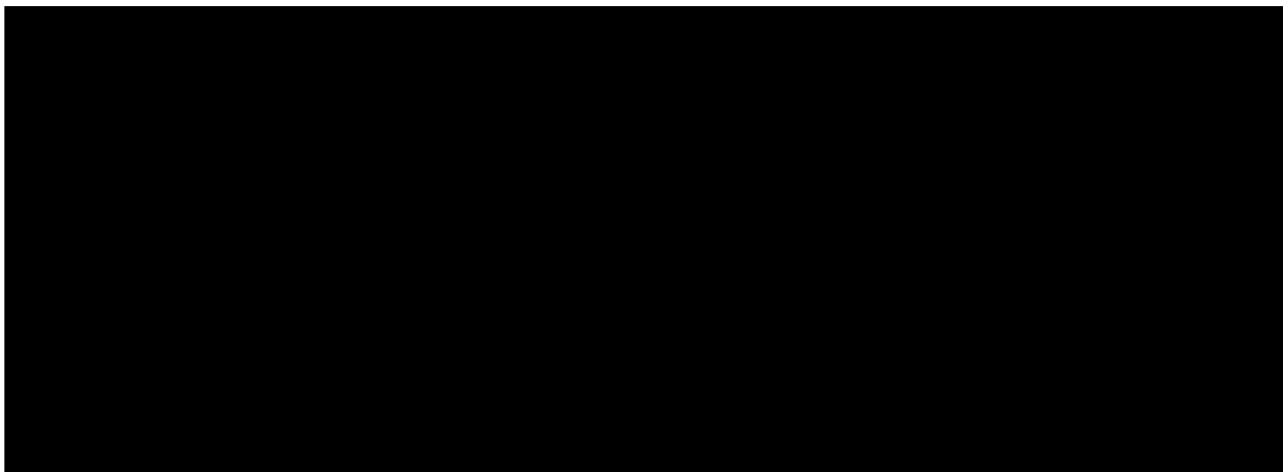


Figure 4.16. SEC-RI elugram overlays showing the polymerization kinetics for **ML400-P**.

At the 100 grams NCA scale, the polymerizations were monitored by SEC-RI-MALS and the polymerization time was established. Results can be found in Table 4.13.

PROCESS OPTIMIZATION -PAR STUDY

The PAR study allows us to define a preliminary Process Design Space (range of values for each CPP identified) and a control strategy to properly develop the manufacturing process. In this study, it is defined how the CPPs are controlled via IPCs and the handling of reactions that will be translated into the manufacturing guide. Thus, a preliminary PAR study for the polymerization step was evaluated in the first set of 10 experiments at small scale (1.5 grams of L-Lys(TFA)-NCA), varying the parameters that are most likely to have an impact in the CQAs, according to our *know-how*. Results for **HL50-P** and **ML400-P** are shown in Figure 4.17 and Table 4.8, and Figure 4.18 and Table 4.9 respectively.

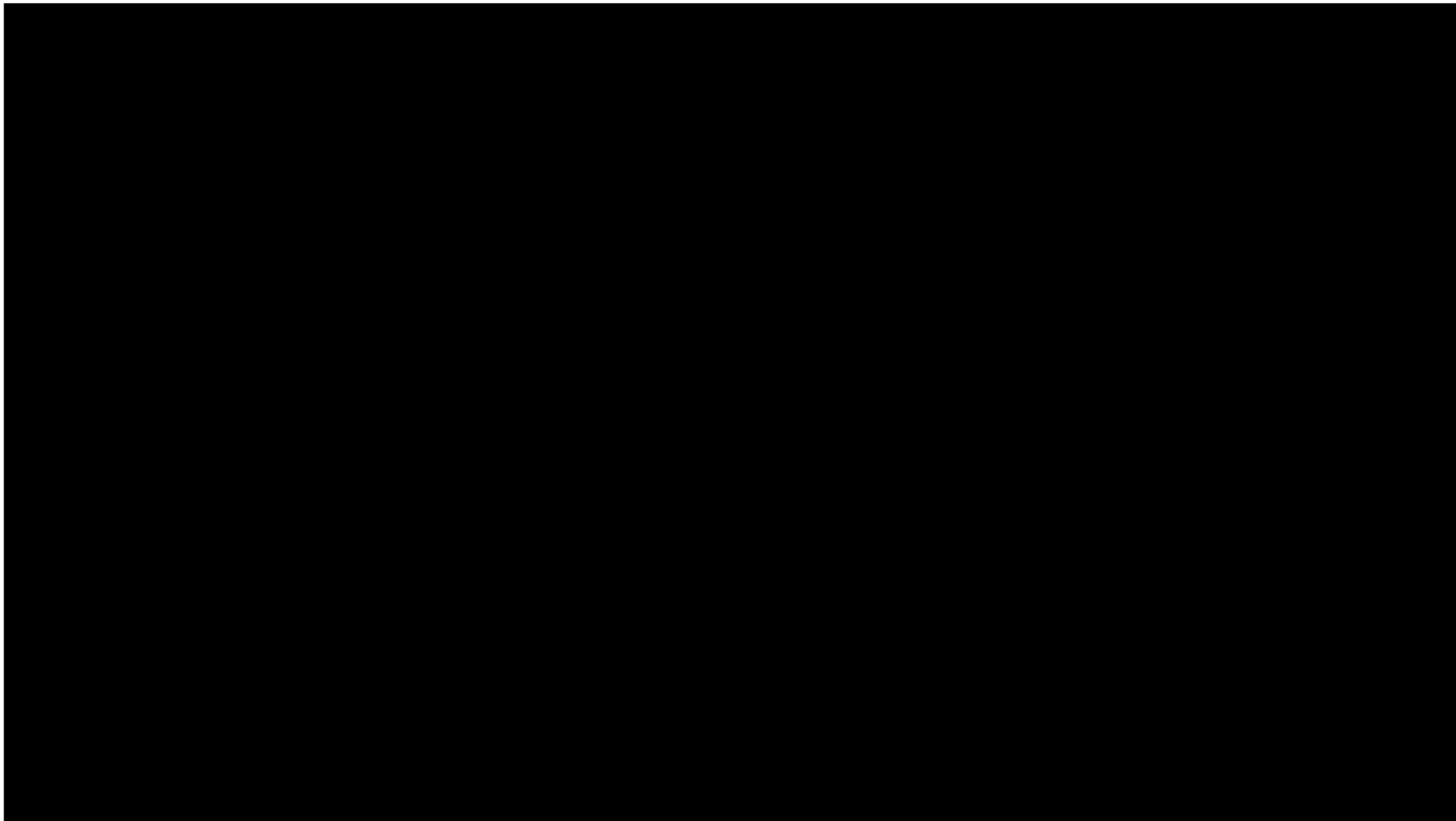


Figure 4.17. SEC-RI from PAR study of **HL50-P**.

Table 4.8. Quantitative results from the PAR study of **HL50-P**.

Trial Number	CPP	Results			Deviation		
		Mw by SEC (kDa)	PDI	DP by Mw	Mw by SEC (kDa)	PDI	DP by Mw
1							
2							
3							
4							
5							
6							
7							
8							
9							
10							

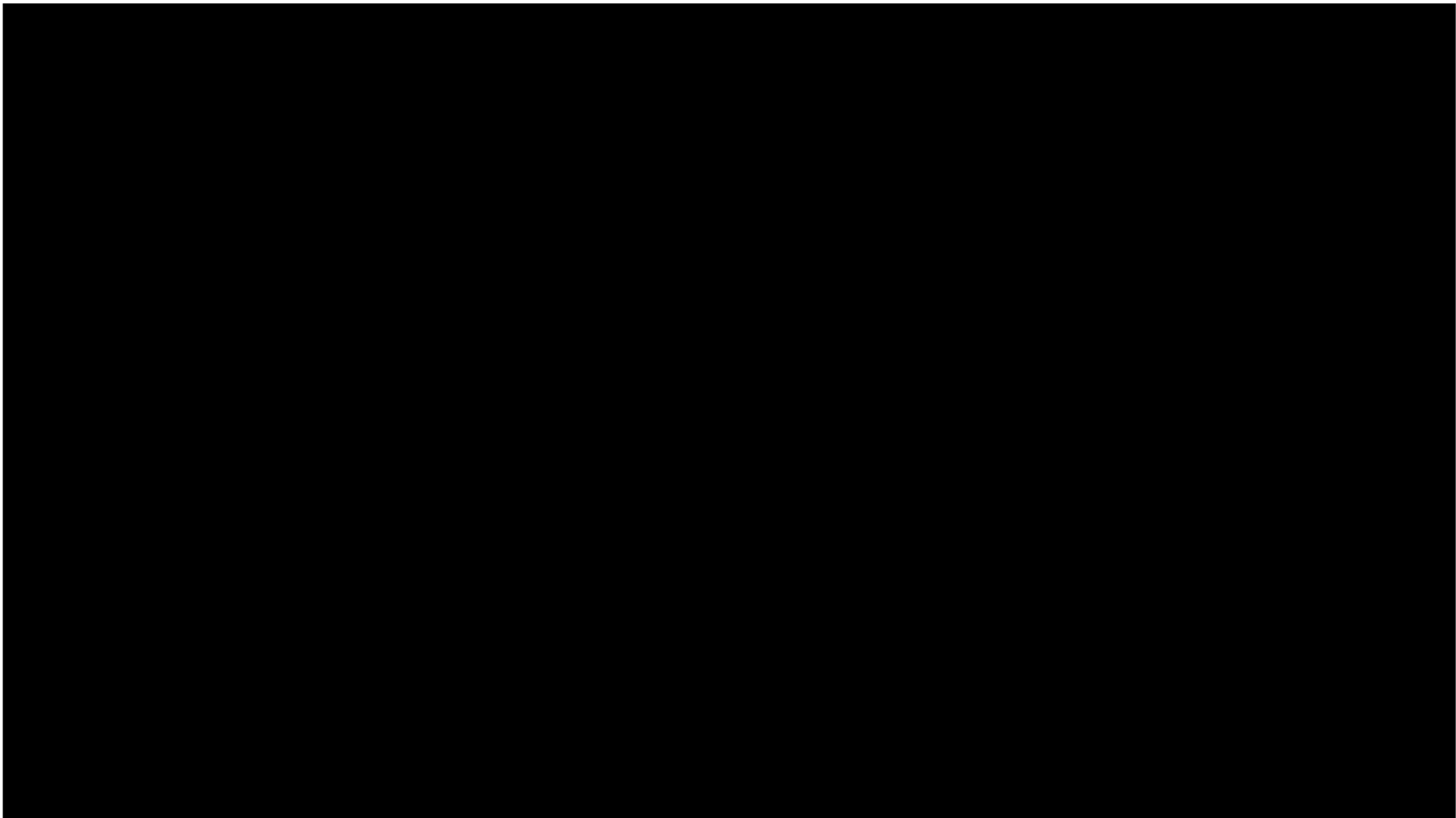


Figure 4.18. SEC-RI from PAR study of **ML400-P**.

Table 4.9. Quantitative results from the PAR study of **ML400-P**.

Trial Number	CPP	Results			Deviation		
		Mw by SEC (kDa)	PDI	DP by Mw	Mw by SEC (kDa)	PDI	DP by Mw
1							
2							
3							
4							
5							
6							
7							
8							
9							
10							

Table 4.10. Summary of PAR study and CPPs identified to control the CQA in the manufacturing process for **HL50** and **ML400** PLys materials.

CPP	PAR for HL50	PAR for ML400

Table 4.10 summarizes the PAR results that allowed us to identify the CPPs of both PLys materials.

Upon concluding the studies into the polymerization step, we next looked into the deprotection reaction. Here, based on our *know-how*, relatively few studies were performed compared with polymerization process. The hydrolyzed PLysHBr was analyzed by SEC-RI-MALS and NMR to see that the tested conditions do not affect the integrity of the final product compared with control (see Figure 4.19 and Table 4.11).

Table 4.11. Quantitative results for **ML400**.

Deprotection Condition Number	Deprotection Condition	Mw by SEC (kDa)	PDI	DP by Mw
Control				
1				
2				
3				

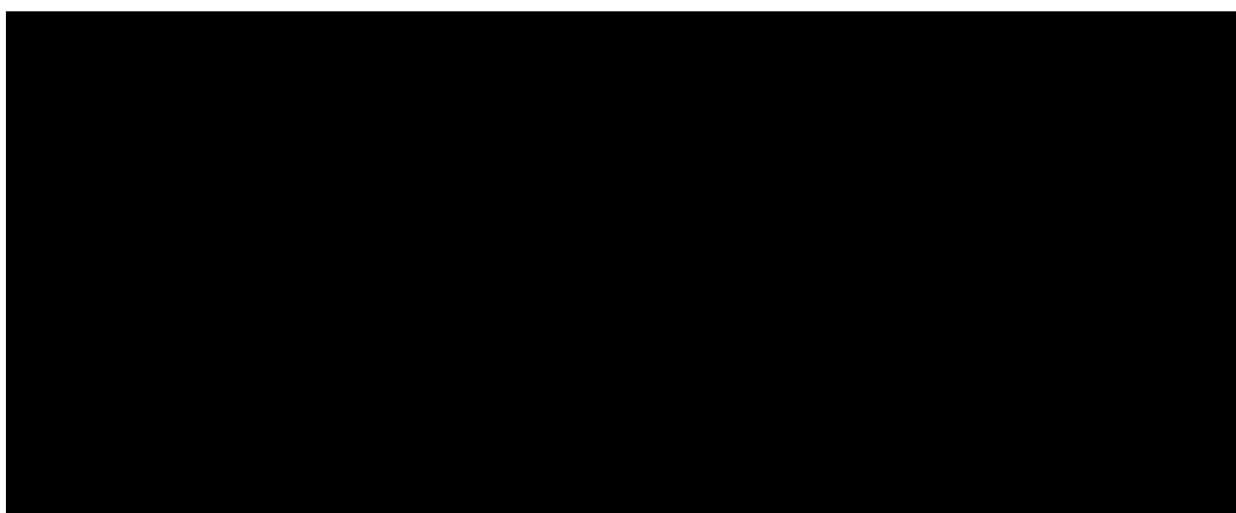
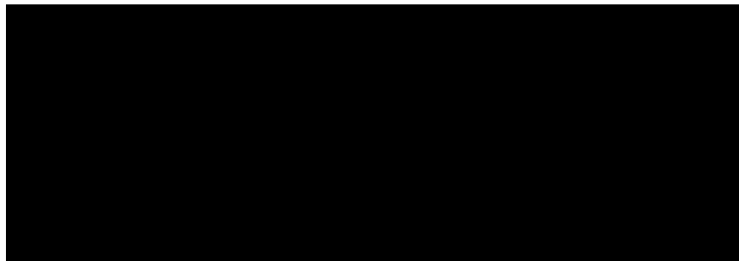


Figure 4.19. (A) SEC- of **ML400**. (B) ¹H NMR of **ML400**.

The deprotection PAR study results shown in Table 4.11 indicated that an increase

in PLysTFA concentration and a decrease in the equivalents of deprotector reagent were both perfectly suitable changes in terms of Mw and DP, given that no drastic changes in Mw distributions or retention time were observed. Neither secondary peaks nor deformation in the main peak appeared in the SEC chromatogram. Finally, the selected conditions to address the CPPs in the deprotection step through basic hydrolysis were:



This allows us to define a design space for operations in the deprotection process and to establish an IPC by NMR at the end of the reaction to check if the TFA hydrolysis has been carried out successfully. Yields for polymerization and deprotection reactions at this stage were not determined.

PILOT BATCHES AND PURIFICATION

Verification of Process Performance

Once the PAR of CPPs defining the CQAs are identified and established at small scale, we can move to the next step of scaling up to the Pilot Batches. These tests were first carried out at 100 grams of NCA scale for each duplicate in the R&D environment. Then, a scale-up in Pilot Unit Clean Room set-up was performed.

The PLys materials obtained in the Pilot Unit Clean Room set-up can be employed in pre-clinical trials to perform GLP TOX studies in animals. To address this, we ensure that the manufacturing process follows the ICH Q11 harmonized guideline “*Development and Manufacture of Drug Substances (Chemical Entities and Biotechnological/Biological Entities)*” to obtain the alpha poly-L-lysine materials as a high quality drug substance.

At this stage the purification process was defined and optimized. The ratio of solvents to precipitation, the number of washes and their volume, the type of drying and drying times, the elimination of impurities, as well as subproducts determination, were all identified and optimized.

Concerning polymerization parameters, as stated previously, for **HL50**, a few problems with the ratio between initiator and NCA were found. Based on the POC and kinetics results, the monomer concentration was fixed and the target DP was adjusted to DP1 in the first 100g batch. Results shown in Table 4.12 indicate that DP values by SEC and NMR are similar to the target. To finish the DP adjustment, in the second Pilot Batch, the target DP was readjusted to DP2 and a good correlation of DP by SEC and NMR was finally obtained. The Pilot Batch results can be observed in Table 4.12 and Figure 4.20.

For polymerization of **ML400**, we decide to stress the target DP to DP1 and DP2 at this scale to establish a comfortable range of operation. Results are very near to the target units by SEC and NMR, they can be observed in Table 4.13 and Figure 4.21.

After 100g batches, we executed the optimization in the Pilot Unit - Clean Rooms at a scale of 1 – 2 Kg of NCA. For both poly-L-lysines, we found good results compared with the 100g batches. For **HL50**, fixing the target DP to DP2 we obtained Mw distributions by SEC-RI-MALS achieving the target units of lysines. Moreover, the increase to double the NCA amount also gives good results in terms of Mw distributions, allowing us to confirm that the manufacturing process is reproducible and scalable. Regarding **ML400**, the values of Mw distributions by SEC-RI-MALS and ratio between MePEG₄ and lysines obtained by NMR are very similar to the theoretical goal for both protected and deprotected materials. The reaction yields for polymerization steps were over 90 %, and for deprotection steps about 80 – 85 %.

A very important fact is that in Figure 20 (A), the SEC elugram for **HL50-P** in DMF shows important differences between retention volume for the POC and R&D Pilot Batches (POC, B02 and B03) compared with the Pilot Batches of the Pilot Unit (B04, B05, C01 and C02). This effect is due to the time analysis between batches. SEC columns show wear associated with time and use, and it is easy to find slight deviations in the retention time with the time for the same sample.

Fortunately, with our approach to calculating Mw distributions of PAA employing RI and MALS giving the absolute Mw, retention time does not have an impact on the Mw. This can be corroborated with the values shown in Table 4.12 which are in good agreement, despite finding important variations in the retention volume. Furthermore, in Figure 4.33 within the Supporting Information, we can see how the Molar Mass Distributions are very similar for all **HL50** batches. These graphic representations are not a function of retention volume and can corroborate the Mw obtained.

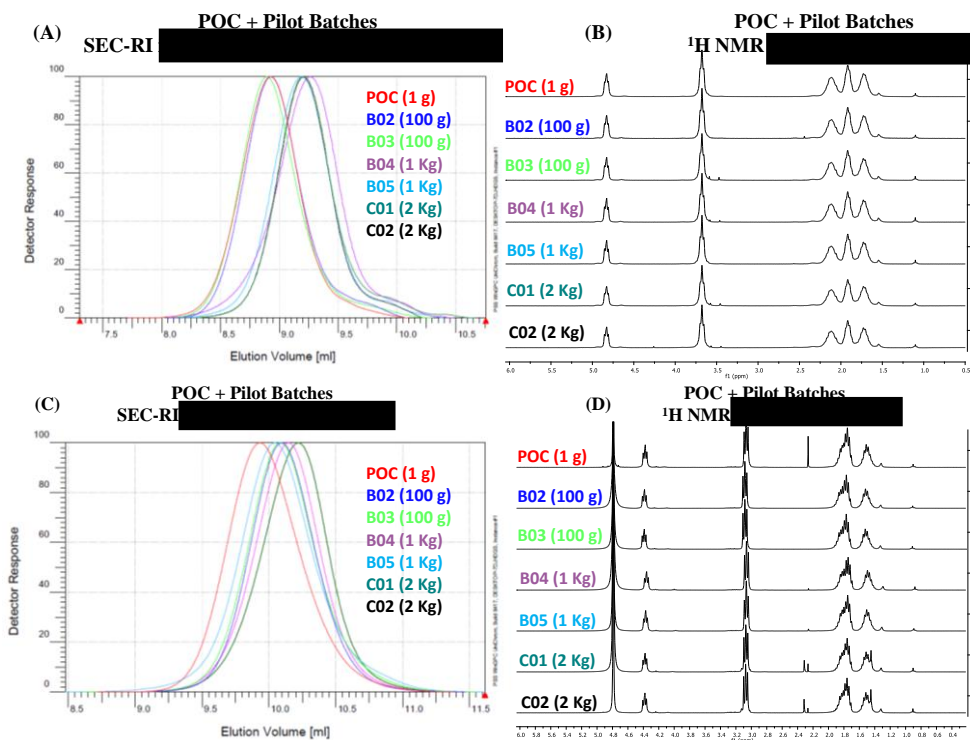


Figure 4.20. HL50-P characterization for POC and Pilot Batches. (A) Overlay SEC-RI. (B) Overlay ¹H NMR. HL50 characterization for POC and Pilot Batches. (C) Overlay SEC-RI. (D) Overlay ¹H NMR.

Table 4.12. Results for **HL50** in Pilot Batches.

Batch	Target	Protected HL50-P	Deprotected HL50
POC			
B02			
B03			
B04			
B05			
C01			
C02			

Table 4.13. Results for **ML400** in Pilot Batches

Batch	Target	Protected ML400-P	Deprotected ML400
POC			
C01			
C02			
C03			

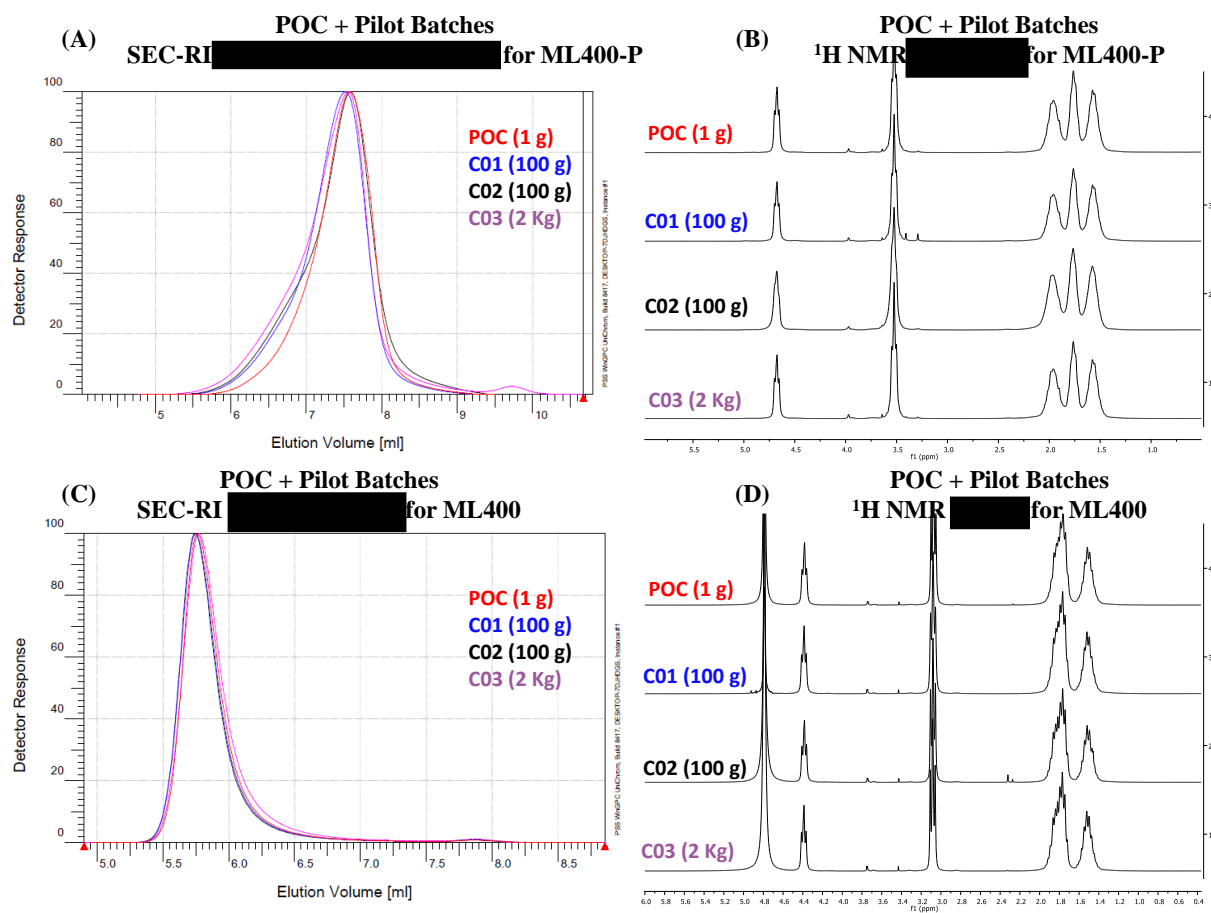


Figure 4.21. ML400-P characterization for POC and Pilot Batches. (A) Overlay SEC-RI. (B) Overlay ¹H NMR. ML400 characterization for POC and Pilot Batches. (C) Overlay SEC-RI. (D) Overlay ¹H NMR.

Table 4.15. Trial data for purification by precipitation of **HL50** Pilot Batch B03.

Step	Work	%

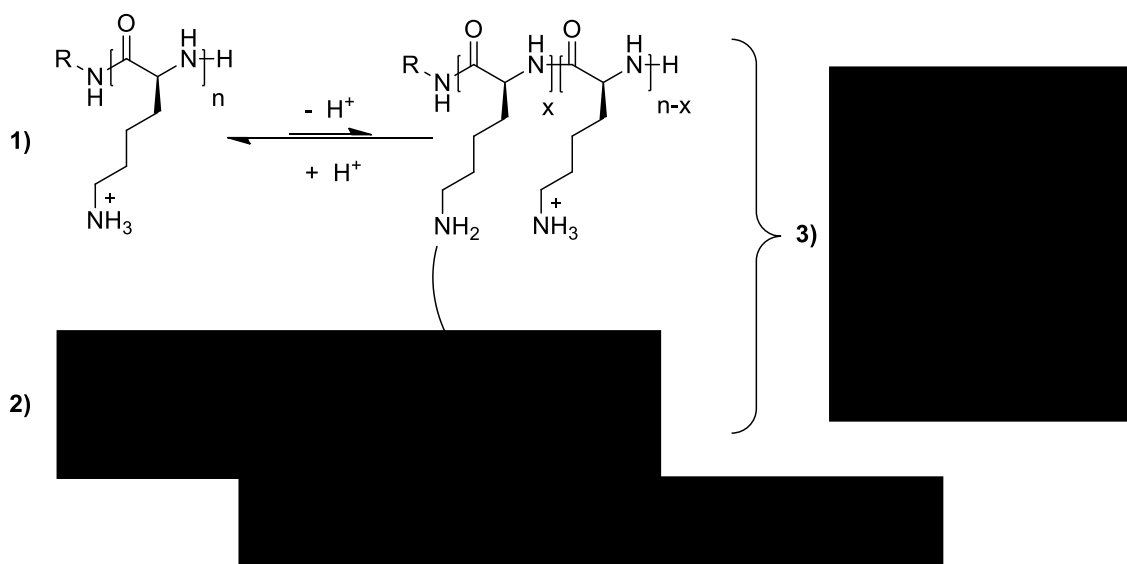
Three more impurities were detected. The manufacturing process were adapted to obtain the impurities levels under the target limits.

IMPURITIES FROM PROCESS

After R&D Pilot Batches optimization, we move to the Pilot Unit – Clean Room set-up to scale-up the process till 1-2 Kg of NCA. Here, some impurities as subproducts were identified and controlled. Again, the process was developed for **HL50**, and then applied to **ML400** finding good results.

SUBPRODUCT 1 formation

We ran the first batch, namely B04, of **HL50** at 1 Kg of L-Lys(TFA)-NCA scale under optimized conditions described previously and, up until the deprotection step, everything worked perfectly. Importantly, the first time after each precipitation, an NMR analysis was carried out to study the process and impurities. Some undesired subproducts were found if the acidification or neutralization was done with a high amount of solvent. See the Scheme 4.3 and the Figure 4.22.



Scheme 4.3. (1) Equilibrium between protonated epsilon amine and free amine. At acidic pH, the free amine population is very low. (2) Solvent activation in acid media and resonant structures. (3) SUBPRODUCT 1 formation.

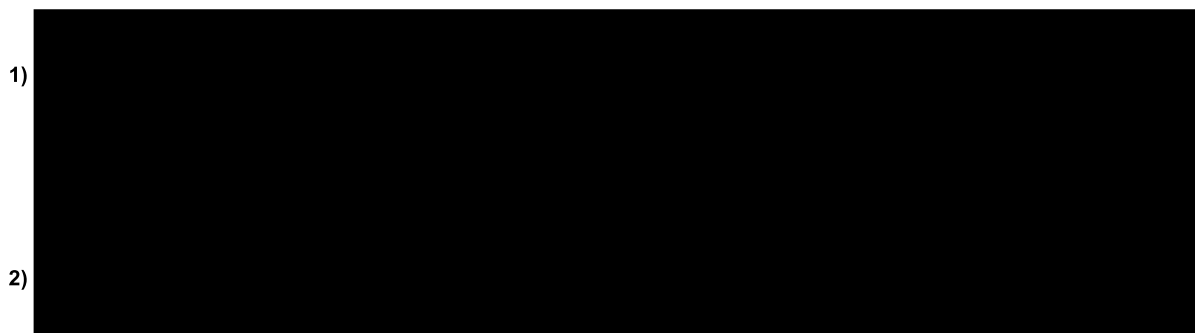
Figure 4.22. Top: ^1H NMR HL50 containing the SUBPRODUCT 1. **Bottom:** ^1H NMR HL50 without SUBPRODUCT 1.

Finally, we determined that if the solvent amount was lower than 5%, the SUBPRODUCT 1 was not formed. Thus, an IPC to control the solvent amount was established.

SUBPRODUCT 2 formation

We found that the solvent level can be a problem in another manufacturing stage

driving the generation of another subproduct called SUBPRODUCT 2. This can be observed in the Scheme 4.4.



Scheme 4.4. (1) SUBPRODUCT 2 formation by mechanism 1 (2) SUBPRODUCT 2 formation by mechanism 1.

We detected and identified the SUBPRODUCT 2 by ^1H NMR as shown in Figure 4.23.

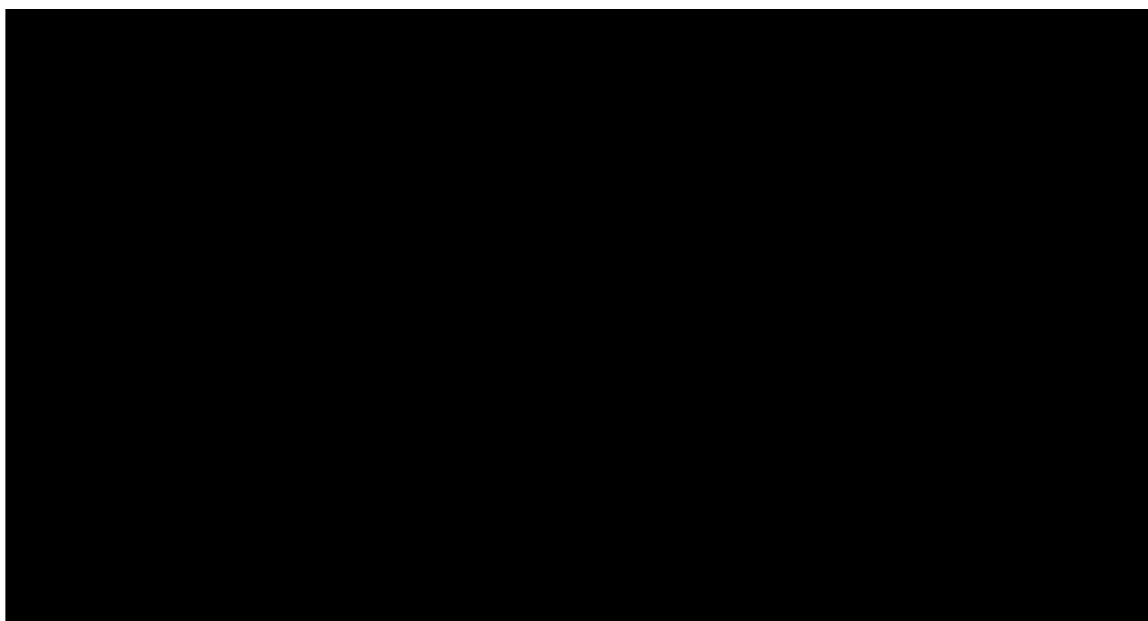


Figure 4.23. ^1H NMR of SUBPRODUCT 2 and **HL50** containing SUBPRODUCT 2.

When we compared the NMR of PLys samples with the NMR of pure SUBPRODUCT 2, we can see a slight chemical displacement in the signals. This could be explained by some kind of interaction between the SUBPRODUCT 2 and PLys epsilon amines. We performed extensive trials to remove the SUBPRODUCT 2 (see Figure 4.24 and 4.25 and Table 4.16), but the only one that worked was the elimination by rotatory evaporation in presence of water. Even so, purification was not easy, and large quantities of water were required to purify just a few milligrams of PLys. Considering large scale synthesis, we would need an industrial rotatory evaporator and this equipment is very expensive and sophisticated. To be sure that the solvent amount complies with the established limit in the final product, we fixed an IPC here to quantify the solvent content by GC-FID, with a limit of $\leq 1\%$.

Given the problems related to this solvent, scientific grounds give us reason to think that the best option could be to remove this solvent and find another solvent to perform the purification. However, there are not many solvents that are both miscible with water and in which the PLys is insoluble. Acetonitrile was considered as an option but was quickly discarded due to its high toxicity [27]. Finally, we decided to maintain the controlled drying process of the PLys materials from the solvent before moving on to the next step in the manufacturing process.

Once drying times were established and solvent subproducts were under control, we ran 4 batches in total for **HL50** and 1 batch for **ML400** at this scale under clean rooms Pilot Unit, taking into account all parameters established throughout the manufacturing process development.

Bioburden and endotoxin impurities

Biological parameters were studied when the PLys materials were intended for use in pre-clinical or clinical trials. This applies to the batches manufactured in the clean rooms Pilot Unit set-up, as well as in GMP. The bioburden and endotoxin impurities can be controlled easily taking the following measures:

- The manufacturing room has a controlled environment with HEPA filters, positive pressure and controlled access.
- Filtration of the product (filtration by 0.22 μm) was carried out as a production stage.
- All the water that makes contact with the product was from the same water production equipment and the endotoxin content has been analyzed (result < 0.0050 EU/mL).
- The containers used for the different manufacturing stages that have been in contact with the product were either of single-use, non-pyrogenic, or previously disinfected.
- A measure to mitigate the risk of contamination in the future cGMP product is to clean all equipment that comes into contact with the product that cannot be of single-use and non-pyrogenic.

Summarizing, the POC results allowed us to define the synthetic route and define the two main steps: polymerization and deprotection. The polymerization times were established through kinetic studies. In the PAR study of the polymerization, CPPs such as the initiator addition, time of NCA in solution, NCA concentration, impurities in NCA, temperature and the stirring speed were defined. Regarding the deprotection PAR study, the protected precursor concentration in solvent, the ratio solvent/water, time, temperature, deprotector reagent equivalents and the rpm for stirring were identified as CPPs, and their acceptable work range was defined. After that, the manufacturing process was studied increasing the NCA scale in the Pilot Batches. Here, we studied and optimized the purification methodology to define the impurities profile and their limits. Also, the solvents ratios and the manufacturing steps were fully defined, as well as the drying times. In order to reach total control over these CPPs, the analytical methodologies were developed to establish the IPCs securing the process performance. Thus, we drew the design space to operate comfortably while ensuring that all the CQAs are within the target limits.

2.2. DESIGN SPACE & CONTROL STRATEGY

The optimization of the design space for the manufacturing process was described in the previous section; the POC, kinetic and PAR studies, as well as the Pilot Batches, granted us the knowledge to identify the CPPs and the impurities profile. According to ICH guidelines, we defined and established the IPCs necessary to control all the parameters securing the CQAs within target limits. The optimized work-flow containing the IPCs can be seen below, along with a table for the defined IPCs, and the CQAs for the CoA including the limits for both PLys materials. Analytical methodologies were developed in parallel and they can be found in section 2.3. ANALYTICAL METHODS DEVELOPMENT. Furthermore, a Risk Analysis for polymerization and deprotection steps were performed for **ML400**. The Risk Analysis information is in M&M section.

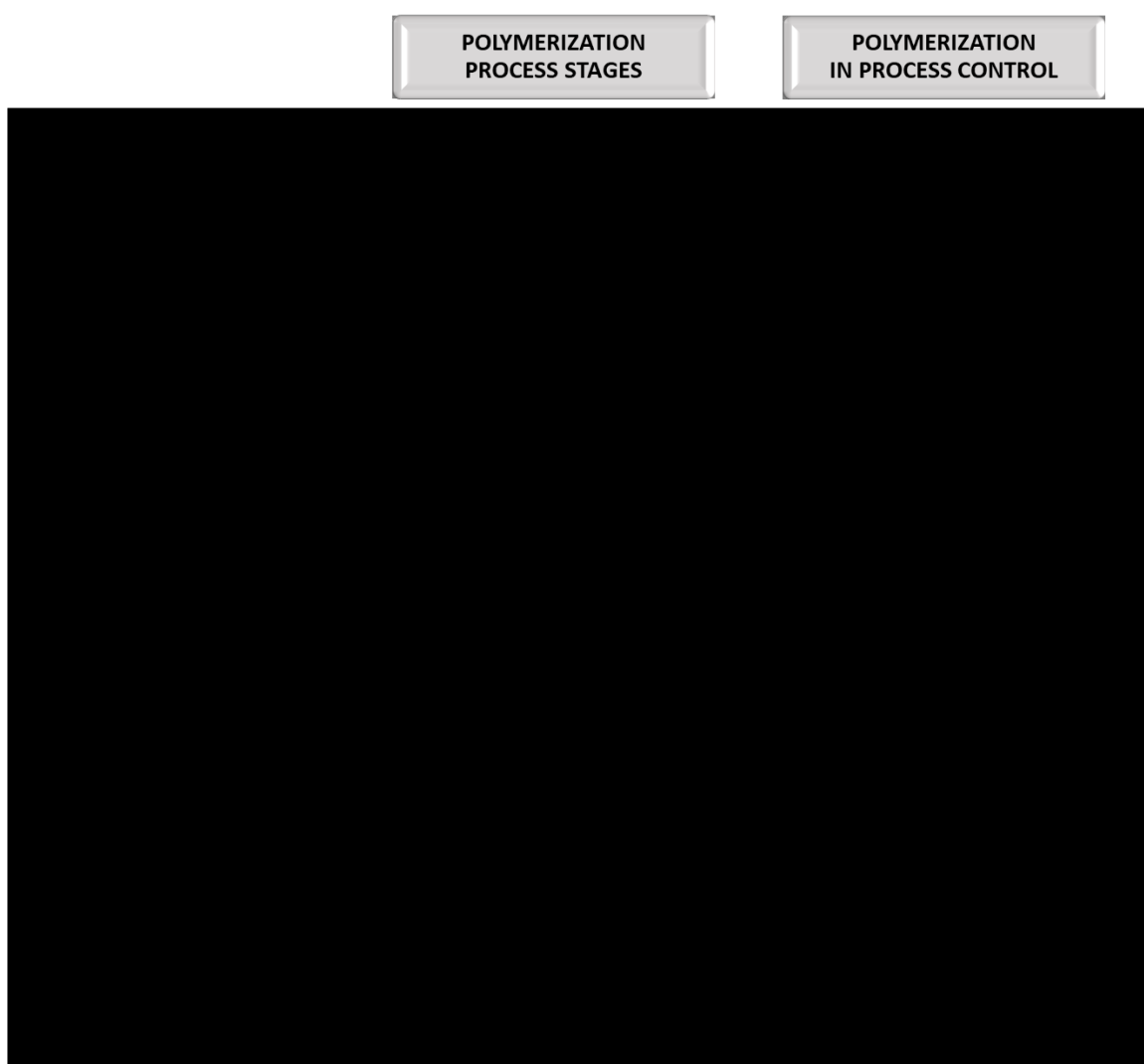


Figure 4.25. Optimized work-flow diagram for polymerization step including the IPCs.

DEPROTECTION
PROCESS STAGES

DEPROTECTION
IN PROCESS CONTROL

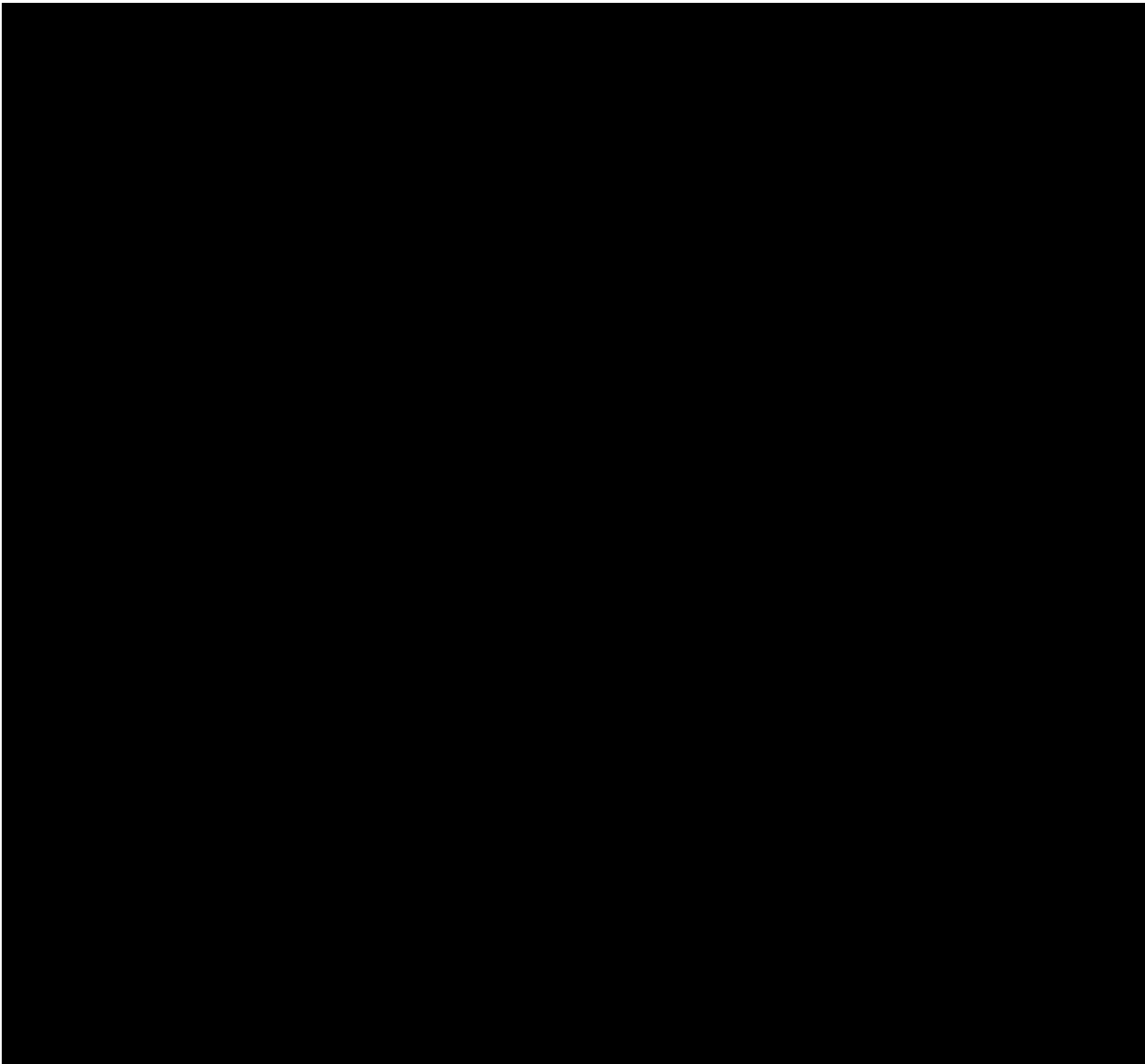


Figure 4.26. Optimized work-flow diagram for deprotection step including the IPCs.

Table 4.17. Summary of IPCs, the techniques used, their limits, the consequences in case that they exceed the limits and the corresponding action to mitigate the out of limit for each step of the manufacturing process and the attribute analyzed for any case.

Stage	IPC technique	Attribute	Limit	Consequence if it exceeds the limit	Action
[Redacted content]					

Table 4.18. Preliminary Limits for CQA in poly-L-lysines final product.

Attribute	Limits for HP50	Limits for MP400
[Redacted content]		

2.3. ANALYTICAL METHODS DEVELOPMENT

All this section has been removed (censored) in order to protect the know-how of the company.

2.4. PROCESS PERFORMANCE: GMP COMPLIANCE AND DATA SUMMARY

Due to customer necessities and the time available to write this thesis dissertation, at the time of writing only **ML400** has moved to GMP compliance.

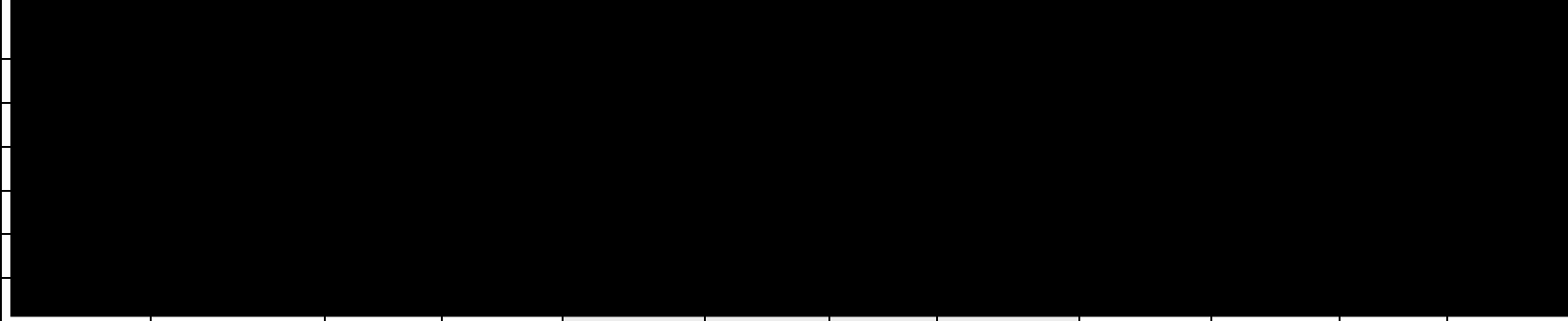
All GMP parameters were managed following and adapting the ICH Q7 harmonized guideline “*Good Manufacturing Practice Guide for Active Pharmaceutical Ingredients*” to alpha poly-L-lysines materials. These include: (i) quality management, (ii) personnel, (iii) building and facilities, (iv) process equipment, (v) documentation and records, (vi) materials management, (vii) production and IPCs, (viii) packaging and identification labelling of products, (ix) storage and distributions, (x) laboratory control, (xi) validation, (xii) change controls, (xiii) rejection and re-use of materials, (xiv) complaints and recalls, (xv) contract manufacturers (including laboratories), and (xvi) agents, brokers, traders, distributors, re-packers and re-labellers [28].

Moreover, the lifecycle of the product was carefully designed, redacted, established and approved, keeping in mind the complete traceability of the final product released. In the lifecycle of the product, the departments involved were: (i) Production, (ii) Quality Control, (iii) Quality Assurance, and also the (iv) Qualified Person, who is the member of the team ultimately responsible for the manufacturing, control, and maintenance of the product according to the established quality standards.

At the GMP stage, all equipment passed the qualification test before use: (i) Design Qualification (DQ), (ii) Installation Qualification (IQ), (iii) Operation Qualification (OQ) and (iv) Process Qualification (PQ). In this sense, all raw materials suppliers were validated by the Quality Assurance Department by auditing their facilities.

Taking into account all the CPPs defined and the IPCs established in the process optimization, we first executed an engineering batch in the GMP Pilot Plant to test the set-up with the optimized conditions. After that, the GMP batch was executed. Results can be found in the next Table 4.24 and Figure 4.30 compared with the POC and Pilot Batches. Also, a cleaning process for ML400 were developed washing the reactors with water and solvents. After all the data collected, we can build the Table 4.25 and 4.26 showing the CoA summary for both PLys materials.

Table 4.24. Results for **ML400** in GMP Pilot Plant.

Batch	Target	Protected ML400-P	Deprotected ML400
POC			
C01			
C02			
C03			
D01			
D04			

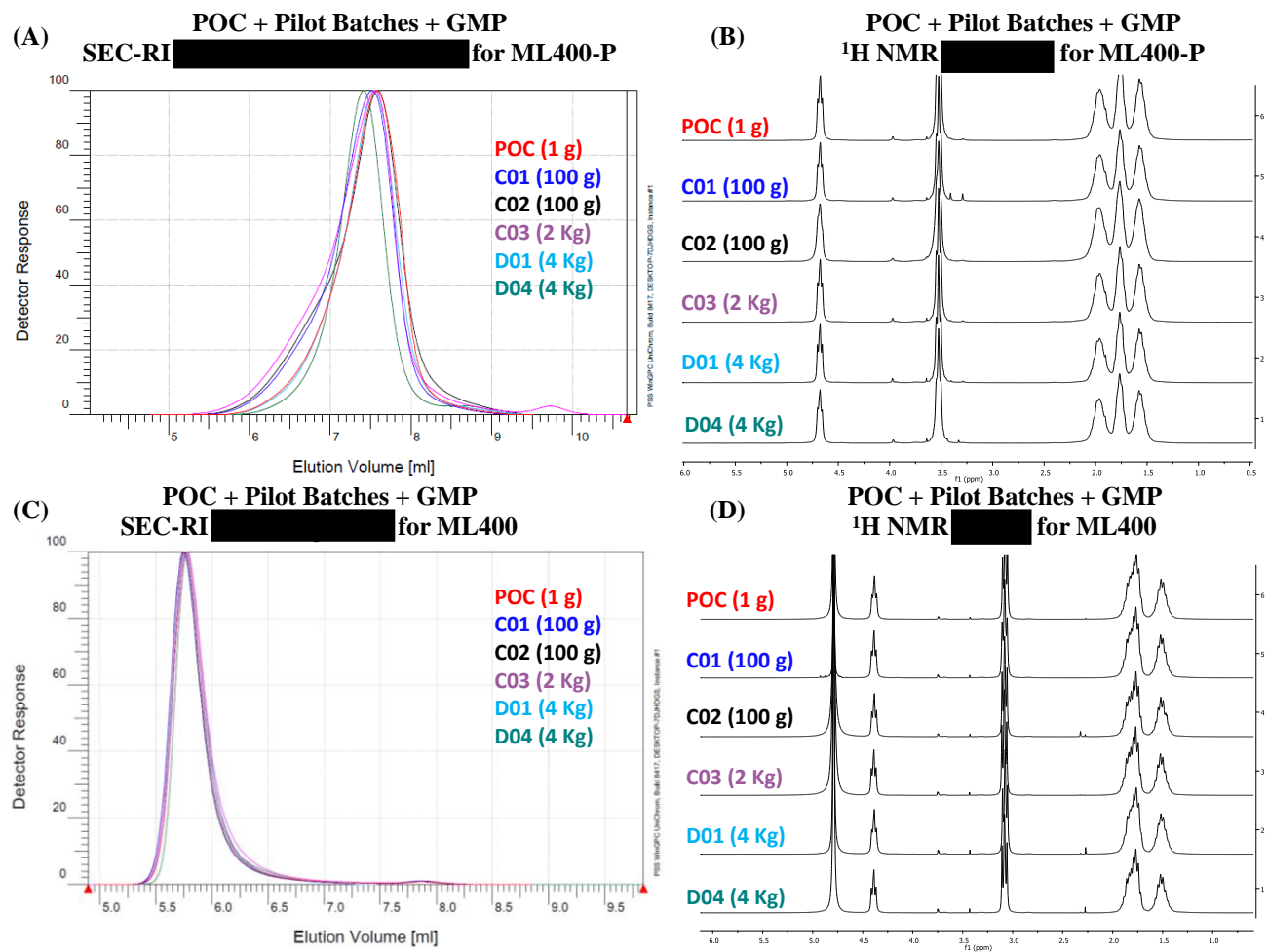


Figure 4.30. ML400-P characterization for POC, Pilot Batches and GMP. (1) Overlay SEC-RI. (2) Overlay ¹H NMR. ML400 characterization for POC, Pilot Batches and GMP. (3) Overlay SEC-RI. (4) Overlay ¹H NMR.

Table 4.25. CoA summaries for **HL50**.

Attribute	Limits	Results						
Batch (NCA scale) [Stage]	-	POC (1g) [POC]	B02 (100g) [Pilot Batch 1]	B03 (100g) [Pilot Batch 2]	B04 (1Kg) [Pilot Batch 3]	B05 (1Kg) [Pilot Batch 4]	C01 (2Kg) [Pilot Batch 5]	C02 (2Kg) [Pilot Batch 6]

Attribute	Limits	Results						
Batch (NCA scale) [Stage]	-	POC (1g) [POC]	B02 (100g) [Pilot Batch 1]	B03 (100g) [Pilot Batch 2]	B04 (1Kg) [Pilot Batch 3]	B05 (1Kg) [Pilot Batch 4]	C01 (2Kg) [Pilot Batch 5]	C02 (2Kg) [Pilot Batch 6]

Table 4.26. CoA summaries for **ML400**.

Attribute	Limits	Results					
Batch (NCA scale) [Stage]	-	POC (1g) [POC]	C01 (100g) [Pilot Batch 1]	C02 (100g) [Pilot Batch 2]	C03 (2Kg) [Pilot Batch 3]	D01 (4Kg) [Engen. Batch GMP]	D04 (4Kg) [GMP]

Attribute	Limits	Results					
Batch (NCA scale) [Stage]	-	POC (1g) [POC]	C01 (100g) [Pilot Batch 1]	C02 (100g) [Pilot Batch 2]	C03 (2Kg) [Pilot Batch 3]	D01 (4Kg) [Engen. Batch GMP]	D04 (4Kg) [GMP]

Based on the number of batches carried out at large scale (Pilot Unit and GMP) together with small-scale productions (POC, PAR, kinetics and Pilot Batches), the next graphics summarize the manufacturing process developed.

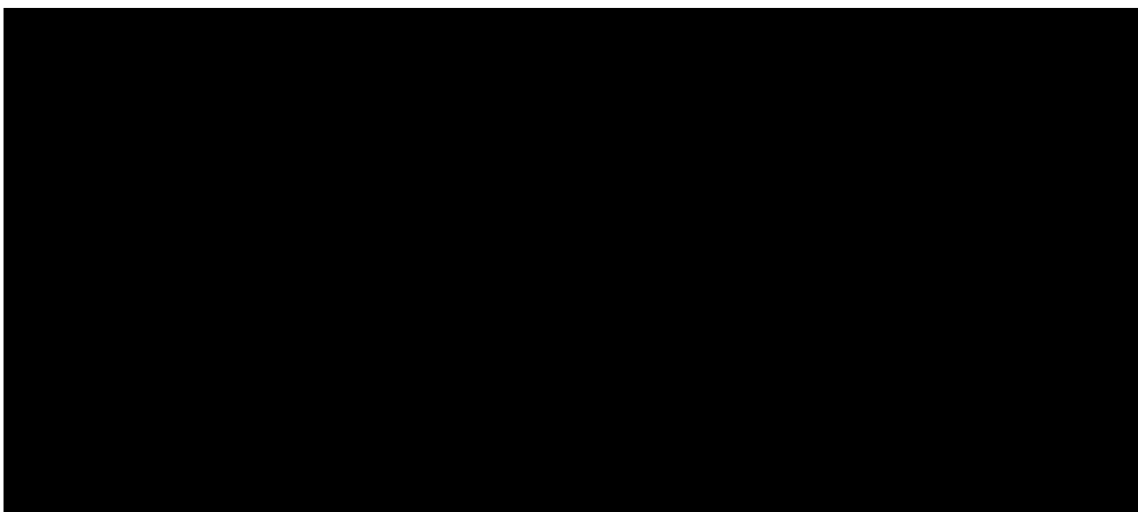


Figure 4.31. Statistic DP data for **HL50**.

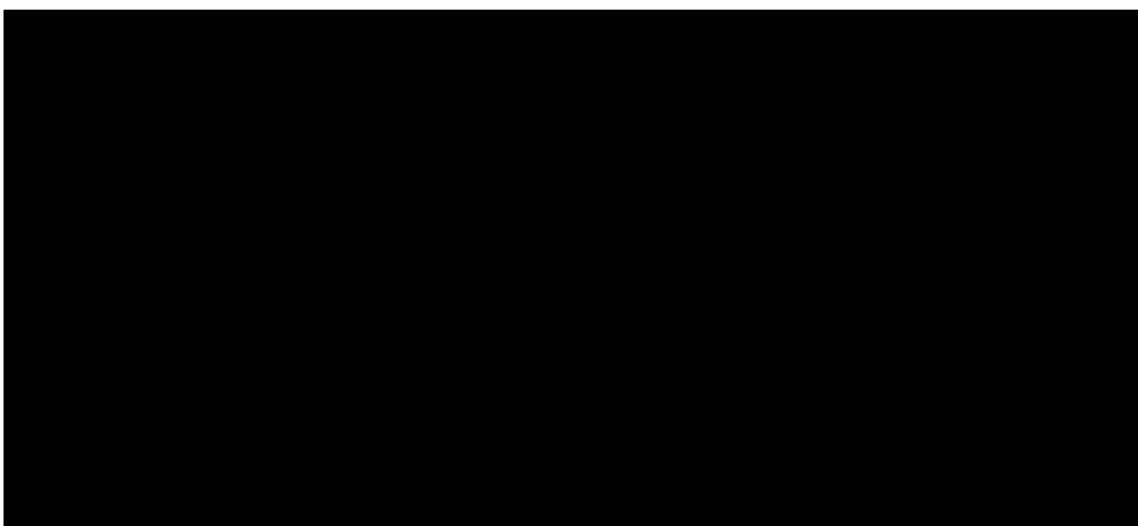


Figure 4.32. Statistic DP data for **ML400**.

The results summarized in Figures 4.31 and 4.32 show that it was necessary to fix the target DP at DP2 to obtain the requested DP. This can be appreciated in the higher deviations found in the POC and kinetics stages. For the Pilot Unit stage for two scales of NCA (1 and 2 Kg), statistic results show high reproducibility and robustness of the manufacturing process developed, resulting in very low deviations in the four techniques employed in protected PLysTFA form and for the final product in hydrobromide salt form.

Contrary to **HL50**, results show how for **ML400**, the target DP was set to the same as the theoretical DP, and the results were close to this value in all cases. This can be attributed to the high quality of NCA employed for the synthesis of large Mw poly-L-lysines. Statistic results show how the manufacturing process developed is reproducible and consistent batch to batch until 4 Kg of NCA.

Based on the results obtained and reported here at different scales, PAR studies, and having identified all CPPs and the necessary IPCs established to guarantee the reproducibility and high quality of our products maintaining the CQA within the specifications, we can say that, manufacturing process currently developed for **HL50** and **ML400** PLys materials is ROBUST, REPRODUCIBLE and SCALABLE. SOPs development and product lifecycle were always under the Quality Assurance Department to guarantee the high quality of poly-L-lysines materials. Besides, we can confirm that these products comply with the quality and the dossier documentation as well as the information package described in the ICH Q11 harmonized guideline “*Development and Manufacture of Drug Substances (Chemical Entities And Biotechnological/Biological Entities)*” to give them the same quality level established for drug substances.

2.5. ICH FORMAL STABILITY

An important aspect in the CMC development is the stability of the final product. To check that the properties and attributes of our poly-L-lysines remain unchanged with time, we performed stability studies adapting the conditions described in the ICH Q1A(R2) “*Stability Testing of New Drug Substances and Products*” guideline. The CQA analyzed to study the stability of both PLys materials were the aspect, the color, the water solubility, the purity, the Mw distributions, the degradation products (initiator and lysine), the water content and the enantiomeric excess. Results are presented below, and as can be observed, our PLys materials are stable up to 36 months at -20°C and maintain the CQAs within target limits. For **ML400** GMP batch D04, we are currently running an official ICH stability study. In order to simplify the data, only the results at 40°C are shown since this is the harshest storage condition. **ML400** is completely stable at 40°C during 6 months.

Table 4.27. Stability studies for **HL50** batch B04, first clean room Pilot Batch.

Batch B04 HL50									
Storage conditions = 1 month 40°C; then at -20°C with shipping closure									
Attribute	Limits	t=0	t=3 months	t=6 months	t=9 months	t=12 months	t=18 months	t=24 months**	t=36 months**

Table 4.28. Stability studies for **ML400** batch D04, first GMP clinical batch.

Batch D04 ML400					
Storage conditions = 40°C with shipping closure					
Attribute	Limits	t=0	t=1 month	t=3 months	t=6 months
[Redacted]					

2.6. SUBMISSION OF CMC PACKAGE

As mentioned previously, the documental CMC package for drug substances is part of the CTD to generate the Investigational New Drug (IND) documentation. These documents are required for the health authorities to commence clinical trials in humans. Defining the goal to generate PAA-based materials that can be employed in clinical trials, all the work within this chapter was executed successfully. The scientific knowledge and the technical information about the manufacturing process as well as analytical techniques to secure the quality level of the defined CQAs, allowed us to illustrate this development for PLys materials achieving their production under GMP compliance.

The present work covers the required activities to generate the CMC documentation. To generate the data, the following parameters have all been defined, addressed, controlled and executed successfully: (i) the PLys materials CQAs and their limits, (ii) the control strategy, (iii) the CPPs, (iv) the raw materials, starting materials and suppliers (v) the analytical techniques and IPCs, and (vi) the risk management activities.

The CMC package for our PLys materials, with the level of drug substance, has been used by the drug product manufacturer to complete the full package documentation CTD-IND to test the products in clinical trials in humans after health agencies approval.

3. CONCLUSIONS

Following the ICH Quality guidelines, it is completely possible to manufacture PAA under drug substance quality grade. Herein, we have developed and optimized the production for two examples of PLys (**HL50** and **ML400**) achieving a robust, reproducible and scalable manufacturing process. Moreover, the analytical techniques to perform a proper physico-chemical characterization have been established and developed to secure that the CQAs are within the target quality range.

According to ICH guidelines, in the early stages of R&D (or POC or bench step), the feasibility study was carried out and the CPPs were then identified and stressed by the PAR study to determine a comfortable operating range in the scale-up. Here, the raw materials were also selected, paying special attention to the L-Lys(TFA)-NCA monomer specifications. In this first step, the IPCs for Mw, PDI, DP and deprotection hydrolysis efficiency were introduced. Then, R&D Pilot Batches were launched in duplicate to obtain the first knowledge about the scale-up parameters, concluding that the feeding ratio between initiator and monomer is a very important key parameter. At this stage, the manufacturing process was adapted to remove the impurities.

This allowed us to develop the workflow diagrams and design the workspace, as well as the manufacturing facilities according to the required quality grade. For preclinical studies of PLys materials, we implemented the clean rooms, called the Pilot Unit, and also the GMP facilities to produce the PAA for preclinical studies in humans. At these stages, the analytical

methodologies were also qualified and validated, permitting the construction of a very complete CoA including all the CQA (physical, chemical and biological), and also the impurities profile, as well as related degradation substances.

Within this work, we have developed an excellent CMC knowledge about the manufacturing process and analytical methodologies for PLys materials considering them as drug substances. This work allows our customers to defend properly their products against the health regulatory authorities and subsequently employ them in regulatory pre-clinical and even clinical studies required to improve patient quality of life.

In summary, by employing the ROP of NCAs via NAM we have developed a robust, reproducible and scalable manufacturing process for alpha poly-L-lysines, as well as all the analytical methodologies required to gain PLys as drug substance at quality grade in GMP compliance following the ICH guidelines.

4. MATERIALS & METHODS

Since the present chapter is a complete guide of the development of the manufacturing process for **HL50** and **ML400** materials, the section of Materials and Methods will be very short to avoid duplication with the above-reported data in the Results and Discussion section.

4.1. MATERIALS

All raw materials are fully described in the section of 2.1.4. SELECTION OF RAW MATERIALS within Results and Discussion.

4.2. METHODS

4.2.1. SYNTHETIC METHODS

All this section has been removed (censored) in order to protect the know-how of the company.

4.2.2. ANALYTICAL METHODS

All analytical methods and physico-chemical characterization techniques are fully described in the section of 2.3. ANALYTICAL METHODS DEVELOPMENT within Results and Discussion.

5. SUPPORTING INFORMATION

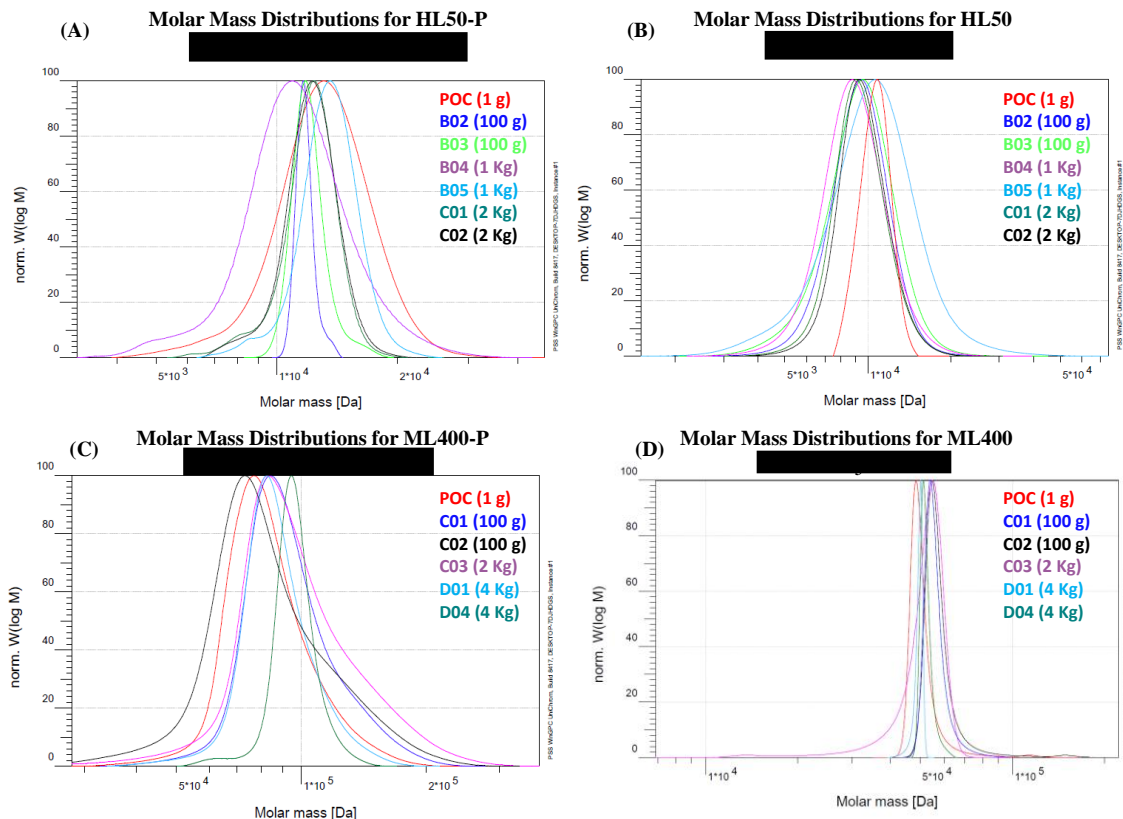


Figure 4.33. Molar Mass Distributions obtained by SEC.

6. REFERENCES

- [1] S. Shima, H. Sakai, POLYLYSINE PRODUCED BY STREPTOMYCES, *Agricultural and Biological Chemistry* 41(9) (1977) 1807-1809.
- [2] S.C. Shukla, A. Singh, A.K. Pandey, A. Mishra, Review on production and medical applications of epsilon-polylysine, *Biochemical Engineering Journal* 65 (2012) 70-81.
- [3] I.L. Shih, Y.T. Van, M.H. Shen, Biomedical applications of chemically and microbiologically synthesized poly(glutamic acid) and poly(lysine), *Mini-Reviews in Medicinal Chemistry* 4(2) (2004) 179-188.
- [4] T. Yoshida, T. Nagasawa, epsilon-Poly-L-lysine: microbial production, biodegradation and application potential, *Applied Microbiology and Biotechnology* 62(1) (2003) 21-26.
- [5] K. Kim, K. Ryu, Y.S. Choi, Y.-Y. Cho, J.Y. Lee, H.S. Lee, H.C. Kang, Effects of the Physicochemical, Colloidal, and Biological Characteristics of Different Polymer Structures between alpha-Poly(L-lysine) and epsilon-Poly(L-lysine) on Polymeric Gene Delivery, *Biomacromolecules* 19(7) (2018) 2483-2495.
- [6] E. Katchalski, I. Grossfeld, M. Frankel, POLY-CONDENSATION OF ALPHA-AMINO ACID DERIVATIVES .3. POLY-LYSINE, *Journal of the American Chemical Society* 70(6) (1948) 2094-2101.
- [7] G.S. Kwon, K. Kataoka, Block copolymer micelles as long-circulating drug vehicles, *Advanced Drug Delivery Reviews* 64 (2012) 237-245.
- [8] M.D. Brown, A. Schatzlein, A. Brownlie, V. Jack, W. Wang, L. Tetley, A.I. Gray, I.F. Uchegbu, Preliminary characterization of novel amino acid based polymeric vesicles as gene and drug delivery agents, *Bioconjugate Chemistry* 11(6) (2000) 880-891.

- [9] R. Herrendorff, P. Hanggi, H. Pfister, F. Yang, D. Demeestere, F. Hunziker, S. Frey, N. Schaeren-Wiemers, A.J. Steck, B. Ernst, Selective in vivo removal of pathogenic anti-MAG autoantibodies, an antigen-specific treatment option for anti-MAG neuropathy, *Proceedings of the National Academy of Sciences of the United States of America* 114(18) (2017) E3689-E3698.
- [10] K.M. Takeda, Y. Yamasaki, A. Dirisala, S. Ikeda, T.A. Tockary, K. Toh, K. Osada, K. Kataoka, Effect of shear stress on structure and function of polyplex micelles from poly(ethylene glycol)-poly(L-lysine) block copolymers as systemic gene delivery carrier, *Biomaterials* 126 (2017) 31-38.
- [11] Y.T. Sun, T.J. Deming, Self-Healing Multiblock Copolypeptide Hydrogels via Polyion Complexation, *Acs Macro Letters* 8(5) (2019) 553-557.
- [12] Y.T. Sun, A.L. Wollenberg, T.M. O'Shea, Y.X. Cui, Z.H. Zhou, M.V. Sofroniew, T.J. Deming, Conformation-Directed Formation of Self-Healing Diblock Copolypeptide Hydrogels via Polyion Complexation, *Journal of the American Chemical Society* 139(42) (2017) 15114-15121.
- [13] S.X. Lv, W.T. Song, Z.H. Tang, M.Q. Li, H.Y. Yu, H. Hong, X.S. Chen, Charge-Conversional PEG-Polypeptide Polyionic Complex Nanoparticles from Simple Blending of a Pair of Oppositely Charged Block Copolymers as an Intelligent Vehicle for Efficient Antitumor Drug Delivery, *Molecular Pharmaceutics* 11(5) (2014) 1562-1574.
- [14] M.P. Bevilacqua, D.J. Huang, B.D. Wall, S.J. Lane, C.K. Edwards, J.A. Hanson, D. Benitez, J.S. Solomkin, T.J. Deming, Amino Acid Block Copolymers with Broad Antimicrobial Activity and Barrier Properties, *Macromolecular Bioscience* 17(10) (2017) 9.
- [15] D. Huesmann, A. Sevenich, B. Weber, M. Barz, A head-to-head comparison of poly(sarcosine) and poly(ethylene glycol) in peptidic, amphiphilic block copolymers, *Polymer* 67 (2015) 240-248.
- [16] A. Birke, J. Ling, M. Barz, Polysarcosine-containing copolymers: Synthesis, characterization, self-assembly, and applications, *Progress in Polymer Science* 81 (2018) 163-208.
- [17] Y. Ohya, S. Takeda, Y. Shibata, T. Ouchi, A. Kano, T. Iwata, S. Mochizuki, Y. Taniwaki, A. Maruyama, Evaluation of polyanion-coated biodegradable polymeric micelles as drug delivery vehicles, *Journal of Controlled Release* 155(1) (2011) 104-110.
- [18] https://starpharma.com/drug_delivery.
- [19] T. Melnyk, S. Dordevic, I. Conejos-Sanchez, M.J. Vicent, Therapeutic potential of polypeptide-based conjugates: Rational design and analytical tools that can boost clinical translation, *Advanced drug delivery reviews* 160 (2020) 136-169.
- [20] A.R. Mazo, S. Allison-Logan, F. Karimi, N.J.A. Chan, W.L. Qiu, W. Duan, N.M. O'Brien-Simpson, G.G. Qiao, Ring opening polymerization of alpha-amino acids: advances in synthesis, architecture and applications of polypeptides and their hybrids, *Chemical Society Reviews* 49(14) (2020) 4737-4834.
- [21] <https://starpharma.com/vivagel>.
- [22] ICH Q11 Development And Manufacture Of Drug Substances (Chemical Entities And Biotechnological/Biological Entities).
- [23] <https://www.fda.gov/about-fda/innovation-fda/what-we-do>.
- [24] M. Glodek, Process Robustness – A PQRI White Paper by PQRI Workgroup Members, in: S. Liebowitz (Ed.) PHARMACEUTICAL ENGINEERING, 2006.
- [25] K.M. de Almeida, M.M. Almeida, F.F. Fingola, H.C. Ferraz, Membrane adsorber for endotoxin removal, *Brazilian Journal of Pharmaceutical Sciences* 52(1) (2016) 171-177.
- [26] I. Conejos-Sanchez, A. Duro-Castano, A. Birke, M. Barz, M.J. Vicent, A controlled and versatile NCA polymerization method for the synthesis of polypeptides, *Polymer Chemistry* 4(11) (2013) 3182-3186.
- [27] M. Greenberg, TOXICOLOGICAL REVIEW OF ACETONITRILE, National Center for Environmental Assessment Office of Research and Development U.S. Environmental Protection Agency Washington, DC, 1999.
- [28] ICH Q7 Good Manufacturing Practice Guide For Active Pharmaceutical Ingredients.

GENERAL DISCUSSION AND FINAL CONCLUSIONS

GENERAL DISCUSSION

Barz et al. stated almost a decade ago that, “*modern life as we know it would be simply impossible without polymers. Natural and synthetic polymers are essential not only in our day-to-day life but have also become increasingly important in biomedical applications*” [1]. Nothing has changed since then, one could even say that polymer impact on society has even exponentially grow, in particular, on biomedical areas where the role of nanomedicine is having a major impact. Poly(Amino Acid)s (PAA)s clearly are a type of polymers with an already demonstrated clinical as well as social benefit [2].

In the past years, PAA-based materials have emerged as candidates to be used as carriers in drug delivery applied on several therapeutic areas [3, 4] such as oncology, gene delivery, and immunotherapy [5, 6]. These materials can also be used against infectious and inflammatory diseases, as diagnostic tools either as predictive biomarkers or as probes for disease monitoring [6]. Surprisingly, for topical administrations and in particular skin applications only a few reports employing PAA-based materials are available [7, 8]. PAA-based materials provide a wide design space using endogenous amino acids that are present in the nature monomers. They can be combined with numerous natural non-poly(amino acid) macromolecules (e.g. HA [9, 10]) or synthetic non-poly(amino acid) macromolecules such as PEG [11], yielding compounds with high functional versatility and other desirable physico-chemical attributes [12]. The high structural versatility, biocompatibility, water-solubility, non-toxicity, and high advances in synthetic techniques make these materials very attractive as drug delivery carriers among other applications [2, 4, 6].

Physico-chemical properties and structural elements implemented during the rational design of the PAA-based materials to be used as drug delivery carriers depend specifically on the final biomedical application, the disease to treat or the administration route, among others [6, 13]. Physico-chemical properties can be modulated in terms of the **manufacturing process** (polymerization techniques, ROP, ATRP, etc.), **size** (small or large), **electrostatic charge** (positive, negative, neutral, or zwitterionic), **conformation** (alpha-helix, beta-sheet, random coil, etc.), **geometry** (sphere, nanotube, etc.), **topology** (linear, star, graft or branched) and **monomer composition** (homo, random, or block). As well as the structural elements such as the **API nature** (hydrophilic or hydrophobic), the **API-carrier interaction** (covalent or non-covalent) and **the supramolecular architecture of the drug delivery system** (micelle, vesicle, polymer-drug conjugate, polyplex, hydrogel, or nanoparticle) [1, 2, 13-15].

Within the current state of the art of PAA-based materials, the vast majority of compounds are in the early stages of R&D and POC [6, 13] with few examples of PAA-based therapeutics in the market or already under clinical evaluation. Unfortunately, as with all advanced therapeutics, it is difficult to achieve the adequate safety:benefit ratio to foster market approval, but not only that, their inherent structural complexity difficults translation as many lack of know-how and consequently, final interest to devote the required resources and risk-taking decisions to successfully reach commercialisation. But what happens when one candidate works? As stated, the process to move a candidate from R&D bench to the market is a long journey. And this path must be performed under GMP regulation. And inside of this GMP regulation, the CMC activities must be applied to support, control, and secure this travel.

CMC activities encompass the development, optimization, and performance of the manufacturing process analytical methodologies, as well as quality management systems, quality grade definition, production, facilities, equipment, laboratory controls, materials, packaging, labeling, and even shipment [16]. Moreover, quality management systems of CMC activities also contain the deviation identification, investigation, and risk management of the manufacturing process as well as the analytical methodologies qualification and validation [16-18].

Within the current framework of this thesis dissertation, the two first chapters have been focused on a work based on R&D activities for PAA-based materials that can be considered inside of the POC stage (or feasibility study or bench stage) before engaging the manufacturing process development. And the final chapter shows two real examples of alpha-poly(L-lysine) for which we performed the CMC process under GMP compliance following the ICH Quality guidelines to achieve the drug substance quality. The optimization and development for (i) manufacturing process, (ii) analytical methodologies, (iii) control strategy, and (iv) submission of results to obtain PAA (concretely alpha-poly-L-lysines) is our main contribution to the current state of the art of the PAA-based materials in the nanomedicine field for drug delivery.

In the first chapter, we focused on the development of the PAA-based materials, concretely in the design and optimization of the production of APAA to drive their self-assembly in micellar structures with different physico-chemical properties [15]. For the hydrophilic block of the amphiphile, we employed the aa according to their electrostatic charge nature using the Glu for anionic charge [19]; Orn for cationic [20]; EG [1, 21, 22] and Sar [23, 24] for neutral; and a random copolymer of Glu and Orn for zwitterionic electrostatic nature. Regarding the hydrophobic segment, we selected the Glu(OBzl) [25] and Phe [13, 26] to generate the alpha-helix secondary structure, and the Val to provide a beta-sheet conformation [27-31].

We carried out this approach adapting the current synthetic methodology of ROP of NCA monomers via NAM widely described in the literature for years [32-35]. We obtained well-defined PAA and APAA in terms of narrow Mw distributions by SEC and good stoichiometry correlation by NMR between the initiator and aa monomer(s). Moreover, hydrolysis techniques to remove the protecting groups to reach the functionalized amino acid were implemented successfully yielding a high percent (> 99 %) of hydrolysis by NMR. All homo and random PAA (18 compounds) were achieved without complications for different DPs for PSar and PGlu, and DP100 for POrn, PArg, and P(Glu-co-Orn)]. For APAA (20 compounds), we found that this technology works better for neutral (PEG, PSar) and anionic (PGlu) PAA than cationic (POrn) or zwitterionic [P(Glu-co-Orn)]. Regarding the secondary structure conformation, APAA containing Glu(OBzl) and Phe showed fewer problems to manufacture than the APAA containing PVal. The poor solubility in common solvents of PVal [30, 31] combined by cationic and zwitterionic hydrophilic segments diffculted their synthesis and proper characterization. Importantly, the secondary structure conformation of the beta-sheet of APAA containing PVal was not confirmed by CD. We design the architectures of these materials based on already published data [27-31].

Other kind of polymeric micelles were also studied bearing a biomolecule as the polymer hydrophobic part yielding the so-called HP-BM micelles. We focused our study on the **TPGS** molecule and in the production of a similar candidate biodegradable and biocompatible employing Sar instead of EG called **TPSS**. **TPGS** is an amphiphilic molecule composed of PEG (hydrophilic) and D-alpha-tocopherol, al called Vitamin E (hydrophobic) and its use is widely described in drug delivery [36]. Many studies are looking at PEG alternatives, being PSar one of the most promising approaches [23, 37-39]. This is due to the already reported PEG-associated side effects that is lately compromising this reference polymeric material in its future development [1, 21]. These associated adverse effects can be mainly summarized as (i) hypersensitivity [21] (ii) non-biodegradability and non-biocompatibility [21, 40], (iii) side effects in the body due to the PEG itself or degradation products, and anti-PEG antibodies formation that could generate undesired immunogenic reactions [40, 41]. PEG substitution is a huge area of interest also in exponential grow within the drug delivery field, and PTS has adopted it as one of its internal interests to look for PAA as PEG substituents. For this reason, **TPSS**, a new biodegradable HP-BM amphiphilic material was developed and properly characterized within this PhD work. A direct comparison with the commercially available PEGylated counterpart not only regarding physico-chemical properties but also their pharmacological properties as skin delivery system. Similar results for both sstem were found regarding Mw distributions by SEC and by MALDI-TOF MS, identity by NMR, and diffusion coefficients by DOSY NMR, as well as an enhancement on skin permeation capabilities with the PSar alternative, demonstrating that HP-BM could be considered a very promising alternative to TPGS in the biomedical field.

These results drive us to select the **PEG-PBG** and **PEG-PPhe** APAA series as well as **TPGS** and **TPSS** to study their self-assembling properties in micellar structures to encapsulate a hydrophobic fluorophore as hydrophobic API model. Encapsulation efficiency and fluorophore load by UV-Vis spectroscopy, secondary conformational structure by CD, CMC by fluorescence spectroscopy and morphology by TEM were determined for the micelles finding good results compared with reported in literature. Moreover, size and Z potential by DLS were determined for micellar formulations prepared by different methodologies. The obtained results allow to conclude that polymeric micelles prepared with APAA as well as HP-BM obtained by ROP of NCAs via NAM are excellent and versatile candidates to encapsulate hydrophobic drugs or APIs to be applied in drug delivery as carriers.

Based on the results for hydrophobic model API encapsulation using the **PEG-PBG** and **PEG-PPhe** polymeric micelles, and motivated by the exploration of PAA-based materials as carriers for skin drug delivery, we decided to develop a platform to transport hydrophobic APIs through the skin. Since the skin drug delivery has been scarcely studied for these materials in the literature.

Recent strategies for the topical administration of APIs to specific skin layers have explored the potential of polymeric formulations of drugs as emulsions, creams, gels, hydrogels, transdermal patches, and wound dressings, and the application of polymers as penetration enhancers [42]. Currently studied polymers include polyacrylates, poloxamers, poly(lactic-co-glycolic acid) [42], polyvinyl alcohols [43], PEG derivatives [44], polysaccharides [42, 45, 46] and PAA [7, 8]. Polysaccharides include naturally occurring polymers produced by algae (e.g., alginate), plants (e.g., cellulose), microbes (e.g., dextran), and animals (e.g., hyaluronic acid) [47]. Hyaluronic acid (HA, also called hyaluronan), a natural heteropolysaccharide with a linear structure discovered by Meyer and Palmer in 1934, contains alternating D-glucuronic acid and *N*-acetyl-D-glucosamide residues [48]. The HA also is widely employed for topical applications due to its versatile properties, such as its biocompatibility, non-immunogenicity, biodegradability and viscoelasticity. Thus, HA is an ideal biomaterial for cosmetic, medical and pharmaceutical applications such as tissue engineering, generate dermal fillers, injectables, to treat specific diseases in the role of drug substance (e.g. osteoarthritis) [49, 50].

We designed a cross-polymer based on HA cross-linked with PGlu through L-lysine named **HA-CP**. **HA-CP** synthesis was developed successfully thanks to the previous optimization with the simplified **PGlu-Lys-PGlu** system without HA. Moreover, the NMR characterization technique as well as SEC, intrinsic viscosity, free amine quantification, and pH monitoring were key to control and understand the cross-linking reaction. After exhaustive physico-chemical characterization of **HA-CP** material, its biological properties as a delivery vehicle into the skin were studied employing *in vitro*, *ex vivo*, and *in vivo* assays,

comparing it with conventional linear HA with similar Mw. Substantial improvements in terms of resistance to HAase degradation, intrinsic human skin permeation capability, and excellent human skin compatibility were observed. Also, the absence of vaginal irritant effect *in vivo* in a rabbit model confirms the good skin compatibility.

Owing to the high skin permeation capability found for **HA-CP**, we decided to study the enhancement capacity of HA-CP in skin drug delivery for hydrophobic APIs encapsulated onto four polymeric micelles based on **PEG114-b-PGlu(OBzl)10**, **PEG114-b-PGlu(OBzl)20**, **PEG114-b-PPhe10**, and **PEG114-b-PPhe20**. Micelles were embedded within the **HA-CP** matrix yielding a hybrid material system with possibilities for topical administration. After *ex vivo* permeation using Franz Diffusion Cells, an excellent capability to go through the stratum corneum and to transport the hydrophobic APIs till the epidermis layer were observed. Four APAA micelles were tested into the **HA-CP**, and the **PEG114-b-PGlu(OBzl)20** and **PEG114-b-PPhe10** micelles showed a higher accumulation in the epidermis. However, the **PEG114-b-PGlu(OBzl)20** micelle was selected to follow the study due to its higher encapsulation capacity and easier synthesis. Thus, the skin permeation of **PEG114-b-PGlu(OBzl)20** micelle was studied by 3 formulations: water, linear HA, and **HA-CP** matrix. And the **HA-CP** formulation showed the highest accumulation in the epidermis layer. Moreover, the **HA-CP** also worked in combination with HP-BM based micelles showing the highest permeation to the epidermis layer for the material containing polysarcosine compared with the PEGylated compound.

The developed technology to prepare cross-linked materials between polysaccharides and PAA was patented [51] and employed in pharmaceutical applications such as the psoriasis treatment enhancing the skin permeation of **PGlu-Fluocinolone** conjugate [52]. These excellent skin properties demonstrated within the frame of this Thesis dissertation are the scientific ground underlying the commercialization and use of the **HA-CP** as an ingredient in cosmetic products currently available under the name of **Biomimetic PBT®** [53]. **HA-CP** is being manufactured at 25 Kg scale.

The current exponential growth on the use of PAA as drug delivery technologies for biomedical applications, motivated us to invest resources in the development of a manufacturing process to produce PAA-based materials at GMP grade. Contrary to the R&D stage in the academy, university, or research institutes, the companies do not share their *know-how* on the manufacturing process, analytical methodologies, facilities, suppliers, quality controls, etc., in scientific journals or databases. Unlike many other commodity polymers employed in pharmaceutical development (e.g. PEG, PLGA, etc.), PAAs lacks a concrete guideline or monography on the recommended strategy for its manufacturing and control processes. Fortunately, ICH guidelines provide excellent and precise information to design a strategy to guaranty that the scientists and manufacturers develop accurately a robust, reproducible, and scalable manufacturing process within a regulated GMP

environment. These guidelines also secure the lifecycle of the product and the traceability of the manufacturing batches. Specifically, the ICH Q11 called “*Development And Manufacture Of Drug Substances (Chemical Entities And Biotechnological/Biological Entities)*” is focused into bring an accurate and detailed pathway to generate new drug substances [54]. And the ICH Q7 “*Good Manufacturing Practice Guide For Active Pharmaceutical Ingredients*” shows how this can be done under GMP compliance [55]. Taking into account that most of these PAA are new materials and that the regulatory agencies expressed their concern on these polymeric nanomedicines in the past we decided to produce the PAA-based materials under the highest regulatory status of drug substance following mainly the ICH guidelines Q11 and Q7. And, as the PLys is the PAA with the highest demand and with the highest publication number (see Figure 4.1), we focused our manufacturing process development and optimization for PLys materials.

We developed and optimized the manufacturing process for two PLys materials (**HL50** and **ML400**) mainly following the ICH Q11 guidelines achieving a robust, reproducible and scalable manufacturing process. Moreover, analytical techniques to perform an adequate physico-chemical characterization were designed, developed, optimized, qualified, and validated. We developed the PLys manufacturing process adapting the FDA scale-up route [56] to our strategy. We developed an outstanding CMC knowledge on the manufacturing process and analytical controls, designing a Control Strategy within GMP compliance or PLys materials as drug substances.

A CMC package documentation over the manufacturing process of both PLys materials was developed. To date, both EMA and FDA have evaluated our CMC package for PLys related materials with very good feedback allowing our partners to clear their path to clinical trials. Materials produced at PTS are currently being tested in humans to treat different pathologies from neurodegenerative disorders to oncology.

FINAL CONCLUSIONS

1. ROP of NCA monomers of alpha aa via NAM methodology has been successfully adapted to generate well-defined narrowly distributed homo and random PAA for different DPs (from 20 to 400) with Mw distributions and stoichiometry between initiator and aa monomers in good agreement with the target values. The living character of this polymerization technique maintains the initiator in the C-terminus and the free amine in the N-terminus being available to act as the initiator to build block copolymers generating well-defined narrowly distributed APAA.
2. PAA and APAA have been synthesized using aa monomers for different nature being (i) cationic (Orn and Arg), (ii) anionic (Glu), (iii) polar (Sar), and (iv) non-polar (Phe and Val) allowing their combination in homo, random and block architectures to modify the

electrostatic charge, the secondary structure conformation, and the hydrophilic – hydrophobic ratio.

3. Physico-chemical characterization techniques to analyze the CQA of the PAA-based materials were developed successfully. The two main characterization techniques developed have been the SEC and NMR. SEC has been employed to obtain the Mw distributions of the protected precursors and the NMR to establish the stoichiometry ratio between initiator and aa monomer(s) composition.
4. Deprotection through acid or basic hydrolysis to remove the protecting groups has been optimized and studied by NMR (> 99 %) in the protected PAA and APAA maintaining the stoichiometry between the initiator and the amino acids.
5. A novel biodegradable alternative to TPGS has been developed containing PSar as PEG substituent. A face-to-face comparison in terms of physical and chemical properties of TPGS and TPSS was carried out finding virtually the same results in terms of Mw distribution, PDI, Vit E content, DC, size, and morphology. Further studies will focus on determining the Critical Aggregation Concentration (CAC) and the antioxidant properties. To note, the obtained results might be susceptible to be patented.
6. Four APAA materials were selected to study their micellar self-assembly properties and their encapsulation efficiency of a hydrophobic API model. Materials were: (i) **PEG114-b-PGlu(OBzl)10**, (ii) **PEG114-b-PGlu(OBzl)20**, (iii) **PEG114-b-PPhe10**, and (iv) **PEG114-b-PPhe20**.
7. A novel **HA-CP** was designed based on HA cross-linked with PGlu through Lys. **HA-CP** was evaluated *in vitro*, *in vivo*, and *ex vivo* as a permeation enhancer in skin drug delivery among other topical applications. HA-CP was directly compared with the parent linear HA with the same Mw demonstrating the advantages on the crosslink strategy in terms of (i) resistance to HAase degradation, (ii) intrinsic human skin permeation capability and (iii) skin compatibility. Moreover, **HA-CP**-based dermo-cosmetic products are currently being marketed under the name of **Biomimetic PBT®**. The current batch production of **HA-CP** is 25 Kg.
8. **HA-CP** was combined with the four polymeric micelles previously mentioned yielding four different hybrid materials (one per micelle). The two hybrid material systems of **HA-CP** with **PEG114-PGlu(OBzl)20** and **PEG114-PPhe10** micelles showed the highest accumulation in the epidermis layer. However, the **PEG114-PGlu(OBzl)20** micelle was selected to follow the study due to its higher encapsulation capacity and easier synthesis. Thus, the skin permeation of **PEG114-PGlu(OBzl)20** micelle was evaluated by three

formulation: (i) water, (ii) linear HA, and (iii) **HA-CP** matrix. And the **HA-CP** formulation showed the highest accumulation in the epidermis layer.

9. The **HA-CP** was also able to form a hybrid carrier with HP-BM-based micelles of **TPGS** and **TPSS** materials. Interestingly, the polysarcosine material showed higher accumulation in the epidermis layer than the PEGylated material.
10. Manufacturing process under drug substance standard quality was developed and fully optimized for two PLys materials (HL50 and ML400) under GMP compliance following mainly two harmonized guidelines: the ICH Q11 “*Development And Manufacture Of Drug Substances (Chemical Entities And Biotechnological/Biological Entities)*” and the ICH Q7 “*Good Manufacturing Practice Guide For Active Pharmaceutical Ingredients*”.
11. A CMC package documentation over the manufacturing process of both PLys materials was developed.

REFERENCES

- [1] M. Barz, R. Luxenhofer, R. Zentel, M.J. Vicent, Overcoming the PEG-addiction: well-defined alternatives to PEG, from structure-property relationships to better defined therapeutics, *Polymer Chemistry* 2(9) (2011) 1900-1918.
- [2] M. Khuphe, P.D. Thornton, Poly(amino acids), in: A. Parambath (Ed.), *Engineering of Biomaterials for Drug Delivery Systems: Beyond Polyethylene Glycol*, Woodhead Publ Ltd, Cambridge, 2018, pp. 199-228.
- [3] A.R. Mazo, S. Allison-Logan, F. Karimi, N.J.A. Chan, W.L. Qiu, W. Duan, N.M. O'Brien-Simpson, G.G. Qiao, Ring opening polymerization of alpha-amino acids: advances in synthesis, architecture and applications of polypeptides and their hybrids, *Chemical Society Reviews* 49(14) (2020) 4737-4834.
- [4] J.V. Gonzalez-Aramundiz, M.V. Lozano, A. Sousa-Herves, E. Fernandez-Megia, N. Csaba, Polypeptides and polyaminoacids in drug delivery, *Expert Opinion on Drug Delivery* 9(2) (2012) 183-201.
- [5] T. Melnyk, S. Dordevic, I. Conejos-Sanchez, M.J. Vicent, Therapeutic potential of polypeptide-based conjugates: Rational design and analytical tools that can boost clinical translation, *Advanced drug delivery reviews* 160 (2020) 136-169.
- [6] A. Duro-Castano, I. Conejos-Sanchez, M.J. Vicent, Peptide-Based Polymer Therapeutics, *Polymers* 6(2) (2014) 515-551.
- [7] M.P. Bevilacqua, D.J. Huang, B.D. Wall, S.J. Lane, C.K. Edwards, J.A. Hanson, D. Benitez, J.S. Solomkin, T.J. Deming, Amino Acid Block Copolymers with Broad Antimicrobial Activity and Barrier Properties, *Macromolecular Bioscience* 17(10) (2017) 9.
- [8] R. Wang, B. Zhou, D.L. Xu, H. Xu, L. Liang, X.H. Feng, P.K. Ouyang, B. Chi, Antimicrobial and biocompatible epsilon-polylysine-gamma-poly(glutamic acid)-based hydrogel system for wound healing, *Journal of Bioactive and Compatible Polymers* 31(3) (2016) 242-259.
- [9] C.G. Zhang, R.L. Zhang, Y. Zhu, W. Wei, Y. Gu, X.Y. Liu, Polymer vesicles prepared from the (L-phenylalanine ethyl ester)-modified hyaluronic acid, *Materials Letters* 164 (2016) 15-18.

- [10] Y. Ohya, S. Takeda, Y. Shibata, T. Ouchi, A. Kano, T. Iwata, S. Mochizuki, Y. Taniwaki, A. Maruyama, Evaluation of polyanion-coated biodegradable polymeric micelles as drug delivery vehicles, *Journal of Controlled Release* 155(1) (2011) 104-110.
- [11] G.S. Kwon, K. Kataoka, Block copolymer micelles as long-circulating drug vehicles, *Advanced Drug Delivery Reviews* 64 (2012) 237-245.
- [12] A. Carlsen, S. Lecommandoux, Self-assembly of polypeptide-based block copolymer amphiphiles, *Current Opinion in Colloid & Interface Science* 14(5) (2009) 329-339.
- [13] O. Zagorodko, J.J. Arroyo-Crespo, V.J. Nebot, M.J. Vicent, Polypeptide-Based Conjugates as Therapeutics: Opportunities and Challenges, *Macromolecular Bioscience* 17(1) (2017).
- [14] A. Lalatsa, A.G. Schatzlein, M. Mazza, B.H.L. Thi, I.F. Uchegbu, Amphiphilic poly(l-amino acids) - New materials for drug delivery, *Journal of Controlled Release* 161(2) (2012) 523-536.
- [15] H.L. Xu, Q. Yao, C.F. Cai, J.X. Gou, Y. Zhang, H.J. Zhong, X. Tang, Amphiphilic poly(amino acid) based micelles applied to drug delivery: The in vitro and in vivo challenges and the corresponding potential strategies, *Journal of Controlled Release* 199 (2015) 84-97.
- [16] R. Wahid, R. Holt, R. Hjorth, F.B. Scorza, Chemistry, manufacturing and control (CMC) and clinical trial technical support for influenza vaccine manufacturers, *Vaccine* 34(45) (2016) 5430-5435.
- [17] N.S. Cauchon, S. Oghamian, S. Hassanpour, M. Abernathy, Innovation in Chemistry, Manufacturing, and Controls-A Regulatory Perspective From Industry, *Journal of Pharmaceutical Sciences* 108(7) (2019) 2207-2237.
- [18] G. Akshatha, V.A. Narayanan, D.S. Sandeep, R.N. Charyulu, Chemistry, Manufacturing and Control (CMC) Evaluations of ANDA Submission in the USA, *Indian Journal of Pharmaceutical Education and Research* 53(3) (2019) 414-420.
- [19] I.L. Shih, Y.T. Van, M.H. Shen, Biomedical applications of chemically and microbiologically synthesized poly(glutamic acid) and poly(lysine), *Mini-Reviews in Medicinal Chemistry* 4(2) (2004) 179-188.
- [20] S.E. Barrett, R.S. Burke, M.T. Abrams, C. Bason, M. Busuek, E. Carlini, B.A. Carr, L.S. Crocker, H. Fan, R.M. Garbaccio, E.N. Guidry, J.H. Heo, B.J. Howell, E.A. Kemp, R.A. Kowtoniuk, A.H. Latham, A.M. Leone, M. Lyman, R.G. Parmar, M. Patel, S.Y. Pechenov, T. Pei, N.T. Pudvah, C. Raab, S. Riley, L. Sepp-Lorenzino, S. Smith, E.D. Soli, S. Staskiewicz, M. Stern, Q. Truong, M. Vavrek, J.H. Waldman, E.S. Walsh, J.M. Williams, S. Young, S.L. Colletti, Development of a liver-targeted siRNA delivery platform with a broad therapeutic window utilizing biodegradable polypeptide-based polymer conjugates, *Journal of Controlled Release* 183 (2014) 124-137.
- [21] K. Knop, R. Hoogenboom, D. Fischer, U.S. Schubert, Poly(ethylene glycol) in Drug Delivery: Pros and Cons as Well as Potential Alternatives, *Angewandte Chemie-International Edition* 49(36) (2010) 6288-6308.
- [22] G.H. Van Domeselaar, G.S. Kwon, L.C. Andrew, D.S. Wishart, Application of solid phase peptide synthesis to engineering PEO-peptide block copolymers for drug delivery, *Colloids and Surfaces B-Biointerfaces* 30(4) (2003) 323-334.
- [23] Y. Xiao, J.Q. Wang, J. Zhang, A. Heise, M.D. Lang, Synthesis and gelation of copolypept(o)ides with random and block structure, *Biopolymers* 107(10) (2017) 9.
- [24] A. Birke, J. Ling, M. Barz, Polysarcosine-containing copolymers: Synthesis, characterization, self-assembly, and applications, *Progress in Polymer Science* 81 (2018) 163-208.

- [25] Z.Y. Song, H.L. Fu, J. Wang, J.S. Hui, T.R. Xue, L.A. Pacheco, H.Y. Yan, R. Baumgartner, Z.Y. Wang, Y.C. Xia, X.F. Wang, L.C. Yin, C.Y. Chen, J. Rodriguez-Lopez, A.L. Ferguson, Y. Lin, J.J. Cheng, Synthesis of polypeptides via bioinspired polymerization of in situ purified N-carboxyanhydrides, *Proceedings of the National Academy of Sciences of the United States of America* 116(22) (2019) 10658-10663.
- [26] S. Niimura, H. Kurosu, A. Shoji, Precise structural analysis of alpha-helical polypeptide by quantum-chemical calculation related to reciprocal side-chain combination of two L-phenylalanine residues, *Journal of Molecular Structure* 970(1-3) (2010) 96-100.
- [27] S.H. Wibowo, A. Sulistio, E.H.H. Wong, A. Blencowe, G.G. Qiao, Functional and Well-Defined -Sheet-Assembled Porous Spherical Shells by Surface-Guided Peptide Formation, *Advanced Functional Materials* 25(21) (2015) 3147-3156.
- [28] A. Sinaga, T.A. Hatton, K.C. Tam, Thermodynamics of micellization of beta-sheet forming poly(acrylic acid)-block-poly(L-valine) hybrids, *Journal of Physical Chemistry B* 112(37) (2008) 11542-11550.
- [29] H.J. Song, G. Yang, P.S. Huang, D.L. Kong, W.W. Wang, Self-assembled PEG-poly(L-valine) hydrogels as promising 3D cell culture scaffolds, *Journal of Materials Chemistry B* 5(9) (2017) 1724-1733.
- [30] H.Y. Zhu, M. Zhu, S.R. Shuai, C. Zhao, Y. Liu, X.H. Li, Z.K. Rao, Y. Li, J.Y. Hao, Effect of polypeptide block length on nano-assembly morphology and thermo-sensitivity of methyl poly(ethylene glycol)-poly(L-valine) copolymer aqueous solutions, *Journal of Sol-Gel Science and Technology* 92(3) (2019) 618-627.
- [31] A. Sinaga, P. Ravi, T.A. Hatton, K.C. Tam, Synthesis of poly(acrylic acid)-block-poly(L-valine) hybrid through combined atom transfer radical polymerization, click chemistry, and nickel-catalyzed ring opening polymerization methods, *Journal of Polymer Science Part a-Polymer Chemistry* 45(13) (2007) 2646-2656.
- [32] T.J. Deming, Methodologies for preparation of synthetic block copolypeptides: materials with future promise in drug delivery, *Advanced Drug Delivery Reviews* 54(8) (2002) 1145-1155.
- [33] H. Lu, J. Wang, Z.Y. Song, L.C. Yin, Y.F. Zhang, H.Y. Tang, C.L. Tu, Y. Lin, J.J. Cheng, Recent advances in amino acid N-carboxyanhydrides and synthetic polypeptides: chemistry, self-assembly and biological applications, *Chemical Communications* 50(2) (2014) 139-155.
- [34] T.J. Deming, Synthesis and Self-Assembly of Well-Defined Block Copolypeptides via Controlled NCA Polymerization, *Hierarchical Macromolecular Structures: 60 Years after the Staudinger Nobel Prize* 11 (2013) 1-37.
- [35] J. Huang, A. Heise, Stimuli responsive synthetic polypeptides derived from N-carboxyanhydride (NCA) polymerisation, *Chemical Society Reviews* 42(17) (2013) 7373-7390.
- [36] C.L. Yang, T.T. Wu, Y. Qi, Z.P. Zhang, Recent Advances in the Application of Vitamin E TPGS for Drug Delivery, *Theranostics* 8(2) (2018) 464-485.
- [37] D. Huesmann, A. Sevenich, B. Weber, M. Barz, A head-to-head comparison of poly(sarcosine) and poly(ethylene glycol) in peptidic, amphiphilic block copolymers, *Polymer* 67 (2015) 240-248.
- [38] K. Son, M. Ueda, K. Taguchi, T. Maruyama, S. Takeoka, Y. Ito, Evasion of the accelerated blood clearance phenomenon by polysarcosine coating of liposomes, *Journal of Controlled Release* 322 (2020) 209-216.
- [39] S.S. Nogueira, Polysarcosine-Functionalized Lipid Nanoparticles for Therapeutic mRNA Delivery, in: A. Schlegel (Ed.) *ACS Appl. Nano Mater.*, 2020, pp. 10634-10645.

- [40] K.D. Hinds, Protein conjugation, cross-linking, and PEGylation, *Biomaterials for Delivery and Targeting of Proteins and Nucleic Acids* (2005) 119-185.
- [41] G.T. Kozma, T. Shimizu, T. Ishida, J. Szebeni, Anti-PEG antibodies: Properties, formation, testing and role in adverse immune reactions to PEGylated nano-biopharmaceuticals, *Advanced drug delivery reviews* 154-155 (2020) 163-175.
- [42] C. Valenta, B.G. Auner, The use of polymers for dermal and transdermal delivery, *European Journal of Pharmaceutics and Biopharmaceutics* 58(2) (2004) 279-289.
- [43] S.A. Castleberry, M.A. Quadir, M. Abu Sharkh, K.E. Shopsowitz, P.T. Hammond, Polymer conjugated retinoids for controlled transdermal delivery, *Journal of Controlled Release* 262 (2017) 1-9.
- [44] A.B. Kutikov, J. Song, Biodegradable PEG-Based Amphiphilic Block Copolymers for Tissue Engineering Applications, *Acs Biomaterials Science & Engineering* 1(7) (2015) 463-480.
- [45] R. Gul, N. Ahmed, K.U. Shah, G.M. Khan, A.U. Rehman, Functionalised nanostructures for transdermal delivery of drug cargos, *Journal of Drug Targeting* 26(2) (2018) 110-122.
- [46] M.C.G. Pella, M.K. Lima-Tenorio, E.T.T. Neto, M.R. Guilherme, E.C. Muniz, A.F. Rubira, Chitosan-based hydrogels: From preparation to biomedical applications, *Carbohydrate Polymers* 196 (2018) 233-245.
- [47] Q. Li, Y.M. Niu, P.F. Xing, C.M. Wang, Bioactive polysaccharides from natural resources including Chinese medicinal herbs on tissue repair, *Chinese Medicine* 13 (2018) 11.
- [48] C. Guarise, M. Pavan, L. Pirrone, D. Renier, SEC determination of cross-link efficiency in hyaluronan fillers, *Carbohydrate Polymers* 88(2) (2012) 428-434.
- [49] S. Berko, M. Maroda, M. Bodnar, G. Eros, P. Hartmann, K. Szentner, P. Szabo-Revesz, L. Kemeny, J. Borbely, E. Csanyi, Advantages of cross-linked versus linear hyaluronic acid for semisolid skin delivery systems, *European Polymer Journal* 49(9) (2013) 2511-2517.
- [50] A. Fakhari, C. Berkland, Applications and emerging trends of hyaluronic acid in tissue engineering, as a dermal filler and in osteoarthritis treatment, *Acta Biomaterialia* 9(7) (2013) 7081-7092.
- [51] D. Morelló-Bolumar, CROSS POLYMERS COMPOSED OF POLYSACCHARIDES AND POLYAMINO ACIDS, AND USES THEREOF (WO 2019/020344 A1), 2019.
- [52] I. Dolz-Perez, M.A. Sallam, E. Masia, D. Morello-Bolumar, M.D.P. del Caz, P. Graff, D. Abdelmonsif, S. Hedtrich, V.J. Nebot, M.J. Vicent, Polypeptide-corticosteroid conjugates as a topical treatment approach to psoriasis, *Journal of Controlled Release* 318 (2020) 210-222.
- [53] <https://www.biomimeticdermocosmetics.com/en/>.
- [54] ICH Q11 Development And Manufacture Of Drug Substances (Chemical Entities And Biotechnological/Biological Entities).
- [55] ICH Q7 Good Manufacturing Practice Guide For Active Pharmaceutical Ingredients.
- [56] <https://www.fda.gov/about-fda/innovation-fda/what-we-do>.

APPENDIX I. THESIS PROJECT, OBJECTIVES, MAIN METHODOLOGY, RESULTS AND CONCLUSIONS IN SPANISH

1. INTRODUCCIÓN Y MARCO TEMÁTICO DE LA TESIS

Barz y Col. dijeron hace 9 años: “*la vida moderna como la conocemos sería imposible sin polímeros. Naturales o sintéticos, los polímeros son esenciales en nuestro día a día y han aumentado su importancia en las aplicaciones biomédicas*” [1]. Nada ha cambiado desde entonces, sino que se ha incrementado su valía en múltiples aplicaciones cotidianas y sobretodo, se ha observado un crecimiento exponencial en el uso de polímeros en áreas biomédicas incluyendo el campo de la nanomedicina siendo los Poli(Amino Ácidos) (PAA) una parte importante de estos [2].

En los últimos años, los materiales basados en PAA han emergido como candidatos para ser usados en administración de fármacos (Active Pharmaceutical Ingredient, API) aplicándose en varias áreas terapéuticas [3, 4] como la oncología, terapia génica o la inmunoterapia para tratar diferentes patologías humanas [5]. Estos materiales pueden usarse también para tratar enfermedades infecciosas o inflamatorias [6]. Los materiales basados en PAA pueden emplearse para el desarrollo de sondas empleadas en diagnóstico molecular tanto como biomarcadores de predicción de la enfermedad como para su monitorización [6]. Sorprendentemente, para aplicaciones tópicas y en piel, hay muy pocos datos empleando materiales basados en PAA [7, 8]. Estos materiales poliméricos son muy versátiles a la vez que seguros, proporcionando múltiples posibilidades de diseño debido a que sus monómeros son amino ácidos (aa) endógenos que están presentes en la naturaleza. Estos monómeros pueden combinarse con otros polímeros naturales que no sean PAA (por ejemplo, el ácido hialurónico (Hyaluronic Acid, HA [9, 10]) o con polímeros sintéticos como por ejemplo el poli(etileno glicol) (PEG) [11], generando compuestos con una gran variedad de tamaños y conformaciones que ofrecen un amplio rango de atributos físico-químicos para diferentes aplicaciones [12]. La alta versatilidad estructural, la biocompatibilidad, la solubilidad en agua, la ausencia de toxicidad y los grandes avances en técnicas sintéticas de polimerización controlada hacen muy atractivos a los PAA para ser empleados en el campo de la nanomedicina [2].

Las propiedades físico-químicas y los elementos estructurales en el diseño racional de los materiales basados en PAA como portadores en la administración de fármacos dependen específicamente de la aplicación final, la enfermedad a tratar o la vía de administración entre otros [6, 13]. Las propiedades físico-químicas se pueden modular en términos de: **el proceso de fabricación** (técnicas de polimerización, ROP, ATRP, etc.), **tamaño** (pequeño o grande), **carga electrostática** (positiva, negativa, neutra o zwitteriónica), **conformación** (hélice-alfa, hoja-beta, ovillo aleatorio, etc.), geometría (esfera, nanotubo, etc.), **topología** (lineal, estrella, injerto o ramificado) y **composición de monómeros** (homo,

aleatorio o bloque). También pueden modularse en base a los elementos estructurales, como la **naturaleza del API** (hidrófila o hidrófoba), la **interacción API-polímero** (covalente o no covalente) y la **arquitectura supramolecular del sistema de administración del fármaco** (micela, vesícula, conjugado polímero-fármaco, poliplejo, hidrogel o nanopartícula) [1, 2, 13-15].

Dentro del estado del arte actual de los materiales basados en PAA, la gran mayoría de los compuestos se encuentran en las primeras etapas de Investigación y Desarrollo (I+D) y/o Prueba de Concepto (Proof of Concept, POC) [6, 13] con pocos ejemplos de medicamentos en ensayos clínicos o comercializados. Desafortunadamente, una cantidad muy baja de ellos serán comercializados, en la mayoría de los casos debido a un desequilibrio en la seguridad-eficacia, pero en muchos otros casos, por falta de recursos o interés de la Industria Farmacéutica. Pero, ¿qué sucede cuando un candidato funciona? Como es bien conocido, el proceso para trasladar a un candidato de la bancada de I+D hasta mercado es un viaje largo. Dicho proceso se debe realizar bajo las normas de Buenas Prácticas de Fabricación (Good Manufacturing Practice, GMP). Y dentro de la normativa GMP, se encuentran las actividades de Química, Fabricación y Control (Chemistry, Manufacturing and Control, CMC), que deben aplicarse para respaldar, controlar y asegurar este viaje.

Las actividades de CMC abarcan el desarrollo, optimización y desempeño de las metodologías analíticas del proceso de fabricación, así como sistemas de gestión de calidad, definición de grado de calidad, producción, instalaciones, equipos, controles de laboratorio, materiales, empaque, etiquetado y el envío [16]. Además, los sistemas de gestión de la calidad de las actividades de CMC también contienen la identificación de desviaciones, la investigación y la gestión de riesgos del proceso de fabricación, así como la calificación y validación de las metodologías analíticas [16-18].

En el marco actual de esta disertación de tesis, los dos primeros capítulos se han centrado en un trabajo basado en actividades de I+D enfocadas en el diseño de nuevos materiales basados en PAA que se pueden considerar dentro de la etapa de POC (o estudio de viabilidad) antes de emprender la fabricación y el proceso de desarrollo. Por el contrario, el capítulo final muestra dos ejemplos reales ya al final de este camino, ya que se están muy cerca de su comercialización. Son dos ejemplos de alfa-poli-L-lisinas para las que se han realizado las actividades de CMC bajo el cumplimiento de GMP siguiendo las pautas de calidad de las guías del Consejo Internacional para la Armonización de Requisitos Técnicos para Productos Farmacéuticos de Uso Humano (International Council for Harmonisation, ICH) para así lograr la calidad y acreditación necesaria de sustancia farmacéutica. La optimización y desarrollo para (i) proceso de fabricación, (ii) metodologías analíticas, (iii) espacio de diseño y (iv) presentación de resultados para la obtención de PAA (concretamente alfa-poli-L-lisinas) es nuestra principal contribución al estado actual del arte de los materiales basados en PAA en el campo de la nanomedicina para la administración de fármacos.

2. OBJETIVOS

La presente disertación de tesis se centra en el diseño y desarrollo de materiales basados en PAA para generar vehículos versátiles bajo condiciones controladas de polimerización fabricados bajo el cumplimiento de las GMP para su uso en aplicaciones de administración de fármacos.

Este objetivo general, involucra varias tareas específicas que se pueden resumir a continuación:

1. Adaptar la metodología sintética descrita en la literatura basada en la polimerización por apertura de anillo (Ring Opening Polymerization, ROP) de monómeros de N-carboxianhídrido (NCA) de alfa-aminoácidos a través del Mecanismo de Amina Normal (Normal, Amine Mechanism, NAM) para obtener PAA y copolímeros de PAA anfifílicos (Amphiphilic Poly(Amino Acid), APAA) bien definidos con una polidispersidad estrecha.

2. Explorar la estrategia sintética para modular las propiedades fisicoquímicas de los APAA tales como carga electrostática (neutra, positiva, negativa y zwitteriónica), conformación secundaria (hélice-alfa, hoja-beta y ovrillo aleatoria) y el balance hidrofílico e hidrofóbico. Además del estudio de los candidatos seleccionados en términos de autoensamblaje en soluciones acuosas en estructuras micelares para encapsular y transportar APIs hidrofobos.

3. Explorar otros tipos de copolímeros de bloques anfifílicos basados en polímeros hidrofílicos que contienen una biomolécula como parte hidrofóbica (Hydrophilic Polymer – BioMolecule, HP-BM). En concreto, diseño y desarrollo de una alternativa biodegradable al D-alfa-tocoferol-poli(etilen glicol)-succinato (TPGS) a base de polisarcosina para sustituir al polietilenglicol como bloque hidrofílico.

4. Diseño y desarrollo de una plataforma novedosa basada en materiales poliméricos entrecruzados de PAA-HA en combinación con APAA para administrar APIs hidrofobos para aplicaciones dérmicas.

5. Desarrollo de técnicas de caracterización físico-química para estudiar los Atributos Críticos de Calidad (Critical Quality Attributes, CQA) en PAA, APAA, HP-BM y micelas poliméricas, así como el polímero entrecruzado para la administración de APIs hidrofobos en la piel.

6. Evaluar el sistema de micelas poliméricas formuladas en el polímero entrecruzado en modelos biológicos relevantes para aplicaciones dérmicas. Evaluación *in vitro* y *ex vivo* en modelos relevantes preclínicamente (líneas celulares y cultivos organotípicos de piel

humana) para evaluar el perfil de seguridad y las propiedades de permeación cutánea de los materiales formulados.

7. Diseñar y desarrollar un proceso de fabricación robusto, reproducible y escalable para generar materiales basados en PAA bajo el cumplimiento de GMP aplicando el grado de estándares de calidad para sustancias farmacéuticas siguiendo las guías ICH.

8. Generar un paquete de documentación CMC sobre el proceso de fabricación de materiales basados en PAA. Esto significa: (i) desarrollar el proceso de escalado (POC y lotes piloto), (ii) identificar los CQA y definir los parámetros críticos del proceso (Critical Process Parameters, CPP) para asegurar la calidad del producto objetivo, (iii) desarrollar las técnicas analíticas y el Controles en proceso (In-Process Controls, IPC), (iv) definir el flujo de trabajo, (v) seleccionar los materiales de partida, (vi) definir la estrategia de control, (vii) diseñar las instalaciones y equipos con la capacidad adecuada para realizar un escalado reproducible y (viii) gestionar la presentación de resultados definiendo los CQAs (físico, químico y biológico), el perfil de impurezas, las sustancias de degradación relacionadas y sus límites para generar el Certificado de Análisis (CoA).

3. METODOLOGÍA PRINCIPAL

3.1. MATERIALES E INSTRUMENTACIÓN

3.1.1. MATERIALES

Todos los reactivos usados durante la tesis fueron de grado analítico o superior, y se usaron sin purificación adicional. Los disolventes usados también eran de grado analítico o superior, y se usaron sin purificación adicional. De manera general, las reacciones llevadas a cabo en disolventes orgánicos se realizaron bajo atmósfera inerte de nitrógeno seco.

3.1.2. INSTRUMENTACIÓN MÁS RELEVANTE

Resonancia Magnética Nuclear (RMN)

Los espectros de RMN se obtuvieron a 27 °C (300 K) mediante un equipo de 300 MHz de Ultrashield™ de Bruker (Billerica MA, EEUU). Los espectros se procesaron con el programa Topspin (Bruker GmbH, Karlsruhe, Alemania). Las muestras se prepararon a una concentración de 10 - 25 mg/mL en el disolvente deuterado correspondiente.

4. RESULTADOS

4.1. MICELAS BASADAS EN POLIAMINO ÁCIDOS AMFIFÍLICOS PARA LA ADMINISTRACIÓN DE FÁRMACOS (CAPÍTULO 2)

En el primer capítulo nos centramos en el desarrollo de materiales basados en PAA, concretamente en el diseño y optimización de la producción de APAA para impulsar su autoensamblaje en estructuras micelares con diferentes propiedades físico-químicas [15]. Para el bloque hidrofílico del material anfifílico, empleamos el aa de acuerdo con su naturaleza de carga electrostática. El ácido glutámico (Glu) fue el aa seleccionado para la carga aniónica [19]; Ornitina (Orn) para la carga catiónica [20]; etilenglicol (EG) [1, 21] y Sarcosina (Sar) [22, 23] para una carga neutra; y un copolímero aleatorio de Glu y Orn para generar la naturaleza electrostática zwitteriónica. Con respecto al segmento hidrofóbico, seleccionamos Glu(OBzl) [24] y fenilalanina (Phe) [13, 25] para generar la estructura secundaria de hélice-alfa, y Valina (Val) para proporcionar una conformación de hoja-beta [26-30].

Para generar estos materiales, adaptamos la metodología sintética actual de poimerización por apertura de anillo (ROP) de monómeros N-carboxianhídidos (NCA) vía NAM ampliamente descrita en la literatura [31-34]. Todos los PAA, tanto homo como aleatorios (18 compuestos) se obtuvieron sin complicaciones para diferentes Grados de Polimerización (Degree of Polymerization, DP). Para los APAA (20 compuestos), encontramos que esta tecnología funciona mejor para los PAA neutros (PEG, PSar) y aniónicos (PGlu), que para los catiónicos (POrn) o zwitteriónicos P(Glu-co-Orn). Con respecto a la conformación de la estructura secundaria, los APAA que contienen Glu(OBzl) y Phe mostraron menos problemas de fabricación que los APAA que contienen PVal. La escasa solubilidad en disolventes comunes de la PVal [29, 30] combinados por segmentos hidrófilos catiónicos y zwitteriónicos dificultó su síntesis y caracterización. Es importante destacar que la conformación de la estructura secundaria de hoja-beta para los APAA que contienen PVal no fue confirmada por CD. Diseñamos las arquitecturas de estos materiales en base a los datos disponibles en las bases de datos [26-30].

También se estudiaron otros tipos de micelas poliméricas. En este caso estas contenían un polímero hidrofílico como cadena soluble en agua y una biomolécula para la parte hidrofóbica (HP-BM). Centramos nuestro estudio en la molécula TPGS y en la producción de un candidato similar biodegradable y biocompatible empleando Sar en lugar de EG llamado **TPSS**. El TPGS es una molécula anfifílica compuesta por PEG (hidrófilo) y D-alfa-tocoferol, también llamado Vitamina E (hidrófoba) y su uso está ampliamente descrito como vehículo en la administración de fármacos [35]. En la última década, se han publicado varios estudios comparando la PSar y el PEG en diferentes materiales [23, 36-38]. El PEG está considerado como polímero hidrofílico de referencia en el campo de transporte de fármacos, pero se han observado en la última década muchos efectos no deseables derivados de su uso crónico tan extendido [1, 21]. Estos inconvenientes son principalmente (i) hipersensibilidad [21], (ii) la no biodegradabilidad y no biocompatibilidad [21], (iii) los

efectos secundarios en el cuerpo debido al PEG en sí o productos de degradación, y la formación de anticuerpos anti-PEG [39, 40]. Por lo tanto, en nuestro caso y como línea prioritaria dentro de la empresa se está buscando alternativas al PEG mediante la utilización de PAA, por ese motivo durante esta tesis doctoral se desarrolló y caracterizó adecuadamente la molécula alternativa de **TPSS**. Este nuevo material anfifílico HP-BM biodegradable se comparó directamente con la versión comercial PEGilada encontrando resultados similares para las distribuciones de Mw por SEC y por MALDI-TOF MS, la identidad y los coeficientes de difusión por RMN.

Los resultados obtenidos nos llevaron a seleccionar las familias de APAA de PEG-PBG y PEG-PPhe, así como el TPGS y **TPSS**, para estudiar sus propiedades de autoensamblaje en estructuras micelares capaces de encapsular un fluoróforo hidrófobo como modelo de API hidrofóbico. Una vez generadas las micelas, se determinó la eficiencia de encapsulación y carga de fluoróforo por espectroscopía UV-Vis, la estructura conformacional secundaria por Dicroísmo Circular, la Concentración de Agregación Crítica por espectroscopía de fluorescencia y su morfología por Microscopía de Transmisión Electrónica, encontrando buenos resultados en comparación con los reportados en literatura. Además, se determinó el tamaño y el potencial Z mediante Dispersión de Luz Dinámica para formulaciones micelares preparadas mediante diferentes metodologías. Los resultados obtenidos nos permiten concluir que la tecnología ROP de NCAs vía NAM es excelente para generar las micelas poliméricas obtenidas con los APAA, así como las obtenidas mediante el enfoque HP-BM. Estas micelas son candidatos excelentes y versátiles como portadores con capacidad de encapsulación de APIs hidrofóbicos y posterior liberación bajo condiciones específicas.

4.2. SISTEMA HÍBRIDO POLIMÉRICO ENTRECruzADO COMO VEHÍCULO CAPAZ DE AUMENTAR LA PERMEACIÓN CUTÁNEA (CAPÍTULO 3)

Basándonos en los resultados obtenidos con la encapsulación del fluoróforo hidrófobo como modelo de API, utilizando las micelas poliméricas PEG-PBG y PEG-PPhe, y motivados por la exploración de materiales basados en PAA como portadores para la administración de fármacos en aplicaciones dérmicas, decidimos desarrollar una plataforma que facilitase la administración tópica en piel, dado que este campo está escasamente estudiado para los PAA.

Las estrategias recientes para la administración tópica de API a capas específicas de la piel han explorado el potencial de las formulaciones poliméricas de fármacos como emulsiones, cremas, geles, hidrogeles, parches transdérmicos y apósitos para heridas, así como la aplicación de polímeros como potenciadores de la permeación [41]. Los polímeros actualmente estudiados incluyen poliácridatos, poloxámeros, poli (ácido láctico-co-glicólico)

[41], alcoholes polivinílicos [42], derivados de PEG [43], polisacáridos [41, 44, 45] y los PAA [8]. Los polisacáridos incluyen polímeros naturales producidos por algas (por ejemplo, alginato), plantas (por ejemplo, celulosa), microbios (por ejemplo, dextrano) y animales (por ejemplo, ácido hialurónico) [46]. El ácido hialurónico (HA, también llamado hialuronato sódico), un heteropolisacárido natural con una estructura lineal descubierto por Meyer y Palmer en 1934, contiene residuos alternados de ácido D-glucurónico y N-acetil-D-glucosamida [47]. El HA también se emplea ampliamente para aplicaciones tópicas debido a sus propiedades versátiles, como su biocompatibilidad, no inmunogenicidad, biodegradabilidad y viscoelasticidad. Así, el HA es un biomaterial ideal para aplicaciones cosméticas, médicas y farmacéuticas como la ingeniería de tejidos, generar rellenos dérmicos, inyectables y para tratar enfermedades específicas como sustancia farmacológica (por ejemplo, osteoartritis) [48, 49].

En este capítulo, diseñamos un polímero entrecruzado basado en HA con entrecruzamiento de PGlu facilitado por la presencia de L-lisina llamado Hyaluronic Acid Cross Polymer (**HA-CP**). La síntesis del **HA-CP** se desarrolló con éxito gracias a la optimización previa con el sistema simplificado entrecruzado de PGlu-Lys-PGlu, sin HA. Además, la técnica de caracterización por RMN, así como por SEC, la viscosidad intrínseca, la cuantificación de aminas libres y la monitorización del pH fueron parámetros clave para controlar y comprender la reacción de entrecruzamiento. Después de una exhaustiva caracterización físico-química del nuevo material **HA-CP**, se estudiaron sus propiedades biológicas como vehículo para administración tópica empleando ensayos *in vitro*, *ex vivo* e *in vivo*, comparándolo con un HA lineal convencional con un Mw similar. Se observaron mejoras sustanciales en términos de resistencia a la degradación de la hialuronidasa, de la capacidad intrínseca de permeación en piel humana y la excelente compatibilidad con la piel humana. Además, la ausencia de efecto irritante vaginal *in vivo* en un modelo de conejo confirmó la buena compatibilidad del **HA-CP** con la piel.

Debido a la alta capacidad de permeación cutánea encontrada para el **HA-CP**, se decidió estudiar la capacidad de mejora del **HA-CP** en la administración de fármacos a través de la piel para API hidrófobos encapsulados en 4 micelas poliméricas basadas en materiales APAA: **PEG114-b-Glu(OBzl)10**, **PEG114-b-PGlu(OBzl)20**, **PEG114-b-PPhe10** y **PEG114-b-PPhe20**. Para ello, las micelas se formularon dentro de la matriz de **HA-CP** produciendo un sistema de material híbrido. Después de la permeación *ex vivo* utilizando celdas de difusión de Franz, se observó una excelente capacidad para atravesar el estrato córneo y transportar los API hidrófobos hasta la capa de la epidermis. De las 4 micelas formuladas en el **HA-CP**, los sistemas de **PEG114-b-PGlu(OBzl)20** y **PEG114-b-PPhe10** fueron los que mayor acumulación en la epidermis mostraron. Sin embargo, seleccionó el sistema híbrido con la micela de **PEG114-b-PGlu(OBzl)20** debido a su mayor capacidad de encapsulación y a que presenta una síntesis más sencilla. Por tanto, la permeación cutánea

de la micela de **PEG114-b-PGlu(OBzl)20** se formuló en tres medios: agua, HA lineal y matriz **HA-CP**. Y la formulación en **HA-CP** mostró la mayor acumulación en la capa de la epidermis.

Además, el nuevo material **HA-CP** también pudo formar un portador híbrido con las micelas tipo HP-BM de **TPGS** y **TPSS** respectivamente. Esta pequeña prueba de concepto es una evidencia del potencial de los materiales de polisarcosina para ser utilizados en la administración tópica de fármacos, ya que el **TPSS** mostró una mayor acumulación en la epidermis que el material PEGilado.

La tecnología desarrollada para preparar materiales reticulados entre polisacáridos y PAA fue patentada [50] y empleada en aplicaciones farmacéuticas como el tratamiento de la psoriasis que mejora la permeación cutánea del conjugado PGlu-fluocinolona [51]. Debido a las excelentes propiedades para la piel observadas en el **HA-CP**, ha hecho que se esté empleando como ingrediente principal en varios productos cosméticos actualmente comercializados bajo el nombre de **Biomimetic PBT** [52]. Actualmente, el proceso de fabricación del **HA-CP** está escalado y optimizado permitiendo su producción en lotes de 25 Kg.

4.3. DESARROLLO DEL PROCESO DE FABRICACIÓN DE ALPHA POLI-L-LISINAS BAJO EL GRADO DE CALIDAD DE SUSTANCIA FÁRMACÉUTICA CONFORME A LAS BUENAS PRÁCTICAS DE FABRICACIÓN (CAPÍTULO 4)

La tendencia actual a utilizar PAA en la administración de fármacos para aplicaciones biomédicas, nos motivó a invertir recursos en el desarrollo de un proceso de fabricación para producir materiales basados en PAA. A diferencia de la etapa de I+D en la academia, universidades o institutos de investigación, las empresas no comparten su tecnología interna en revistas científicas o bases de datos sobre procesos de fabricación, metodologías analíticas, instalaciones, proveedores, controles de calidad, etc. A diferencia de muchos otros polímeros empleados en el desarrollo farmacéutico (por ejemplo, PEG, PLGA, etc.), los PAA carecen de una guía concreta o monografía sobre la estrategia recomendada para sus procesos de fabricación y control. Afortunadamente, las guías ICH proporcionan una excelente y precisa información para diseñar una estrategia que garantice que los científicos y los fabricantes sean capaces de desarrollar con precisión un proceso de fabricación robusto, reproducible y escalable dentro de un entorno GMP regulado si requieren de los conocimientos adecuados. Estas guías también garantizan el ciclo de vida del producto y la trazabilidad de los lotes de fabricación. Específicamente, la guía ICH Q11 denominada “*Desarrollo y Fabricación de Sustancias Farmacéuticas (Entidades Químicas y Entidades Biotecnológicas/Biológicas)*” está enfocada en mostrar una ruta precisa y detallada para generar nuevas sustancias farmacéuticas [53]. Y la guía ICH Q7 llamada “*Guía de Buenas*

Prácticas de Fabricación de Ingredientes Farmacéuticos Activos” muestra cómo se puede hacer esto de acuerdo con el cumplimiento de las GMP [54]. Teniendo en cuenta que la mayoría de estos PAA son materiales nuevos y que las agencias reguladoras expresaron su preocupación por estas nanomedicinas poliméricas en el pasado, decidimos producir los materiales basados en PAA bajo el estándar regulatorio más alto de sustancia farmacéutica siguiendo principalmente las guías ICH Q11 y Q7. Y, como la poli-L-lisina (PLys) es el PAA con mayor demanda y con el mayor número de publicaciones (ver Figura 4.1), enfocamos el desarrollo y optimización de nuestro proceso de fabricación para PLys.

Se desarrolló y optimizó el proceso de fabricación de dos PLys (**HL50** y **ML400**) siguiendo principalmente la guía ICH Q11 logrando un proceso de fabricación robusto, reproducible y escalable. Además, se diseñaron, desarrollaron, optimizaron, cualificaron y validaron técnicas analíticas para realizar una adecuada caracterización físico-química. El proceso de fabricación de PLys se desarrolló adaptando la ruta de escalado de la FDA [55] a nuestro enfoque.

Se elaboró un paquete documental CMC para las dos PLys mencionadas. Hasta la fecha, tanto la EMA como la FDA han evaluado nuestro paquete CMC para materiales relacionados con PLys con muy buenos comentarios permitiendo a nuestros socios despejar el camino hacia los ensayos clínicos. Los materiales producidos en Polypeptide Therapeutic Solutions S.L. forman parte de nanofármacos que se están probando actualmente en humanos dentro de diferentes ensayos clínicos para tratar diferentes patologías, desde trastornos neurodegenerativos hasta en oncología.

5. CONCLUSIONES

1. La tecnología de ROP de los monómeros NCA de alfa aa mediante la metodología NAM se ha adaptado con éxito para generar PAA, tanto de composición homogénea como aleatoria bien definidos y con perfiles de Mw homogéneos para diferentes DPs (de 20 a 400) obteniendo buenos resultados con respecto al objetivo. El carácter vivo de esta técnica de polimerización permite que el iniciador se mantenga en el extremo C-terminal y permitiendo que la amina libre esté disponible en el extremo N-terminal para actuar como iniciador para construir copolímeros de bloque generando APAA bien definidos.
2. Se han sintetizado PAA y APAA utilizando monómeros de aa de diferente naturaleza siendo: (i) catiónicos (Orn y Arg), (ii) aniónicos (Glu), (iii) polares (Sar) y (iv) apolares (Phe y Val), permitiendo su combinación en arquitecturas homogéneas, aleatorias y en bloque para modificar la carga electrostática, la conformación de la estructura secundaria y la relación hidrofílica-hidrofóbica.
3. Se desarrollaron con éxito técnicas de caracterización físico-química para analizar los CQAs de los materiales basados en PAA. Las dos principales técnicas de caracterización

desarrolladas han sido el SEC y el RMN. Se ha empleado SEC para obtener las distribuciones de Mw de los precursores protegidos y la RMN para establecer la relación de estequiometría entre el iniciador y la composición de monómero(s) de aa.

4. Se ha optimizado y estudiado por RMN la desprotección mediante hidrólisis ácida y básica para eliminar los grupos protectores de los materiales basados en PAA

5. Se ha desarrollado una nueva alternativa biodegradable al TPGS que contiene PSar como polímero hidrófilo en lugar de PEG llamado **TPSS**. Se realizó una comparación cara a cara en términos de propiedades físicas y químicas de TPGS y **TPSS** encontrando prácticamente los mismos resultados en términos de distribución de Mw, polidispersidad, contenido de Vitamina E, coeficiente de difusión, tamaño y morfología. Los estudios posteriores se centrarán en determinar la concentración de agregación crítica y las propiedades antioxidantes. Además, los resultados son susceptibles de ser patentados.

6. Se seleccionaron cuatro materiales basados en APAA para estudiar sus propiedades de autoensamblaje micelar y su eficiencia de encapsulación de un fluoróforo hidrófilo como modelo de API hidrofóbico. Los materiales seleccionados fueron: (i) **PEG114-b-PGlu(OBzl)10**, (ii) **PEG114-b-PGlu(OBzl)20**, (iii) **PEG114-b-PPhe10** y (iv) **PEG114-b-PPhe20**.

7. Se diseñó un nuevo polímero entrecruzado basado en HA reticulado con PGlu a través de lisina llamado **HA-CP**. El compuesto **HA-CP** se evaluó *in vitro*, *in vivo* y *ex vivo* como un portador en la administración de fármacos a través de la piel para aplicaciones tópicas en comparación directamente con un HA lineal con el mismo Mw encontrando excelentes resultados y mejoras en términos de: (i) resistencia a la degradación de hialuronidasa, (ii) capacidad intrínseca de permeación de la piel humana y (iii) compatibilidad con la piel. Además, se ha comercializado una serie de productos dermo-cosméticos basados en **HA-CP** bajo el nombre de **Biomimetic PBT**. Actualmente, el proceso de fabricación del **HA-CP** está escalado y optimizado permitiendo su producción en lotes de 25 Kg.

8. El **HA-CP** se combinó con las 4 micelas poliméricas mencionadas anteriormente dando lugar a 4 materiales híbridos (uno por micela). Los sistemas del material híbrido de **HA-CP** con micelas de **PEG114-PGlu(OBzl)20** y **PEG114-PPhe10** mostraron la mayor acumulación en la capa de la epidermis.

9. El **HA-CP** se formuló para obtener un vehículo híbrido con micelas basadas en HP-BM con los materiales **TPGS** y **TPSS** respectivamente. El vehículo híbrido de polisarcosina mostró una mayor acumulación en la capa de la epidermis comparado con la versión PEGilada.

10. El proceso de fabricación bajo el estándar de calidad de sustancia farmacéutica se desarrolló y optimizó completamente para dos PLys (**HL50** y **ML400**) dentro de la normativa GMP siguiendo las guías armonizadas ICH Q11 “*Desarrollo y Fabricación de Sustancias Farmacéuticas (Entidades Químicas y Entidades Biotecnológicas/Biológicas)*” y la ICH Q7 “*Guía de Buenas Prácticas de Fabricación de Ingredientes Farmacéuticos Activos*”.

11. Se ha elaborado un paquete de documentación de CMC sobre el proceso de fabricación de ambas PLys.

6. REFERENCIAS

- [1] M. Barz, R. Luxenhofer, R. Zentel, M.J. Vicent, Overcoming the PEG-addiction: well-defined alternatives to PEG, from structure-property relationships to better defined therapeutics, *Polymer Chemistry* 2(9) (2011) 1900-1918.
- [2] M. Khuphe, P.D. Thornton, Poly(amino acids), in: A. Parambath (Ed.), *Engineering of Biomaterials for Drug Delivery Systems: Beyond Polyethylene Glycol*, Woodhead Publ Ltd, Cambridge, 2018, pp. 199-228.
- [3] A.R. Mazo, S. Allison-Logan, F. Karimi, N.J.A. Chan, W.L. Qiu, W. Duan, N.M. O'Brien-Simpson, G.G. Qiao, Ring opening polymerization of alpha-amino acids: advances in synthesis, architecture and applications of polypeptides and their hybrids, *Chemical Society Reviews* 49(14) (2020) 4737-4834.
- [4] J.V. Gonzalez-Aramundiz, M.V. Lozano, A. Sousa-Herves, E. Fernandez-Megia, N. Csaba, Polypeptides and polyaminoacids in drug delivery, *Expert Opinion on Drug Delivery* 9(2) (2012) 183-201.
- [5] T. Melnyk, S. Dordevic, I. Conejos-Sanchez, M.J. Vicent, Therapeutic potential of polypeptide-based conjugates: Rational design and analytical tools that can boost clinical translation, *Advanced drug delivery reviews* 160 (2020) 136-169.
- [6] A. Duro-Castano, I. Conejos-Sanchez, M.J. Vicent, Peptide-Based Polymer Therapeutics, *Polymers* 6(2) (2014) 515-551.
- [7] M.P. Bevilacqua, D.J. Huang, B.D. Wall, S.J. Lane, C.K. Edwards, J.A. Hanson, D. Benitez, J.S. Solomkin, T.J. Deming, Amino Acid Block Copolymers with Broad Antimicrobial Activity and Barrier Properties, *Macromolecular Bioscience* 17(10) (2017) 9.
- [8] R. Wang, B. Zhou, D.L. Xu, H. Xu, L. Liang, X.H. Feng, P.K. Ouyang, B. Chi, Antimicrobial and biocompatible epsilon-polylysine-gamma-poly(glutamic acid)-based hydrogel system for wound healing, *Journal of Bioactive and Compatible Polymers* 31(3) (2016) 242-259.
- [9] Y. Ohya, S. Takeda, Y. Shibata, T. Ouchi, A. Kano, T. Iwata, S. Mochizuki, Y. Taniwaki, A. Maruyama, Evaluation of polyanion-coated biodegradable polymeric micelles as drug delivery vehicles, *Journal of Controlled Release* 155(1) (2011) 104-110.
- [10] C.G. Zhang, R.L. Zhang, Y. Zhu, W. Wei, Y. Gu, X.Y. Liu, Polymer vesicles prepared from the (L-phenylalanine ethyl ester)-modified hyaluronic acid, *Materials Letters* 164 (2016) 15-18.
- [11] G.S. Kwon, K. Kataoka, Block copolymer micelles as long-circulating drug vehicles, *Advanced Drug Delivery Reviews* 64 (2012) 237-245.
- [12] A. Carlsen, S. Lecommandoux, Self-assembly of polypeptide-based block copolymer amphiphiles, *Current Opinion in Colloid & Interface Science* 14(5) (2009) 329-339.

- [13] O. Zagorodko, J.J. Arroyo-Crespo, V.J. Nebot, M.J. Vicent, Polypeptide-Based Conjugates as Therapeutics: Opportunities and Challenges, *Macromolecular Bioscience* 17(1) (2017).
- [14] A. Lalatsa, A.G. Schatzlein, M. Mazza, B.H.L. Thi, I.F. Uchegbu, Amphiphilic poly(l-amino acids) - New materials for drug delivery, *Journal of Controlled Release* 161(2) (2012) 523-536.
- [15] H.L. Xu, Q. Yao, C.F. Cai, J.X. Gou, Y. Zhang, H.J. Zhong, X. Tang, Amphiphilic poly(amino acid) based micelles applied to drug delivery: The in vitro and in vivo challenges and the corresponding potential strategies, *Journal of Controlled Release* 199 (2015) 84-97.
- [16] R. Wahid, R. Holt, R. Hjorth, F.B. Scorza, Chemistry, manufacturing and control (CMC) and clinical trial technical support for influenza vaccine manufacturers, *Vaccine* 34(45) (2016) 5430-5435.
- [17] N.S. Cauchon, S. Oghamian, S. Hassanpour, M. Abernathy, Innovation in Chemistry, Manufacturing, and Controls-A Regulatory Perspective From Industry, *Journal of Pharmaceutical Sciences* 108(7) (2019) 2207-2237.
- [18] G. Akshatha, V.A. Narayanan, D.S. Sandeep, R.N. Charyulu, Chemistry, Manufacturing and Control (CMC) Evaluations of ANDA Submission in the USA, *Indian Journal of Pharmaceutical Education and Research* 53(3) (2019) 414-420.
- [19] I.L. Shih, Y.T. Van, M.H. Shen, Biomedical applications of chemically and microbiologically synthesized poly(glutamic acid) and poly(lysine), *Mini-Reviews in Medicinal Chemistry* 4(2) (2004) 179-188.
- [20] S.E. Barrett, R.S. Burke, M.T. Abrams, C. Bason, M. Busuek, E. Carlini, B.A. Carr, L.S. Crocker, H. Fan, R.M. Garbaccio, E.N. Guidry, J.H. Heo, B.J. Howell, E.A. Kemp, R.A. Kowtoniuk, A.H. Latham, A.M. Leone, M. Lyman, R.G. Parmar, M. Patel, S.Y. Pechenov, T. Pei, N.T. Pudvah, C. Raab, S. Riley, L. Sepp-Lorenzino, S. Smith, E.D. Soli, S. Staskiewicz, M. Stern, Q. Truong, M. Vavrek, J.H. Waldman, E.S. Walsh, J.M. Williams, S. Young, S.L. Colletti, Development of a liver-targeted siRNA delivery platform with a broad therapeutic window utilizing biodegradable polypeptide-based polymer conjugates, *Journal of Controlled Release* 183 (2014) 124-137.
- [21] K. Knop, R. Hoogenboom, D. Fischer, U.S. Schubert, Poly(ethylene glycol) in Drug Delivery: Pros and Cons as Well as Potential Alternatives, *Angewandte Chemie-International Edition* 49(36) (2010) 6288-6308.
- [22] A. Birke, J. Ling, M. Barz, Polysarcosine-containing copolymers: Synthesis, characterization, self-assembly, and applications, *Progress in Polymer Science* 81 (2018) 163-208.
- [23] Y. Xiao, J.Q. Wang, J. Zhang, A. Heise, M.D. Lang, Synthesis and gelation of copolypept(o)ides with random and block structure, *Biopolymers* 107(10) (2017) 9.
- [24] Z.Y. Song, H.L. Fu, J. Wang, J.S. Hui, T.R. Xue, L.A. Pacheco, H.Y. Yan, R. Baumgartner, Z.Y. Wang, Y.C. Xia, X.F. Wang, L.C. Yin, C.Y. Chen, J. Rodriguez-Lopez, A.L. Ferguson, Y. Lin, J.J. Cheng, Synthesis of polypeptides via bioinspired polymerization of in situ purified N-carboxyanhydrides, *Proceedings of the National Academy of Sciences of the United States of America* 116(22) (2019) 10658-10663.
- [25] S. Niimura, H. Kurosu, A. Shoji, Precise structural analysis of alpha-helical polypeptide by quantum-chemical calculation related to reciprocal side-chain combination of two L-phenylalanine residues, *Journal of Molecular Structure* 970(1-3) (2010) 96-100.
- [26] S.H. Wibowo, A. Sulistio, E.H.H. Wong, A. Blencowe, G.G. Qiao, Functional and Well-Defined -Sheet-Assembled Porous Spherical Shells by Surface-Guided Peptide Formation, *Advanced Functional Materials* 25(21) (2015) 3147-3156.

- [27] A. Sinaga, T.A. Hatton, K.C. Tam, Thermodynamics of micellization of beta-sheet forming poly(acrylic acid)-block-poly(L-valine) hybrids, *Journal of Physical Chemistry B* 112(37) (2008) 11542-11550.
- [28] H.J. Song, G. Yang, P.S. Huang, D.L. Kong, W.W. Wang, Self-assembled PEG-poly(L-valine) hydrogels as promising 3D cell culture scaffolds, *Journal of Materials Chemistry B* 5(9) (2017) 1724-1733.
- [29] H.Y. Zhu, M. Zhu, S.R. Shuai, C. Zhao, Y. Liu, X.H. Li, Z.K. Rao, Y. Li, J.Y. Hao, Effect of polypeptide block length on nano-assembly morphology and thermo-sensitivity of methyl poly(ethylene glycol)-poly(L-valine) copolymer aqueous solutions, *Journal of Sol-Gel Science and Technology* 92(3) (2019) 618-627.
- [30] A. Sinaga, P. Ravi, T.A. Hatton, K.C. Tam, Synthesis of poly(acrylic acid)-block-poly(L-valine) hybrid through combined atom transfer radical polymerization, click chemistry, and nickel-catalyzed ring opening polymerization methods, *Journal of Polymer Science Part a-Polymer Chemistry* 45(13) (2007) 2646-2656.
- [31] T.J. Deming, Methodologies for preparation of synthetic block copolypeptides: materials with future promise in drug delivery, *Advanced Drug Delivery Reviews* 54(8) (2002) 1145-1155.
- [32] H. Lu, J. Wang, Z.Y. Song, L.C. Yin, Y.F. Zhang, H.Y. Tang, C.L. Tu, Y. Lin, J.J. Cheng, Recent advances in amino acid N-carboxyanhydrides and synthetic polypeptides: chemistry, self-assembly and biological applications, *Chemical Communications* 50(2) (2014) 139-155.
- [33] T.J. Deming, Synthesis and Self-Assembly of Well-Defined Block Copolypeptides via Controlled NCA Polymerization, *Hierarchical Macromolecular Structures: 60 Years after the Staudinger Nobel Prize* 262 (2013) 1-37.
- [34] J. Huang, A. Heise, Stimuli responsive synthetic polypeptides derived from N-carboxyanhydride (NCA) polymerisation, *Chemical Society Reviews* 42(17) (2013) 7373-7390.
- [35] C.L. Yang, T.T. Wu, Y. Qi, Z.P. Zhang, Recent Advances in the Application of Vitamin E TPGS for Drug Delivery, *Theranostics* 8(2) (2018) 464-485.
- [36] D. Huesmann, A. Sevenich, B. Weber, M. Barz, A head-to-head comparison of poly(sarcosine) and poly(ethylene glycol) in peptidic, amphiphilic block copolymers, *Polymer* 67 (2015) 240-248.
- [37] K. Son, M. Ueda, K. Taguchi, T. Maruyama, S. Takeoka, Y. Ito, Evasion of the accelerated blood clearance phenomenon by polysarcosine coating of liposomes, *Journal of Controlled Release* 322 (2020) 209-216.
- [38] S.S. Nogueira, Polysarcosine-Functionalized Lipid Nanoparticles for Therapeutic mRNA Delivery, in: A. Schlegel (Ed.) *ACS Appl. Nano Mater.*, 2020, pp. 10634–10645.
- [39] K.D. Hinds, Protein conjugation, cross-linking, and PEGylation, *Biomaterials for Delivery and Targeting of Proteins and Nucleic Acids* (2005) 119-185.
- [40] G.T. Kozma, T. Shimizu, T. Ishida, J. Szebeni, Anti-PEG antibodies: Properties, formation, testing and role in adverse immune reactions to PEGylated nano-biopharmaceuticals, *Advanced drug delivery reviews* 154-155 (2020) 163-175.
- [41] C. Valenta, B.G. Auner, The use of polymers for dermal and transdermal delivery, *European Journal of Pharmaceutics and Biopharmaceutics* 58(2) (2004) 279-289.
- [42] S.A. Castleberry, M.A. Quadir, M. Abu Sharkh, K.E. Shopsowitz, P.T. Hammond, Polymer conjugated retinoids for controlled transdermal delivery, *Journal of Controlled Release* 262 (2017) 1-9.

- [43] A.B. Kutikov, J. Song, Biodegradable PEG-Based Amphiphilic Block Copolymers for Tissue Engineering Applications, *Acs Biomaterials Science & Engineering* 1(7) (2015) 463-480.
- [44] R. Gul, N. Ahmed, K.U. Shah, G.M. Khan, A.U. Rehman, Functionalised nanostructures for transdermal delivery of drug cargos, *Journal of Drug Targeting* 26(2) (2018) 110-122.
- [45] M.C.G. Pella, M.K. Lima-Tenorio, E.T.T. Neto, M.R. Guilherme, E.C. Muniz, A.F. Rubira, Chitosan-based hydrogels: From preparation to biomedical applications, *Carbohydrate Polymers* 196 (2018) 233-245.
- [46] Q. Li, Y.M. Niu, P.F. Xing, C.M. Wang, Bioactive polysaccharides from natural resources including Chinese medicinal herbs on tissue repair, *Chinese Medicine* 13 (2018) 11.
- [47] C. Guarise, M. Pavan, L. Pirrone, D. Renier, SEC determination of cross-link efficiency in hyaluronan fillers, *Carbohydrate Polymers* 88(2) (2012) 428-434.
- [48] S. Berko, M. Maroda, M. Bodnar, G. Eros, P. Hartmann, K. Szentner, P. Szabo-Revesz, L. Kemeny, J. Borbely, E. Csanyi, Advantages of cross-linked versus linear hyaluronic acid for semisolid skin delivery systems, *European Polymer Journal* 49(9) (2013) 2511-2517.
- [49] A. Fakhari, C. Berklund, Applications and emerging trends of hyaluronic acid in tissue engineering, as a dermal filler and in osteoarthritis treatment, *Acta Biomaterialia* 9(7) (2013) 7081-7092.
- [50] D. Morelló-Bolumar, CROSS POLYMERS COMPOSED OF POLYSACCHARIDES AND POLYAMINO ACIDS, AND USES THEREOF (WO 2019/020344 A1), 2019.
- [51] I. Dolz-Perez, M.A. Sallam, E. Masia, D. Morello-Bolumar, M.D.P. del Caz, P. Graff, D. Abdelmonsif, S. Hedtrich, V.J. Nebot, M.J. Vicent, Polypeptide-corticosteroid conjugates as a topical treatment approach to psoriasis, *Journal of Controlled Release* 318 (2020) 210-222.
- [52] <https://www.biomimeticdermocosmetics.com/en/>.
- [53] ICH Q11 Development And Manufacture Of Drug Substances (Chemical Entities And Biotechnological/Biological Entities).
- [54] ICH Q7 Good Manufacturing Practice Guide For Active Pharmaceutical Ingredients.
- [55] <https://www.fda.gov/about-fda/innovation-fda/what-we-do>.